

Copyright

by

Valentina Marzia Rossi

2016

The Dissertation Committee for Valentina Marzia Rossi Certifies that this is the approved version of the following dissertation:

Mixed-Energy Shallow-Marine Systems with Emphasis on Tidal Influence

Committee:

Ronald J. Steel, Supervisor

Wonsuck Kim, Co-Supervisor

Cornel Olariu

William Fisher

Sergio Longhitano

**Mixed-Energy Shallow-Marine Systems with Emphasis on Tidal
Influence**

by

Valentina Marzia Rossi, Laurea Magistrale

**Mixed-Energy Shallow-Marine Systems with Emphasis on Tidal
Influence**

Presented to the Faculty of the Graduate School of

The University of Texas at Austin

in Partial Fulfillment

of the Requirements

for the Degree of

Doctor of Philosophy

The University of Texas at Austin

December 2016

Dedication

To my mom, my dad, my sister, and Julio.

“The mountains are calling and I must go” – John Muir

“In every walk with nature one receives far more than he seeks” – John Muir

*“... non vogliate negar l'esperienza,
di retro al sol, del mondo senza gente.*

*Considerate la vostra semenza:
fatti non foste a viver come bruti,
ma per seguir virtute e canoscenza”*

Dante Alighieri, Divina Commedia, Inferno canto XXVI, 116-120

Acknowledgements

I would like to thank all the people that helped me throughout my PhD. My family and Julio for their constant support and help. Ron Steel, my co-advisor, for his help and great geological discussions. Wonsuck Kim, my co-supervisor, for his help and for his great support. Cornel Olariu, for great discussions and for helping me to improve all my research ideas. Sergio Longhitano (and Marta), for his help and support, and for the great time in the field. Donatella Mellere, for constant support and for motivating me. Domenico Chiarella, for his help in the field and not only. The PI's of the Lajas Project, and in particular Bob Dalrymple, for his great help in the field and for great discussions.

I would also like to thank Vicente and Graciela, that made me feel like at home in Argentina, and made my field experience there unforgettable. All my friends in Ron's and Wonsuck's research groups, Jinyu, Yang, Xiaojie, Logan, Austin, Allison, Anastasia, Brandee, Si, Shunli, YeJin, Max, WoongMo.

Finally, I would like to thank the companies and institutions that have supported my research: Statoil, VNG Norge, Woodside and BHP Billiton, the RioMAR consortium, GSA, IAS and the Ronald K. DeFord Field Scholarship Fund.

Mixed-Energy Shallow-Marine Systems with Emphasis on Tidal Influence

Valentina Marzia Rossi, PhD

The University of Texas at Austin, 2016

Supervisors: Ronald J. Steel and Wonsuck Kim

This research investigates mixed-energy shallow marine depositional systems (i.e., subject to the influence of river, wave and tidal currents), with particular emphasis on the role of tidal currents in controlling the final stratigraphic product. In modern coastal areas and in the rock record, many sedimentary systems bear the signature of changing and overlapping coastal processes. Understanding the evolution of the mixed tidal systems and their stratigraphic expression is fundamental both to the science of dynamic stratigraphy and for a proper exploitation of the stored natural resources. The research was carried out using four datasets: an outcrop dataset of measured sedimentological sections from the Jurassic Lajas Formation, Argentina; a dataset of previously published literature of process variability and sedimentary structures; a dataset of numerical simulations produced with Delft3D software; and an outcrop dataset of measured sedimentological sections from the Pleistocene Siderno Strait, Italy.

The data here presented highlight the great degree of process variability in the rock record, and the importance of tidal currents in controlling deltaic morphology and stratigraphic architecture. The strata of the Lajas Formation show a clear process partitioning in different reaches of the deltaic system (proximal vs. distal and regressive vs. transgressive). In particular, tidal currents strongly reworked the delta front at times,

creating sand-rich and amalgamated sandbodies. This project demonstrates that disentangling the signals of river, wave and tidal currents in the stratigraphy leads to a better interpretation of ancient mixed-energy systems. The study of the literature database shows that some sedimentary structures can be considered reliable indicators of a particular process (river, waves or tides), whereas other structures cannot be tied with confidence to any particular process. A process probability value is calculated for each sedimentary structure, and thus quantifies process variability and its uncertainty. This work encourages a new, more detailed and more quantified field methodology for facies sedimentology. The numerical modeling of tide-influenced deltas using Delft3D shows how different degrees of tidal influence in river-dominated deltas affect delta morphology and stratigraphy, when tidal currents are flowing perpendicularly to the shoreline. Increasing tidal influence induces deeper and more stable distributary channels that act as efficient conduits for sediment transport basinward. The delta-front geometry is also affected by tidal current reworking, evolving into a compound clinoform geometry. The research on the Siderno Strait, in contrast, highlights tidal influence on deltaic stratigraphic evolution when tidal currents flow parallel to the coastline. River-dominated deltas entering the tide-dominated strait tend to show a deflection of the delta-front sands in a direction parallel to the dominant tidal current. The delta-front sands became reworked by tidal currents into large dune fields within the strait.

Table of Contents

List of Tables	xii
List of Figures	xiv
Chapter 1: Introduction	1
Problems and Significance.....	1
Objectives	3
Overview of Chapters	4
Chapter 2: The role of tidal, wave and river currents in the evolution of mixed-energy deltas: Example from the Lajas Formation (Argentina)	4
Chapter 3: Quantifying process regime in ancient shallow marine mixed-energy depositional systems: what are sedimentary structures really telling us?	5
Chapter 4: Impact of tidal currents on delta-channel deepening, stratigraphic architecture and sediment bypass beyond the shoreline	5
Chapter 5: Tidal and Fluvial Processes Interplay in an Early Pleistocene, Delta-Fed, Strait Margin (Calabria, southern Italy).....	6
References.....	7
Chapter 2: The role of tidal, wave and river currents in the evolution of mixed-energy deltas: Example from the Lajas Formation (Argentina)	11
Abstract.....	11
introduction	12
Geological setting	16
The Lajas Formation	17
Methodology	18
Facies associations and depositional environments.....	20
Facies Association 1 (Coastal Plain).....	25
Facies Association 1.1 (Upper Coastal Plain).....	25
Facies Association 1.2 (Lower Delta Plain)	27

Facies Association 1.3 (Lower Delta-Plain Interdistributary Bays)	30
Facies Association 1.4 (Lower Delta Plain)	31
Process summary	34
Facies Association 2 (Delta Front and Subaqueous Platform)	35
Facies Association 2.1 (Delta-Front Mouth Bars)	35
Facies Association 2.2 (Tidally Reworked Bars and Dunes)	39
Facies Association 2.3 (Subaqueous Platform)	45
Facies Association 2.4 (Shoreface)	49
Process summary	51
Facies Association 3 (Prodelta and Offshore)	52
Facies Association 3.1 (Prodelta)	52
Facies Association 3.2 (Offshore/Offshore Transition)	52
Process summary	54
Facies Association 4 (Tidal Inlet and Estuary)	54
Facies Association 4.1 (Tidal Inlet)	54
Facies Association 4.2 (Estuary)	58
Process summary	63
Stratigraphic architecture and stacking patterns	64
Discussion	69
Vertical and lateral process variability in the Lajas Formation	69
Lower Lajas Palaeogeography	72
Sediment partitioning and reservoirs implications	79
Comparison with modern systems	82
Conclusions	84
Acknowledgements	86
References	86
Chapter 3: Quantifying process regime in ancient shallow marine mixed-energy depositional systems: what are sedimentary structures really telling us?	95
Abstract	95
Introduction	96

Quantifying shallow-marine mixed-energy systems	98
Example 1: Las Lajas Fm. outcrop (Neuquén Basin)	103
Example 2: sedimentary logs database	106
Discussion	110
Process Probability Graph (PPG).....	110
Limitations of the methodology	111
Conclusions.....	112
Acknowledgements.....	113
References.....	113
 Chapter 4: Impact of tidal currents on delta-channel deepening, stratigraphic architecture, and sediment bypass beyond the shoreline	 116
Abstract.....	116
Introduction.....	117
Methodology	118
Fluvio-deltaic channel and shoreline evolution	119
Subaqueous delta platform and stratal development	122
Discussion	125
Sediment partitioning.....	125
Tidal processes in modern river deltas.....	128
Conclusions.....	129
Acknowledgments.....	130
References.....	130
 Chapter 5: Tidal and fluvial process interplay in an early Pleistocene, delta-fed, strait margin (Calabria, southern Italy).....	 132
Abstract.....	132
Introduction.....	133
General geological setting of the Siderno Basin.....	137
General tectonic setting.....	137
Neogene-to-Quaternary stratigraphy of the Siderno Basin.....	138
Facies and facies associations.....	140

Facies Association 1 (shelf mudstones and marlstones).....	141
Facies Association 2 (river-dominated, tide-influenced deltaic deposits)	143
Facies Association 3 (deflected, tide-dominated delta-front).....	147
Facies Association 4 (tidal strait-margin complex)	150
Facies Association 5 (shoreface and lagoon complex).....	152
Discussion: marginal-marine sedimentation along the Siderno Strait northern margin	155
Deltaic vs. tidal strait processes	155
River-flood deposits in straits	156
Intensity of tidal current reworking of the delta front.....	156
The early Pleistocene Siderno strait-margin evolution and the onset of a tidal circulation	160
Conclusions.....	163
Acknowledgments.....	164
References.....	164
Appendix A: Correlation panel of the Lajas outcrop at Lohan Mahuida	169
Appendix B: Supplementary material for process probability calculations	171
References.....	176
Appendix C: Supplementary material for the modeling simulations (Delft3D)..	185
References.....	190
Bibliography	192

List of Tables

Table 1.1: List of facies present in the Lower Lajas Formation at Lohan Mahuida.	21
Table 3.1: Table of the main shallow marine sedimentary structures. This table is based on an extensive literature review, and it assigns a percentage to each sedimentary structure, that represents the probability for a certain structure to be the result of wave (P(w)), tidal (P(t)), or river currents (P(r)). For example, if eight out of ten papers recognize a sedimentary structure as the result of tidal currents, two as the result of river currents and zero as related to wave/storm currents, the percentages are as follow: Pw=0%, Pt=80%, and Pr=20%. Some sketches are redrawn after De Raaf et al. (1977); Boersma and Terwindt (1981); Dalrymple et al. (1990); Nio and Yang (1991); Dalrymple (2010).	100
Table 3.2: List of references, location and age of the case studies used for the analysis of sedimentary logs.	102
Table 5.1: List of facies	142
Table B.1: Complete list of references used to calculate the percentages of each sedimentary structure.	171
Table B.2: Within unidirectional cross-strata it is possible in some cases to distinguish between tabular and trough cross-strata. Percentages have been calculated for tabular (2D) cross-strata and trough (3D) cross-strata.	175

Table B.3: Percentages related to inverse grading and inverse-to-normal grading. This structure is very diagnostic of river processes. However, the number of papers referencing it is very limited. For this reason this structure is shown only in the Appendix.	175
Table C.1: Complete list of the 24 runs used in this study	186
Table C.2: Data used to calculate A* and H* in all the runs and in modern deltas. Data for modern deltas is from Thompson (1968), Allen et al. (1979), Caline and Huong (1992), Guillen and Palanques (1992), Carriquiry and Sánchez (1999), Lambiase et al. (2002), Syvitski and Saito (2007), Baitis (2008), Kim et al. (2009), Sassi et al. (2011), Shaw et al. (2013), Shaw and Mohrig (2014), Cummings et al. (2016).	187

List of Figures

- Figure 1.1: Location of the study area in the Neuquén Basin of Argentina; map of the Neuquén Basin (modified after Spalletti et al., 2000) during the post-rift back-arc phase. Possible highlands inherited from syn-rift topography are highlighted in dashed red and yellow.16
- Figure 1.2: (A) Satellite image of the study area (Lohan Mahuida hill, yellow box). (B) Google Earth image of the study outcrop belt. Dashed white line represents the base of shelf deposits and the arrow shows the average progradation direction of the whole system (approximately north-west). Circles with black contour represent the location of measured sections. Circle with red contour represents the location of a less detailed log. (C) Photomosaic of Lohan Mahuida Hill; coloured lines match the colouring of different units in the correlation panel.....20
- Figure 1.3: (A) Clast-supported conglomerates and pebbly sandstones infilling channelized features of Facies Association 1.1. Hammer for scale is 32.5 cm long. (B) Facies Association 1.1 channels composed of pebbly sandstones cutting into marine sediments (red surface, representing a Sequence Boundary). The field notebook is 19 cm long27
- Figure 1.4: Clast-supported conglomerate showing inverse grading. Hammer for scale is 32.5 cm long27
- Figure 1.5: Facies Association 1.2 channel with low-relief, incising into heterolithic dark mudstones. Load and flame structures are present in the lower part of the body. Rose diagrams show palaeocurrents.....29

Figure 1.6: Coarsening-upward and thickening-upward sandbody, ranging from heterolithic muddy sediments up to upper fine–lower medium sandstones, characterized by moderate bioturbation. Hammer for scale is 32.5 cm long.....31

Figure 1.7: (A) Stratigraphic interval (yellow strip) with Facies Association 1.4 deposits. The base of the channels is marked by an erosion surface and sometimes by mudstone rip-up clasts. (B) Internal erosional surfaces typical of Facies Association 1.4 marked by an increase in grain size. (C) Increasing/decreasing organic debris concentration along the toesets and bottomsets of the cross-strata. (D) 20 to 15 cm thick cross-strata showing bundling.....34

Figure 1.8: Flood-Interflood cyclicity in Facies Association 2.1 deposits. (A) Photograph of a coarsening-upward sandbody. The deposit becomes coarser and cleaner upward. Red arrows point to event beds, whereas white arrows point to finer-grained interbeds. Hammer for scale is 32.5 cm long. (B) Detail of finer-grained interbeds characterized by fine scale alternations of organic debris and sandy laminae, and the presence of bioturbation. The pencil is 15 cm long.38

Figure 1.9: (A) Facies Association 1.4 deposits overlain by a coarsening-upward sandbody characterized by well-developed inclined strata. Person for scale is *ca* 1.8 m tall. (B) Abundant soft-sediment deformation and oversteepened cross-strata in Facies Association 2.1 deposits. These features are interpreted as fluvial signals. (C) Distal reach of a coarsening-upward sandbody, showing high degree of bioturbation and only few remnants of HCS. (D) Bi-directional cross-strata in the upper portion of a Facies Association 2.1 sandbody. The field notebook is 19 cm long.....39

Figure 1.10: (A) Overview of amalgamated sandbodies of Facies Association 2.2. (B) Compound cross-bedding typical of the sandbodies of Facies Association 2.2. Note that individual small-scale cross-strata are separated by reactivation surfaces. Hammer for scale is 32.5 cm long. (C) Abandonment surface between Facies Association 2.1 and Facies Association 2.2 sandbodies. This surface is rich in mud chips, wood/plant fragments and is very bioturbated. Some shell fragments are also present. (D) Double drapes in the toeset region of a Facies Association 2.2 sandbody. Pencil is 15 cm long.....43

Figure 1.11: (A) Laterally accreting sandbody of Facies Association 2.2. Note the presence of large (up to 35 m high) accretion surfaces; the total extent of the sandbody is more than 300 m. Person for scale (circled; *ca* 1.8 m tall). (B) Detail of sandbody shown in (A). Yellow lines show large-scale accretion surfaces (yellow arrow shows their main dip direction); white lines highlight set-climbers cross-strata (white arrow shows their dip direction). Pencil for scale is 15 cm long. (C) Bundled cross-strata. Hammer is 32.5 cm long.....44

Figure 1.12: (A) Subtidal bar deposits *ca* 5 m thick (red arrows mark their basal and top surfaces). Note the internal accretion surfaces in the lower bar deposits (yellow lines). (B) River signals: Poor sorting; coaly fragments. (C) Double organic drapes. Hammer head for scale is 17.5 cm.48

Figure 1.13: Bar in the subaqueous platform. (A) Photograph and line drawing of a 5 m thick bar cut into coaly shales. The bar (yellow) is clinostratified and at the top is slightly incised by soft-sediment deformed sandstones (orange). (B) Marine bioturbation on a bed plane. (C) Compound internal architecture of the bar. In red master bedding, in yellow foresets and superimposed cross-strata. Hammer for scale is 32.5 cm long. .49

Figure 1.14: Fine-grained amalgamated sandstones with hummocky cross-stratification (HCS).....50

Figure 1.15: Photographic panel of Facies Association 4.1 deposits cropping out in Section 1. Facies Association 4.1 has an erosional base marked by pebbles and shell fragments. The infill is characterized by stacked cross-strata bounded by low-angle inclined master surfaces. The thickness of the smaller cross-stratal sets decreases upward. Hammer for scale is 32.5 cm long (red circle).....57

Figure 1.16: Fence diagram of Facies Association 4.1 deposits cropping out in Section 1. The base is erosional, overlain by normally graded pebbly sandstone with shell fragments. The overlying deposits are cross-stratified, but the size of the cross-strata decreases upward. The upper compound body (red colour) is coarser grained and more poorly sorted than the sediments underneath, probably indicating an interval of high-energy currents.....57

Figure 1.17: Photographic panel and line drawing of Facies Association 4.2 (marked by yellow lines in the photopanel). Unit 1 (brown colour) is composed of poorly sorted cross-strata. Unit 2 (grey colour) is a clinostratified unit. In the middle part (Unit 3, grey and yellow colours) large-scale 3D cross-strata and channels are present but, in places, the structures are destroyed by liquefaction (yellow colour). At the top, Unit 4 (dark grey colour) erodes the previous deposits and it is marked at the base by shell and wood fragments.....62

Figure 1.18: (A) Two-dimensional compound cross-strata, 50 cm to 1 m thick. Hammer for scale is 32.5 cm long. (B) Rhythmic lamination in the bottomsets of large-scale cross-strata, where the organic fragments are concentrated and are associated with bioturbation. (C) Accumulation of Eunerineidae gastropods preserved in an early-cemented horizon. The pencil is 15 cm long. (D) Sigmoidal cross-strata. The Jacob's staff is 140 cm long.....63

Figure 1.19: Correlation panel based on measured sections (S1 to S9). The outcrop belt is *ca* 7 km long and total stratigraphic thickness is *ca* 300 m. The overall succession is progradational (from deep-water deposits of the Los Molles Formation to upper coastal-plain deposits, Facies Association 1.1), but it is complicated by several regressive to transgressive cycles. The cross-section is slightly oblique to strike, with progradation from south-west (right) to north-east (left). A higher resolution version of this figure is available in Appendix A.68

Figure 1.20: Schematic logs illustrating the differences between a mixed-energy delta (based on the Lajas Formation) and classical river-dominated, wave-dominated and tide-dominated deltas (based on Willis, 2005; Bhattacharya, 2010; Charvin et al., 2010; Olariu et al., 2010). Different colours represent a process dominance: red river (R), yellow waves (W) and blue tides (T). Purple represents mixed tide and river processes, green represents mixed tide and wave processes, and brown represents a mix of all three processes. M = mud; vf = very fine sand; f = fine sand; m = medium sand; c = coarse sand; vc = very coarse sand; g = gravel.72

Figure 1.21: Photomosaic of Lohan Mahuida hillside (Section 1). Different colours refer to the correlation panel. The relative importance of the three processes [river (F), wave (W) and tidal (T) currents] throughout the succession (i.e. time changes) have been highlighted.....76

Figure 1.22: Palaeogeographic sketch map (not to scale) of the north-westerly Lajas deltaic system (regressive phase). This palaeogeography is based on the morphology of partially analogous modern examples in Taiwan, Kamchatka, Fraser River and Wax Lake Delta. (A) The palaeogeographic reconstruction shows a complex deltaic system. Moving from proximal to distal locations, fluvial-dominated, gravelly channels of the upper delta-plain pass downstream to sand-dominated, tide-influenced lower delta-plain channels. Distributary channels can be laterally adjacent to either the interdistributary bay areas (filled by organic-rich muds, marine influenced fine-grained deposits and small crevasse deltas), or to shoreface deposits. Further seaward a subaqueous platform is developed, passing into delta front and prodelta/shelf environments. This transition is accompanied by an increasing tidal and wave influence. The black line traced in the middle of the delta emphasizes that the two style of lower delta-plain channels (amalgamated or isolated in muddy sediments) can either co-exist or alternate through time. Colour-coded as Fig. 1.19. (B) Inset map showing details of the distributary channels, subaqueous platform bars and delta front in the case of a lower delta-plain dominated by bifurcating channels. (C) Inset map showing details of the distributary channels, subaqueous platform bars and delta front in the case of a lower delta-plain dominated by braided channels.....77

Figure 1.23: Plan view of panels (B) and (C) of Fig. 1.22. Different colours represent a process dominance: red river, yellow waves, and blue tides. Orange represents mixed wave and river processes, purple mixed tide and river processes, and green mixed tide and wave processes. The maps highlight the high lateral process variability in mixed-energy deltas. Different processes co-exist and interact at the same time in different areas of the delta system.....78

Figure 1.24: Speculative reconstruction of the Lajas palaeogeography. Two river systems or two main distributary reaches of the same system developed on the eastern and western side of a structural element (fold or fault; thick dashed red line). The eastern side underwent relative uplift and a thinner Lajas Formation succession was deposited here (Quattrocchio et al., 1996; Martínez et al., 2008), whereas the western side was located in an area of higher subsidence (based on missing biozones in the uplifted area and expanded stratigraphic section in the subsiding area; Martínez et al., 2008). Tidal currents reworked the deltaic deposits present to the west more efficiently (Lohan Mahuida area). Between the two main fluvial/deltaic fairways (yellow, orange, green and brown lines) a sheltered area with more wave influence was probably present (dashed blue line). Background image from Google Earth.....79

Figure 1.25: (A) Conceptual model of a compound clinoform, showing the subaerial delta and the subaqueous delta (modified from Swenson et al., 2005). (B) Plan view of the Mahakam delta, showing the subaqueous limit of the subtidal platform (redrawn after Roberts & Sydow, 2003).82

Figure 3.1: Process variability of mixed-energy deltas. (A) Simplified sketch of a deltaic system where river, wave and tidal processes are active at the same time. These processes can be active either in different parts of the delta system or in the same area, and they can vary through time. Process dominance is represented via a color-coded ternary diagram: yellow represents wave processes (W), red river processes (R) and blue tidal processes (T). In some areas more than one process can be active (i.e. purple represents co-existing tidal and river processes, green represents co-existing tidal and wave processes). This map is an example of the inherent complexity of mixed-energy systems. (B) Niger Delta; images from Google Earth. White rectangle in the inset shows the location within the delta of the image. (C) Copper River Delta; image from <http://earthobservatory.nasa.gov/>.97

Figure 3.2: Example of how to calculate compound percentages. According to Table 3.1, sigmoidal cross strata have $P_w=7\%$, $P_t=71\%$, $P_r=22\%$. However, the foresets of these cross-strata are draped by mud ($P_w=6\%$, $P_t=86\%$, $P_r=8\%$). Therefore the total percentages that take into account both characteristics are: $P_w=6\%$, $P_t=79\%$, $P_r=15\%$. This bed is located at 7 m from the bottom of the parasequence. Photo courtesy of Keith Adamson.101

Figure 3.3: Location of the sedimentary logs published in the literature used to calculate the proportions of facies and processes in different environments and sub-environments.103

Figure 3.4: Sedimentological log of the described deltaic parasequence (A) and vertical (i.e. temporal) process changes (B). (A) shows the “classical” sedimentological log measured through the parasequence, whereas the probability graph shows the occurrence of river, wave and tidal processes through time. Yellow represents wave processes (W), red fluvial processes (R) and blue tidal processes (T). The lower part of the parasequence shows high probability of being the result of wave action. The middle part of the parasequence shows a complex mixture of wave, river and tidal processes. The upper part of the parasequence shows similar probabilities of being the result of fluvial and tidal currents. 105

Figure 3.5: Relation between sedimentary structures and hydrodynamic processes (river, wave, tide); n represents the total number of facies units (stratal units characterized by the same structure) counted to calculate the percentages.....107

Figure 3.6: Sedimentary structures and processes in deltaic environment; n represents the total number of facies units counted to calculate the percentages.108

Figure 3.7: Sedimentary structures and processes in shelf bars and ridges; n represents the total number of facies units counted to calculate the percentages.109

Figure 3.8: Relations between sedimentary structures and different environments; n represents the total number of facies units counted to calculate the percentages.....110

Figure 4.1: Topographic surfaces collected at 7.2 yr (final run time), showing shoreline morphologies and distributary channel networks for deltas simulated under different tidal amplitudes (A) and sand:mud ratios.119

Figure 4.2: Relationship between dimensionless tidal amplitude and channel depth (A^* and H^*). Modern deltas are labeled with their names; bars show range of variability.....121

Figure 4.3: (A-D) Stratigraphic cross sections for model runs with a substrate sand:mud ratio of 50:50. (E-H) Plan-view images of the deltas. Dashed lines show the locations of the cross sections in A-D. A - tidal amplitude.123

Figure 4.4: (A) Normalized delta-front slopes for the model runs with a substrate sand:mud ratio of 50:50. (B) Slopes for the model runs with a substrate sand:mud ratio of 25:75 and 100:0 for tidal amplitude $A=0$ and $A=1.5$ m, and two tide-influenced and tide-dominated modern deltas (Cummings et al., 2016).....125

Figure 4.5: Suspended and bedload sediment (sed) fluxes, sea level, and flow velocity versus normalized time at four locations from upstream (1) to downstream (4) (Fig. C.3) along the main distributary channel in the model runs with a substrate sand:mud ratio of 50:50. (A) Tidal amplitude $A=1.5$ m. (B) $A=0$ m.....126

Figure 4.6: Percentages of sand and mud calculated radially from the delta apex to the shoreline and from the shoreline to the prodelta (Fig. C.4). The shoreline position is marked by a dashed line. A - tidal amplitude.127

Figure 5.1: (A) Regional-scale structural sketch of the Calabro-Peloritani Arc, showing the main Plio-Pleistocene shear zones responsible for the south-eastward tectonic migration towards the Ionian Basin (modified from Tansi et al., 2007). (B) Paleogeographic reconstruction of the Siderno Strait during the Pleistocene, with the studied sector indicated in the rectangle. Note the occurrence of other adjacent tidal straits. (C) Simplified geological map of the central-eastern sector of the Siderno Basin, showing the main tidal sand bodies and the area documented in this work (modified from Cavazza et al., 1997).136

Figure 5.2: Detailed facies map of the studied area (see location in Fig. 5.1C). The present-day exposures of the lower-middle Pleistocene succession form elongate bodies. Cross-section A-A' is in Fig. 5.9.139

Figure 5.3: Main stratigraphic logs measured across the studied succession.140

Figure 5.4: (A) Shelf mudstones and marlstones belonging to *FA1*. Arrows indicate the sharp contact with the overlying *FA3* tidal sandstones. (B) Detail of the surface separating *FA1* from the overlying *FA2-FA3* tidal cross-stratified sandstones.143

Figure 5.5: Overview of *FA2* deposits. (A) Typical erosional surfaces of *facies 2a*; note how *facies 2b* is eroded by *facies 2a*. (B) Undulate erosional surfaces. (C) Tidal foreset lamination within *facies 2b* erosionally overlain by the deposits of *facies 2a*. (D) Soft sediment deformation in *facies 2a*.145

Figure 5.6: Outcrop photographs of *FA3*. (A) Piano Fossati section showing large-scale cross-stratification with abundant three-dimensional cross-strata. (B) Line-drawing of the photograph in A. Note cross-cutting sets and the dominant foreset dip towards the left (E-SE). (C) Piano Crasto section, which lies down-current from the section shown in A and B (see Fig. 5.2), shows, instead, dominant two-dimensional cross-strata with unimodal foreset direction. (D) Details of the photo in panel C, showing internal features of the tidal cross strata. (E) Cliff exposure in Mt della Torre, showing alternation of *FA2* and *FA3* deposits, with *FA3* deposits becoming more abundant towards the top. (F) Detail of the cliff in (E), showing the interfingering between *FA2* and *FA3*. 149

Figure 5.7: Outcrops of *FA4*. (A) Vertical transition at the Monte della Torre section between *FA3* and *FA4* (dotted line). (B) Detail of cross-stratified biocalcarenites of *facies 4a*. (C) Carbonate mounds of *facies 4b*, organized in a lateral compensation pattern. (D) Close-up view from the previous photograph. (E) Conglomerates and sandstones of *facies 4c* at Piano Fossati. (F) Detail from the previous photograph..... 153

Figure 5.8: Deposits belonging to *FA5*. (A) Cross-laminated foreshore sandstones (*facies 5a*) overlain by lagoonal fine-grained, bioclastic sandstones (*facies 5b*). (B) Alternation of mudstones and bioclastic sandstones interpreted as lagoonal deposits (rectangle indicates the detail in panel C). (C) Bioclastic-rich interval encased in muddy sediments (*facies 5b*). For location, see rectangle in (B). (D) Laminated, fine-grained sandstones interpreted as aeolian deposits overlying *facies 5b* (Jacob staff for scale is 1.1 m tall)..... 154

Figure 5.9: (A) Cross-section reconstructed along the trace A'-A indicated in Fig. 5.2.

(B) Conceptual depositional model showing the relationships between river-dominated deltaic deposits and tidal cross-strata interpreted in the present work.....159

Figure 5.10: Palaeogeographic reconstructions showing the evolution of the northern margin of the Siderno Strait (inset), and the associated tide-dominated passageway during the early-middle Pleistocene. (A) At the end of the early Gelasian transgression, non-tidal open-shelf mudstones filled an inherited topography incised into older deposits during a previous stage of relative sea-level fall. (B) A subsequent phase of regional-scale tectonic activity in this part of the Calabro-Peloritani Arc was probably the cause of the onset of tide-modulated current exchange between the Tyrrhenian and the Ionian seas in the Siderno Strait (as well as in the adjacent Catanzaro and Messina straits; see reconstruction in Fig. 5.1C). Block-faulting of this part of the Siderno Strait margin caused the uplift of the Piano Fossati high, creating a 3.5-km-wide passageway that became dominated by strong tidal currents with a dominant SE-directed flow. Deltas prograded into this narrow corridor from the Serre Massif, but due to the presence of strong tidal currents, the delta front deposits became skewed. (C) The continued transgression caused the delta to back-step, and deposition became dominated by bioclastic tidal dunes and in-situ carbonate factories. (D) Highstand sedimentation caused coastal progradation and, possibly, the closure of this sector of the Siderno Strait margin.....162

Figure A.1: Correlation panel of the Lajas Formation at Lohan Mahuida. The cross-section is slightly oblique to strike, but overall the progradation is from the south-west to north-east. Stratigraphic surfaces are color-coded as follows: red represents sequence boundaries, blue represents flooding surfaces, green represents maximum flooding surfaces. Solid lines represent 3rd order surfaces, dashed lines represents 4th order and 5th order surfaces.170

Table C.1: Complete list of the 24 runs used in this study.186

Figure C.1: Location of the two deepest channels (white rectangles) used to calculate H* (see Table C.2). The shoreline position is marked by the black line.188

Figure C.2: Final shoreline rugosity for all model runs.188

Figure C.3: Position of the four locations along the main distributary channel in which the width-averaged parameters shown in Fig. 4.5 (base level, flow velocity, suspended sediment flux, bedload sediment flux) have been calculated. (A) Locations in the 50:50 run with $A=1.5$ m. (B) Locations in the 50:50 run with $A=0$ m.189

Figure C.4: Position of the transects along which the percentages of sand and mud in the deltaic deposits (Fig. 4.6) have been calculated. (A) Position of the transects in the 50:50 run with $A=0$. (B) Position of the transects in the 50:50 run with $A=1.5$ m. The subaerial delta transects include deposits from the delta apex to the shoreline. The subaqueous delta transects include deposits from the shoreline to the prodelta.190

Chapter 1: Introduction

PROBLEMS AND SIGNIFICANCE

Tides, and more specifically tidal currents, are an important agent of erosion, sand transport and deposition in many shallow marine environments, and therefore there are both commercial and scientific reasons to improve our knowledge of tide-influenced processes, environments and depositional successions. Since the 1950's our knowledge of tidal processes and tidal deposits has evolved, passing from a focus on intertidal environments and estuaries (Boersma and Terwindt, 1981; Clifton, 1982; De Boer, 1998) to a more comprehensive analysis of tidal processes (e.g., Dalrymple and Choi, 2007; Dalrymple, 2010; Longhitano et al., 2012b; Plink-Björklund, 2012).

The first works on tidal deposits started mainly in Europe (The Netherlands, England and France), although important work was conducted in the Bay of Fundy as well (Davis Jr and Dalrymple, 2011). These studies however were mainly focusing on tidal flat environments, on the different elements and sub-environments present within tidal flats, and on sediment composition (Klein, 1963; Klein and Sanders, 1964; de Jong, 1977). Great emphasis was also given to the use of tidal flat deposits to calculate paleotidal ranges (Klein, 1971). One of the first works that tried to establish new criteria for the recognition of tidal influence was the work on tidal bundles by Visser (1980), allowing more precise and definitive recognition of tidal deposits in the rock record. Since then, focus on tidal deposits shifted from the intertidal flats to subtidal cross-stratified sandbodies (e.g., Allen, 1981; Allen and Homewood, 1984; Dalrymple, 1984; De Mowbray and Visser, 1984).

In the last decades, tidal processes and tide-influenced environments have received renewed attention. For example, recent studies of the detailed characteristics of subtidal sandbodies provided new refined criteria to recognize tidal dunes and to distinguish them from tidal bars (despite similar dimensions) in the rock record (e.g., Olariu et al., 2012a; Olariu et al., 2012b). Several studies focused on the role that falling or rising sea level has on tidal processes (as detected in transgressive vs. regressive deposits), showing that tidal signals can be strengthened and better preserved in transgressive as well as lowstand system tracts (Cattaneo and Steel, 2003; Guzman and Fisher, 2006; Steel et al., 2012; Chen et al., 2014). Other studies focused on new models for estuaries, on the occurrence of tidal facies in relation to the infilling of previously incised valleys, both on the inner shelf as well as at the shelf edge (e.g., Dalrymple et al., 1992; Cummings et al., 2006). In contrast, tidal deposits developed on the open shelf have been significantly understudied, but recent new research provided the first detailed overview of shelf bars and ridges (e.g., Reynaud and Dalrymple, 2012) and the first detailed recognition of these deposits in the rock record (Schwarz, 2012; Leva López et al., 2016). Finally, several studies focused on the characteristics of tidal deposits in different environments (e.g., estuaries, open coast tidal flats, shorefaces) in relation to the tidal range and tidal current speed, showing that even microtidal systems, when topographically constricted, can produce tide-dominated deposits (Yang et al., 2005; Dashtgard et al., 2009; Dashtgard et al., 2012; Longhitano et al., 2012b).

Recently, many works have started to focus on the influence that all three processes (river, waves, and tides), sometimes in an intricate manner, can exert on sedimentary successions (e.g., Ainsworth et al., 2011; Vakarelov et al., 2012; Ainsworth et al., 2015). Modern coastal depositional systems show a very high degree of lateral variability, as coastal processes (river, wave, and tidal currents) can rapidly change in

space (e.g., Ainsworth et al., 2011; Olariu, 2014). In the rock record, shallow-marine sedimentary successions bear the signature not only of spatially changing, along-strike environments, but also of cross-shelf time changes in the dominant coastal processes (Yoshida et al., 2007). These changes can be related to autogenic or allogenic factors (Yoshida et al., 2007; Olariu, 2014). The complexity of coastal environments present in the Holocene is arguably present also in ancient depositional systems, and therefore it can impact the distribution and characteristics of petroleum reservoirs. Additionally, tectonic activity can play a key role in controlling depositional environments, as it affects relative sea-level, coastline morphology and sediment yield. In particular, tectonically-confined basins represent interesting case studies, as their structural configuration causes some processes to be dampened (e.g., waves), and others to be amplified (e.g., tidal currents). The hydrodynamic conditions developed in these basins are therefore very complex, and strongly affect sediment dispersal routes and deposition (Anastas et al., 1997; Frey and Dashtgard, 2011; Longhitano et al., 2012a; Longhitano and Steel, 2016).

Recently, numerical modeling has also proved to be a useful tool to study the influence of different processes on coastal environments (van Maren et al., 2004; Dastgheib et al., 2008; Hillen, 2009; Edmonds et al., 2010; Geleynse et al., 2011; Hillen et al., 2014).

OBJECTIVES

The objectives of the research in this dissertation are:

1. and to provide more quantitative evaluation of the stratigraphic signatures of mixed-energy deltas in the rock record. In particular, this research focused on a study of the Jurassic Lajas Delta system, in the Neuquén Basin (Argentina), and showed how tidal currents had a major reworking impact on transgressed river mouth bars whose tops became broad

subaqueous delta platforms, in areas that were more rapidly subsiding than adjacent areas.

2. To develop a more detailed and quantitative methodology for outcrop facies sedimentology, leading to recognition and disentangling the relative importance of wave, tidal and river processes in the rock record.
3. To investigate the influence of tidal currents compared to fluvial processes on deltaic depositional systems, and in particular to examine the sensitivity of distributary channels to tides. This research focused on the analysis of numerical simulations (Delft3D), which modeled river deltas affected by different tidal amplitudes.
4. To characterize the architecture and depositional processes of tide-influenced straits (tectonically-confined basins). In particular, focus was on the marginal zones of tidal straits, where river-fed deltas interact with tidal currents flowing axially within the strait.

OVERVIEW OF CHAPTERS

Chapter 2: The role of tidal, wave and river currents in the evolution of mixed-energy deltas: Example from the Lajas Formation (Argentina)

Chapter Two presents the analysis and interpretation of field data from the Jurassic Lajas Formation (Neuquén Basin, Argentina) and the results of this work have been published in *Sedimentology* (Rossi and Steel, 2016). This research was part of the Lajas Project (funded by Statoil, Woodside, VNG Norge and BHP Billiton), in collaboration with the University of Manchester, Queen's University and the Universidad Nacional de La Plata.

The lower Lajas Formation is interpreted as a sand-rich, mixed-energy deltaic system. It is characterized by an overall regressive trend but punctuated by several

regressive-transgressive cycles, showing a marked process variability both laterally and vertically. In general, wave influence increased in the distal and lateral reaches of the deltaic system; river influence increased toward the most proximal areas; tidal influence was strongest on the delta front and subaqueous delta platform areas, with enhancement of tidal reworking across the subaqueous platform during slight transgressive water deepening, possibly caused by subsidence that was greater than in adjacent, less tidally affected areas. Strong tidal currents were responsible for the reworking of delta-front sediments, producing amalgamated, sand-rich tidal bars and dunes.

Chapter 3: Quantifying process regime in ancient shallow marine mixed-energy depositional systems: what are sedimentary structures really telling us?

Chapter Three presents a new methodology that aims at quantifying process variability in sedimentary successions. This research has been submitted to the *Journal of Sedimentary Research*.

This research is based on an extensive literature review of the most common sedimentary structures. Each structure is assigned a probability of having been the result of wave, tide or river currents, and the vertical integration of process probabilities of individual beds in a rock succession creates probability graphs. This methodology can be efficiently coupled to classical facies analysis, and it can be a useful tool to quantify in more detail process variability in ancient systems.

Chapter 4: Impact of tidal currents on delta-channel deepening, stratigraphic architecture and sediment bypass beyond the shoreline

Chapter Four presents the analysis of a series of numerical simulations conducted in collaboration with Lamar University, Indiana University, and the Department of Civil, Architectural and Environmental Engineering at the University of Texas at Austin. This research has been published in *Geology* (Rossi et al., 2016).

Delft3D generated numerical simulation of deltas that has been used to investigate the effects of tides on deltaic morphology and stratigraphy. The key results of this work show that an increase in tidal amplitude causes more rugose planform shoreline patterns and the development of deeper and more stable distributary channels. These channels act as efficient conduits for ebb-enhanced currents to bypass sediment across the delta plain and to extend the channels basinward, across the subaqueous delta platform. The delta-front profile is also affected by increasing tidal influence, as it changes from concave to convex, with the development of a compound geometry for higher tidal amplitudes.

Chapter 5: Tidal and Fluvial Processes Interplay in an Early Pleistocene, Delta-Fed, Strait Margin (Calabria, southern Italy)

Chapter Five presents the results of a field-based study of the northern margin of the Siderno paleostrait (southern Italy). This research has been submitted for publication to *Marine and Petroleum Geology*.

In this study, syndepositional tectonic activity produced a complex coastal morphology, with the development of a *ca.* 3.5 km-wide local, marine passageway. This configuration caused strong interaction between fluvially-derived deltaic sediments and tidal currents (flowing roughly parallel to the strait margin). Tidal currents strongly reworked the distal deltaic deposits into dune fields that were oriented at a high angle with respect to the deltaic progradation direction.

REFERENCES

- Ainsworth, R. B., Vakarelov, B. K., Lee, C., MacEachern, J. A., Montgomery, A. E., Ricci, L. P., and Dashtgard, S. E., 2015, Architecture and Evolution of A Regressive, Tide-Influenced Marginal Marine Succession, Drumheller, Alberta, Canada: *Journal of Sedimentary Research*, v. 85, no. 6, p. 596-625.
- Ainsworth, R. B., Vakarelov, B. K., and Nanson, R. A., 2011, Dynamic spatial and temporal prediction of changes in depositional processes on clastic shorelines: toward improved subsurface uncertainty reduction and management: *AAPG bulletin*, v. 95, no. 2, p. 267-297.
- Allen, J. R. L., 1981, Lower Cretaceous tides revealed by cross-bedding with mud drapes: *Nature*, v. 289, no. 5798, p. 579-581.
- Allen, P. A., and Homewood, P., 1984, Evolution and mechanics of a Miocene tidal sandwave: *Sedimentology*, v. 31, no. 1, p. 63-81.
- Anastas, A. S., Dalrymple, R. W., James, N. P., and Nelson, C. S., 1997, Cross-stratified calcarenites from New Zealand: subaqueous dunes in a cool-water, Oligo-Miocene seaway: *Sedimentology*, v. 44, no. 5, p. 869-891.
- Boersma, J. R., and Terwindt, J. H. J., 1981, Neap-spring tide sequences of intertidal shoal deposits in a mesotidal estuary: *Sedimentology*, v. 28, no. 2, p. 151-170.
- Cattaneo, A., and Steel, R. J., 2003, Transgressive deposits: a review of their variability: *Earth-Science Reviews*, v. 62, no. 3-4, p. 187-228.
- Chen, S., Steel, R. J., Dixon, J. F., and Osman, A., 2014, Facies and architecture of a tide-dominated segment of the Late Pliocene Orinoco Delta (Morne L'Enfer Formation) SW Trinidad: *Marine and Petroleum Geology*, v. 57, no. 0, p. 208-232.
- Clifton, H. E., 1982, Estuarine deposits, *in* Scholle, P. A., and Spearing, D., eds., *Sandstone Depositional Environments*: Tulsa, OK, American Association of Petroleum Geologists, p. 179-189.
- Cummings, D. I., Arnott, R. W. C., and Hart, B. S., 2006, Tidal signatures in a shelf-margin delta: *Geology*, v. 34, no. 4, p. 249-252.
- Dalrymple, B. W., 2010, Tidal depositional systems, *in* James, N. P., and Dalrymple, B. W., eds., *Facies models*, Volume 4, Geological Association of Canada, p. 201-231.
- Dalrymple, R. W., 1984, Morphology and internal structure of sandwaves in the Bay of Fundy: *Sedimentology*, v. 31, no. 3, p. 365-382.
- Dalrymple, R. W., Zaitlin, B. A., and Boyd, R., 1992, Estuarine facies models: conceptual basis and stratigraphic implications: perspective: *Journal of Sedimentary Research*, v. 62, no. 6.
- Dalrymple, R. W., and Choi, K., 2007, Morphologic and facies trends through the fluvial-marine transition in tide-dominated depositional systems: A schematic framework for environmental and sequence-stratigraphic interpretation: *Earth-Science Reviews*, v. 81, no. 3-4, p. 135-174.
- Dashtgard, S. E., Gingras, M. K., and MacEachern, J. A., 2009, Tidally Modulated Shorefaces: *Journal of Sedimentary Research*, v. 79, no. 11, p. 793-807.

- Dashtgard, S. E., MacEachern, J. A., Frey, S. E., and Gingras, M. K., 2012, Tidal effects on the shoreface: Towards a conceptual framework: *Sedimentary Geology*, v. 279, no. 0, p. 42-61.
- Dastgheib, A., Roelvink, J. A., and Wang, Z. B., 2008, Long-term process-based morphological modeling of the Marsdiep Tidal Basin: *Marine Geology*, v. 256, no. 1-4, p. 90-100.
- Davis Jr, R. A., and Dalrymple, R. W., 2011, *Principles of tidal sedimentology*, Springer Science & Business Media.
- De Boer, P. L., 1998, Intertidal sediments: composition and structure, *in* Eisma, D., ed., *Intertidal Deposits. River Mouths, Tidal Flats, and Coastal Lagoons*: Boca Raton, CRC Press, p. 345-361.
- de Jong, J. D., 1977, Dutch tidal flats: *Sedimentary Geology*, v. 18, no. 1, p. 13-23.
- De Mowbray, T., and Visser, M. J., 1984, Reactivation surfaces in subtidal channel deposits, Oosterschelde, Southwest Netherlands: *Journal of Sedimentary Research*, v. 54, no. 3, p. 811-824.
- Edmonds, D., Slingerland, R., Best, J., Parsons, D., and Smith, N., 2010, Response of river-dominated delta channel networks to permanent changes in river discharge: *Geophysical Research Letters*, v. 37, no. 12, p. L12404.
- Frey, S. E., and Dashtgard, S. E., 2011, Sedimentology, ichnology and hydrodynamics of strait-margin, sand and gravel beaches and shorefaces: Juan de Fuca Strait, British Columbia, Canada: *Sedimentology*, v. 58, no. 6, p. 1326-1346.
- Geleynse, N., Storms, J. E. A., Walstra, D.-J. R., Jagers, H. R. A., Wang, Z. B., and Stive, M. J. F., 2011, Controls on river delta formation; insights from numerical modelling: *Earth and Planetary Science Letters*, v. 302, no. 1-2, p. 217-226.
- Guzman, J. I., and Fisher, W. L., 2006, Early and middle Miocene depositional history of the Maracaibo Basin, western Venezuela: *AAPG bulletin*, v. 90, no. 4, p. 625-655.
- Hillen, M. M., 2009, Wave reworking of a delta: process-based modelling of sediment reworking under wave conditions in the deltaic environment [Master thesis: TU Delft].
- Hillen, M. M., Geleynse, N., Storms, J. E. A., Walstra, D. J. R., and Groenenberg, R. M., 2014, Morphodynamic modelling of wave reworking of an alluvial delta and application of results in the standard reservoir modelling workflow, *in* Martinus, A. W., Ravnås, R., Howell, J. A., Steel, R. J., and Wonham, J. P., eds., *From Depositional Systems to Sedimentary Successions on the Norwegian Continental Margin (Special Publication 46 of the IAS)*, Volume 46, International Association of Sedimentologists, p. 167-186.
- Klein, G. D., 1963, Bay of Fundy intertidal zone sediments: *Journal of Sedimentary Research*, v. 33, no. 4.
- Klein, G. D., 1971, A Sedimentary Model for Determining Paleotidal Range: *Geological Society of America Bulletin*, v. 82, no. 9, p. 2585-2592.
- Klein, G. D., and Sanders, J. E., 1964, Comparison of sediments from Bay of Fundy and Dutch Wadden Sea tidal flats: *Journal of Sedimentary Research*, v. 34, no. 1.

- Leva López, J., Rossi, V. M., Olariu, C., and Steel, R. J., 2016, Architecture and recognition criteria of ancient shelf ridges; an example from Campanian Almond Formation in Hanna Basin, USA: *Sedimentology*.
- Longhitano, S. G., Chiarella, D., Di Stefano, A., Messina, C., Sabato, L., and Tropeano, M., 2012a, Tidal signatures in Neogene to Quaternary mixed deposits of southern Italy straits and bays: *Sedimentary Geology*, v. 279, no. 0, p. 74-96.
- Longhitano, S. G., Mellere, D., Steel, R. J., and Ainsworth, R. B., 2012b, Tidal depositional systems in the rock record: A review and new insights: *Sedimentary Geology*, v. 279, no. 0, p. 2-22.
- Longhitano, S. G., and Steel, R. J., 2016, Deflection of the progradational axis and asymmetry in tidal seaway and strait deltas: insights from two outcrop case studies, *Paralic Reservoir*: London, Geological Society - Special Publication.
- Olariu, C., 2014, Autogenic process change in modern deltas: lessons for the ancient, *in* Martinius, A. W., Ravnås, R., Howell, J. A., Steel, R. J., and Wonham, J. P., eds., *From Depositional Systems to Sedimentary Successions on the Norwegian Continental Margin* Volume 46, International Association of Sedimentologists, p. 149-166.
- Olariu, C., Steel, R. J., Dalrymple, R. W., and Gingras, M. K., 2012a, Tidal dunes versus tidal bars: The sedimentological and architectural characteristics of compound dunes in a tidal seaway, the lower Baronia Sandstone (Lower Eocene), Ager Basin, Spain: *Sedimentary Geology*, v. 279, p. 134-155.
- Olariu, M. I., Olariu, C., Steel, R. J., Dalrymple, R. W., and Martinius, A. W., 2012b, Anatomy of a laterally migrating tidal bar in front of a delta system: Esdolomada Member, Roda Formation, Tremp-Graus Basin, Spain: *Sedimentology*, v. 59, no. 2, p. 356-U332.
- Plink-Björklund, P., 2012, Effects of tides on deltaic deposition: Causes and responses: *Sedimentary Geology*, v. 279, no. 0, p. 107-133.
- Reynaud, J.-Y., and Dalrymple, R. W., 2012, Shallow-marine tidal deposits, *in* Davis Jr, R. A., and Dalrymple, B. W., eds., *Principles of Tidal Sedimentology*: New York, Springer, p. 335-370.
- Rossi, V. M., Kim, W., Leva López, J., Edmonds, D., Geleynse, N., Olariu, C., Steel, R. J., Hiatt, M., and Passalacqua, P., 2016, Impact of tidal currents on delta-channel deepening, stratigraphic architecture, and sediment bypass beyond the shoreline: *Geology*, v. 44, no. 11, p. 927-930.
- Rossi, V. M., and Steel, R. J., 2016, The role of tidal, wave and river currents in the evolution of mixed-energy deltas: Example from the Lajas Formation (Argentina): *Sedimentology*, v. 63, no. 4, p. 824-864.
- Schwarz, E., 2012, Sharp-based marine sandstone bodies in the Mulichinco Formation (Lower Cretaceous), Neuquén Basin, Argentina: remnants of transgressive offshore sand ridges: *Sedimentology*, p. no-no.
- Steel, R. J., Plink-Björklund, P., and Aschoff, J., 2012, Tidal Deposits of the Campanian Western Interior Seaway, Wyoming, Utah and Colorado, USA, *in* Davis Jr, R. A., and Dalrymple, R. W., eds., *Principles of Tidal Sedimentology*, Springer Netherlands, p. 437-471.

- Vakarelov, B. K., Ainsworth, R. B., and MacEachern, J. A., 2012, Recognition of wave-dominated, tide-influenced shoreline systems in the rock record: Variations from a microtidal shoreline model: *Sedimentary Geology*, v. 279, p. 23-41.
- van Maren, D. S., Hoekstra, P., and Hoitink, A. J. F., 2004, Tidal flow asymmetry in the diurnal regime: bed-load transport and morphologic changes around the Red River Delta: *Ocean Dynamics*, v. 54, no. 3-4, p. 424-434.
- Visser, M., 1980, Neap-spring cycles reflected in Holocene subtidal large-scale bedform deposits: a preliminary note: *Geology*, v. 8, no. 11, p. 543-546.
- Yang, B. C., Dalrymple, R. W., and Chun, S. S., 2005, Sedimentation on a wave-dominated, open-coast tidal flat, south-western Korea: summer tidal flat – winter shoreface: *Sedimentology*, v. 52, no. 2, p. 235-252.
- Yoshida, S., Steel, R. J., and Dalrymple, R. W., 2007, Changes in Depositional Processes—An Ingredient in a New Generation of Sequence-Stratigraphic Models: *Journal of Sedimentary Research*, v. 77, no. 6, p. 447-460.

Chapter 2: The role of tidal, wave and river currents in the evolution of mixed-energy deltas: Example from the Lajas Formation (Argentina)¹

ABSTRACT

Many modern deltas show complex morphologies and architectures related to the interplay of river, wave and tidal currents. However, methods for extracting the signature of the individual processes from the stratigraphic architecture are poorly developed. Through an analysis of facies, palaeocurrents and stratigraphic stacking patterns in the Jurassic Lajas Formation, this paper: (i) separates the signals of wave, tide and river currents; (ii) illustrates the result of strong tidal reworking in the distal reaches of deltaic systems; and (iii) discusses the implications of this reworking for the evolution of mixed-energy systems and their reservoir heterogeneities. The Lajas Formation, a sand-rich, shallow-marine, mixed-energy deltaic system in the Neuquén Basin of Argentina, previously defined as a tide-dominated system, presents an exceptional example of process variability at different scales. *Tidal signals* are predominantly located in the delta front, the subaqueous platform and the distributary channel deposits. Tidal currents vigorously reworked the delta front during transgressions, producing intensely cross-stratified, sheet-like, sandstone units. In the subaqueous platform, described for the first time in an ancient outcrop example, the tidal reworking was confined within subtidal channels. The intensive tidal reworking in the distal reaches of the regressive delta front could not have been predicted from knowledge of the coeval proximal reaches of the regressive delta front. The *wave signals* occur mainly in the shelf or shoreface deposits.

¹ This chapter has been published as: Rossi, V. M., and Steel, R. J., 2016, The role of tidal, wave and river currents in the evolution of mixed-energy deltas: Example from the Lajas Formation (Argentina): *Sedimentology*, v. 63, no. 4, p. 824-864. I was the primary author of this work.

The *fluvial signals* increase in abundance proximally but are always mixed with the other processes.

The Lajas system is an unusual clean-water (i.e. very little mud is present in the system), sand-rich deltaic system, very different from the majority of mud-rich, modern tide-influenced examples. The sand-rich character is a combination of source proximity, syndepositional tectonic activity and strong tidal-current reworking, which produced amalgamated sandstone bodies in the delta-front area, and a final stratigraphic record very different from the simple coarsening-upward trends of river-dominated and wave-dominated delta fronts.

INTRODUCTION

A deltaic system can typically be defined as a sedimentary body that progrades basinward into a standing body of water, built by fluvial processes in combination with a more or less pronounced reworking through waves and tides. Although it is common to classify deltas as fluvial-dominated, wave-dominated and tide-dominated, the analysis of many examples shows that the basic types can be considered merely as relatively unusual end-members of a continuum (Willis et al., 1999; Bhattacharya and Giosan, 2003; Dalrymple et al., 2003; Olariu and Bhattacharya, 2006; Olariu et al., 2010). Mixed-energy deltas should therefore be much more common in the stratigraphic record than currently recognized. The study of mixed-energy deltas usually involves very complex systems, where all three processes are active at the same time, but the strength and preservation potential of each individual process changes in space, even over short distances (few hundreds of metres), as well as in time (Ta et al., 2002a; Plink-Björklund, 2008; Ainsworth et al., 2011). Therefore, it becomes important to identify and separate the signals of the three main processes (rivers, waves and tides) through the stratigraphy, and to understand what controls their latero-vertical partitioning. Ainsworth et al. (2008,

2011) and Vakarelov and Ainsworth (2013) have emphasized the high degree of variability that can occur in modern deltas and other coastal systems but research has yet to form a clear methodology tested on ancient cases. An important point to make is that the classical ternary diagram for delta classification (e.g. Galloway, 1975; Vakarelov and Ainsworth, 2013) does not fully reflect or explain the great complexity and variability in mixed-energy deltaic systems.

Recognition of the controlling processes acting on a delta system is very important not only for a correct reservoir characterization, but also to better assess the regional palaeogeography (for example, fetch necessary for wave development; irregularity of coastline and connection to open ocean to allow propagation of the tidal wave). Few models have been proposed for mixed-energy deltas (e.g. Galloway, 1976; Ta et al., 2002a; Roberts and Sydow, 2003; Willis and Gabel, 2003; Plink-Björklund, 2012; Amir Hassan et al., 2013; Ichaso and Dalrymple, 2014). Sand-rich deltas are far less known because many of the modern examples are fine-grained and mud-rich systems (Ta et al., 2002a; Roberts & Sydow, 2003), and because they occur mostly in the Indo-Pacific zone, draining large, low gradient areas with a humid-tropical climate. Although many important deltaic hydrocarbon reservoirs are muddy and heterolithic, for example the Jurassic reservoirs of the Mid-Norwegian Continental shelf (Martinius et al., 2001, 2005; Ichaso & Dalrymple, 2014; Thrana et al., 2014), others are cleaner cross-bedded sandstones, evidently originated from cleaner water systems (Mellere & Steel, 1996; Pontén & Plink-Björklund, 2007, 2009; Tānavsū-Milkeviciene & Plink-Björklund, 2009).

The Jurassic Lajas Formation in the Neuquén Basin of Argentina is a delta and estuary complex that has been traditionally interpreted as tide-dominated (McIlroy et al., 2005; Spalletti et al., 2010). New results show that the Lajas Formation is an exceptional

example of a mixed-energy system with process variability at different scales (bed scale, parasequence scale and sequence scale) and it provides insight on what to expect in the rock record from a sand-rich mixed-energy deltaic system. The outcrop exposures of the Lajas Formation in the study area clearly show how a mixed-energy delta system differs significantly from classical river-dominated or wave-dominated deltas. The front of river-dominated deltas usually is characterized by parallel-laminated or structureless event beds, unidirectional (seaward directed) current ripples and only occasional cross-strata, with stressed trace fossil assemblages (e.g. Mutti et al., 2000; Olariu et al., 2010). The front of wave-dominated deltas usually contains clean sandstones dominated by hummocky cross-stratification (HCS), swaley cross-stratification (SCS) and wave and combined-flow ripple lamination, with abundant and diverse trace fossils (e.g. Bhattacharya & Giosan, 2003; Charvin et al., 2010). The front of tide-dominated deltas (Willis et al., 1999; Pontén & Plink-Björklund, 2009; Tānavsū-Milkeviciene & Plink-Björklund, 2009) is characterized by a stacking of well-ordered cross-strata (sometimes with prominent mud drapes and bi-directional palaeocurrents), as well as a high degree of internal tidal scour surfaces (often filled by heterolithic or muddy strata). Neap–Spring tidal bundling, rhythmic lamination and wavy/lenticular/flaser bedding with bi-directional ripples are also common (e.g. Bhattacharya & Willis, 2001; Pontén & Plink-Björklund, 2009). Intervals of stacked sets of cross-strata are often channelized, and fluid mud layers can also be present (e.g. Martinius et al., 2001; Dalrymple et al., 2003; Ichaso & Dalrymple, 2014). Trace fossils are less diverse than in wave-dominated settings, and can show clear evidence of stress (MacEachern et al., 2010).

The focus of the present paper is the Lajas Formation, cropping out on the hillside of Lohan Mahuida in the southern Neuquén Basin (Fig. 1.1). The objectives of this work are: (i) to show how to separate the signals of wave, tide and river currents in an ancient,

sand-rich mixed-energy system; (ii) to illustrate the result of strong tidal reworking in the distal reaches of deltaic systems; and (iii) to discuss the implications of this for the evolution of mixed-energy systems and for reservoir heterogeneities.

The hypothesis is that in a mixed-energy tide-influenced delta the main tidal signals will be found in the delta front, subaqueous platform and, to a lesser extent, in the distributary channels, because these are the zones where the tidal wave becomes more constricted and tidal-current speed is accelerated. Wave signals will be preserved mainly in the prodelta/shelf areas and/or occasionally in shorefaces developed laterally to the main fluvial and tidal inputs. Fluvial signals will be predominant in the lower and upper delta plain, assuming that the tidal wave does not penetrate great distances inland (Tänavsuu-Milkeviciene & Plink-Björklund, 2009). What makes the Lajas delta system more complex in the study area is that the distal reaches of the system became intensively reworked at times by tidal currents because of periodic transgression caused by syndepositional tectonic downwarping, possibly augmented by autogenic responses.

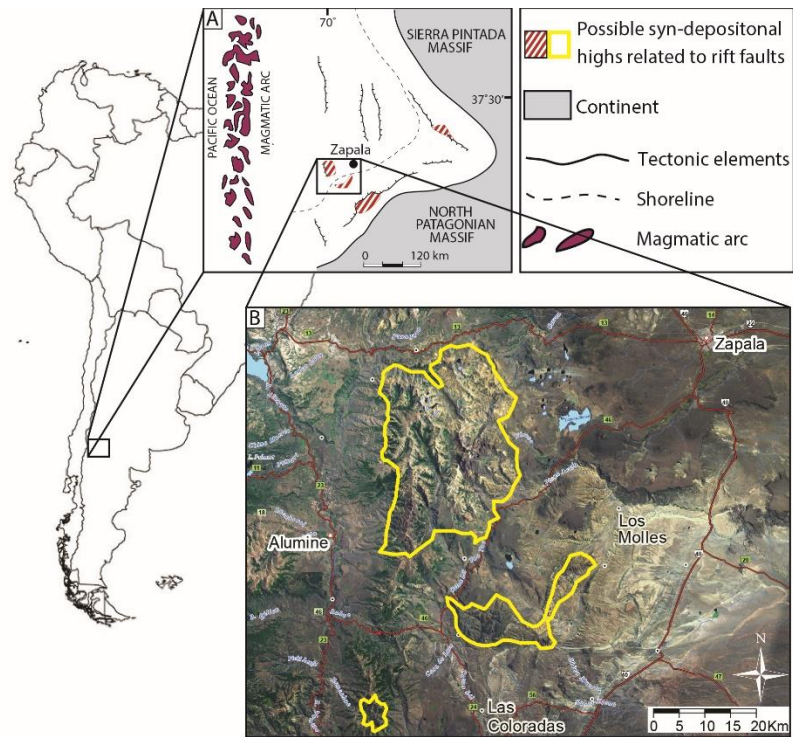


Figure 1.1: Location of the study area in the Neuquén Basin of Argentina; map of the Neuquén Basin (modified after Spalletti et al., 2000) during the post-rift back-arc phase. Possible highlands inherited from syn-rift topography are highlighted in dashed red and yellow.

GEOLOGICAL SETTING

The Neuquén Basin is located in west-central Argentina and in central Chile (Fig. 1.1), *ca* 33° to 40° south, just north of the Patagonian Massif, on the eastern side of the Andes (Franzese et al., 2006; Spalletti et al., 2010). The Neuquén Basin has been bounded for most of its history (Fig. 1.1A) by the cratonic areas of the Sierra Pintada Massif on the north-east margin, by the North Patagonian Massif to the south and by the Andean magmatic arc on the active western margin of the Gondwanan–South American Plate (Spalletti et al., 2010).

During the Early Triassic to earliest Jurassic, thermomechanical collapse of a Late Palaeozoic orogenic belt led to the development of isolated half grabens, dominated by continental volcanoclastic deposits passing upward into lacustrine and shallow-marine sediments (Vergani et al., 1995; Franzese et al., 2006). During the Early Jurassic the change from mechanical to thermal subsidence led to the formation of broader depocentres (for example, the Neuquén Basin), formed by the amalgamation of previous isolated troughs, and to widespread incursion of marine sedimentation (Vergani et al., 1995; Franzese et al., 2003). The development of the magmatic arc in this region and the formation of extensional back-arc basins began in the Early–Middle Jurassic and was completed by Late Jurassic time (Franzese et al., 2003). The detailed tectonics of the back-arc basin development in the Jurassic are still emerging, and it seems unlikely that this period is simply ‘postrift’ with homogeneous subsidence. Instead, localized highlands (Fig. 1.1A and B) related to re-activated syn-rift faults were probably present, as also suggested by thicknesses variations in Jurassic deposits across tectonic elements (Quattrocchio et al., 1996; Martínez et al., 2008). Since the Middle Cretaceous Andean compressional tectonics have induced tectonic inversion, caused uplift of a foreland thrust belt and led to the formation of a retro-arc foreland basin which, in turn, caused the closure of the connections between the previous back-arc basins and the Proto-Pacific Ocean (Franzese et al., 2003).

The Lajas Formation

The Bajocian–Bathonian Lajas Formation (Rosenfeld, 1978; Zavala, 1996; McIlroy et al., 1999; Martínez et al., 2002) was deposited during a back-arc phase of basin development and had a widespread development sub-parallel to the magmatic arc. However, most research has focused on a segment of the Lajas Formation developed within the Neuquén Embayment and drained mainly from the cratonic areas to the east

(McIlroy et al., 2005). The Lajas succession in this area varies from 800 to 180 m in thickness (McIlroy et al., 2005) and has been interpreted by previous workers (Brandsæter et al., 2005; McIlroy et al., 2005; Morgans-Bell & McIlroy, 2005; Spalletti et al., 2010) as a tide-dominated succession of tidal flat, tidal channel and deltaic deposits that were formed within the open-mouthed (Neuquén) embayment where tidal currents were prominent and wave action was minimal. The Lajas Formation overlies and interfingers with the muddy Los Molles Formation deep-water slope deposits and it is overlain by the fluvial deposits of the Challacó Formation, so that in most areas this prism of alluvial to deep marine deposits is infilling the back-arc basin. Available biostratigraphic data in the Neuquén Embayment constrains the period of Lajas deposition to some 4.5 Myr (Morgans-Bell & McIlroy, 2005). The Lajas Formation essentially represents the ‘shelf’ that bridged the fluvial to deep-water systems of the basin, with shelf-margin progradation mainly from the southern and eastern margins of the basin (Burgess et al., 2000; McIlroy et al., 2005; Morgans-Bell & McIlroy, 2005). Palynological studies in the Lajas Formation (Martínez et al., 2002) recognized a warm–cool–warm climatic fluctuation. There is evidence that the Lajas Formation in the present Lohan Mahuida study area was subject to greater subsidence (as suggested by greater thickness of the Lajas Formation and a more complete biozone record) compared to the adjacent areas around Los Molles to the east (Quattrocchio et al., 1996; Martínez et al., 2008).

METHODOLOGY

This study entails a facies, palaeocurrent and stratigraphic stacking-pattern analysis of the well-exposed Lower Lajas Formation along the mountainsides of Lohan Mahuida (Fig. 1.2), along the Picun Leufu River to the south-west of the town of Zapala (Neuquén Province). A 300 m thick succession of the Lower Lajas Formation was

examined. The outcrop cliffs extend for about 7 km and are NNE–SSW oriented (oblique to the NNW regional transport direction, but with a downdip component to the NNE). The spatial and vertical process variability through the succession has been analyzed through the use of a series of sedimentological sections along the 7 km long hillside, together with high-resolution digital photomosaics (Gigapan software©). The measured sections have been supplemented with photographs, field sketches, palaeocurrent data, analysis of sedimentary structures, grain size, sorting and bioturbation variability. Additionally, a less detailed sedimentological log has been measured *ca* 10 km to the west of the main outcrop belt, along the Picun Leufu River (Fig. 1.2).

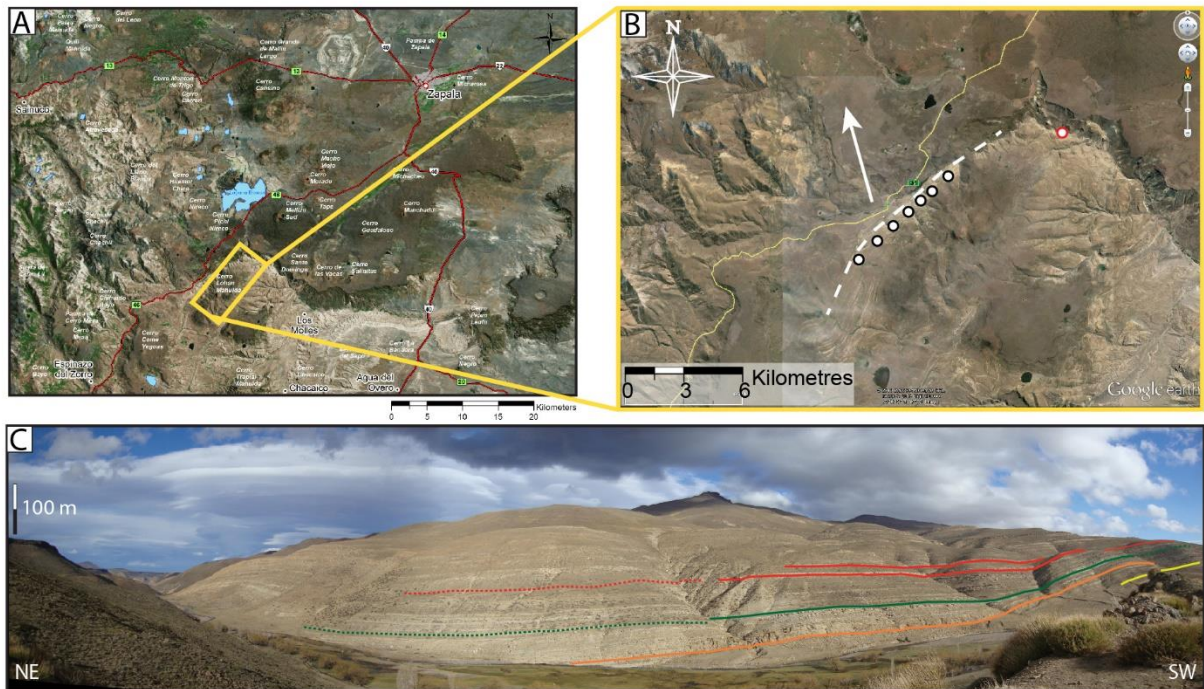


Figure 1.2: (A) Satellite image of the study area (Lohan Mahuida hill, yellow box). (B) Google Earth image of the study outcrop belt. Dashed white line represents the base of shelf deposits and the arrow shows the average progradation direction of the whole system (approximately north-west). Circles with black contour represent the location of measured sections. Circle with red contour represents the location of a less detailed log. (C) Photomosaic of Lohan Mahuida Hill; coloured lines match the colouring of different units in the correlation panel.

FACIES ASSOCIATIONS AND DEPOSITIONAL ENVIRONMENTS

Four major facies associations (FA) have been recognized. Within each of them, sub-associations will be described in more detail. Table 1.1 presents all of the facies used.

Table 1.1: List of facies present in the Lower Lajas Formation at Lohan Mahuida.

F	Processes	Lithology	Sedimentary structures	Texture	Bed/Set thickness [cm]	Organic matter	Bioturbation	Interpretation
1	F	Pebbly sst and conglomerates	Structureless, trough cross-bedding, inverse or normal grading	Poor sorting, sub-angular clasts	30 -100	-	Absent	Channel fill in the upper delta plain
2a	F	Coarse lag with pebbles, coal/wood fragments, mud rip-up clasts	Structureless (erosionally based)	Poor sorting	5 - 10	Wood and plant fragments	Absent	Coarse lag at the base of channels
2b	T/W	Shell lags (with possible pebbles and wood fragments)	Structureless, normal grading, or cross-strata	Poor to moderate sorting	5 - 20	yes	Absent to scarce	Discontinuous sheets of lag deposits lying above erosive ravinement surfaces or flooding surfaces; coarse lag at the base of channels
3	T/W	Silt/mud with thick articulated and broken shells (e.g., <i>Modiolus</i> , <i>Oysters</i> , <i>Trigonia</i> , <i>Alectryonia</i> , <i>Eunerineidae</i>)	Structureless	Poor sorting	30 - 60	-	High	<i>in situ</i> shell accumulations (interdistributary bays, lagoons, shelf)
4	T/W	Sst with shells, wood fragments, sparse granules	Structureless	Poor sorting	-	Yes (wood fragments)	Abundant (many mud-filled burrows)	Bioturbated surfaces overlying abandonment surfaces or high frequency ravinement surfaces
5a	F (T)	Fine-lower medium sst	Structureless, normal grading (load and flame structures)	Moderate to good sorting	10 - 50	-	Absent to scarce	Fluvial channel fill; proximal crevasse sub-delta; estuarine channel fill; mouth bars
5b	T (F)	Upper fine-lower medium sst	Structureless, mud rip-up clasts	Good sorting	150 - >300	-	Scarce to moderate	Estuarine channel fill

Table 1.1: Continued

F	Processes	Lithology	Sedimentary structures	Texture	Bed/Set thickness [cm]	Organic matter	Bioturbation	Interpretation
6	F	Lower medium-upper medium sst	Soft-sediment deformed cross-strata/ Soft-sediment deformation	Moderate to poor sorting; disorganized	30 - 200	Scarce/absent	Absent	Fluvial channel fill; river-dominated distributary channels and mouth bars
7a	F	Lower medium-coarse (up to pebbly) sst	Trough cross-strata	Poor to moderate sorting	10 - 50	As drapes (not cyclic)	Scarce	Upper and lower delta plain channel fill; base of estuarine incision
7b	F (minor T)	Upper fine-upper medium sst	Cross-strata	Moderate sorting	7 - 30	As drapes over cross-strata toesets (rarely cyclic)	Weak to moderate	Lower delta plain channel infill with minor tidal influence; proximal crevasse sub-delta; mouth bars
7c	T (F)	Lower medium to upper medium sst	Planar cross-strata (in places bi-directional)	Moderate to good sorting	10 - 80	As drapes on foresets	Moderate to abundant	Estuarine channel fill; distributary channels; tidally reworked delta front mouth bars; tidal bars and dunes on delta front and subaqueous platform
7d	T	Lower medium to upper medium sst	Sigmoidal cross-strata	Moderate to good sorting	20- 80	As drapes	Moderate	Delta front mouth bars; tidal bars and dunes on delta front and subaqueous platform; estuarine channel fill
7e	T	Lower medium to upper medium sst	Tidal bundles	Moderate to good sorting	10 - 30	As single or double drapes	Moderate to abundant	Estuarine channel fill; tidally influenced distributary channels; tidally reworked delta front mouth bars; tidal bars and dunes

Table 1.1: Continued

F	Processes	Lithology	Sedimentary structures	Texture	Bed/Set thickness [cm]	Organic matter	Bioturbation	Interpretation
7f	T	Lower fine to upper medium sst	Large trough and planar cross-strata	Moderate to good sorting	20-60 up to 100	Yes (cyclic drapes in toesets and bottomsets)	Moderate to abundant	Estuarine channel infill; tidally reworked delta front mouth bars; tidal bars and dunes
7g	T	Upper medium-lower coarse sst	Trough cross-strata	Poor to moderate sorting	7 -15	Plant debris	Abundant	Tidal inlet fill
8	T	Lower fine to upper medium sst	Compound bedforms	Moderate to good sorting	Compound bedforms <500; cross-strata 5-15	As drapes (especially in bottomsets and toesets)	Moderate to abundant	Estuarine channel fill; tidally reworked delta front mouth bars; tidal bars and dunes on delta front and subaqueous platform
9a	F/T	Lower fine to lower medium sst	Current ripples, climbing ripples	Moderate to good sorting	< 5	In places as drapes on ripple foresets	Absent to scarce	River-dominated to tide-influenced mouth bars; lower delta-plain channel infill
9b	T	Lower fine to lower medium sst	Bi-directional, set-climber ripples	Moderate to good sorting	< 5	As drapes on ripple foresets	Moderate	Tidally-reworked mouth bars; tidal bars & dunes on delta front and subaqueous platform; estuarine channel fill
9c	W	Lower fine to lower medium	Symmetrical ripples and combined flow ripples	Good sorting	< 5	-	Abundant	Wave-influenced to wave-dominated deposits
10a	F/T/ W	Heterolithic alternations of sandy siltstones and organic-rich mudstones/ coaly shales	Planar bedding, faint lamination, low-angle lamination, flaser and wavy bedding	Good to moderate sorting	0.5 - 5	Abundant to moderate	Absent to scarce	Lower delta plain interdistributary bays; distal crevasse subdelta; distal delta front; bottomsets of tidal bars and dunes; tidal flats; subaqueous platform

Table 1.1: Continued

F	Processes	Lithology	Sedimentary structures	Texture	Bed/Set thickness [cm]	Organic matter	Bioturbation	Interpretation
10b	F/T	Heterolithic alternations of fine sandstones and siltstones	Planar bedding, structureless beds to plane-parallel laminated	Good to moderate sorting	0.5 - 5	Scarce	Absent to moderate	Lower delta plain; subaqueous platform; tidal flats
10c	F/W/T	Muddy heterolithics (with silt, very fine sst)	Planar bedding, plane-parallel lamination, wavy, lenticular bedding	Moderate to poor sorting (partially due to mottling)	1 -2 (silty / sandy strata)	Some plant debris	High	Prodelta/offshore
11	T	Organic-rich siltstones and fine sst	Rhythmic lamination	Good sorting	few mm - 2 cm	Abundant	Moderate	Tidally reworked mouth bars; bottomsets of dunes and bars
12	W	Very fine-fine sst	SCS/HCS	Good sorting	20 - 150	Scarce/absent	Moderate to abundant	Shoreface; wave-reworked mouth bars; prodelta/offshore (HCS)
13	W/F/T	Siltstones-very fine-fine sst	Low-angle lamination	Good sorting	cm- dm scale	Scarce/absent	Abundant	Wave-influenced to wave-dominated deposits (; toesets of larger bedforms; crevasse splay subdelta (interdistributary bays); mouth bars
14	F/W/T	Very fine - lower medium sst	Parallel lamination	Good sorting	cm- dm scale	Scarce	Moderate	Wave-influenced to wave-dominated deposits; mouth bars; tidal flats
15	T/W	Very fine - lower medium sst	Flaser bedding	Moderate to good sorting	few cm	Moderate	Moderate	Mouth bars; tidal flats; interdistributary bays; bottomsets of larger bedforms; subaqueous platform

Facies Association 1 (Coastal Plain)

Facies Association 1 (FA 1) includes depositional elements of upper coastal plain and lower coastal plain, such as fluvial channels, distributary channels, interdistributary bays and crevasse deltas. Facies Association 1 is present mainly in the studied upper part of the Lajas Formation, but it is also found around 170 m above the base of the Lajas Formation. This facies association usually presents an unconformable lower boundary which can be traced at the scale of the outcrop belt. Facies associations 1.2 and 1.3 interfinger with deposits of FA 2 in the upper half of the studied Lajas Formation, whereas in the lower half FA 1.4 probably has an unconformable contact with FA 2 deposits.

Facies Association 1.1 (Upper Coastal Plain)

Facies Association 1.1 is characterized by channelized sharp-based sandbodies, organized in upward-fining packages up to 6 m thick (Fig. 1.3); they are mainly composed of pebbly sandstones (up to 5 cm sub-angular pebbles in an upper medium–lower medium sandstone matrix; F1) but, in a few places (for example, Section 2), clast-supported conglomerates with pebbles up to 5 cm in diameter are present (Fig. 1.3A and 4). In places, reverse grading in these deposits has been observed (Fig. 1.4). The main sedimentary structures are sets of trough cross-strata and soft-sediment deformation (F7a and F6). In the finer-grained intervals, cross-strata contain organic debris/mud drapes, which do not show any cyclic organization (F7a). Wood fragments and logs have been found in this unit. No large-scale internal accretion surfaces have been recognized.

Facies Association 1.1 presents a variety of clasts derived from metamorphic rocks and magmatic rocks, as well as mud rip-up clasts. This unit is highly erosional, and

cuts down into marine sediments, highly bioturbated and characterized by HCS (Fig. 1.3B).

Interpretation: Facies Association 1.1 is interpreted as channels in an upper coastal-plain environment, because it is composed of bodies lacking any prominent marine influence or reworking, whereas terrestrial influence predominates. The deposits are coarse-grained, ranging from pebbly sandstones to conglomerates with no or very limited bioturbation (Figs 1.3 and 1.4). The inverse-graded beds can represent high sediment-concentration river-flood events. As a comparison, in the modern Fraser River system the major grain-size change from wandering gravel-bed river (entirely in the freshwater non-tidal reach) to sand-bed channel occurs tens of kilometres upstream from the delta front (Dashtgard et al., 2012).

Facies Association 1.1 represents the coarsest deposits encountered in the examined portion of the Lajas Formation. Because of the sudden increase in grain size (up to pebbles) and a basinward shift in facies (from marine sediments to coarse-grained channels) it is proposed that the extensive erosional base (at the scale of the whole outcrop belt) of this unit is a sequence boundary.

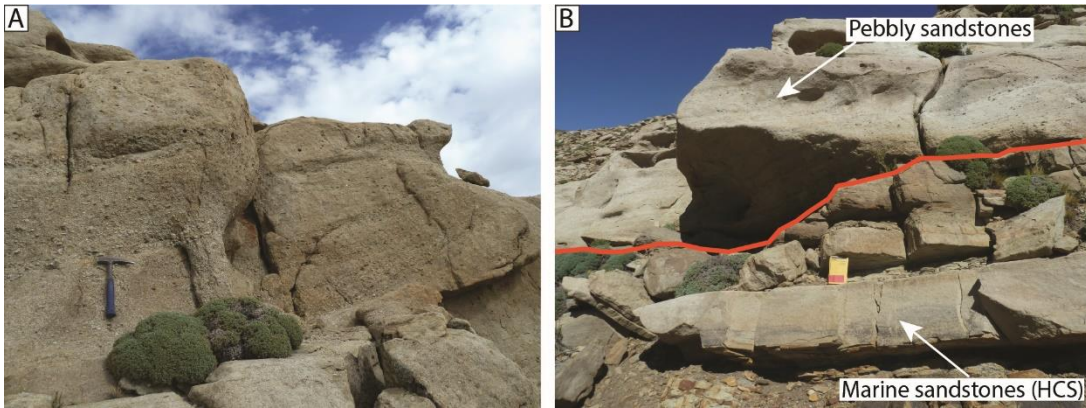


Figure 1.3: (A) Clast-supported conglomerates and pebbly sandstones infilling channelized features of Facies Association 1.1. Hammer for scale is 32.5 cm long. (B) Facies Association 1.1 channels composed of pebbly sandstones cutting into marine sediments (red surface, representing a Sequence Boundary). The field notebook is 19 cm long.



Figure 1.4: Clast-supported conglomerate showing inverse grading. Hammer for scale is 32.5 cm long.

Facies Association 1.2 (Lower Delta Plain)

Facies Association 1.2 is characterized by channelized, erosionally to sharp-based sandbodies, 1 to 4 m thick and few hundreds of metres wide (Fig. 1.5); these bodies incise into FA 1.3 deposits, in places associated with load and flame structures (F5a).

They are composed of lower and upper medium-grained sandstones moderately to poorly sorted with abundant soft-sediment deformation and mainly trough cross-stratification (Fig. 1.5; F5a, F6, F7a and F7b). Granules and pebble-size material together with abundant mud rip-up clasts, coal and wood fragments are very common. The stratigraphically lower channelized sandbodies can show weak to moderate bioturbation throughout the deposits [bioturbation index (BI) 1 to 2], with an impoverished trace fossil assemblage characterized by small vertical and horizontal burrows, the toesets of the cross-strata (in places bi-directional, F7c) are draped by organic fragments (although not always in an orderly manner, F7b), and compound cross-bedding is observed very infrequently. In places, ripple cross-lamination (F9a) can be the dominant sedimentary structure associated with very shallow channelized bodies or it represents the uppermost infill of thicker bodies (upward fining and reduction in cross-strata size). The stratigraphically higher channelized sandbodies are coarser grained, they have rip-up clasts, wood fragments and pebble-size material at the base of the incision (F2a), and they are characterized by decimetre to half-metre-scale trough cross-stratification and contorted bedding with scarce to absent draping along the foresets (F6 and F7a). Furthermore, there is no inclined accretion internal structure in these units. Palaeocurrent data are quite scattered (Fig. 1.5 and Figure A.1), but the predominant direction is towards the north-east.

Interpretation: Facies Association 1.2 is mainly characterized by shallow and relatively narrow channels that cut into non-marine to brackish fine-grained deposits (Fig. 1.5). This association has been interpreted as lower delta-plain distributary channels a few hundred metres wide, in which marine influence is gradually lost upward (i.e. towards more proximal environments). The limited to absent marine bioturbation and abundance of coal and wood fragments, as well as pebble-size material, indicate a strong

terrestrial influence. However, a trend has been observed within the distributary channels. The stratigraphically lower channels are characterized by more bioturbation and draped foresets than the stratigraphically higher ones which, in contrast, contain more pebble-sized material and wood fragments. The interpretation is that the stratigraphically lower channels were closer to the river mouth, and therefore more subject to marine (i.e. tidal) influence, especially during low river discharge periods (brackish water with tidal influence; see also Dalrymple & Choi, 2007). The stratigraphically higher channels were located in a more landward position, where there is no detectable influence of marine processes. Similar trends have also been observed in the Tilje Formation (Ichaso & Dalrymple, 2014). These channels represent a basinward shift of facies and they are likely to be associated with progradational pulses of the system, possibly suggestive of downcutting related to high-frequency relative base-level falls (see Appendix A).



Figure 1.5: Facies Association 1.2 channel with low-relief, incising into heterolithic dark mudstones. Load and flame structures are present in the lower part of the body. Rose diagrams show palaeocurrents.

Facies Association 1.3 (Lower Delta-Plain Interdistributary Bays)

Facies Association 1.3 is characterized by few metres thick weakly to non-bioturbated and faintly laminated to low-angle laminated sandy siltstones and organic rich black mudstones (Fig. 1.5; F10a, F10b and F13). In places flaser and wavy bedding is present in these fine-grained deposits (F10a and F15). Facies Association 1.2 usually cuts into this type of deposit. Facies Association 1.3 is also characterized by accumulations of shells (F3), composed of thick articulated and broken shells (including *Modiolus*, *Oysters*, *Trigonia* and *Alectryonia*). The shells are usually preserved in silty-muddy sediments with no physical structures and a high degree of bioturbation (BI 5 to 6). The main trace fossils are *Rhizocorallium*, *Paleophycus*, *Thalassinoides* and *Arenicolites*. Scattered coarsening-upward and thickening-upward bodies 50 cm to 1 m thick are present (Fig. 1.6). These bodies range from upper fine to lower medium sandstones, with planar cross-bedding or ghosts of trough cross-bedding, but they can also be structureless (F5a and F7b); they are usually moderately bioturbated.

Interpretation: Facies Association 1.3 is interpreted as interdistributary bays into which channels of FA 1.2 incise. The small-scale, coarsening-upward and thickening-upward fine to medium-grained sandstone bodies have been interpreted as crevasse splay deltas (Fig. 1.6). Crevasse splay deltas and more bioturbated shell-bearing sediments are interpreted as being deposited in interdistributary bays or lagoons. Some of these shell-bearing sediments are interpreted as *in situ* accumulations of shells, based on the fine-grained nature of the deposits, high bioturbation index, the fact that most of the shells are articulated and that they do not show any preferential orientation. *In situ* shell accumulations could also represent high-frequency flooding events. Facies Association 1.3 deposits are preferentially preserved in the upper part of the study succession,

possibly indicating a higher aggradation rate at the time of their deposition, as opposed to the lower part of the studied succession, characterized by more amalgamated sandbodies.

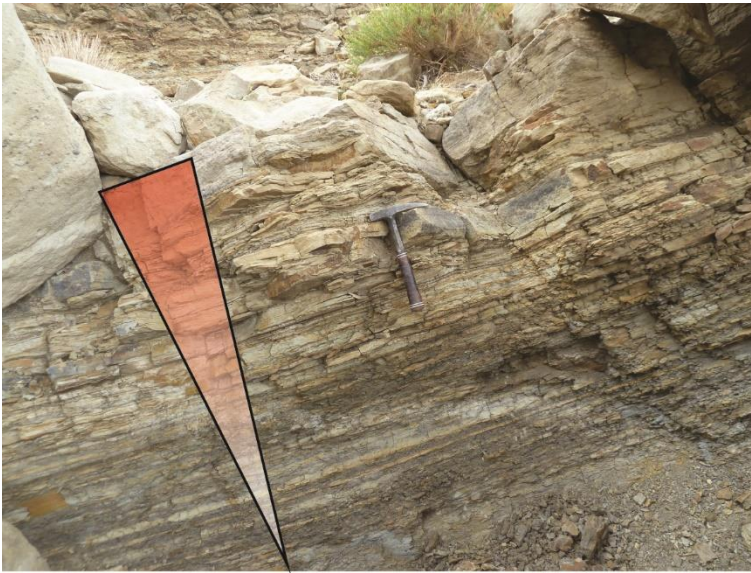


Figure 1.6: Coarsening-upward and thickening-upward sandbody, ranging from heterolithic muddy sediments up to upper fine–lower medium sandstones, characterized by moderate bioturbation. Hammer for scale is 32.5 cm long.

Facies Association 1.4 (Lower Delta Plain)

Facies Association 1.4 is characterized by 3 to 7 m thick amalgamated sandbodies (Fig. 1.7) that are relatively coarse-grained (occasionally pebbly) and have abundant plant fragments, as well as frequent erosional surfaces coated and highlighted by mud clasts and coarser grain sizes (Fig. 1.7B). These sandbodies usually are cross-stratified (F7a, F7b, F7c and F7e) and incise into sandy heterolithic deposits, which are plane-parallel laminated (F10b). Towards the northeast, this facies association contains frequent internal erosional surfaces marked by pebbles, whereas towards the south-west the amount of soft-sediment deformation increases (F6). In general, bioturbation is rare.

Where bioturbation is moderate to high, trace fossils colonize specific bed surfaces or heterolithic and finer-grained deposits. Trace fossils include *Dactyloidites ottoi*, *Ophiomorpha* and *Planolites*. Palaeocurrents are directed mainly towards the north and north-west, but there is also a component towards the south and south-east.

A distinctive example of this sandstone body type, shown in Fig. 1.7A, is a 7 m thick, erosively based unit with rip-up clasts at its base. It cuts down into underlying heterolithic deposits. The body is entirely cross-stratified, with stacked sets 15 to 20 cm thick (F7b, F7c and F7e). The cross-strata are organized into 0.8 to 1.7 m thick co-sets that begin with an erosion surface overlain by mud clasts, granules and pebbles. Within each of these units the grain size is constant (lower medium) or slightly fining upward (from lower coarse or upper very coarse to lower medium). The fining-up trend is also accompanied by a reduction in set thickness, and sometimes culminates in ripple-laminated horizons (F9a). The toesets and bottomsets of the individual cross-sets show, in places (Fig. 1.7C), a trend of increasing and then decreasing concentration of organic debris (see also Martinius & Gowland, 2011). These organic debris laminae (which can be as thick as 1 or 2 cm) bound sandy foresets, therefore defining tidal bundles (F7e). The cross-strata also show reactivation surfaces (Fig. 1.7D).

Interpretation: Facies Association 1.4 is interpreted to be deposited within amalgamated, broad and shallow distributary channels (around 0.8 to 1.7 m deep), because of the presence of basal erosion surfaces, overlying coarse deposits (deepest reaches of channels), and the upward thinning and fining tendency of the bodies. The upward thinning and fining of such units may result from periods of waning-flood discharge from the feeder system, or may indicate accreting bars above the initial thalweg-fill deposits. The coarse grain size, basal erosion surfaces, plant and wood fragments, multiple channelized erosional surfaces and abundant soft-sediment

deformation point towards an increased terrestrial (fluvial) influence in the Lajas succession, marking a change to peak progradation in the Lajas system. Facies Association 1.4 is interpreted to have been deposited in braided distributary channels. The presence of increasing/decreasing organic debris concentration draping sandy foresets points towards tidal reworking and/or tidal modulation of river flow within the distributaries. Because of the sudden increase in grain size (up to pebbles), basinward shift in facies (from FA 2 deposits to coarse-grained channels without part of the typical FA 2 sequence, as is typical of mixed-energy deltas) and extensive erosional base (at the scale of the whole outcrop belt), the lower boundary of this unit has been interpreted as a sequence boundary (see Appendix A).

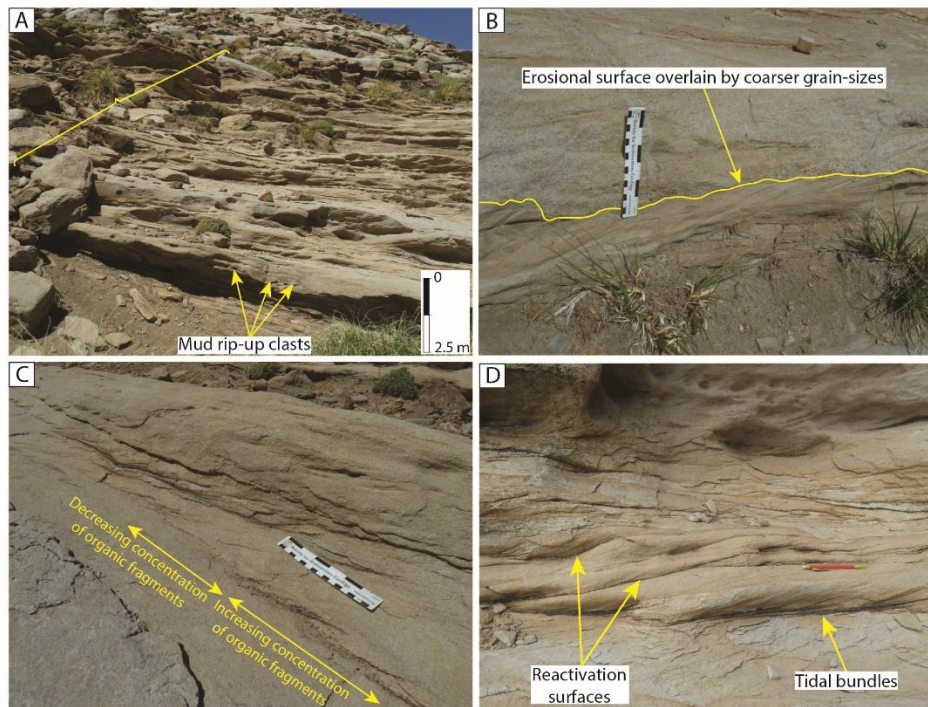


Figure 1.7: (A) Stratigraphic interval (yellow strip) with Facies Association 1.4 deposits. The base of the channels is marked by an erosion surface and sometimes by mudstone rip-up clasts. (B) Internal erosional surfaces typical of Facies Association 1.4 marked by an increase in grain size. (C) Increasing/decreasing organic debris concentration along the toesets and bottomsets of the cross-strata. (D) 20 to 15 cm thick cross-strata showing bundling.

Process summary

Facies Association 1 shows a predominant river influence. Tidal influence is almost absent, and is only weakly expressed in the heterolithic fine-grained sediments in the interdistributary bays, as wavy and flaser bedding, and possibly as sporadic organaceous drapes on the toesets of cross-strata. As also described by Tānavsū-Milkeviciene & Plink-Björklund (2009), the tidal wave apparently does not penetrate great distances inland in this mixed-energy type of delta. River influence is recognized by grain size and sorting of the deposits, as well as abundant wood and plant fragments and

the lack of bioturbation. Sporadic drapes on the foresets of cross-strata could represent tidal modulation of river flows (FA 1.2), but the absence of any organization in the drapes seems to make this hypothesis unlikely, at least in FA 1.1 (see also Ichaso & Dalrymple, 2014). Facies Association 1.4 shows the same strong terrestrial influence as FA 1.1 and FA 1.2 (coarse-grained sediment such as granules and pebbles, poor sorting, abundant plant debris and a high degree of internal erosional surfaces). However, FA 1.4 also contains tidal modulation, expressed as increasing/decreasing organic-fragment concentrations and tidal bundling of foresets (Fig. 1.7; see also Martinus & Gowland, 2011). These observations point towards a pre dominance of river processes, but modulated by tidal action.

Facies Association 2 (Delta Front and Subaqueous Platform)

Facies Association 2 (FA 2) includes depositional elements of the delta front and subaqueous platform, such as mouth bars, tidally reworked mouth bars, subtidal channels and shorefaces. Facies Association 2 is predominant in both the upper and lower parts of the Lower Lajas Formation at Lohan Mahuida. In the lower half, FA 2 interfingers with muddy shelfal deposits, whereas in the upper part it is in lateral contact with interdistributary bay and lower delta-plain distributary deposits (FA 1.2 and FA 1.3).

Facies Association 2.1 (Delta-Front Mouth Bars)

Facies Association 2.1 is characterized by coarsening-upward sandbodies up to 4 m thick and a few hundred metres wide. These sandbodies show characteristic, well-developed, metre-scale inclined strata (Figs 1.8 and 1.9A), ripple lamination (F9a), cross-stratification (F6 and F7c), parallel lamination (F14) or (F6) soft-sediment deformation (Fig. 1.9B). The sandbodies show a coarsening-upward trend, usually from lower fine-grained sandstones, silty heterolithic deposits or coaly shales with thin sandstone beds to

lower medium-grained thicker sandstone beds (Fig. 1.8). This coarsening and thickening trend is accompanied by a change from dirty sandstones near the base to cleaner sandstones at the top. In some cases, the lower part of a sandbody can show alternation between medium or fine-grained sandstone beds (usually structureless, parallel laminated or cross-stratified; Fig. 1.8, red arrows; F5a, F14 and F7b) and organic-rich, finely (rhythmically) laminated intervals (Fig. 1.8B, white arrows; F11). Many FA 2.1 sandbodies are characterized by plane-parallel or wavy lamination, but sedimentary structures can also show an upward increase in scale, from rippled laminae, flaser-beds, low-angle and plane-parallel lamination up to larger cross-strata sets, 12 to 18 cm thick. In places, bi-directional cross-stratification is present (Fig. 1.9D). Abundant mud clasts also occur. Palaeocurrents are variable, but the dominant components are to the north/north-west and to the east (see Appendix A). Where palaeocurrent data from large-scale inclined bedding and smaller cross-strata are available, they show a similar direction, indicating forward-accretion (see Appendix A). Bioturbation is sparse in the most proximal sandbodies, but it can be abundant in the more distal ones. Towards the distal reaches, the sandbodies continue to show a coarsening-upward trend, but there is an increase in bioturbation, reduction in size of sedimentary structures, increase in mud content and association with a few decimetre thick, well-sorted fine-grained SCS, HCS and low-angle laminae (F12 and F13). Commonly the sedimentary structures are obliterated by bioturbation and only a few scattered remnants are preserved (Fig. 1.9C).

In a few places, especially towards the southwest, FA 2.1 sandbodies are characterized by soft-sediment deformation (Fig. 1.9B). These bodies show a well-developed coarsening-up trend, from muddy sediments with wavy lamination (F10a), to upper fine-grained sets of small cross-strata, to lower-upper medium sigmoidal cross-strata 20 to 30 cm thick (Fig. 1.9B; F7b, F7c and F7d). The cross-stratified packages can

also contain intervals of climbing ripple lamination (F9a), indicating fall-out from high suspended-sediment concentrations. The cross-strata can be locally deformed (Fig. 1.9B), or a bigger portion of the sandbodies can be intensely soft-sediment deformed (F6) with the presence of water-escape pipes (Fig. 1.9B).

Interpretation: The dominant feature in FA 2.1 is an upward-coarsening and thickening of the sandbodies, a few hundred metres long and up to 4 m thick. They are interpreted as mouth-bar deposits, representing the unconfined deposits accumulated at the mouths of the distributary channels as they first enter the basin and start bifurcating. These mouth bars are located in the most proximal portion of the subaqueous platform deposits, as discussed below.

Mouth-bar deposits by definition are symptomatic of river influence and, where soft-sediment deformation, climbing ripples and plane-parallel lamination dominate the mouth-bar deposits, they signify very strong river influence (Wright, 1977; Tye & Coleman, 1989; Olariu & Bhattacharya, 2006; Olariu et al., 2010). Structureless or cross-stratified sandstones (event beds) in the lower part of some bar deposits (Fig. 1.8, red arrows) are likely to be emplaced during high discharge periods and are indicative of river floods. The presence of tidal rhythmites and bioturbation (Fig. 1.8B, white arrows), on the other hand, indicates marine-current (tides) reworking which preferentially occurs during interflood periods, when low-discharge conditions induce higher salinity (saline water can penetrate further inland), and allow other currents (for example, tidal currents) or wave processes to redistribute the sediments deposited by fluvial processes. Similar patterns have been described also in the McMurray Formation (Jablonski, 2012; Jablonski & Dalrymple, 2014), although in a more landward setting (i.e. within the innermost part of the fluvial to marine transition zone), and in the Tilje Formation (Ichaso & Dalrymple, 2014). These type of FA 2.1 deposits have therefore been interpreted as

tide-influenced mouth bars dominated by seasonal river discharge. The bar geometry is most likely to be dominated by river processes (length to width ratio of *ca* 2:1; Reynolds, 1999), while tides only rework sediment during low-discharge periods, as also described in the Chimney Rock Tongue by Plink-Björklund (2012). The observed trend from sand-rich mouth-bar deposits to intensely bioturbated coarsening-upward packages associated with a few decimeter thick SCS, HCS and low-angle laminae (Fig. 1.9C) points towards a lateral and/or distal deepening trend, which can occur over only a few hundred metres. These more distal packages can in places show a mixture of tidal and wave indicators (such as bi-directional cross-strata, low-angle laminae and remnants of HCS; Fig. 1.9C and D). This variability can represent a relative increase in wave energy in the more distal portions of the delta system or suggest that some mouth bars originally were influenced more by wave processes.

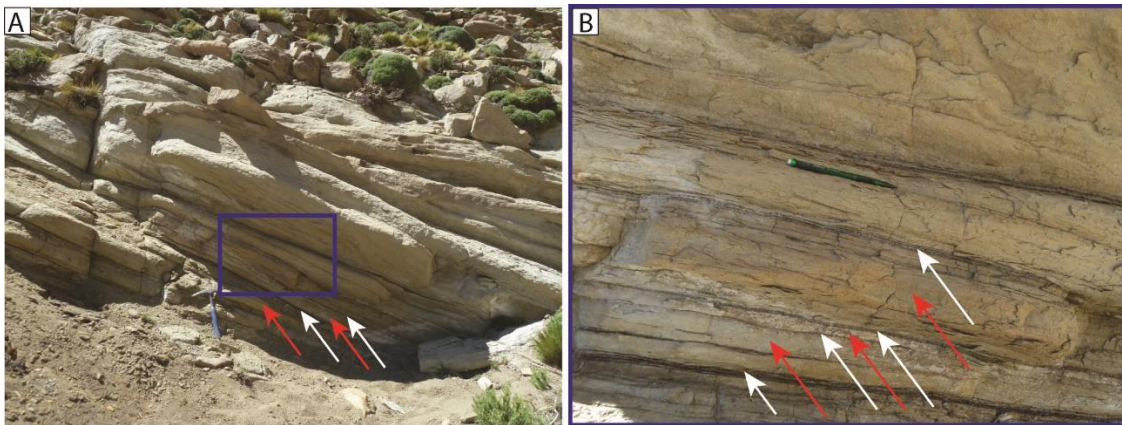


Figure 1.8: Flood-Interflood cyclicity in Facies Association 2.1 deposits. (A) Photograph of a coarsening-upward sandbody. The deposit becomes coarser and cleaner upward. Red arrows point to event beds, whereas white arrows point to finer-grained interbeds. Hammer for scale is 325 cm long. (B) Detail of finer-grained interbeds characterized by fine scale alternations of organic debris and sandy laminae, and the presence of bioturbation. The pencil is 15 cm long.

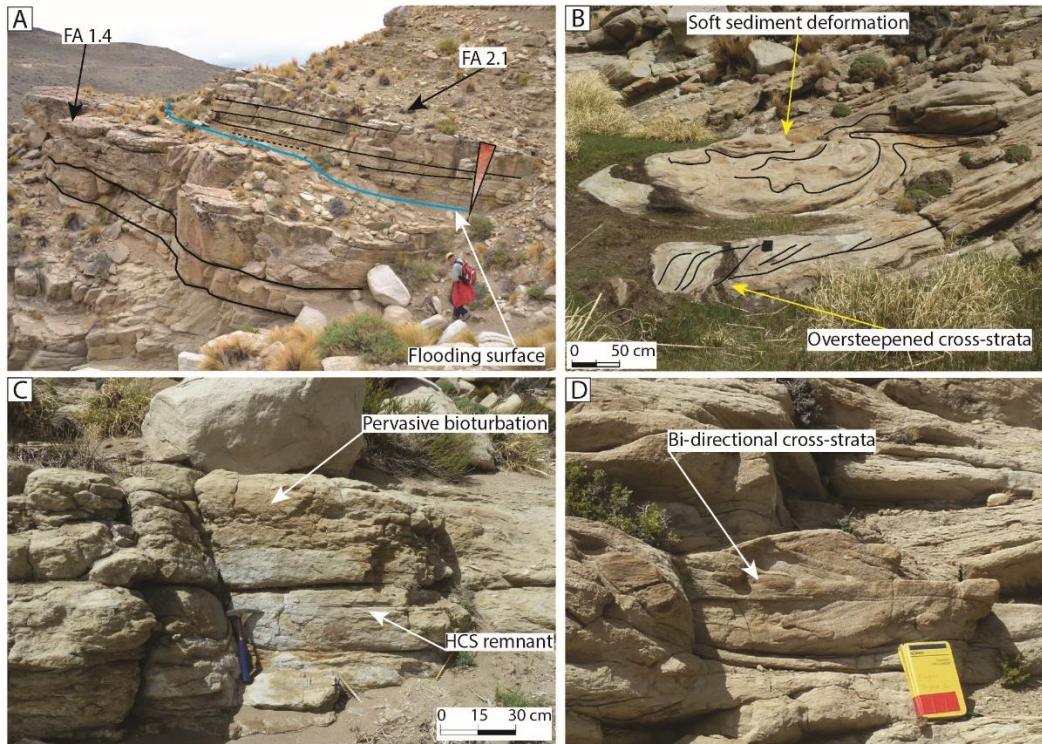


Figure 1.9: (A) Facies Association 1.4 deposits overlain by a coarsening-upward sandbody characterized by well-developed inclined strata. Person for scale is *ca* 1.8 m tall. (B) Abundant soft-sediment deformation and oversteepened cross-strata in Facies Association 2.1 deposits. These features are interpreted as fluvial signals. (C) Distal reach of a coarsening-upward sandbody, showing high degree of bioturbation and only few remnants of HCS. (D) Bi-directional cross-strata in the upper portion of a Facies Association 2.1 sandbody. The field notebook is 19 cm long.

Facies Association 2.2 (Tidally Reworked Bars and Dunes)

Facies Association 2.2 is characterized by intensely cross-stratified and amalgamated sandbodies a few metres thick (Figs 1.10 and 1.11A). These bodies are characterized by up to 4 m thick inclined beds or foresets that can be followed along the outcrop belt for hundreds of metres, and they can trend obliquely or in the same direction

to many of the rippled and thinner cross-stratified sets that occur within the larger bodies. The sandbodies can be channelized or flat-based amalgamated bodies (Fig. 1.10A).

The sandbodies usually show a broad coarsening-upward grain size, from lower fine to upper medium-grained. They are also moderate to well-sorted and with sub-angular grains. The degree of bioturbation is usually moderate and dominated by *Dactyloidites ottoi*, although *Cruziana*, *Ophiomorpha*, *Planolites* and *Macaronichnus* trace fossils are also present. The dominant sedimentary structure is cross-stratification (in places sigmoidal cross-strata and bi-directional cross-strata; F7c and F7d), with very frequent compound cross-bedding (Fig. 1.10B; F8). Set-climber cross-strata and ripples (Fig. 1.11B; F7c and F9b) and reactivation surfaces within the cross-strata are very common. The coarsening-upward trend of the body is accompanied by an increase in the size of the preserved bedforms. In the lower part of the bodies, there are heterolithic wavy to low-angle laminae (F10a), ripple cross-lamination with mud/organic drapes (F9a), or flaser bedding (F15), followed by planar cross-strata (two-dimensional dunes), whereas in the upper part of the bodies trough cross-strata (three-dimensional dunes) or larger scale planar cross-strata can occur (F7c and F7f). From bottom to top, the sandstones become cleaner, and there is less organic debris, concentrated in thick laminae draping bottomsets and toesets (as single drapes or double drapes; Fig. 1.10D). In places, there is a bundled or cyclic thickness change in the foresets and bottomsets along the length of the unit (Fig. 1.11C; F7e). In some places, thin (few decimetres thick) and sharp-based to erosionally based shelly beds are present (F2b), with thick shells mostly preserved in a stable hydrodynamic position. Shell fragments can also be aligned along the foresets of cross-strata.

Thin (few decimetres) heterolithic intervals or very bioturbated surfaces (Fig. 1.10C) can separate sandbodies of FA 2.2 from FA 2.1 sandbodies (F4, F10a and F10b).

These bioturbated surfaces contain large shell fragments, wood fragments and sparse granules. Trace fossils are abundant and, although many are sand-filled, few of them are filled with mud. Palaeocurrents are variable, but the main components are eastward, northward and southward (see Appendix A). Overall this association is sand-rich, with only modest fine-grained deposits preserved, and it occurs abundantly in the lower half of the study succession (see Appendix A).

Interpretation: The cross-stratified sandstone bodies that characterize FA 2.2 are interpreted as bars and compound dunes based on their internal flow/migration configuration (based on the work of Olariu et al., 2012, in the Baronia Formation). They are interpreted to have been deposited during very intensive tidal reworking of the original mouth bars on the front of the delta. Larger dunes climbing over smaller dunes produced upward thickening and slight upward-coarsening patterns during this reworking. Many of the features observed in these sandbodies indicate strong tidal influence, such as the presence of sigmoidal cross-bedding, bi-directional cross-strata, reactivation surfaces, mud/organic debris drapes and cyclic changes in foreset and bottomset thickness; furthermore compound cross-bedding is a quite typical feature of shallow-marine tidal environments (Dalrymple et al., 1978; Allen & Homewood, 1984; Dalrymple, 1984). Strong delta-front currents are commonly flood tidal currents (Dalrymple, 2010; Dalrymple & Choi, 2007). Facies Association 2.2 sandbodies are inferred to have an aspect ratio strongly controlled by tidal currents. High-energy conditions favoured the removal of fine-grained material, leaving clean, cross-bedded sandstones, although the water column appears to have been rich in organic fragments. These environmental conditions encouraged the colonization by *Dactyloidites*, which has been shown to be favoured by the presence of phytodetrital remains (Fürsich & Bromley, 1985; de Gibert et al., 1995; Agirrezabala & de Gibert, 2004). Highly bioturbated

surfaces rich in shells and wood fragments can be interpreted as abandonment surfaces or high-frequency tidal-ravinement surfaces; this interpretation is consistent with such surfaces occurring between FA 2.1 and FA 2.2 deposits. Abundance and type of bioturbation, especially the great amount of *Dactyloidites ottoi* bioturbation, indicates a marine environment. Sharp-based shell beds are likely to represent the local tidal-ravinement action at the base of channels (Dalrymple et al., 2003; Willis & Gabel, 2003) or could possibly represent storm events (Kidwell et al., 1986; Kidwell & Bosence, 1991; Fürsich & Oschmann, 1993).

Facies Association 2.2 sandbodies are interpreted in terms of extensive tidal reworking of the original FA 2.1 delta-front mouth bars. During high-frequency flooding and tidal-current influx, probably due to repeated tectonic subsidence against an uplifting syn-sedimentary high block, tidal currents in fairways from the south heavily reworked the outer parts of the delta front and produced intensely cross-bedded compound dunes and tidal bars. An alternative hypothesis is that intense tidal reworking occurred during deltaic progradation or on abandoned delta lobes after lobe switching, as suggested also by Plink-Björklund (2012). The result is highly amalgamated (both laterally and vertically) tidally reworked sandbodies (FA 2.2) with only remnants of the original mouth bars remaining (FA 2.1). The reworked delta-front area therefore became an amalgamated sandy environment.

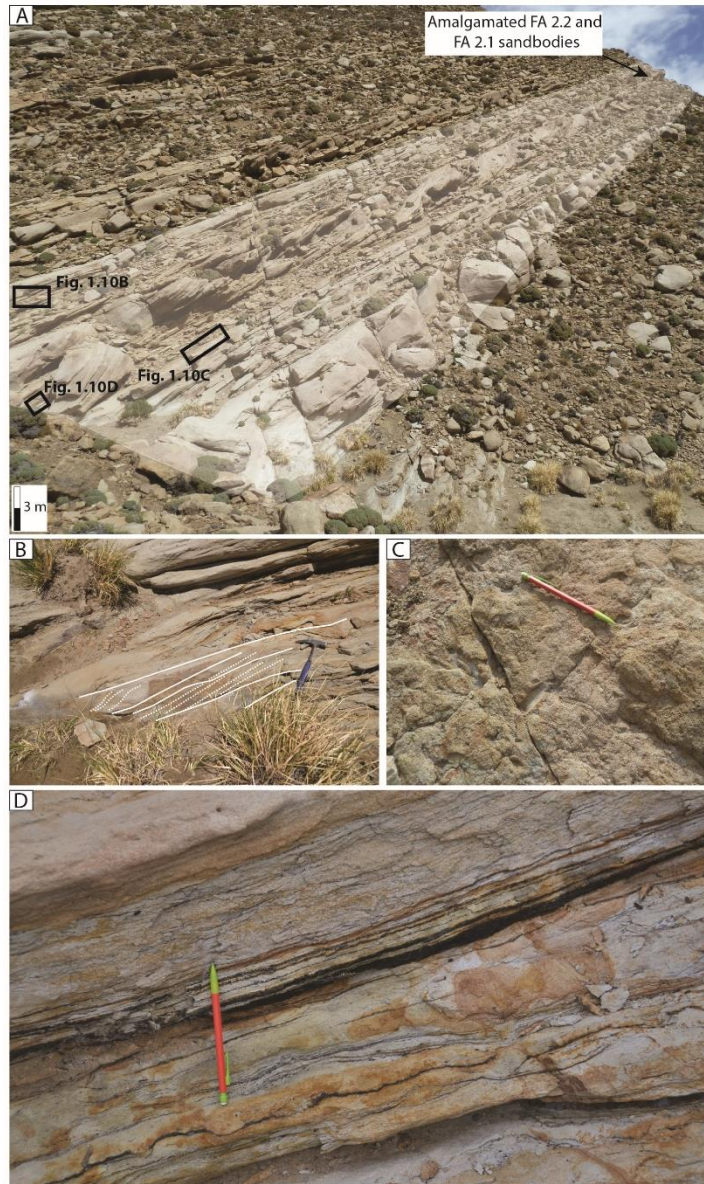


Figure 1.10: (A) Overview of amalgamated sandbodies of Facies Association 2.2. (B) Compound cross-bedding typical of the sandbodies of Facies Association 2.2. Note that individual small-scale cross-strata are separated by reactivation surfaces. Hammer for scale is 32.5 cm long. (C) Abandonment surface between Facies Association 2.1 and Facies Association 2.2 sandbodies. This surface is rich in mud chips, wood/plant fragments and is very bioturbated. Some shell fragments are also present. (D) Double drapes in the toeset region of a Facies Association 2.2 sandbody. Pencil is 15 cm long.

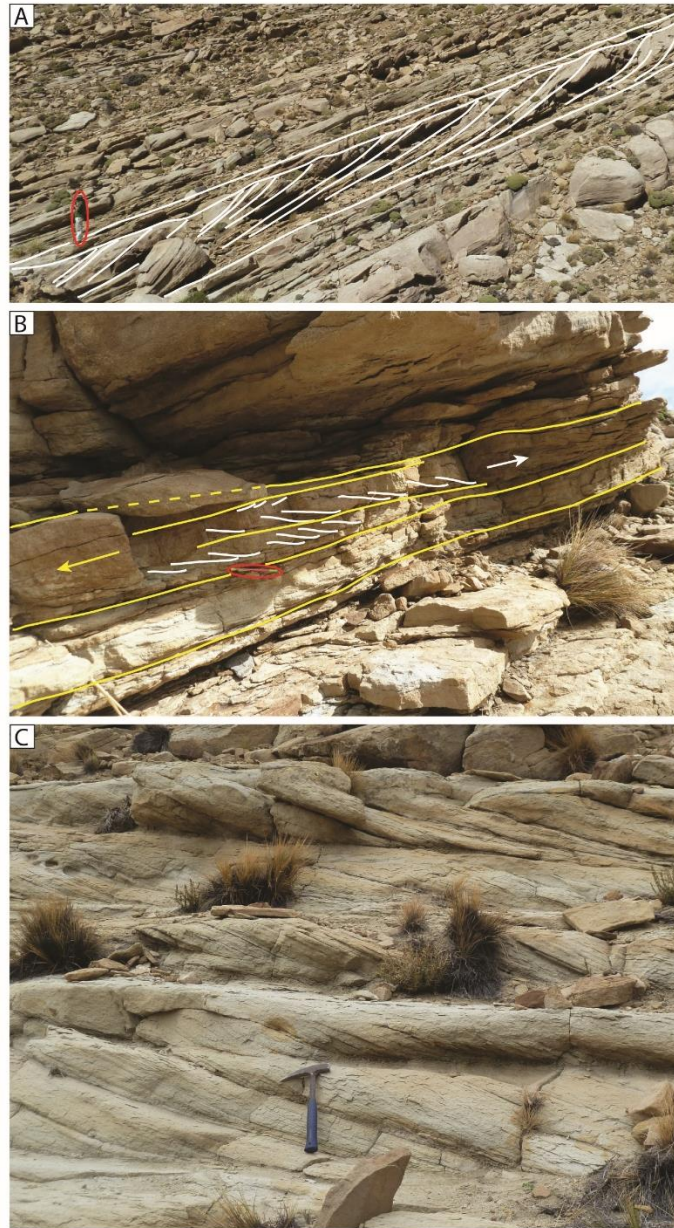


Figure 1.11: (A) Laterally accreting sandbody of Facies Association 2.2. Note the presence of large (up to 35 m high) accretion surfaces; the total extent of the sandbody is more than 300 m. Person for scale (circled; *ca* 1.8 m tall). (B) Detail of sandbody shown in (A). Yellow lines show large-scale accretion surfaces (yellow arrow shows their main dip direction); white lines highlight set-climbers cross-strata (white arrow shows their dip direction). Pencil for scale is 15 cm long. (C) Bundled cross-strata. Hammer is 32.5 cm long.

Facies Association 2.3 (Subaqueous Platform)

Facies Association 2.3 is characterized by heterolithic and fine-grained bioturbated sediments (F10a and F10b) within which channelized or mounded cross-stratified sandbodies (a maximum of 5 m thick and a few hundred metres wide) occur (Figs 1.12 and 1.13). Facies Association 2.3 sandbodies consist of upper fine or lower medium-grained sandstones, moderately sorted. The thickness of these bodies varies between 2.5 m and 5 m and internally they are cross-stratified or, in rare cases, structureless. The sandbodies can show either fining-upward or coarsening-upward trends. Cross-strata can be up to 1 m thick, and can show a characteristic cyclic variation in foreset thickness, double and single drapes (mainly composed of organic debris; Fig. 1.12C) and reactivation surfaces (F7e). In places formset cross-strata and sigmoidal cross-strata have been recognized (F7d). Compound cross-bedding is a ubiquitous feature (Figs 1.12 and 1.13; F8). Bed surfaces can be bioturbated (*Paleophycus*, *Arenicolites*, *Dactyloidites*, escape features and other unspecified burrows; Fig. 1.13B). Palaeocurrents are directed mainly towards the north and north-east, but there is also a component towards the south-east and north-west.

As an example, in Section 6 (see Appendix A), laterally accreting sandstone bodies are present (Figs 1.12 and 1.13) in FA 2.3. Most of the sandbodies have a sharp or erosional base (marked by pebbles, mudstone rip-up clasts and/or shell fragments; F2a and F2b), but in places it can be more gradational. Internally, the sandbodies are cross-stratified (Figs 1.12A, 1.12C, 1.13A and 1.13C), and they contain both planar and trough cross-strata (F7c and F7f) which, in most cases, show palaeocurrent indicators at high angle to the larger scale inclined beds, although in some sandbodies they show the same dip direction. As an example, one of these bodies (Fig. 1.12) is characterized by cross-strata about 40 cm thick (up to 1 m), although usually cross-strata are smaller near the

base of the body. Cross-strata are defined by grain-size variations (from upper medium to upper fine) or by organic-fragment drapes; they show tidal bundles (F7e), consisting of sandy foresets enclosed between double or single drapes of organic fragments (Fig. 1.12C). The sandbody is very rich in coaly fragments (Fig. 1.12B) and few shell fragments are present. Sparse *Dactyloidites ottoi* bioturbation is present. Another sandbody (Fig. 1.13), present in a stratigraphically higher position, shows very clear inclined strata on a scale of 5 m, and is truncated at the top by a structureless sandbody (Fig. 1.13A and C). Each inclined stratum contains ripple laminae (some of which dip up-slope) and it is bounded at the top by a finer-grained interlayer, but upward larger scale cross-strata are present (F8). *Dactyloidites ottoi* and escape structures are frequent, while bedding planes are intensely bioturbated by marine trace fossils (Fig. 1.13B). These bodies are always associated, both laterally and vertically, with FA 2.4 deposits.

Interpretation: The dominant elements of FA 2.3 are sandbodies that are channelized (up to 5 m deep and a few hundred metres wide) with laterally or forward accreting and upward-fining infill or are mounded (in strike view) upward-coarsening and thickening units a few hundred metres long (see Appendix A). The channelized sandbodies usually cut into heterolithic sediments or coaly shales (Figs 1.12 and 1.13). These sandbodies are interpreted as subtidal channel deposits developed by tidal reworking in the subaqueous delta platform, a phenomenon frequently observed in tide-influenced to tide-dominated systems (Kuehl et al., 1997; Roberts & Sydow, 2003; Swenson et al., 2005). These subtidal channels presumably are connected in a landward direction with the distributary channels, given the presence of pebbles, wood and coaly fragments. These deposits are characterized by internal compound architecture (typical of tidal sandbodies in shallow-marine environments; Fig. 1.13C), intense marine bioturbation (Fig. 1.13B), double organic drapes and tidal bundling of cross-strata (Fig.

1.12C) which indicate a tidal-current influence or reworking in a subtidal environment. Nonetheless the presence of granules, pebbles, wood fragments and coaly fragments (for example, Fig. 1.12B) indicate influence of riverine currents. The erosional bases of the sandbodies, marked by pebble-sized basement lithics and mudstone rip-up clasts, can represent tidal ravinement surfaces, or they can be related to episodes of stronger tidal currents during spring cycles and of strong fluvial outflow.

The intensity and type of bioturbation both within the sandbodies and in closely related sediments clearly indicates a marine environment, as well as their close association with FA 2.4 deposits (discussed below). The subaqueous delta platform (subtidal delta platform or subaqueous delta; Roberts & Sydow, 2003; Swenson et al., 2005; Helland-Hansen & Hampson, 2009) is a shallow and relatively flat area extending from the subaerial lower delta plain up to the rollover point of the delta front. It develops as the subaqueous platform reach of a compound clinoform, between the subaerial and delta-front portions (Kuehl et al., 1997; Pirmez et al., 1998; Roberts & Sydow, 2003; Swenson et al., 2005; Xue et al., 2010). This subaqueous platform characteristically includes: (i) subtidal channels (continued from the subaerial distributaries) filled by tidal bars; (ii) compound dunes; and (iii) fine-grained background sediments.

The intensely cross-bedded sandstone component (large tidal bars and compound dunes) of FA 2.3 deposits is probably similar to that described in FA 2.2, attributed to strong reworking by tidal currents impinging and spreading into the Lohan Mahuida deltas. However, the reworking of FA 2.3 deposits was preferentially confined into channels of the subaqueous platform and had a less dramatic effect in the areas lateral to the channels. It did not produce the widespread sheet-like tidal reworking that was common more seaward in FA 2.2, presumably because FA 2.3 was more protected in the proximal reaches of the system.

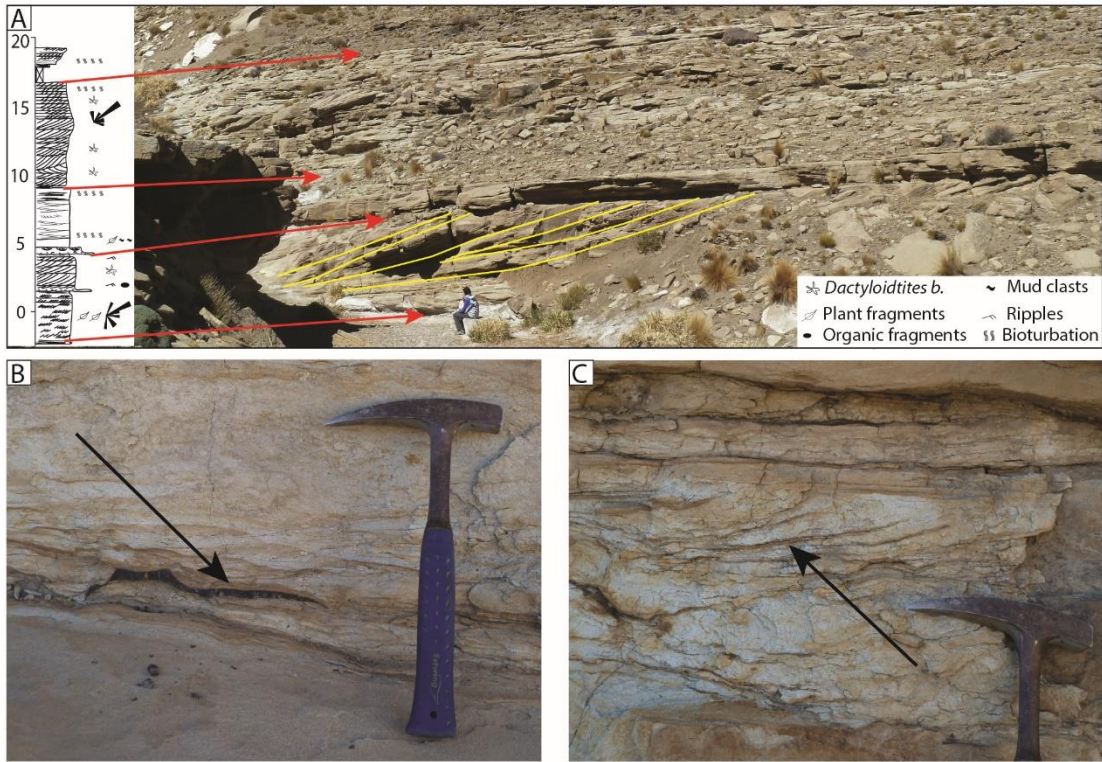


Figure 1.12: (A) Subtidal bar deposits *ca* 5 m thick (red arrows mark their basal and top surfaces). Note the internal accretion surfaces in the lower bar deposits (yellow lines). (B) River signals: Poor sorting; coaly fragments. (C) Double organic drapes. Hammer head for scale is 17.5 cm.

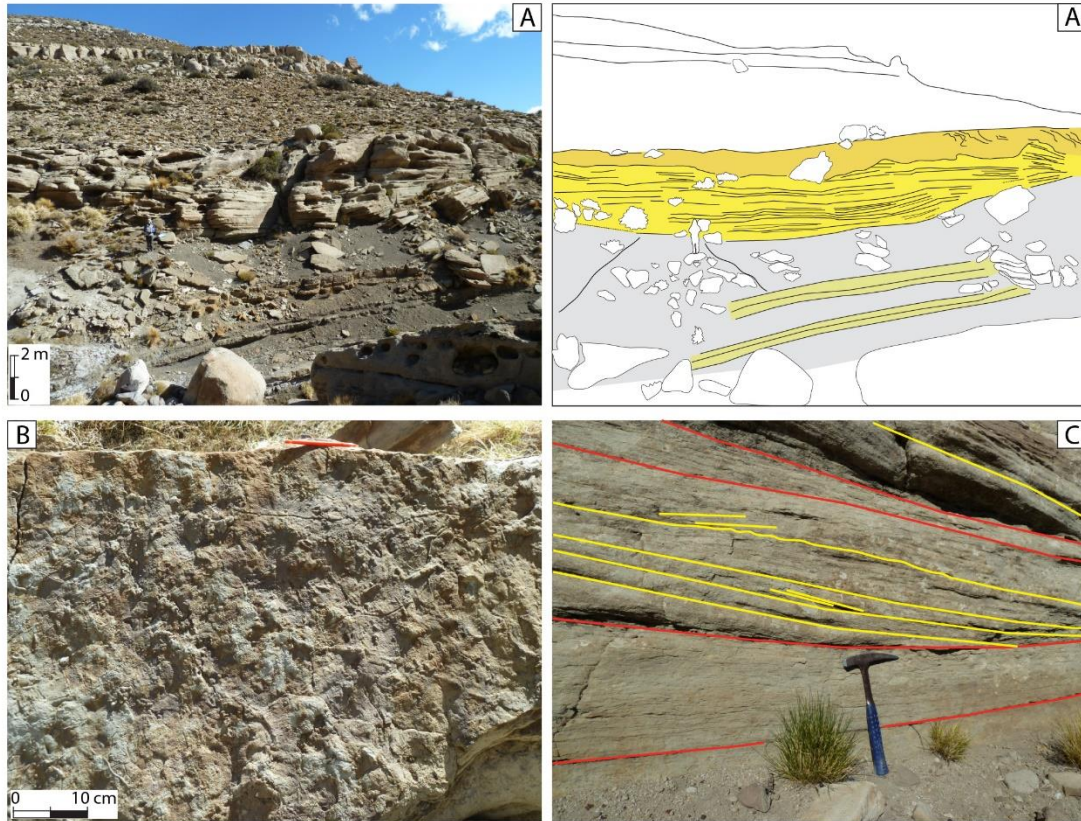


Figure 1.13: Bar in the subaqueous platform. (A) Photograph and line drawing of a 5 m thick bar cut into coaly shales. The bar (yellow) is clinostratified and at the top is slightly incised by soft-sediment deformed sandstones (orange). (B) Marine bioturbation on a bed plane. (C) Compound internal architecture of the bar. In red master bedding, in yellow foresets and superimposed cross-strata. Hammer for scale is 32.5 cm long.

Facies Association 2.4 (Shoreface)

Facies Association 2.4 is characterized by very fine and fine-grained sandstones with low-angle laminae, and SCS and HCS, which can be isolated or amalgamated (F12 and F13). The trace fossil assemblage is diverse and abundant and includes *Skolithos*, *Planolites*, *Ophiomorpha*, *Thalassinoides* and *Arenicolites*.

In Section 5 (Fig. 1.14) very fine sandstone packages up to 2 m thick overlie FA 2.1 deposits and are cut by FA 1.4 deposits. These very fine sandstones are very well-sorted, sharp-based, and characterized by amalgamated HCS. Other examples (Section 2) include coarsening-upward packages less than a metre thick characterized by fine-grained heterolithics (F10c) at the base followed by fine-grained sandstone beds with low-angle laminae and swales (F12 and F13) and lower medium sandstone beds with ripples and small cross-strata (F9a and F9c). These sandstone beds are intensely bioturbated by *Skolithos* and other burrowers.

Interpretation: The fine-grained sandbodies of FA 2.4 are characterized everywhere by hummocky and swaley stratification, low-angle laminae, and symmetrical ripples. These features, together with abundant and diverse trace fossil assemblages, indicate a marine environment. Facies Association 2.4 has been interpreted as wave-influenced to wave-dominated lateral shoreface deposits, based on its stratigraphic position and relation with other facies associations.

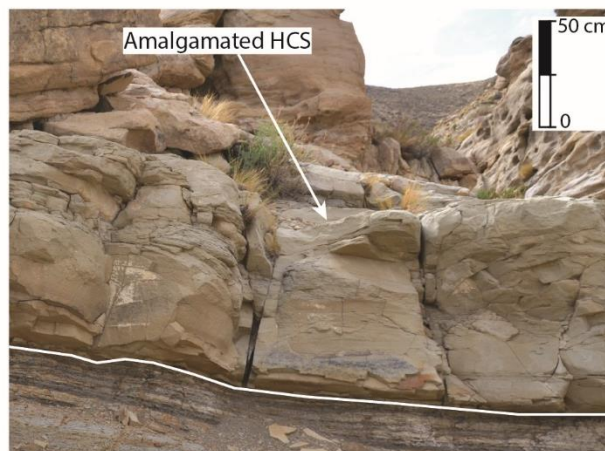


Figure 1.14: Fine-grained amalgamated sandstones with hummocky cross-stratification (HCS).

Process summary

Facies Association 2 shows an unusually strong tidal influence, except for FA 2.4. Tidal reworking is identified by the abundant compound cross-bedding, set-climber ripples and small cross-strata on the lee side of bigger bedforms and bars, as well as double mud/organic drapes, tidal bundles within cross-stratified sets and reactivation surfaces. Another indication of strong subtidal reworking is the good sorting of sand grains and scarcity of fine-grained sediments. Tidal currents rework previously deposited river and wave-influenced sediments of the Lajas delta system. *River influence* is expressed mainly by the large amount of coaly fragments, event beds in unreworked mouth bars, and by the presence of pebbles and granules. The strongest tidal reworking occurs in FA 2.2 deposits, but it decreases into the more proximal reaches of FA 2.3 and FA 2.1 deposits. Tidal-current reworking occurred preferentially in the distal part of the prograding deltaic tongues (FA 2.2); this reworking could have happened due to high-frequency flooding related to repeated tectonic subsidence, to lobe abandonment, or to stronger tidal currents present in the delta front and subaqueous platform environments. Facies Associations 2.3 and 2.1 are more proximal, and while they still show tidal-reworking features, they also show stronger river signals. In particular FA 2.1 deposits, located closer to the river mouths and accreting during progradational phases, are composed mainly of riverine event beds, while tidal currents are able to rework only the fine-grained interflood deposits. *Wave influence* is the least important, but can be significant locally, probably lateral to the main sediment fairways, where river and tidal currents were less strong. Wave-influenced deposits can occur during flooding events, but they can also be present during progradational phases, because in mixed-energy systems processes can change rapidly in space (Roberts & Sydow, 2003; Ainsworth et al.,

2008). The high degree of bioturbation associated with FA 2 indicate an overall subaqueous (marine) environment.

Facies Association 3 (Prodelta and Offshore)

Facies Association 3 (FA 3) includes prodelta and offshore-transition deposits. Facies Association 3 is characterized by the most abundant fine-grained deposits encountered in the study area. This facies association dominates the lower half of the study succession and interfingers with FA 2.1 and FA 2.2 deposits.

Facies Association 3.1 (Prodelta)

Facies Association 3.1 is characterized by 2 to 8 m thick siltstones, muddy heterolithic deposits or heterolithic sandy-silty deposits, containing a large amount of mud (F10). Facies Association 3.1 gradually coarsens upward as the mud and silt content decreases, and transitions into FA 2.1 deposits. In a few places, 2 to 3 m thick coarsening-upward packages from muddy siltstones to fine sandstones with HCS have been observed (F12). The dominant sedimentary structures are wavy, lenticular bedding and plane-parallel lamination (F10c and F14). The degree of bioturbation is usually moderate to high, and it obliterates most of the primary sedimentary structures.

Facies Association 3.2 (Offshore/Offshore Transition)

Facies Association 3.2 is characterized by fine-grained, muddy deposits (F10c) within which fine-grained sandstone bodies up to 2 m thick are encased. Shell fragments (with the bivalve *Trigonia* being the most common) are frequent and sometimes they produce lags capping sandstone beds (F2b). They occur as both parautochthonous (as pavements and stringers) and allochthonous (as beds and lenses) assemblages (Kidwell et al., 1986). The degree of bioturbation is moderate to high (*Ophiomorpha*, *Macaronichnus*, *Arenicolites*, *Thalassinoides* and *Planolites*).

The sandstones bodies are very fine to fine-grained and well-sorted. The most common sedimentary structure is HCS (F12). Hummocky cross-stratification sets vary in thickness from 20 cm up to 1.5 m, and HCS wavelength is usually 2 to 3 m. Ripple-lamination (both symmetrical and asymmetrical), low-angle lamination and plane-parallel lamination are also present (F9a, F9c, F13 and F14), but subordinate. Less frequently, dune-formed cross-strata (both planar and trough) are present, ranging in grain size from fine to lower medium (F7c and F7f). Sets vary in thickness from 10 to 50 cm. Dune cross-strata sets can be encased within sandstone beds characterized by HCS, or they can be isolated and up to 2 m thick.

Interpretation: Facies Association 3.1 and Facies Association 3.2 are interpreted, respectively, as prodelta and offshore/offshore-transition deposits. Facies Association 3 represents the most distal deposits of the Lajas Formation, because of the abundance of trace fossils, abundance of fine-grained, heterolithic deposits and marine mudstone, and because of its vertical and lateral association with FA 2.1 and FA 2.2. The fine-grained nature of the sediments and the degree of bioturbation point towards a low-energy setting. Conditions at the time of deposition were probably close to fully marine, but the low ichnogenera diversity and the presence of opportunists indicate a fairly stressed environment. The coarsening-upward packages are interpreted as the distal reaches of prograding deltaic lobes. Where the coarsening-upward packages are capped by HCS, they could either represent distal wave-influenced mouth bar or distal shoreface deposits (Ichaso & Dalrymple, 2014). Isolated cross-stratified packages are interpreted as transgressive shelf sandstones (see also Ichaso & Dalrymple, 2014) and indicate strong sediment reworking through marine currents (probably tidal currents). Overall at this site, river-derived sediments were being transported close to the offshore-transition zone, where they were exposed to wave action and reworking, as well as to tidal-current

reworking. Waves were the predominant process, especially in FA 3.2. Based on HCS wavelength, water depths are estimated to have been *ca* 40 to 60 m and the fetch was greater than 80 km (based on the methodology described in Myrow et al., 2008).

Process summary

The high level of bioturbation and fine-grained character of the sediments suggest a distal setting (prodelta to offshore transition) for the deposition of FA 3. In this context, river influence can be inferred only by the presence of poor sorting in many of the sandstone beds, interpreted as beds that were less reworked by waves and tides. Overall, waves were the predominant process in FA 3.2, producing and preserving HCS with metre-scale wavelength in very fine and fine-grained sandstones. Nonetheless, tidal currents were also present (FA 3.1 and FA 3.2), and effectively reworked the coarser grained sediments into 2D and 3D cross-strata.

Facies Association 4 (Tidal Inlet and Estuary)

Facies Association 4 (FA 4) includes tidal inlet and estuarine deposits and occurs at about 170 m from the base of the Lajas Formation at Sections 1, 3/4 and 7 (see Appendix A). Facies Association 4 is associated with a transgressive event recognized across the whole outcrop belt through a deepening trend and overall retrogradational stacking pattern. In places, a transgressive lag deposit can be observed, characterized by highly bioturbated sediments rich in shell fragments.

Facies Association 4.1 (Tidal Inlet)

Facies Association 4.1 is characterized by channelized and cross-stratified sandstone bodies. The best example of FA 4.1 deposits occurs in Section 1 (see Supporting Information). It is a 4 m deep and 1 km wide (see Appendix A) sandbody cutting into siltstones and heterolithic sediments (F10). Its base is marked by pebbles,

shell fragments, wood and organic fragments (Figs 1.15 and 1.16; F2b). The beds are normally graded, from pebbly sandstones with sub-rounded pebbles and granules to upper medium, poorly sorted sandstones with trough cross-bedding (*ca* 10 cm thick cross-strata; F2b). The channel infill generally fines upward and the size of the cross-stratal sets decreases upward.

The *lower part of the infill* is characterized by 20 to 80 cm thick sets of planar cross-strata (Fig. 1.15). The cross-strata are lower to upper medium-grained sandstones with moderate–good sorting (F7c). The foresets have a thickness range from 2 to 5 cm, and are highlighted by organic-rich interlaminae, but in the bottomset region the organic-rich laminae become a few millimetres thick.

The *middle part of the channel infill* (Fig. 1.15) is characterized by lower medium-grained sandstones with moderate-good sorting and smaller cross-strata (*ca* 10 cm thick, both planar and trough cross-strata). A sigmoidal cross-strata is very well-preserved in this interval (F7d); its bottomsets are characterized by organic-fragment concentration and ripple laminae while the foresets contain very well defined laminae 5 mm to 1 cm thick.

The *upper part of the channel infill* is a compound body, with 7 to 15 cm thick upper medium to lower coarse-grained, poorly sorted, cross-strata (Fig. 1.16; F7 g). Palaeocurrents are mainly directed towards the north and east but, in more detail, the lower part of the succession shows predominantly east-directed palaeocurrents, whereas the upper part has east and north-south directed palaeocurrents (Fig. 1.16). *Dactyloidites ottoii* bioturbation is widespread throughout the deposits. Similar deposits have been recognized also in Sections 3/4 and 7 (see Appendix A). Laterally and above this unit, muddy siltstones and fine–very fine sandstones, characterized by hummocky strata and low-angle lamination, are present (see Appendix A).

Interpretation: Facies Association 4.1 is interpreted as tidal inlet deposits or as deep tidal channel deposits associated with a tidal inlet, due to its close association with underlying heterolithic sediments (F10), the immediately overlying and adjacent wave-dominated facies (fine and very fine sandstones with HCS and low-angle lamination) and coarse-grained cross-bedded sediments with a fining-upward trend (Hayes, 1980; Rieu et al., 2005). Pebble-sized material is probably related to strong tidal currents or to tidal ravinement surfaces. Palaeocurrents are mainly east-oriented but, in more detail, the lower part of the tidal inlet has east-directed palaeocurrents, whereas the upper part has more north-directed palaeocurrents with a slight bi-directional component (Fig. 1.16). Therefore, the main currents are likely to be tidal currents. The barrier into which the inlet cuts has been largely destroyed during transgression and only the part of the inlet channel that hung lower than the base of the barrier has been preserved (e.g. Rieu et al., 2005; FitzGerald et al., 2012). The overlying thin wave-dominated strata are the culmination of the transgression as the barrier got cannibalized and overlain by offshore mudstones.

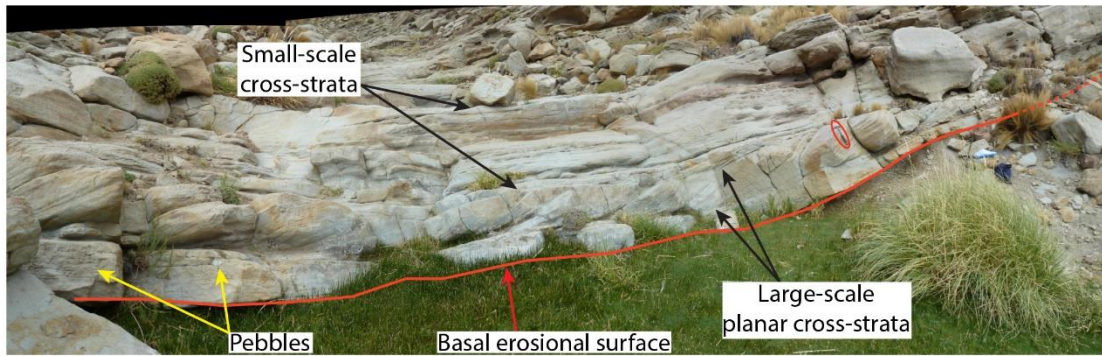


Figure 1.15: Photographic panel of Facies Association 4.1 deposits cropping out in Section 1. Facies Association 4.1 has an erosional base marked by pebbles and shell fragments. The infill is characterized by stacked cross-strata bounded by low-angle inclined master surfaces. The thickness of the smaller cross-stratal sets decreases upward. Hammer for scale is 32.5 cm long (red circle).

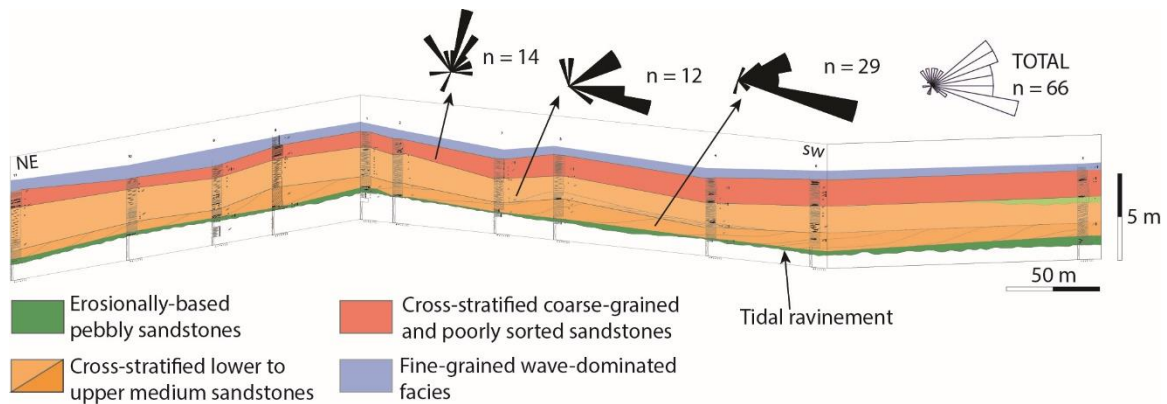


Figure 1.16: Fence diagram of Facies Association 4.1 deposits cropping out in Section 1. The base is erosional, overlain by normally graded pebbly sandstone with shell fragments. The overlying deposits are cross-stratified, but the size of the cross-strata decreases upward. The upper compound body (red colour) is coarser grained and more poorly sorted than the sediments underneath, probably indicating an interval of high-energy currents.

Facies Association 4.2 (Estuary)

In Section 1, FA 4.1 deposits are overlain and partially eroded by an up to 15 m thick sandstone unit with a complex internal architecture and more than 3 km of lateral extent (Fig. 1.17). The base of the body is erosional, in places marked by basement-derived sub-angular and sub-rounded pebbles (*ca* 1 to 2 cm long), and rip-up clasts (up to 14 cm long), and it incises into underlying fine-grained deposits and wave-dominated sandstones (see Appendix A). This unit is capped by dark brown mudstones (up to 7 m thick), rich in plant fragments. The lateral termination of the sandstone body is abrupt. The FA 4.2 sandstone body is erosively based and extensively cross-stratified and it can be subdivided into four units (Fig. 1.17).

Unit 1: At the base of the body, poorly sorted, coarse-grained cross-strata (F7a) are preserved in places above the erosional base of the unit (Unit 1, in Fig. 1.17). However, this facies is replaced, near the lateral termination of the unit, by thinly bedded (5 to 8 cm thick) upper fine sandstones with plane-parallel lamination and subordinate flaser bedding (F14 and F15). These beds are burrowed by *Skolithos* and *Planolites*.

Unit 2: Compound cross-strata (Unit 2, Fig. 1.17), with well-developed master surfaces are developed in Unit 2 (F8). Along the master surfaces there are 8 to 15 cm thick cross-strata or ripple laminae. The sandstones are lower fine-grained to upper medium-grained with moderate sorting. Mud rip-up clasts are present.

Unit 3: This unit is characterized by channels and by non-channelized large-scale planar and trough cross-strata cross-cutting one another (middle and upper parts of the body, Fig. 1.17). Non-channelized cross-strata have a lateral (preserved) extent of tens of metres and a preserved thickness ranging from 20 to 60 cm (F7f), although some sets can reach 1 m in thickness (Fig. 1.18A). Smaller sets of cross-strata can migrate in the opposite direction to the bigger ones (F7c). Low-angle laminae can also be present (F13)

and they represent toesets of bigger cross-strata. Non-channelized cross-strata usually display compound geometries (Fig. 1.18A); they are separated by master surfaces, over which new cross-strata migrate. Reactivation surfaces are also a common feature. Cross-strata vary in grain size from lower fine (mainly the bottomsets) to lower medium sandstones, usually moderately to well-sorted. Cross-strata foreset thickness varies between 5 cm and 10 cm. Within the foresets, laminae can be defined by grain-size variations or by organic fragments and can show organized changes in thickness (Fig. 1.18A; F7e). The bottomset and toeset regions tend to concentrate organic fragments, which alternate with 5 to 8 mm thick upper very fine to lower fine sandstones forming thin rhythmic lamination or ripple lamination (Fig. 1.18B; F9b and F11). Vertical and horizontal burrows are both present.

Channels present in Unit 3 can either be composed of structureless sandstones (for example, Fig. 1.18A) or they can be cross-stratified (F7f and F5b). Cross-strata are upper medium and lower medium sandstones, with moderate to poor sorting. Water-escape structures can be present. Channel thickness varies from 0.6 to 2 m.

Part of Unit 3 is in places characterized by structureless upper fine to lower medium, moderately to well-sorted sandstones (Fig. 1.17). Within these structureless sandstones mud chip horizons distorted by deformation are present (F5b). It is clear that the passage between the cross-strata and structureless sandstones is gradational, because following laterally the same sets of cross-strata, they become gradually disrupted until they are completely structureless. Subordinate facies associated with the cross-bedded units and structureless sandstones are represented by low-angle and plane-parallel laminated fine-grained sandstones with symmetrical ripples (F9c, F13 and F14).

Unit 4: This unit has an erosional base, marked by thick shell fragments, sub-rounded granules, mud chips and wood fragments (F2b). The internal architecture is

characterized by cross-strata, some of which display a well-developed sigmoidal shape (Fig. 1.18D; F7c and F7d). Oppositely directed ripples and bi-directional cross-strata are also a common feature (F9b). Cross-stratal foresets are usually 3 to 4 cm thick, defined by organic fragments or by grain-size variations, from lower coarse to upper medium sandstone. The sorting is moderate to poor, with grains up to very coarse sandstone.

Bioturbation occurs throughout Units 2, 3 and 4 and is dominated by *Dactyloidites ottoi*, but *Planolites* and *Macaronichnus* are also present. *Planolites* and small escape structures tend to be concentrated in the organic-rich thinly laminated bottomsets. Although bioturbation is widespread, it usually concentrates on bed planes.

Scattered gastropod (*Eunerineidae*; Kollmann, 2014) shell concentrations, associated with subangular granules and coarse sandstones, are randomly but markedly present within this unit (Fig. 1.18C). Sometimes they are clearly associated with erosional features (channels), but in most cases they have been the locus of early cementation, and form concentric dark red concretions.

Interpretation: Facies Association 4.2 is interpreted as an estuarine sandbody. The lateral extent of this unit is more than 3 km, and its thickness is up to 15 m. The base of the unit is erosional, in places marked by pebbles, mudstone rip-up clasts and poorly sorted, cross-stratified sandstones, which are interpreted as remnants of possible fluvial deposits (Unit 1). The parallel-laminated thin sandstone beds close to the margin of the outcropping estuary can represent tidal flat deposits. Units 2 and 3 are characterized by compound cross-strata, large-scale 2D and 3D cross-strata cross-cutting one another. The cross-strata sometimes show grain-size bundling in the foresets, sigmoidal shape, reactivation surfaces and rhythmic lamination in the toesets and bottomsets; these are characteristic tidal signals. Units 2 and 3 represent the main channelized estuarine bars (cf. Clifton & Phillips, 1980; De Mowbray & Visser, 1984; Nichols & Biggs, 1985;

Wightman & Pemberton, 1997). Horizons with rip-up clasts line the base of channels, where currents were strongest. Structureless intervals can be due to liquefaction of rapidly deposited sediments (Wightman & Pemberton, 1997). Subordinate low-angle laminated fine-grained sandstones with wave ripple laminae can represent subordinate wave-influenced deposits. *Eunerineidae* gastropods lived semi-infaunally in a shallow subtidal environment and shells were accumulated during high-energy events by winnowing in chaotic assemblages within their environment (Kollmann, 2014). Unit 4 has an erosional base marked by a shell lag, granules and wood fragments which, together with the presence of sigmoidal cross-strata, bi-directional cross-strata and ripples, indicate the influence of strong tidal currents. Unit 4 is also interpreted as an estuarine channel. Finally, the mudstones that cap the sandstone body can represent open bay or marsh deposits. Overall, this estuarine association shows very similar characteristics in terms of facies, sedimentary structures and internal architecture to some deposits described in the McMurray Formation, and it seems to have comparable dimensions to some of the estuarine units there described (High Hill river section, see Wightman & Pemberton, 1997, in particular units 3 and 4).

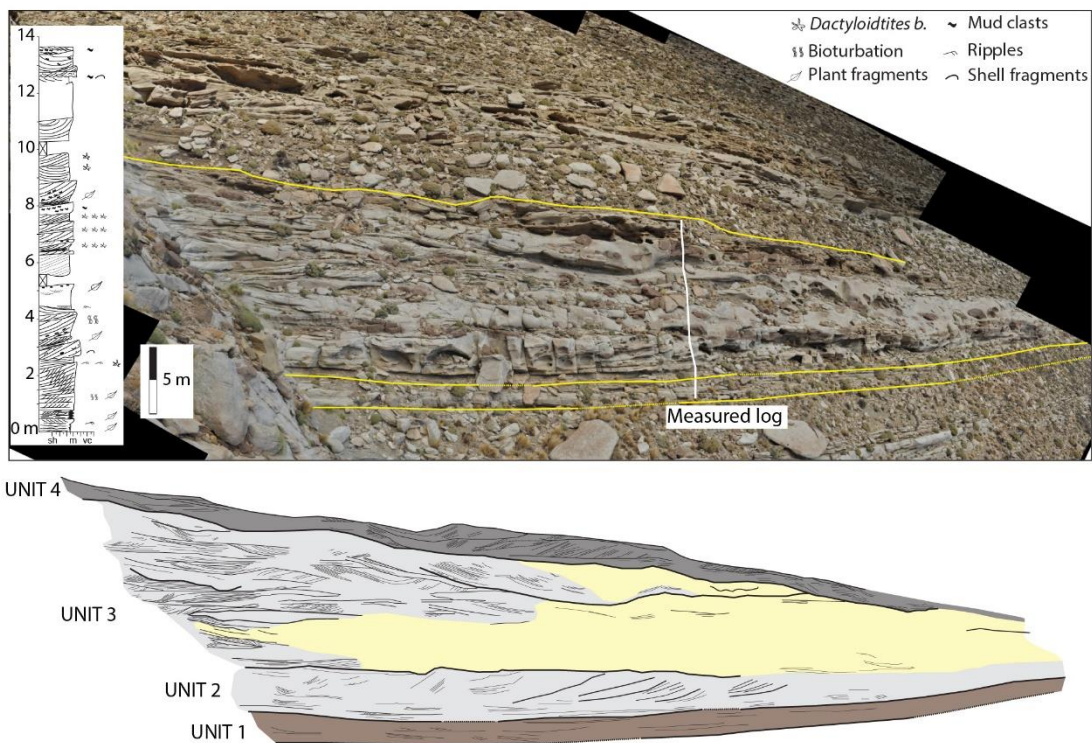


Figure 1.17: Photographic panel and line drawing of Facies Association 4.2 (marked by yellow lines in the photopanel). Unit 1 (brown colour) is composed of poorly sorted cross-strata. Unit 2 (grey colour) is a clinostratified unit. In the middle part (Unit 3, grey and yellow colours) large-scale 3D cross-strata and channels are present but, in places, the structures are destroyed by liquefaction (yellow colour). At the top, Unit 4 (dark grey colour) erodes the previous deposits and it is marked at the base by shell and wood fragments.

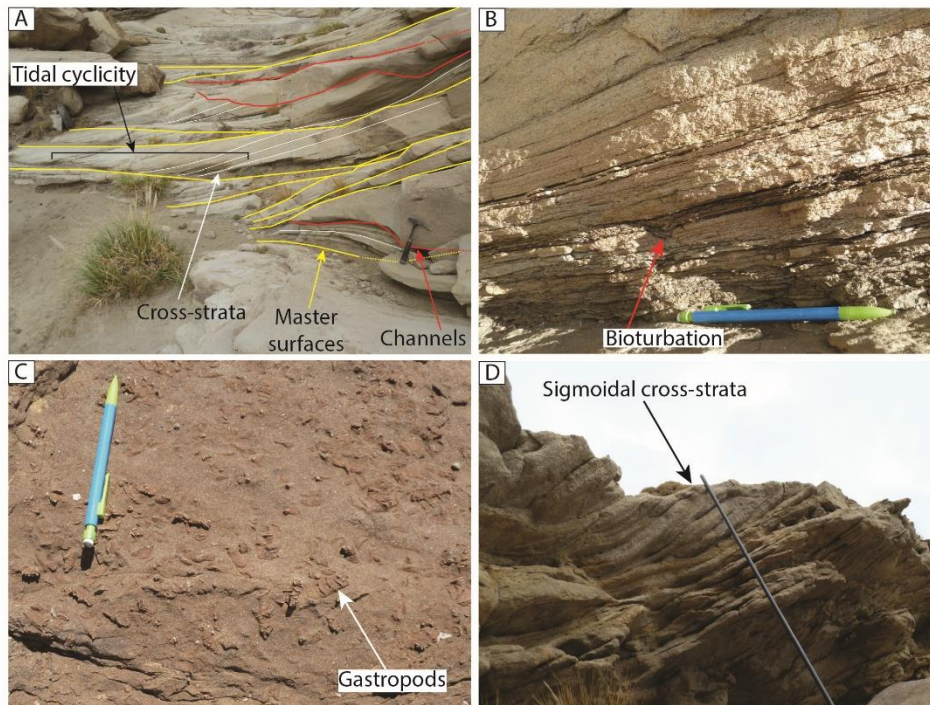


Figure 1.18: (A) Two-dimensional compound cross-strata, 50 cm to 1 m thick. Hammer for scale is 32.5 cm long. (B) Rhythmic lamination in the bottomsets of large-scale cross-strata, where the organic fragments are concentrated and are associated with bioturbation. (C) Accumulation of Eunerineidae gastropods preserved in an early-cemented horizon. The pencil is 15 cm long. (D) Sigmoidal cross-strata. The Jacob's staff is 140 cm long.

Process summary

Facies Association 4 is characterized by a stacked succession of marine bioturbated, moderately to well-sorted cross-stratified sandstones. Bioturbation is widespread but tends to be concentrated on bedding planes, marking a pause in sedimentation. Compound dunes and single 2D sigmoidal dunes are a common feature of high-energy tidal estuaries. Double mud drapes and rhythmic lamination in the bottomsets and toesets also indicate tidal influence. In the estuarine body, scattered

gastropods and shell concentrations indicate strong reworking by marine currents (Clifton, 1982; Kidwell, 1982; Kidwell & Bosence, 1991; Wightman & Pemberton, 1997). These units are therefore interpreted as tide-dominated. Finer-grained sandstones dominated by HCS and low-angle lamination are associated with these tide-dominated sandbodies, and they represent wave-dominated to wave-influenced deposits.

STRATIGRAPHIC ARCHITECTURE AND STACKING PATTERNS

The Lajas Formation occurs within an overall regressive succession, from the deep-water mudstones and slope turbidites of the Los Molles Formation to the Lajas delta-front and delta-plain deposits (Fig. 1.19). The general Lajas depositional environment is interpreted as a mixed-energy tide-influenced delta system (see also Willis, 2005), with associated subenvironments: upper coastal plain, lower coastal plain (including distributary channels, interdistributary bays and lagoons), laterally developed shorefaces, subaqueous delta platform, delta front and prodelta. An approximately 300 m thick succession of the Lower Lajas Formation was examined. A particular feature of this overall regressive deltaic succession is that its distal to middle reaches were intensely reworked by tidal currents (FA 2.2). This tidal reworking is likely to have happened during periods of transgression perhaps augmented by autogenic lobe switching and abandonment.

Two depositional sequences, 150 m and 140 m thick, respectively, are bounded by three sequence boundaries showing erosional surfaces and abrupt changes in facies and grain size. In the correlation panel (Fig. 1.19) a sequence boundary has been interpreted near the base of the succession. Sequence boundary 1 (SB 1) separates sharp-based delta-front sandstones from shelfal deposits (most of the latter deposits are covered and not clearly cropping out) in the south-westernmost part of the outcrop belt. This

surface has been interpreted as a sequence boundary because FA 2.1 deposits begin in a very abrupt manner, without any gradual coarsening-upward trend from prodelta/distal delta-front deposits as seen in younger sediments. Towards the north-east (i.e. further basinward) the sequence boundary passes into a correlative conformity, as the abrupt nature of the boundary is gradually lost. The lower half of the succession is capped by a second sequence boundary (SB 2). This sequence boundary underlies distributary channel deposits (FA 1.4) that cut into delta-front and lateral shoreface deposits (FA 2.1, FA 2.2 and FA 2.4), without any intervening subaqueous platform deposits (FA 2.3), as seen in the upper half of the succession. Sequence boundary 2 is an erosional surface traceable at the scale of the whole outcrop belt (7 km) that incised (up to 13 m) into FA 2 deposits, almost completely removing transgressive shoreface deposits (FA 2.4, see Fig. 1.19). This erosional surface (in contrast to SB 1) is marked by an increase in grain size (up to pebbles), with localized conglomerates. The overlying deposits (FA 1.4) are coarse-grained amalgamated channels which could indicate limited accommodation space. The third sequence boundary (SB 3) is located near the top of the study interval, at the base of coarse-grained upper coastal-plain deposits (FA 1.1) that directly overlie and erode transgressive marine deposits. The nature of sequence boundary 3 is similar to that of sequence boundary 2, but developed in more proximal environments. Sequence boundary 3 is a highly erosional surface traceable at the scale of the whole outcrop belt. It erodes (up to 15 m) FA 1.3 deposits and transgressive FA 2.4 deposits. It is marked by an increase in grain size (conglomerates and pebbly sandstones).

At a smaller scale, eight higher frequency (possibly fourth-order) cycles (on average 35 m thick) of relative sea-level change occur, modulating the overall regressive pattern and the two main sequences. These cycles can be divided into regressive packages (if they are shallowing upward) and transgressive packages (if they are deepening

upward). Different cycles are separated by flooding surfaces (in places coinciding with a sequence boundary) or by maximum flooding surfaces (i.e. points of turnaround from transgression to a new episode of regression). In the lower 150 m of the succession, there are three regressive–transgressive (R–T) cycles. The first regressive package starts at SB 1; it is characterized by a shallowing upward trend as deltaic tongues (FA 2) prograde in the basin (Fig. 1.19). The transgressive package begins with a flooding surface, marked by offshore/prodelta deposits overlying FA 2 deposits of the regressive package. This transgressive package is characterized by a backstepping of the deltaic tongues and culminates in a maximum flooding surface marked by fine-grained very bioturbated deposits (FA 3). The following two R–T cycles have similar characteristics (Fig. 1.19). The regressive packages mark a new episode of deltaic progradation (FA 2.1 and FA 2.2) following a maximum flooding surface, while the transgressive packages are prodeltaic/offshore deposits (FA 3) or shoreface deposits (FA 2.4) overlying FA 2.1 and FA 2.2 deposits. The last transgressive package is truncated by sequence boundary 2 (Fig. 1.19). These three regressive cycles are developed in delta front to shelf settings, and they pass downward into the muddy slope deposits of the Los Molles Formation that can be seen to contain slope turbidites in this area.

The central part of the stratigraphic succession, up to 50 m thick, is dominated by two regressive cycles and one transgressive cycle. The first regressive package is characterized by FA 1.4 deposits overlying sequence boundary 2. Facies Association 1.4 coarse-grained channelized deposits are amalgamated, probably due to limited accommodation space, and they are capped by a transgressive surface that marks a backstepping of the system. This surface is highly bioturbated and in places (for example, Section 6, Fig. 1.19) overlain by wave-influenced deposits. The transgressive package is

characterized mainly by tidal inlet deposits (FA 4.1). The following regressive package is characterized by a renewed deltaic progradation (FA 2.1 and FA 2.2 in Fig. 1.19).

The uppermost 90 m of the Lower Lajas succession are highly aggradational but also characterized by four transgressive–regressive (T–R) cycles (Fig. 1.19). Given the overall regressive nature of the succession, these cycles are generally developed in more proximal environments (for example, subaqueous platform channels and minor shoreface deposits, lower delta-plain interdistributary bays with isolated distributary channels, and upper coastal-plain deposits) than the lower ones. From south-west to north-east there is a proximal to distal component of change. The T–R cycles are bounded by erosional surfaces which show a strong concentration of distributary channels (Fig. 1.19) cutting into lower delta plain and subaqueous platform deposits (FA 1.3 and FA 2.3). These surfaces are overlain by FA 4.2 and FA 1.2 channels (in places with tidal influence) and by FA 2.4 and FA 2.3 deposits in the interfluves, which define transgressive packages. These erosional surfaces have been interpreted as high-frequency sequence boundaries that coincide with transgressive surfaces. For example, the first high-frequency erosional surface is filled in by thick estuarine deposits (FA 4.2) capped by marshes or open bay deposits. The orientation of the outcrop belt (south-west/north-east) provides a near strike section in which incisions are evident. The regressive packages are composed mainly of FA 2.1, FA 2.3 and FA 1.3 deposits. The regressive–transgressive cycles developed in a more distal setting record HST and LST regressive intervals and TST packages, while cycles developed in a more proximal setting are composed mainly of TST and HST deposits (LST deposits are probably developed more basinward due to the overall progradation of the system).

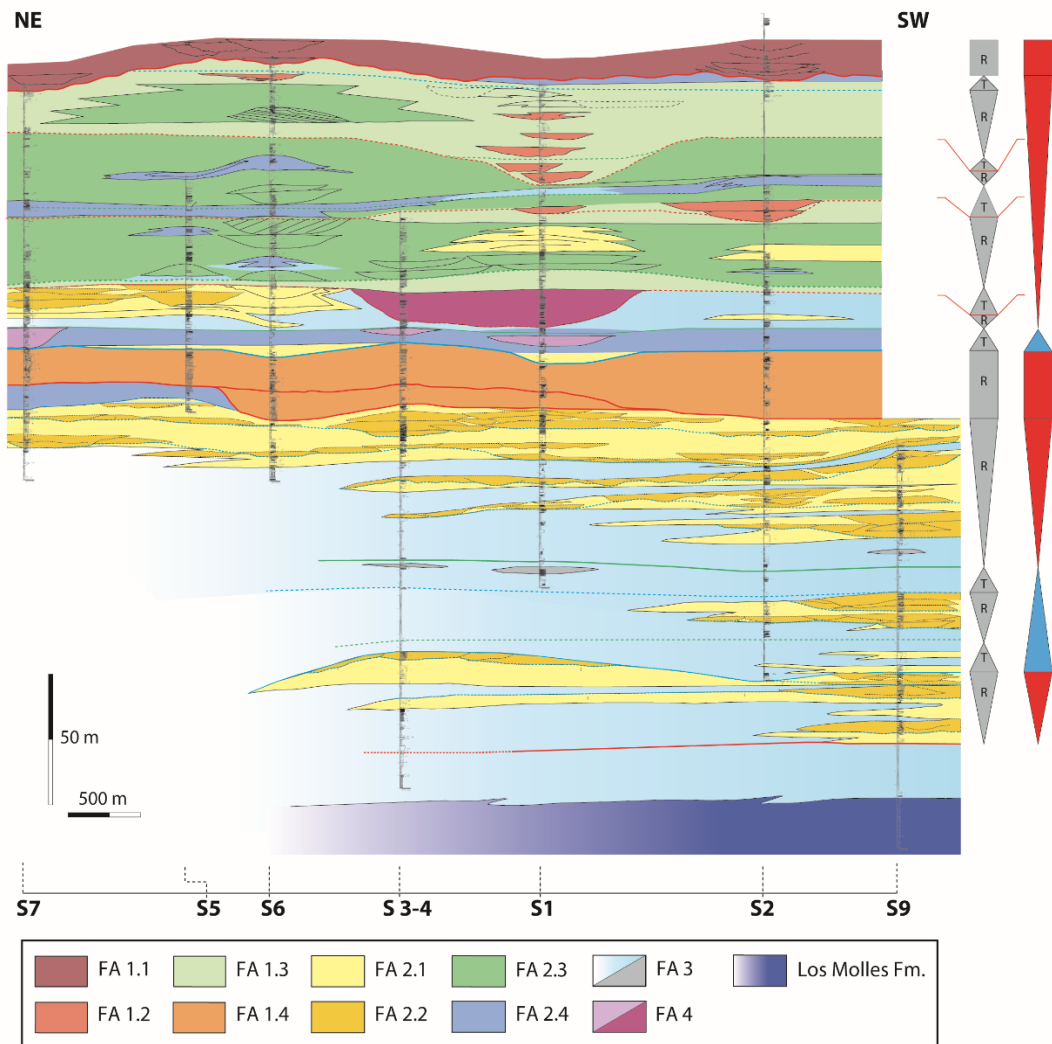


Figure 1.19: Correlation panel based on measured sections (S1 to S9). The outcrop belt is *ca* 7 km long and total stratigraphic thickness is *ca* 300 m. The overall succession is progradational (from deep-water deposits of the Los Molles Formation to upper coastal-plain deposits, Facies Association 1.1), but it is complicated by several regressive to transgressive cycles. The cross-section is slightly oblique to strike, with progradation from south-west (right) to north-east (left). A higher resolution version of this figure is available in Appendix A.

DISCUSSION

Vertical and lateral process variability in the Lajas Formation

In the Lajas system at Lohan Mahuida, the three process components (waves, tides and river currents) were active at the same time and spatially overlap with one another, creating a mixed-energy delta system that differs significantly from classical river-dominated, wave-dominated or tide-dominated deltas (Fig. 1.20).

The main *tidal signals* are strongest on the delta front, subaqueous platform and, to a lesser extent, in the distributary channel deposits. Tidal processes are recognized by small to large (possibly sigmoidal) cross-strata, in places with double mud or organic drapes; cross-strata and ripples that climb upward on the lee face of larger scale bedforms or bars; occasional sustained tidal bundling of dune-foreset thickness that reflects the varying strength of currents during spring and neap tidal periods; abundant reactivation surfaces; compound cross-bedding; rhythmic lamination in fine-grained sediments; and cyclic change in organic/mud draping along the foresets of individual cross-strata.

The *wave signals* are strongest on the shelf, shoreface or prodelta region, where they develop hummocky cross-stratification (HCS) with metre-scale wavelengths; or in bottomsets of dunes, where there are wave ripples and possibly combined-flow ripples. Occasionally shoreface deposits are likely to be developed on spits that were off-axis with respect to the main distributary channels. These shoreface deposits are characterized by amalgamated HCS beds or by small coarsening-upward stratal packages, with small 3D cross-strata, swales and combined-flow ripples.

The *fluvial signals* are always mixed with the other processes, but their distinctive signal comes as river-flood pulses that can be recognized by intervals or lenses of coarse-grained or pebbly sediment within sharp and erosionally based beds. These fluvial strata are then invariably partially reworked by waves or tides in the distal delta-front region.

The most easily recognizable fluvial sediments are moderate to poorly sorted, and associated with wood and plant fragments and other large quantities of organic debris.

In the Lajas system there was a broad spatial and temporal partitioning of the three processes. Fluvial signals in the stratigraphy are strongest landward, whereas wave signals are strongest in the most distal strata or in lateral areas with respect to the main river input (Figs 1.21, 1.22 and 1.23). Tidal signals are the least predictable, but they show the strongest influence in the delta front and subaqueous platform deposits (as also shown in other cases, e.g. Dalrymple & Choi, 2007). An additional complexity in the partitioning of wave, river and tidal signals is that they not only change spatially, but they can also change temporally (Fig. 1.21; cf. Ta et al., 2002a; Plink-Björklund, 2012; Olariu, 2014). Through time, landward and seaward movements of the shoreline, accompanied by changes in coastal morphology, enhanced or reduced the influence of any of the three processes, thus further complicating process partitioning in the stratigraphy. Lateral facies transitions related to process changes can be extremely abrupt in mixed-energy systems (Ainsworth et al., 2011; Olariu, 2014). Vertical process (and facies) variability is related to time and spatial changes in process dominance in different sub-environments, and can be caused by allogenic or autogenic processes. Instead lateral process variability is more likely to be related to autogenic causes. For example, the change between subtidal channels and wave-influenced lateral shorefaces (Fig. 1.19) is probably related to autogenic processes, i.e. it occurs without any obvious change in external forcing (see also Olariu, 2014). On the contrary, the change from tide-reworked delta-front deposits to amalgamated, tidally modulated braided distributary channels (Fig. 1.19) is more likely to be related to an allogenic change in relative-base level. This process partitioning is important because it controls the distribution of sand, which in the Lajas system is

concentrated in areas of strong tides and river currents (delta-front and tide-influenced subaqueous channels).

As a general rule, sediment sorting is indicative of the degree of marine reworking: better sorted sediments are more likely to be the product of wave and/or tidal reworking, whereas more poorly sorted sediments are likely to be river-borne (see also Plink-Björklund, 2012). Similar process distributions (river influence stronger in proximal and distal distributary channels, tidal influence stronger in the subaqueous platform and delta-front areas, wave influence stronger in more distal settings and areas lateral to the main river mouth) have also been recognized in the Tilje Formation (Ichaso & Dalrymple, 2014).

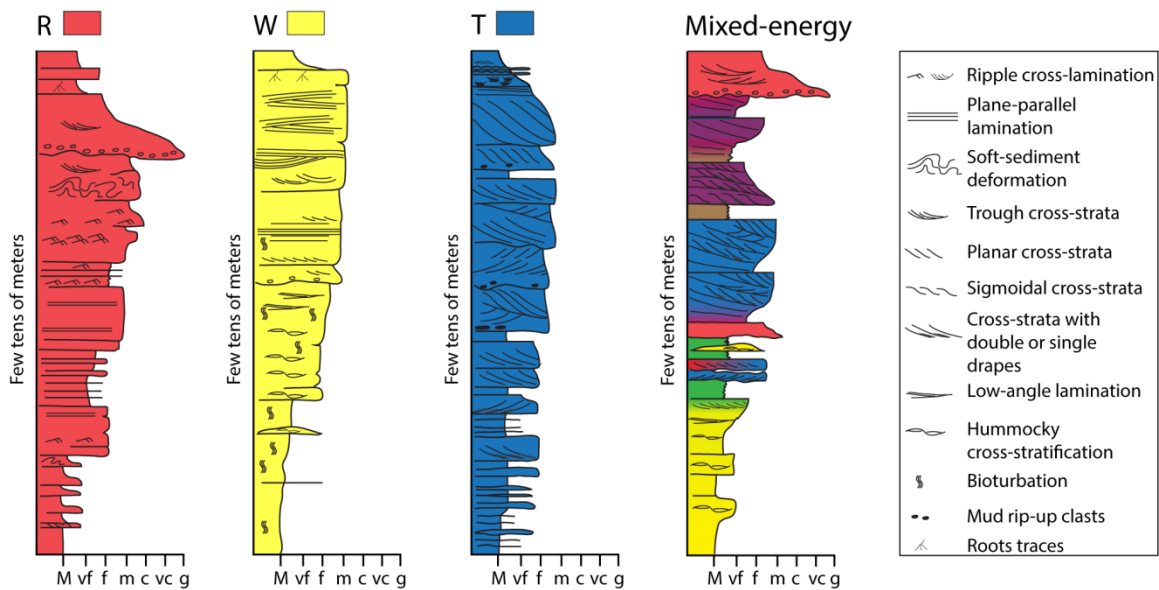


Figure 1.20: Schematic logs illustrating the differences between a mixed-energy delta (based on the Lajas Formation) and classical river-dominated, wave-dominated and tide-dominated deltas (based on Willis, 2005; Bhattacharya, 2010; Charvin et al., 2010; Olariu et al., 2010). Different colours represent a process dominance: red river (R), yellow waves (W) and blue tides (T). Purple represents mixed tide and river processes, green represents mixed tide and wave processes, and brown represents a mix of all three processes. M = mud; vf = very fine sand; f = fine sand; m = medium sand; c = coarse sand; vc = very coarse sand; g = gravel.

Lower Lajas Palaeogeography

A palaeogeographic reconstruction of the Lajas delta system based on all the observations presented in this paper is shown in Fig. 1.22. The palaeogeographic sketch map shows two possible scenarios for the lower delta. One scenario involves shallow, amalgamated and relatively coarse-grained distributary channels, probably braided in nature (FA 1.4) and the other is given by finer grained, small and isolated distributary channels encased in laminated mudstones (FA 1.2). Facies Association 1.4 produces an

extensive unit in the lower half of the studied succession, while Facies Association 1.2 constitutes a large portion of the upper part of the succession (Fig. 1.19).

The palaeogeographic sketch map hypothesizes that the two styles of lower delta-plain channels (FA 1.4 and FA 1.2) can potentially co-exist in different portions of a larger scale delta system, as a function of different discharges through different branches of the distributive system. These channels were probably parts of relatively small, coarse-grained, sandy rivers. Alternatively, these two styles did not co-exist, but appeared and dominated at different times. In other words, during periods of steeper depositional gradients and falling relative-base level, FA 1.4 developed in the lower delta plain, whereas during periods of high aggradation FA 1.2 would have developed (a very similar reconstruction has been suggested also for the Pleistocene to Holocene evolution of the Orinoco Delta; Warne et al., 2002). In both cases, when the distributary channels entered the basin, they would have created distributary-mouth bar deposits (FA 2.1). Channel continuation across the subaqueous platform allowed the formation of subtidal channel deposits (FA 2.3). Different processes can co-exist and overlap in mixed-energy deltas. Figure 1.23 shows how complex this interaction can be.

In order to justify the coarse-grained nature of the upper delta plain (conglomerates and pebbly sandstones with no sign of point bar development) and the sand-rich character of the delta front (medium-grained and fine-grained sandstones), the interpretation is that the main source area was not very far away and gradients were possibly high (due to syn-depositional tectonic activity). A high gradient system would also justify a limited landward penetration of the tidal wave into the fluvial reach. An additional consideration is that tidal-current reworking in the Lohan Mahuida area was much stronger than in areas to the east (Los Molles area, see Kurcinka, 2014). This observation, coupled with a significantly thicker Lajas Formation succession in the Lohan

Mahuida compared with the Los Molles area (Quattrocchio et al., 1996; Martínez et al., 2008), and with biostratigraphic data suggesting an expanded stratigraphic section in Lohan Mahuida area compared to missing biozones in the Los Molles area (Martínez et al., 2008), suggests coeval tectonic downwarping at Lohan Mahuida. This might have played an important role in controlling tidal current strength by modifying shoreline morphology (i.e. creating an embayment) and bathymetry. In Lohan Mahuida, the Lajas deltaic system was strongly reworked by tidal currents, creating unique, sand-rich deposits in the delta-front and subtidal channels. Furthermore, between the Lohan Mahuida and Los Molles areas (*ca* 18 km apart) a succession *ca* 70 m thick where wave-influenced facies associations prevail has been recognized (Fig. 1.2). Figure 1.24 shows a possible reconstruction of the Lajas system at a larger scale. Figure 1.24 shows two main feeder river systems separated by a tectonic element (a fault or a fold) projected northward from the crestal trend of an uplifted Palaeozoic–Triassic block (Fig. 1.24). In this scenario, the systems to the east of the lineament are on an area of relative uplift, whereas the systems to the west are on an area of relative subsidence. The part of the deltaic system to the west was subject to much stronger reworking by tidal currents than the part of the system to the east. The tidal wave was probably entering the Neuquén Basin from the north or the west, and the subsiding area to the west of the inferred tectonic lineament would have provided an embayed coastline morphology favouring tidal-current enhancement. Given the poor constraints in the literature on the palaeogeography of the Neuquén Basin, it is not possible to rule out the likelihood that the Lajas system was bigger, and that the systems recognized in the Lohan Mahuida and Los Molles areas were in fact different distributary reaches of the same river, diverted by tectonic elements (possibly a fault or a fold). Furthermore, palaeocurrent data from different stratigraphic levels of the Lajas Formation at Lohan Mahuida (coloured arrows,

Fig. 1.24) seem to suggest a trend parallel or perpendicular to the fault and/or fold element, therefore pointing to an influence of this tectonic element on the development of the depositional systems. The deltaic system in the lower half of the studied Lajas Formation was characterized by palaeocurrents directed mainly towards the north and north-east. The depositional systems present in central part of the succession (developed above a sequence boundary and characterized by an increase in grain size, FA 1.4) show palaeocurrents directed mainly towards the north-west. In the upper part of the succession palaeocurrents are directed mainly towards the north and north-east. Additionally, there are palaeocurrents directed towards the south and east, which have been interpreted as due to (flood) tidal currents.

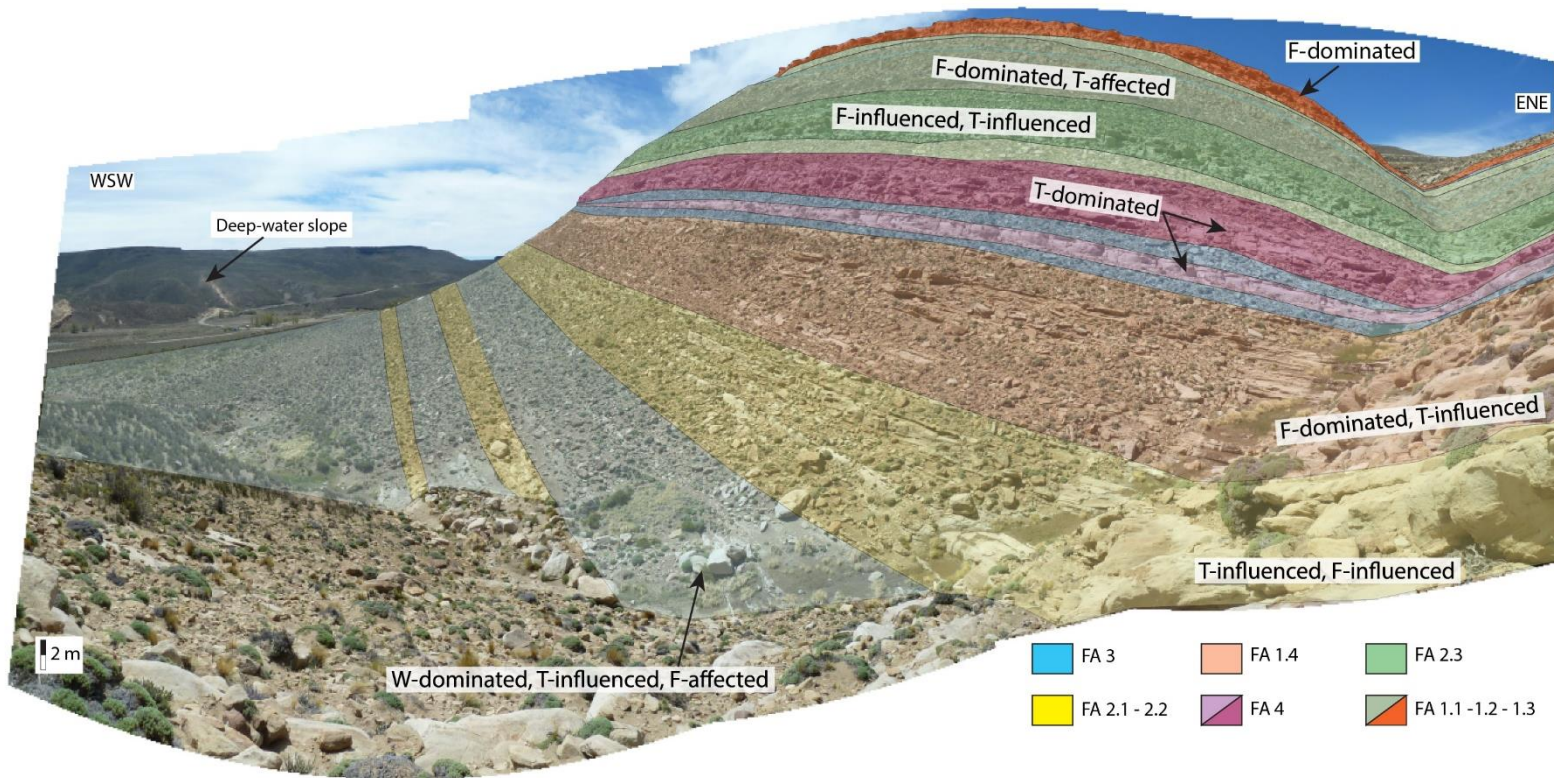


Figure 1.21: Photomosaic of Lohan Mahuida hillside (Section 1). Different colours refer to the correlation panel. The relative importance of the three processes [river (F), wave (W) and tidal (T) currents] throughout the succession (i.e. time changes) have been highlighted

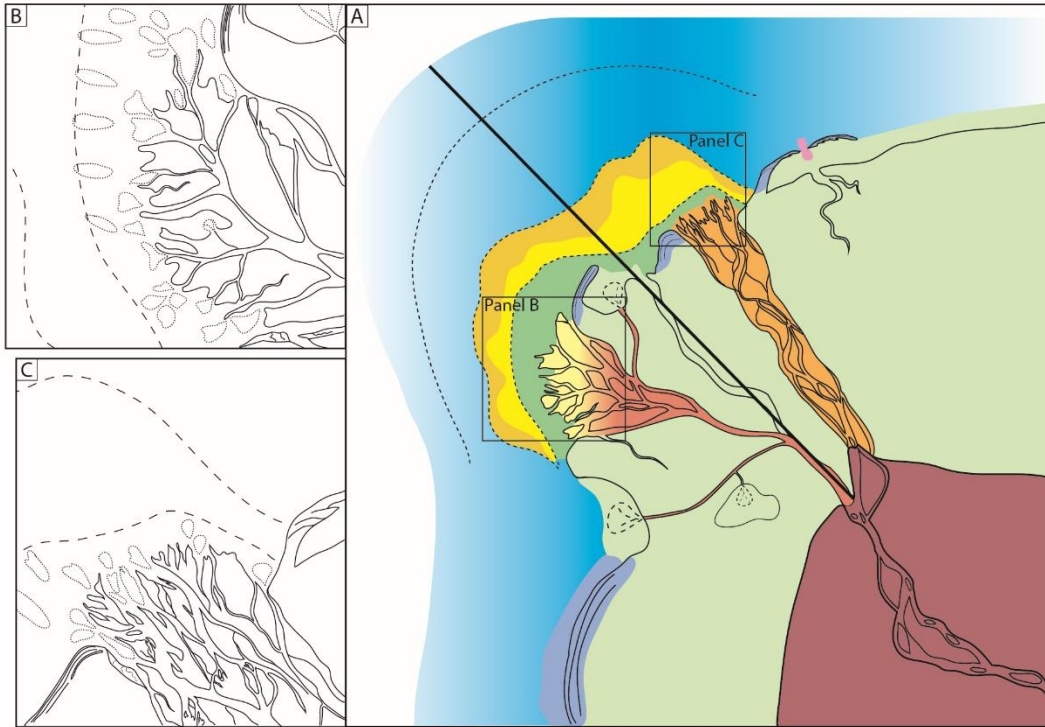


Figure 1.22: Palaeogeographic sketch map (not to scale) of the north-westerly Lajas deltaic system (regressive phase). This palaeogeography is based on the morphology of partially analogous modern examples in Taiwan, Kamchatka, Fraser River and Wax Lake Delta. (A) The palaeogeographic reconstruction shows a complex deltaic system. Moving from proximal to distal locations, fluvial-dominated, gravelly channels of the upper delta-plain pass downstream to sand-dominated, tide-influenced lower delta-plain channels. Distributary channels can be laterally adjacent to either the interdistributary bay areas (filled by organic-rich muds, marine influenced fine-grained deposits and small crevasse deltas), or to shoreface deposits. Further seaward a subaqueous platform is developed, passing into delta front and prodelta/shelf environments. This transition is accompanied by an increasing tidal and wave influence. The black line traced in the middle of the delta emphasizes that the two style of lower delta-plain channels (amalgamated or isolated in muddy sediments) can either co-exist or alternate through time. Colour-coded as Fig. 1.19. (B) Inset map showing details of the distributary channels, subaqueous platform bars and delta front in the case of a lower delta-plain dominated by bifurcating channels. (C) Inset map showing details of the distributary channels, subaqueous platform bars and delta front in the case of a lower delta-plain dominated by braided channels.

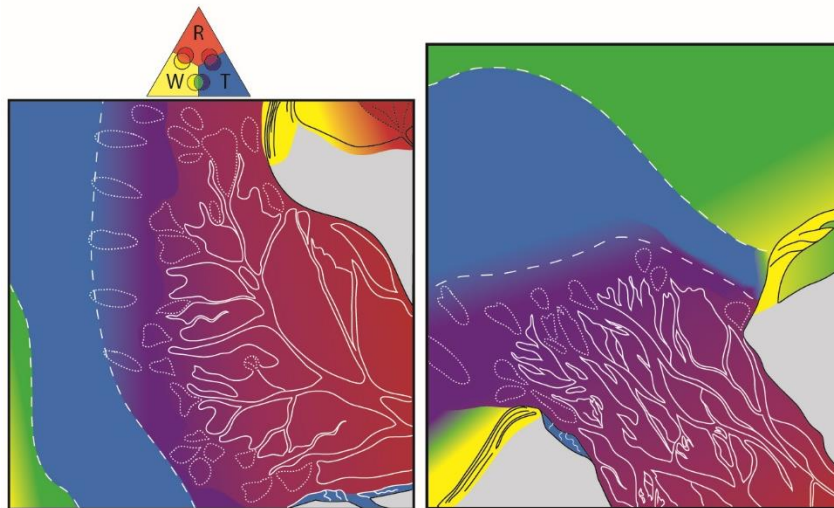


Figure 1.23: Plan view of panels (B) and (C) of Fig. 1.22. Different colours represent a process dominance: red river, yellow waves, and blue tides. Orange represents mixed wave and river processes, purple mixed tide and river processes, and green mixed tide and wave processes. The maps highlight the high lateral process variability in mixed-energy deltas. Different processes co-exist and interact at the same time in different areas of the delta system.

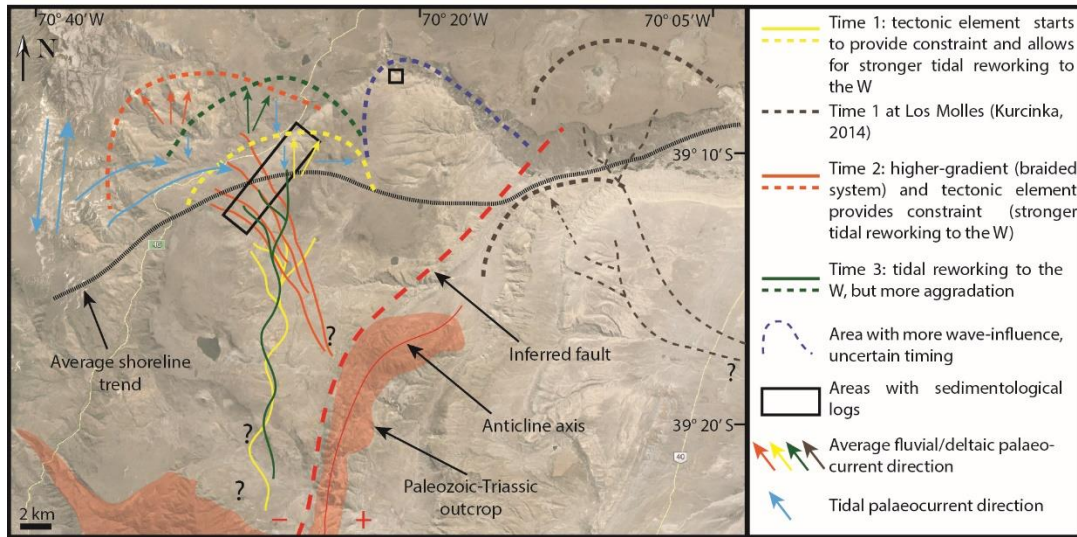


Figure 1.24: Speculative reconstruction of the Lajas palaeogeography. Two river systems or two main distributary reaches of the same system developed on the eastern and western side of a structural element (fold or fault; thick dashed red line). The eastern side underwent relative uplift and a thinner Lajas Formation succession was deposited here (Quattrocchio et al., 1996; Martínez et al., 2008), whereas the western side was located in an area of higher subsidence (based on missing biozones in the uplifted area and expanded stratigraphic section in the subsiding area; Martínez et al., 2008). Tidal currents reworked the deltaic deposits present to the west more efficiently (Lohan Mahuida area). Between the two main fluvial/deltaic fairways (yellow, orange, green and brown lines) a sheltered area with more wave influence was probably present (dashed blue line). Background image from Google Earth.

Sediment partitioning and reservoirs implications

From the above discussion it is clear that there were complex interactions between wave, tidal and fluvial processes, both in time and space, creating highly variable deltaic morphology (Figs 1.22 and 1.23) and heterogeneous architectural elements. Ultimately, these interactions controlled not only delta morphology, but also sand partitioning across different zones of the system. Facies Association 1.3 deposits are fine-grained with FA 1.2 channels isolated within muddy heterolithic deposits. Along the main sediment

fairways or during periods of increased gradient the distributary channels are shallow and coarse-grained (FA 1.4).

It is widely accepted (Nittrouer et al., 1996; Pirmez et al., 1998; Walsh et al., 2004; Swenson et al., 2005; Helland-Hansen & Hampson, 2009; Xue et al., 2010; Goodbred & Saito, 2012) that reworking by marine processes (waves and tides) generates a subaqueous platform (compound clinoform geometry, Fig. 1.25), which in modern delta examples is generally muddy, partially because it has been mainly reported from large sub-tropical deltas (Van Andel, 1967; Xue et al., 2010). The heterolithic subaqueous platform of the Lajas Formation was cut by isolated, sandy channels, filled by bars up to 5 m thick. In the Lajas system sand was transported even further seaward onto the delta front, where it was strongly reworked by tidal currents into amalgamated bars, whereas the remaining mud was mainly going through the system and deposited on the shelf and slope (Los Molles Formation). Subaqueous platforms reported from modern examples show a wide range of widths, mainly dependent on the energy of the marine environment (Roberts & Sydow, 2003; Swenson et al., 2005; Xue et al., 2010). Well-developed subaqueous platforms can extend for tens of kilometres, for example, Ganges-Brahmaputra (Kuehl et al., 1997; Goodbred & Kuehl, 1999) or Amazon (Nittrouer et al., 1996); others can be 5 to 10 km wide, for example, Mahakam (Roberts & Sydow, 2003, and Fig. 1.25 in this work) and, in some cases, the subaqueous platform is only a few kilometres wide (e.g. Xue et al., 2010). It can be expected that the wider the subaqueous platform, the finer the deposits will be at the rollover point of the delta front, due to the morphodynamic partitioning of sediment in the subaerial and subaqueous delta (see also Swenson et al., 2005). In the Ganges-Brahmaputra system, the subaqueous platform extends out to a depth of up to 30 m and it is composed of fine sand, while the foresets and bottomsets (delta front and prodelta/shelf) are muddy (Kuehl et al., 1997). Given the

very large amount of sand present in the Lajas system, both in the subaqueous platform and in the delta front, here it is assumed that the former was not very wide, probably only a few kilometres. Alternatively it can be expected that when and where there is a development of amalgamated, coarse-grained distributary channels (FA 1.4) in the lower coastal plain, the subaqueous platform is very limited or does not exist, and the delta-front deposits are very sandy and composed of amalgamated bars. On the other hand, FA 2.3 deposits encased in muddy sediments in the subaqueous platform would be strictly associated with more isolated distributary channels (FA 1.2) and in this case it is likely that the delta front would also be less sand-rich. Deltaic tongues gradually fine and thin over distances of a few kilometres and pass into bioturbated muddy sandstones.

Recognition of the mixed-energy character of a deltaic system is extremely important also for reservoir characterization. Lateral facies transitions within the studied units in the Lajas mixed-energy system can be very abrupt (even in a few hundred metres, see Fig. 1.19) and would have major impact on reservoir modelling and characterization. As an example, FA 2.3 channels (500 to 1000 m wide) in the subaqueous platform (Fig. 1.19) are encased in heterolithic deposits and adjacent to small wave-influenced sandbodies (FA 2.4) or mouth-bar deposits (FA 2.1). The distance between different sandbodies (either wave or tide-influenced) varies between less than 100 m to *ca* 1 km. On the other hand, delta-front deposits and amalgamated channels related to sequence boundaries (Fig. 1.19) are more laterally continuous (minimum 6 to 7 km). Fourth-order sequence boundaries can produce localized incisions filled by stacked distributary channels or estuarine deposits up to 15 m thick. These incisions are *ca* 500 to 1000 m wide in proximal settings of the lower delta plain, while they are 3 km wide further downdip, where estuarine deposits occur.

The relative importance of river, wave and tidal currents has a major impact on reservoir properties. Fluvial-dominated deposits tend to be coarser-grained, poorly sorted, and contain a high concentration of poorly organized plant and wood fragments, while tide-influenced and wave-influenced deposits are finer grained and better sorted.

Furthermore, the relative importance of river, wave or tidal currents impacts sandbody geometry and flow properties (Brandsæter et al., 2005). For example, FA 2.1 mouth bars are likely to have an aspect ratio determined by river processes (length to width ratio of *ca* 2:1), with tidal currents reworking sediments only during low-discharge periods and creating possible horizontal and vertical permeability barriers. On the contrary, FA 2.2 sandbodies are strongly reworked by tidal currents, and they can be channelized or non-channelized. Where FA 2.2 sandbodies are non-channelized, they are likely to have a greater aspect ratio.

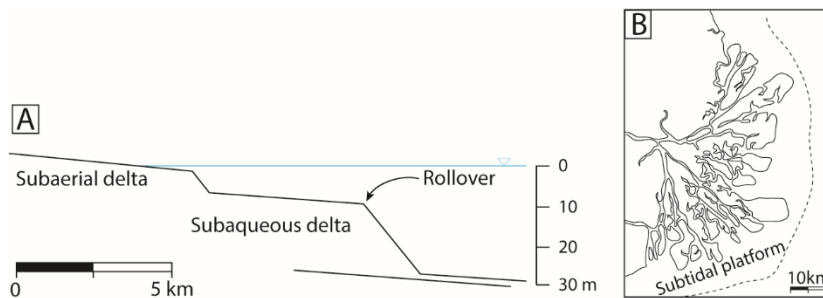


Figure 1.25: (A) Conceptual model of a compound clinoform, showing the subaerial delta and the subaqueous delta (modified from Swenson et al., 2005). (B) Plan view of the Mahakam delta, showing the subaqueous limit of the subtidal platform (redrawn after Roberts & Sydow, 2003).

Comparison with modern systems

In the modern, there are few well-described examples of mixed-energy deltas. The Mahakam delta (Fig. 1.25B) shows strong river and tidal influence, with minor wave

reworking (Roberts & Sydow, 2003). The Mekong delta shows an evolution from strongly tide-influenced to wave-influenced and tide-influenced through time, as the delta prograded and moved out of a protected embayment (Ta et al., 2002a,b; Xue et al., 2010). In the Holocene Mekong River delta deposits, subaqueous platform facies (mainly silts and sands with wavy and flaser bedding, cross-lamination, small cross-strata and parallel lamination) show tidal influence accompanied in places by wave influence (Ta et al., 2002b). Another possible good analogue for the Lajas system is the north-west Borneo coast (Crevello et al., 1997; Lambiase et al., 2003; Saller & Blake, 2003). Here, transtensional and transpressional tectonics affected the shelf and slope areas (Crevello et al., 1997; Saller & Blake, 2003) and they influenced deltaic deposition as well as sedimentary processes (Lambiase et al., 2003). As pointed out before, many of these modern systems occur in the Indo-Pacific zone and tend to be mud-rich, whereas the ancient example of the Lajas deltas is extremely sand-rich. Possible additional modern analogues for such a system can be found in Canada and Alaska, in the Fraser and Copper river deltas, respectively (Galloway, 1976; Carle & Hill, 2009; Ayranci et al., 2012; Dashtgard et al., 2012). Both of these systems are developed close to the sediment source (coastal range) and are quite sandy. The Fraser River delta shows a very sandy delta front and development of many subtidal channels. The Copper River delta shows clear influence of waves (barrier islands and sand spits), tides (tidal channels) and rivers (braided system).

The ternary diagram based on Galloway (1975) does not encompass the great complexity and variability in mixed-energy deltaic systems (see also Lambiase et al., 2002; Vakarelov & Ainsworth, 2013). Mixed-energy deltas show a high degree of process variability both in space and time. When thinking about changes in process regime or depositional systems through time, there is a tendency to associate these events

with base-level changes associated with the formation of incised valleys, estuaries and deltas (Dalrymple et al., 1992). However, when dealing with mixed-energy deltas, changes in dominant processes can easily occur at shorter time scales (Olariu, 2014) due to autogenic processes (for example, the Mekong delta; Ta et al., 2002a,b). These changes are very important, because they control the distribution of architectural elements and their heterogeneities, sediment partitioning and also delta morphology.

CONCLUSIONS

The Lajas Formation provides a fine example of a sand-rich mixed-energy delta, where it is possible to recognize process variability at different scales (bed scale, delta lobe scale and delta complex scale). It also provides the first description of subaqueous platform deposits in an ancient outcrop example.

The Lajas Formation is characterized by an overall regressive trend, from distal shelf deposits adjacent to the deep-water slope deposits of the Los Molles Formation up to upper delta plain and alluvial deposits. The succession is punctuated by several regressive–transgressive cycles (Fig. 1.19), developed by the basinward–landward transiting of the Lajas delta system. Within each cycle it is possible to recognize the varying influence and signals of waves, tides and river currents. The *tidal signals* are: (i) small to large (sigmoidal) cross-strata with double mud or organic drapes; (ii) cross-strata and ripples that climb upward on the lee face of larger scale bedforms or bars; (iii) occasional sustained tidal bundling of dune-foreset thickness; (iv) abundant reactivation surfaces; (v) compound cross-bedding; (vi) rhythmic lamination in fine-grained sediments; and (vii) cyclic change in organic/mud draping along the foresets of individual cross-strata. The *wave signals* are: (i) (amalgamated) hummocky cross-stratification (HCS) sets with metre-scale wavelengths; (ii) wavy beds; (iii) low-angle lamination; (iv) wave and combined-flow ripples and (v) swales. The *fluvial signals* are always mixed

with the other processes, but they are recognized as: (i) intervals or lenses of coarse-grained or pebbly sediment within sharp and erosionally based beds; (ii) intervals with poor sorting; and (iii) large quantities of wood, plant fragments and organic debris.

Overall, wave influence decreased and river influence increased in the succession upward through time, due to the overall progradational trend of the succession. In other words, wave energy was stronger in the distal and lateral reaches of the delta system, whereas river currents were stronger in more proximal areas. Tidal energy was stronger in the delta front and subaqueous platform areas. Strong tidal currents played a key role in the reworking of sediments in the delta front and subaqueous platform, producing tidal bars and compound dunes. The final stratigraphic record is strongly influenced by this reworking, so that these deltaic deposits are very different from the simple coarsening-upward trend typical of river-dominated and wave-dominated deltas. The Lajas system at Lohan Mahuida was probably influenced by syndepositional tectonic activity, that controlled the locus of strong tidal reworking and the development of sequence boundaries associated with abrupt increase in grain sizes.

Lateral and vertical process variability (and therefore facies changes) can be extremely abrupt in mixed-energy systems. Vertical process variability can be caused by allogenic or autogenic processes, whereas lateral process variability is more likely to be related to autogenic causes.

The Lajas system is a clean-water sand-rich deltaic system, very different from the majority of modern tide-influenced examples that are extremely muddy. The availability of sand is probably related to the closeness of the source area, possibly enhanced by tectonic activity. Another important factor that contributed to create sand-rich deposits is the high degree of reworking by marine processes, especially tidal currents. The sand-rich character of the Lajas Formation has important implications for

the assessment of the main sand belts in this Formation in the Neuquén subsurface. It may also improve current understanding of the expected reservoir architecture of mixed-energy systems such as the reservoirs of the Tilje, Ile and Garn formations in the oil fields of the Norwegian Continental Shelf. The main sandbodies are located in the fairways of the distributary channels, in the subaqueous platform (as isolated sandbodies) and in the delta-front (as amalgamated sandbodies).

ACKNOWLEDGEMENTS

This study is part of the Lajas Project, a collaborative project between the University of Texas at Austin, the University of Manchester, Queen's University and the Universidad Nacional de La Plata. The authors are very thankful to Statoil, Woodside, VNG Norge and BHP Billiton for economic support to the Lajas Project. We would like to thank the Lajas Project PIs Steve Flint and Gonzalo Veiga for guidance and discussion, and in particular project PI Robert Dalrymple for great help in the field. The authors are thankful to Heinz Kollmann for useful discussion. The authors would also like to thank Allard Martinius and Piret Plink-Björklund for very constructive comments that helped to greatly improve the manuscript.

REFERENCES

- Agirrezabala, L. M., and de Gibert, J. M., 2004, Paleodepth and Paleoenvironment of *Dactyloidites otto* (Geinitz, 1849) from Lower Cretaceous Deltaic Deposits (Basque-Cantabrian Basin, West Pyrenees): *PALAIOS*, v. 19, no. 3, p. 276-291.
- Ainsworth, R. B., Flint, S. S., and Howell, J. A., 2008, Predicting coastal depositional style: influence of basin morphology and accommodation to sediment supply ratio within a sequence stratigraphic framework: Recent advances in models of shallow-marine stratigraphy: *SEPM Special Publication*, v. 90, p. 237-263.
- Ainsworth, R. B., Vakarelov, B. K., and Nanson, R. A., 2011, Dynamic spatial and temporal prediction of changes in depositional processes on clastic shorelines: toward improved subsurface uncertainty reduction and management: *AAPG bulletin*, v. 95, no. 2, p. 267-297.

- Allen, P. A., and Homewood, P., 1984, Evolution and mechanics of a Miocene tidal sandwave: *Sedimentology*, v. 31, no. 1, p. 63-81.
- Amir Hassan, M. H., Johnson, H. D., Allison, P. A., and Abdullah, W. H., 2013, Sedimentology and stratigraphic development of the upper Nyalau Formation (Early Miocene), Sarawak, Malaysia: A mixed wave- and tide-influenced coastal system: *Journal of Asian Earth Sciences*, v. 76, no. 0, p. 301-311.
- Ayranci, K., Lintern, D. G., Hill, P. R., and Dashtgard, S. E., 2012, Tide-supported gravity flows on the upper delta front, Fraser River delta, Canada: *Marine Geology*, v. 326–328, no. 0, p. 166-170.
- Bhattacharya, J. P., 2010, Deltas, *in* Dalrymple, B. W., and James, N. P., eds., *Facies models*, Volume 4, Geological Association of Canada, p. 233-264.
- Bhattacharya, J. P., and Giosan, L., 2003, Wave-influenced deltas: geomorphological implications for facies reconstruction: *Sedimentology*, v. 50, no. 1, p. 187-210.
- Bhattacharya, J. P., and Willis, B. J., 2001, Lowstand Deltas in the Frontier Formation, Powder River Basin, Wyoming: Implications for Sequence Stratigraphic Models: *AAPG Bulletin*, v. 85, no. 2, p. 261-294.
- Brandsæter, I., McIlroy, D., Lia, O., Ringrose, P., and Næss, A., 2005, Reservoir modelling and simulation of Lajas Formation outcrops (Argentina) to constrain tidal reservoirs of the Halten Terrace (Norway): *Petroleum Geoscience*, v. 11, no. 1, p. 37-46.
- Burgess, P. M., Flint, S., and Johnson, S., 2000, Sequence stratigraphic interpretation of turbiditic strata: An example from Jurassic strata of the Neuquén basin, Argentina: *Geological Society of America Bulletin*, v. 112, no. 11, p. 1650-1666.
- Carle, L., and Hill, P. R., 2009, Subaqueous Dunes of the Upper Slope of the Fraser River Delta (British Columbia, Canada): *Journal of Coastal Research*, v. 25, no. 2, p. 448-458.
- Charvin, K., Hampson, G. J., Gallagher, K. L., and Labourdette, R., 2010, Intra-parasequence architecture of an interpreted asymmetrical wave-dominated delta: *Sedimentology*, v. 57, no. 3, p. 760-785.
- Clifton, H. E., 1982, Estuarine deposits, *in* Scholle, P. A., and Spearing, D., eds., *Sandstone Depositional Environments*: Tulsa, OK, American Association of Petroleum Geologists, p. 179-189.
- Clifton, H. E., and Phillips, R. L., 1980, Lateral trends and vertical sequences in estuarine sediments, Willapa Bay, Washington, *in* Field, M. E., Bouma, A. H., Colburn, I. P., Douglas, R. G., and Ingle, J. C., eds., *Quaternary Depositional Environments of the Pacific Coast*, Volume Pacific Coast Paleogeography Symposium 4, Society of Economic Paleontologists and Mineralogists Pacific Section, p. 55-71.
- Crevello, P., Morley, C., Lambiase, J., and Simmons, M., The Interaction of Tectonics and Depositional Systems on the Stratigraphy of the Active Tertiary Deltaic Shelf Margin of Brunei Darussalam, *in* *Proceedings Proceedings of the Petroleum Systems of SE Asia and Australasia Conference 1997*, p. 767-772.
- Dalrymple, B. W., 2010, Tidal depositional systems, *in* James, N. P., and Dalrymple, B. W., eds., *Facies models*, Volume 4, Geological Association of Canada, p. 201-231.

- Dalrymple, R. W., 1984, Morphology and internal structure of sandwaves in the Bay of Fundy: *Sedimentology*, v. 31, no. 3, p. 365-382.
- Dalrymple, R. W., Baker, E. K., Harris, P. T., and Hughes, M. G., 2003, Sedimentology and stratigraphy of a tide-dominated, foreland-basin delta (Fly River, Papua New Guinea), *in* Sidi, F. H., Nummedal, D., Imbert, P., Darman, H., and Posamentier, H. W., eds., *Tropical Deltas of Southeast Asia—Sedimentology, Stratigraphy, and Petroleum Geology*, Volume 76, SEPM Special Publication, p. 147-173.
- Dalrymple, R. W., and Choi, K., 2007, Morphologic and facies trends through the fluvial–marine transition in tide-dominated depositional systems: A schematic framework for environmental and sequence-stratigraphic interpretation: *Earth-Science Reviews*, v. 81, no. 3–4, p. 135-174.
- Dalrymple, R. W., Knight, R. J., and Lambiase, J. J., 1978, Bedforms and their hydraulic stability relationships in a tidal environment, Bay of Fundy, Canada: *Nature*, v. 275, p. 100-104.
- Dalrymple, R. W., Zaitlin, B. A., and Boyd, R., 1992, Estuarine facies models; conceptual basis and stratigraphic implications: *Journal of Sedimentary Research*, v. 62, no. 6, p. 1130-1146.
- Dashtgard, S., Venditti, J., Hill, P., Sisulak, C., Johnson, S., and La Croix, A., 2012, Sedimentation across the tidal-fluvial transition in the lower Fraser River, Canada: *Sediment. Rec.*, v. 10, p. 4-9.
- de Gibert, J. M., Martinell, J., and Domènech, R., 1995, The rosetted feeding trace fossil *Dactyloidites ottoi* (Geinitz) from the Miocene of Catalonia: *Geobios*, v. 28, no. 6, p. 769-776.
- De Mowbray, T., and Visser, M. J., 1984, Reactivation surfaces in subtidal channel deposits, Oosterschelde, Southwest Netherlands: *Journal of Sedimentary Research*, v. 54, no. 3, p. 811-824.
- FitzGerald, D., Buynevich, I., and Hein, C., 2012, Morphodynamics and Facies Architecture of Tidal Inlets and Tidal Deltas, *in* Davis Jr, R. A., and Dalrymple, R. W., eds., *Principles of Tidal Sedimentology*, Springer Netherlands, p. 301-333.
- Franzese, J., Spalletti, L., Pérez, I. G., and Macdonald, D., 2003, Tectonic and paleoenvironmental evolution of Mesozoic sedimentary basins along the Andean foothills of Argentina (32°–54°S): *Journal of South American Earth Sciences*, v. 16, no. 1, p. 81-90.
- Franzese, J. R., Veiga, G. D., Schwarz, E., and Gómez-Pérez, I., 2006, Tectonostratigraphic evolution of a Mesozoic graben border system: the Chachil depocentre, southern Neuquén Basin, Argentina: *Journal of the Geological Society*, v. 163, no. 4, p. 707-721.
- Fürsich, F. T., and Bromley, R. G., 1985, Behavioural interpretation of a rosetted spreite trace fossil: *Dactyloidites ottoi* (Geinitz): *Lethaia*, v. 18, no. 3, p. 199-207.
- Fürsich, F. T., and Oschmann, W., 1993, Shell beds as tools in basin analysis: the Jurassic of Kachchh, western India: *Journal of the Geological Society*, v. 150, no. 1, p. 169-185.

- Galloway, W. E., 1975, Process framework for describing the morphologic and stratigraphic evolution of deltaic depositional systems, *in* Broussard, M. L., ed., *Deltas, Models for Exploration*, p. 87-98.
- Galloway, W. E., 1976, Sediments and stratigraphic framework of the Copper River fan-delta, Alaska: *Journal of Sedimentary Research*, v. 46, no. 3, p. 726-737.
- Goodbred Jr, S. L., and Saito, Y., 2012, Tide-dominated deltas, *in* Davis Jr, R. A., and Dalrymple, B. W., eds., *Principles of Tidal Sedimentology*, Springer Netherlands, p. 129-149.
- Goodbred, S. L., and Kuehl, S. A., 1999, Holocene and modern sediment budgets for the Ganges-Brahmaputra river system: Evidence for highstand dispersal to flood-plain, shelf, and deep-sea depocenters: *Geology*, v. 27, no. 6, p. 559-562.
- Hayes, M. O., 1980, General morphology and sediment patterns in tidal inlets: *Sedimentary Geology*, v. 26, no. 1-3, p. 139-156.
- Helland-Hansen, W., and Hampson, G. J., 2009, Trajectory analysis: concepts and applications: *Basin Research*, v. 21, no. 5, p. 454-483.
- Ichaso, A. A., and Dalrymple, R. W., 2014, Eustatic, tectonic and climatic controls on an early synrift mixed-energy delta, Tilje Formation (early Jurassic, Smørbukk Field, offshore mid-Norway), *in* Martinius, A. W., Ravnås, R., Howell, J. A., Steel, R. J., and Wonham, J. P., eds., *Depositional Systems to Sedimentary Successions on the Norwegian Continental Shelf, Volume 46*, International Association of Sedimentologists Special Publication, p. 339-388.
- Jablonski, B. V. J., 2012, Process Sedimentology and Three-Dimensional Facies Architecture of a Fluvially Dominated, Tidally Influenced Point Bar: Middle McMurray Formation, Lower Steepbank River Area, Northeastern Alberta, Canada [MSc MSc Thesis]: Queen's University.
- Jablonski, B. V. J., and Dalrymple, B. W., 2014, Fluvial Seasonality: A Predictive Tool for Deciphering the Sedimentological Complexity of Inclined Heterolithic Stratification Deposited on Large-Scale Tidal-Fluvial Point Bars?, CSPG/CSEG/CWLS GeoConvention 2013, (Integration: Geoscience engineering Partnership), AAPG/CSPG©2014: Calgary TELUS Convention Centre & ERCB Core Research Centre, Calgary, AB, Canada, 6-12 May 2013.
- Kidwell, S. M., Time scales of fossil accumulation: patterns from Miocene benthic assemblages, *in* Proceedings Third North American Paleontological Convention, Proceedings 1982, Volume 1, p. 295-300.
- Kidwell, S. M., and Bosence, D. W. J., 1991, Taphonomy and time-averaging of marine shelly faunas, *in* Allison, P. A., and Briggs, D. E. G., eds., *Taphonomy: Releasing the Data Locked in the Fossil Record*. : New York, Plenum Press, p. 115-209.
- Kidwell, S. M., Fürsich, F. T., and Aigner, T., 1986, Conceptual Framework for the Analysis and Classification of Fossil Concentrations: *Palaios*, v. 1, no. 3, p. 228-238.
- Kollmann, H. A., 2014, The extinct Nerineoidea and Acteonelloidea (Heterobranchia, Gastropoda): a palaeobiological approach: *Geodiversitas*, v. 36, no. 3, p. 349-383.
- Kuehl, S. A., Levy, B. M., Moore, W. S., and Allison, M. A., 1997, Subaqueous delta of the Ganges-Brahmaputra river system: *Marine Geology*, v. 144, no. 1-3, p. 81-96.

- Kurcinka, C., 2014, Sedimentology and facies architecture of the tide-influenced, river-dominated delta-mouth bars in the lower Lajas Formation (Jurassic), Argentina [MSc MSc Thesis]: Queen's University.
- Lambiase, J. J., Damit, A. R., Simmons, M. D., Abdoerrias, R., and Hussin, A., 2003, A Depositional model and the stratigraphic development of modern and ancient tide-dominated deltas in NW Borneo, *in* Sidi, F. H., Nummedal, D., Imbert, P., Darman, H., and Posamentier, H. W., eds., *Tropical Deltas of Southeast Asia—Sedimentology, Stratigraphy, and Petroleum Geology* Volume SEPM Special Publication 76, p. 109-123.
- Lambiase, J. J., Rahim, A. A. b. A., and Peng, C. Y., 2002, Facies distribution and sedimentary processes on the modern Baram Delta: implications for the reservoir sandstones of NW Borneo: *Marine and Petroleum Geology*, v. 19, no. 1, p. 69-78.
- MacEachern, J. A., Pemberton, S. G., Gingras, M. K., and Bann, K. L., 2010, Ichnology and facies models, *in* James, N. P., and Dalrymple, R. W., eds., *Facies models*, Volume 4, Geological Association of Canada.
- Martínez, M. A., Prámparo, M. B., Quattrocchio, M. E., and Zavala, C. A., 2008, Depositional environments and hydrocarbon potential of the Middle Jurassic Los Molles Formation, Neuquén Basin, Argentina: palynofacies and organic geochemical data: *Revista Geológica de Chile*, v. 35, no. 2, p. 279-305.
- Martínez, M. A., Quattrocchio, M. E., and Zavala, C. A., 2002, Análisis palinofacial de la Formación Lajas (Jurásico Medio), Cuenca Neuquina, Argentina. Significado paleoambiental y paleoclimático: *Revista Española de Micropaleontología*, v. 34, no. 1, p. 81-104.
- Martinius, A. W., and Gowland, S., 2011, Tide-influenced fluvial bedforms and tidal bore deposits (Late Jurassic Lourinhã Formation, Lusitanian Basin, Western Portugal): *Sedimentology*, v. 58, no. 1, p. 285-324.
- Martinius, A. W., Kaas, I., Næss, A., Helgesen, G., Kjærefjord, J. M., and Leith, D. A., 2001, Sedimentology of the heterolithic and tide-dominated tilje formation (Early Jurassic, Halten Terrace, Offshore Mid-Norway), *in* Martinsen, O. J., and Dreyer, T., eds., *Sedimentary Environments Offshore Norway — Palaeozoic to Recent*, Volume Volume 10, Norwegian Petroleum Foundation Special Publications, p. 103-144.
- Martinius, A. W., Ringrose, P. S., Brostrøm, C., Elfenbein, C., Næss, A., and Ringås, J. E., 2005, Reservoir challenges of heterolithic tidal sandstone reservoirs in the Halten Terrace, mid-Norway: *Petroleum Geoscience*, v. 11, no. 1, p. 3-16.
- McIlroy, D., Flint, S., Howell, J. A., and Timms, N., 2005, Sedimentology of the tide-dominated Jurassic Lajas Formation, Neuquén Basin, Argentina: Geological Society, London, Special Publications, v. 252, no. 1, p. 83-107.
- McIlroy, D., Flint, S. S., and Howell, J. A., 1999, Applications of high-resolution sequence stratigraphy to reservoir prediction and flow unit definition in aggradational tidal successions, *in* Hentz, T., ed., *Advanced Reservoir Characterization for the 21st Century.*, Volume 19, GCSSEPM Special Publications, p. 121-132.

- Mellere, D., and Steel, R. J., 1996, Tidal sedimentation in Inner Hebrides half grabens, Scotland: the Mid-Jurassic Bearreraig Sandstone Formation: Geological Society, London, Special Publications, v. 117, no. 1, p. 49-79.
- Morgans-Bell, H. S., and McIlroy, D., 2005, Palaeoclimatic implications of Middle Jurassic (Bajocian) coniferous wood from the Neuquén Basin, west-central Argentina: Geological Society, London, Special Publications, v. 252, no. 1, p. 267-278.
- Mutti, E., Tinterri, R., Di Biase, D., Fava, L., Mavilla, N., Angella, S., and Calabrese, L., 2000, Delta-front facies associations of ancient flood-dominated fluvio-deltaic systems: *Rev. Soc. Geol. Espana*, v. 13, no. 2, p. 165-190.
- Myrow, P. M., Lukens, C., Lamb, M. P., Houck, K., and Strauss, J., 2008, Dynamics of a Transgressive Prodeltaic System: Implications for Geography and Climate Within a Pennsylvanian Intracratonic Basin, Colorado, U.S.A: *Journal of Sedimentary Research*, v. 78, no. 8, p. 512-528.
- Nichols, M. M., and Biggs, R. B., 1985, Estuaries, *in* Davis Jr, R. A., ed., *Coastal Sedimentary Environments*: New York, Springer-Verlag, p. 77-186.
- Nittrouer, C. A., Kuehl, S. A., Figueiredo, A. G., Allison, M. A., Sommerfield, C. K., Rine, J. M., Faria, L. E. C., and Silveira, O. M., 1996, The geological record preserved by Amazon shelf sedimentation: *Continental Shelf Research*, v. 16, no. 5-6, p. 817-841.
- Olariu, C., 2014, Autogenic process change in modern deltas: lessons for the ancient, *in* Martinius, A. W., Ravnås, R., Howell, J. A., Steel, R. J., and Wonham, J. P., eds., *From Depositional Systems to Sedimentary Successions on the Norwegian Continental Margin Volume 46*, International Association of Sedimentologists, p. 149-166.
- Olariu, C., and Bhattacharya, J. P., 2006, Terminal Distributary Channels and Delta Front Architecture of River-Dominated Delta Systems: *Journal of Sedimentary Research*, v. 76, no. 2, p. 212-233.
- Olariu, C., Steel, R. J., Dalrymple, R. W., and Gingras, M. K., 2012, Tidal dunes versus tidal bars: The sedimentological and architectural characteristics of compound dunes in a tidal seaway, the lower Baronia Sandstone (Lower Eocene), Ager Basin, Spain: *Sedimentary Geology*, v. 279, p. 134-155.
- Olariu, C., Steel, R. J., and Petter, A. L., 2010, Delta-front hyperpycnal bed geometry and implications for reservoir modeling: Cretaceous Panther Tongue delta, Book Cliffs, Utah: *AAPG bulletin*, v. 94, no. 6, p. 819-845.
- Pirmez, C., Pratson, L. F., and Steckler, M. S., 1998, Clinoform development by advection-diffusion of suspended sediment: Modeling and comparison to natural systems: *Journal of Geophysical Research: Solid Earth*, v. 103, no. B10, p. 24141-24157.
- Plink-Björklund, P., 2008, Wave-to-tide facies change in a Campanian shoreline complex, Chimney Rock Tongue, Wyoming-Utah, USA, *in* Hampson, G. J., Steel, R. J., Burgess, P. M., and Dalrymple, B. W., eds., *Recent advances in models of shallow-marine stratigraphy: SEPM Special Publication, Volume 90*, p. 265-291.

- Plink-Björklund, P., 2012, Effects of tides on deltaic deposition: Causes and responses: *Sedimentary Geology*, v. 279, no. 0, p. 107-133.
- Pontén, A., and Plink-Björklund, P., 2007, Depositional environments in an extensive tide-influenced delta plain, Middle Devonian Gauja Formation, Devonian Baltic Basin: *Sedimentology*, v. 54, no. 5, p. 969-1006.
- , 2009, Process Regime Changes Across a Regressive to Transgressive Turnaround in a Shelf-Slope Basin, Eocene Central Basin of Spitsbergen: *Journal of Sedimentary Research*, v. 79, no. 1, p. 2-23.
- Quattrocchio, M. E., Zavala, C. A., García, V., and Volkheimer, W., Paleogeographic changes during the Middle Jurassic in the southern part of the Neuquén Basin, Argentina, *in* Proceedings Advances in Jurassic Research. Transtec Publications, Geo Research Forum, Switzerland, 1996, Volume 1-2, p. 467-484.
- Reynolds, A. D., 1999, Dimensions of paralic sandstone bodies: AAPG bulletin, v. 83, no. 2, p. 211-229.
- Rieu, R., van Heteren, S., van der Spek, A. J. F., and De Boer, P. L., 2005, Development and Preservation of a Mid-Holocene Tidal-Channel Network Offshore the Western Netherlands: *Journal of Sedimentary Research*, v. 75, no. 3, p. 409-419.
- Roberts, H. H., and Sydow, J., 2003, Late Quaternary stratigraphy and sedimentology of the offshore Mahakam delta, east Kalimantan (Indonesia), *in* Sidi, F. H., Nummedal, D., Imbert, P., Darman, H., and Posamentier, H. W., eds., *Tropical Deltas of Southeast Asia—Sedimentology, Stratigraphy, and Petroleum Geology*, Volume 76, SEPM Special Publication, p. 125-145.
- Rosenfeld, U., 1978, Litología y sedimentología de la formación Lajas (Jurásico Medio) en la parte austral de la Cuenca Neuquina, Argentina: *Acta Geológica Lilloana*.
- Saller, A., and Blake, G., 2003, Sequence stratigraphy and syndepositional tectonics of upper Miocene and Pliocene deltaic sediments, offshore Brunei Darussalam, *in* Sidi, F. H., Nummedal, D., Imbert, P., Darman, H., and Posamentier, H. W., eds., *Tropical Deltas of Southeast Asia — Sedimentology, Stratigraphy, and Petroleum Geology* SEPM Special Publication 76, p. 219-234.
- Spalletti, L., Veiga, G., and Schwarz, E., 2010, Facies and stratigraphic sequences of the Mesozoic Neuquén Basin (Western Argentina): continental to deep marine settings. , *in* del Papa, C. A., R., ed., *Field Excursion Guidebook*, 18th International Sedimentological Congress, Mendoza, Argentina, FE-C3 Mendoza, Argentina, p. 1-79.
- Swenson, J. B., Paola, C., Pratson, L., Voller, V. R., and Murray, A. B., 2005, Fluvial and marine controls on combined subaerial and subaqueous delta progradation: Morphodynamic modeling of compound-clinoform development: *Journal of Geophysical Research: Earth Surface*, v. 110, no. F2, p. 1-16.
- Ta, T. K. O., Nguyen, V. L., Tateishi, M., Kobayashi, I., Saito, Y., and Nakamura, T., 2002a, Sediment facies and Late Holocene progradation of the Mekong River Delta in Bentre Province, southern Vietnam: an example of evolution from a tide-dominated to a tide- and wave-dominated delta: *Sedimentary Geology*, v. 152, no. 3-4, p. 313-325.

- Ta, T. K. O., Nguyen, V. L., Tateishi, M., Kobayashi, I., Tanabe, S., and Saito, Y., 2002b, Holocene delta evolution and sediment discharge of the Mekong River, southern Vietnam: *Quaternary Science Reviews*, v. 21, no. 16–17, p. 1807-1819.
- Tänavsuu-Milkeviciene, K., and Plink-Björklund, P., 2009, Recognizing Tide-Dominated Versus Tide-Influenced Deltas: Middle Devonian Strata of the Baltic Basin: *Journal of Sedimentary Research*, v. 79, no. 12, p. 887-905.
- Thrana, C., Næss, A., Leary, S., Gowland, S., Brekken, M., and Taylor, A., 2014, Updated depositional and stratigraphic model of the Lower Jurassic Åre Formation, Heidrun Field, Norway, *From Depositional Systems to Sedimentary Successions on the Norwegian Continental Margin*, John Wiley & Sons, Ltd, p. 253-289.
- Tye, R. S., and Coleman, J. M., 1989, Evolution of Atchafalaya lacustrine deltas, south-central Louisiana: *Sedimentary Geology*, v. 65, no. 1–2, p. 95-112.
- Vakarelov, B. K., and Ainsworth, R. B., 2013, A hierarchical approach to architectural classification in marginal-marine systems: Bridging the gap between sedimentology and sequence stratigraphy: *AAPG bulletin*, v. 97, no. 7, p. 1121-1161.
- Van Andel, T. H., 1967, The Orinoco Delta: *Journal of Sedimentary Petrology*, v. 37, no. 2, p. 297-310.
- Vergani, G. D., Tankard, A. J., Belotti, H. J., and Welsink, H. J., 1995, Tectonic Evolution and Paleogeography of the Neuquén Basin, Argentina, *in* Tankard, A. J., Suarez Soruco, R., and Welsink, H. J., eds., *Petroleum Basins of South America*: Tulsa, OK, AAPG Memoir 62, p. 383-402.
- Walsh, J. P., Nittrouer, C. A., Palinkas, C. M., Ogston, A. S., Sternberg, R. W., and Brunskill, G. J., 2004, Clinoform mechanics in the Gulf of Papua, New Guinea: *Continental Shelf Research*, v. 24, no. 19, p. 2487-2510.
- Warne, A. G., Guevara, E. H., and Aslan, A., 2002, Late Quaternary Evolution of the Orinoco Delta, Venezuela: *Journal of Coastal Research*, v. 18, no. 2, p. 225-253.
- Wightman, D. M., and Pemberton, S. G., 1997, The Lower Cretaceous (Aptian) McMurray Formation: an overview of the Fort McMurray area, northeastern, Alberta, *in* Pemberton, S. G., and James, D. P., eds., *Petroleum Geology of the Cretaceous Mannville Group, Western Canada Volume 18*, Canadian Society of Petroleum Geologists p. 312-344.
- Willis, B. J., 2005, Deposits of tide-influenced river deltas, *in* Giosan, L., and Bhattacharya, J. P., eds., *River Deltas - Concepts, Models, and Examples*, Volume 83, SEPM Special Publication, p. 87-129.
- Willis, B. J., Bhattacharya, J. P., Gabel, S. L., and White, C. D., 1999, Architecture of a tide-influenced river delta in the Frontier Formation of central Wyoming, USA: *Sedimentology*, v. 46, no. 4, p. 667-688.
- Willis, B. J., and Gabel, S. L., 2003, Formation of Deep Incisions into Tide-Dominated River Deltas: Implications for the Stratigraphy of the Segó Sandstone, Book Cliffs, Utah, U.S.A: *Journal of Sedimentary Research*, v. 73, no. 2, p. 246-263.
- Wright, L. D., 1977, Sediment transport and deposition at river mouths: A synthesis: *Geological Society of America Bulletin*, v. 88, no. 6, p. 857-868.

- Xue, Z., Liu, J. P., DeMaster, D., Van Nguyen, L., and Ta, T. K. O., 2010, Late Holocene Evolution of the Mekong Subaqueous Delta, Southern Vietnam: *Marine Geology*, v. 269, no. 1–2, p. 46-60.
- Zavala, C. A., Sequence stratigraphy in continental to marine transitions. An example from the middle Jurassic Cuyo Group, South Neuquen Basin, Argentina, *in* Proceedings Advances in Jurassic Research Dürnten, Switzerland, 1996, Trans Tech Publications, GeoResearch Forum, p. 285-294.

Chapter 3: Quantifying process regime in ancient shallow marine mixed-energy depositional systems: what are sedimentary structures really telling us?²

ABSTRACT

Interpreting the whole range of river, wave and tidal interaction recorded in shallow-marine, coastal successions can be challenging. The complexity arises because sedimentary structures produced by all three processes can be fully or partially preserved in the same stratal packages, and many of these structures are not diagnostic of a specific process.

We therefore present a new methodology that assigns (percentage) the likely wave (w), tide (t) and river (r) process variability for a bed or stratal unit via a library of sedimentary structures and their non-unique process generators. Each bed or bedset can be characterized by a specific structure or multiple structures (taking also into account lateral variations). Percentage values of wave/tide/river processes of different structures can be averaged to create a final compound process probability for each bed. Vertical integration of process probability for individual beds in a rock succession creates probability graphs. The methodology has been applied on a 15 meters thick parasequence of the Jurassic Lajas Fm., Argentina, and is seen to efficiently couple classical facies analysis and surficial process studies to quantify process variability in ancient systems. The methodology here presented should help future studies that aim at a quantification of process variability, and it can point out current biases present in the scientific community.

² This Chapter has been submitted to JSR as: Rossi, V. M., Perillo, M. M., Steel, R. J., Olariu, C., Quantify process regime in ancient shallow marine mixed-energy depositional systems: what are sedimentary structures really telling us? I was the primary author of this work.

INTRODUCTION

Many shallow-marine coastal systems are characterized by the interplay of river, wave, and tidal currents (Yoshida et al., 2007; Plink-Björklund, 2008; Ainsworth et al., 2011; Vakarelov et al., 2012; Olariu, 2014; Rossi and Steel, 2016). The complexity of mixed-energy systems arises because the dominant process can change over short spatial and temporal scales (Yoshida et al., 2007; Ainsworth et al., 2011). For these reasons, predicting the evolution and resulting architecture of ancient mixed-energy shallow marine depositional systems is particularly challenging. The sedimentary structures produced by fluvial, wave, and tidal processes can be preserved so as to produce very complex stratal packages in mixed-energy systems. Therefore, in order to understand the role of different processes in such depositional systems and to successfully predict their evolution there is a need for quantifying the variability present in the stratigraphic record. The use of quantitative databases has been proven useful and is considerably growing (e.g., Colombera et al., 2012a; Colombera et al., 2016), as databases allow to store information from both modern and ancient systems in order to better characterize limited subsurface data. Many of the databases are used to characterize heterogeneities or architectures of reservoirs (Colombera et al., 2012a). The work presented in this paper can be used to improve these predictions, adding detail information on sedimentary structures and processes.

Ainsworth et al. (2011) proposed a classification of mixed-energy coastal systems (MECS), which emphasizes the extremely high spatial variability of these systems. Ainsworth et al. (2011) classification methodology is based on the thickness (and presumed time span) recorded by the dominant process. The study here presented builds upon their work and uses a quantitative approach to MECS, based on the probability of each sedimentary structure being associated with a physical process. Due to the inherent

complexity and heterogeneity of process distributions (e.g. Fig. 3.1) even over short distances (Ta et al., 2002; Ainsworth et al., 2011), MECS require a more inclusive analysis than simply weighting a most dominant sedimentary structure. Here we propose, once all facies characteristics are collected, assigning a ‘percentage of process’ indicator to each sedimentary structure (or facies), leading to a process probability index. To exemplify this methodology, a 15 m thick deltaic parasequence of the Jurassic Lajas Formation, in the Neuquén Basin (Argentina) is analyzed.

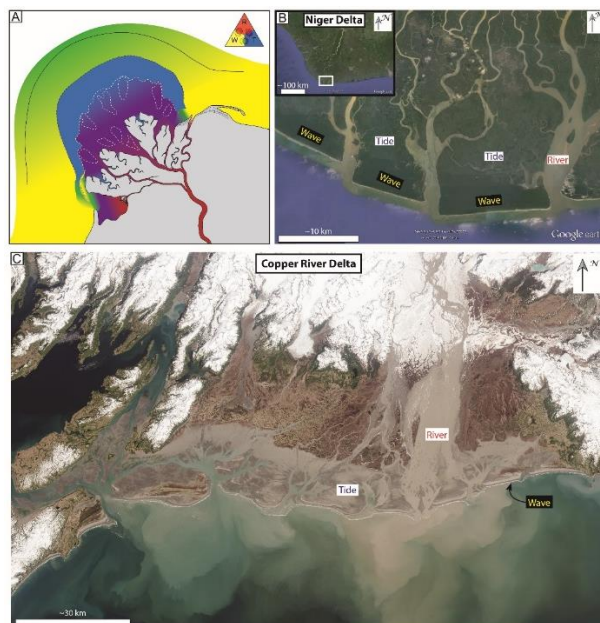


Figure 3.1: Process variability of mixed-energy deltas. (A) Simplified sketch of a deltaic system where river, wave and tidal processes are active at the same time. These processes can be active either in different parts of the delta system or in the same area, and they can vary through time. Process dominance is represented via a color-coded ternary diagram: yellow represents wave processes (W), red river processes (R) and blue tidal processes (T). In some areas more than one process can be active (i.e. purple represents co-existing tidal and river processes, green represents co-existing tidal and wave processes). This map is an example of the inherent complexity of mixed-energy systems. (B) Niger Delta; images from Google Earth. White rectangle in the inset shows the location within the delta of the image. (C) Copper River Delta; image from <http://earthobservatory.nasa.gov/>.

QUANTIFYING SHALLOW-MARINE MIXED-ENERGY SYSTEMS













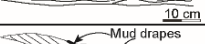

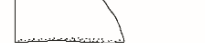
In order to distinguish and quantify the structures generated by waves, tides and river currents in shallow marine environments, we undertook an extensive literature review of ancient, modern and experimental works of the most common sedimentary structures (e.g., Jopling and Walker, 1968; Dalrymple et al., 1978; Allen, 1982; Kvale et al., 1989; Dumas et al., 2005). From this review (a complete list can be found in Appendix B) it is concluded that some common sedimentary structures are not uniquely connected with a single process (waves, tides and river currents), and thus they cannot be used with sufficient reliability to interpret a particular process domination. For example, current ripples have been described from river, wave, and tide-dominated settings (e.g. Dalrymple et al., 1978; Allen, 1982), while other structures, such as two-dimensional symmetrical ripples, are more confidently tied to waves (e.g. Dumas et al., 2005).

In order to overcome such ambiguity and quantify uncertainty, each sedimentary structure has been assigned a percentage (Table 3.1) that represents the frequency of association of each structure to a certain process (waves, tides, or river currents) in the literature (see Appendix B). The lower part of Table 3.1 takes into account characteristics such as grain sorting and bioturbation intensity. This additional information can be used to validate and refine the interpretation based on the sedimentary structures, and to decide whether the hydrodynamic interpretation agrees with this other interpretation.

This methodology is not intended as a replacement of classical facies analysis and of the use of facies models. The first step in the study of all sedimentary successions is the detailed characterization of the depositional environments through facies analysis. The methodology here presented can be used in a second phase, using the sedimentary structures, in order to quantify the role of wave, tides, and river currents on the deposition of the study succession (or in different subenvironments).

This methodology provides a tool, more refined than 'normal', that gives to each sedimentary structure a probability or likelihood of reflecting dominant process (P(w), P(t) and P(r)). For example, repeated mud drapes have 86% probability of being the result of tidal currents, 8% probability of being the results of river currents, and only 6% probability of being the results of wave currents. Since in reality different structures can be present at the same time (for example, sigmoidal cross-strata with mud or organic-draped foresets, Fig. 3.2), it is possible to sum two or more percentages to obtain a combined percentage (in this case the result is 79% probability of being the result of tidal currents, 15% probability of being the result of river currents, and 6% probability of being the result of wave action).

Table 3.1: Table of the main shallow marine sedimentary structures. This table is based on an extensive literature review, and it assigns a percentage to each sedimentary structure, that represents the probability for a certain structure to be the result of wave (P(w)), tidal (P(t)), or river currents (P(r)). For example, if eight out of ten papers recognize a sedimentary structure as the result of tidal currents, two as the result of river currents and zero as related to wave/storm currents, the percentages are as follow: P_w=0%, P_t=80%, and P_r=20%. Some sketches are redrawn after De Raaf et al. (1977); Boersma and Terwindt (1981); Dalrymple et al. (1990); Nio and Yang (1991); Dalrymple (2010).

Sedimentary structures (shallow marine)				
Structure	Sketch	P(w)	P(t)	P(r)
Symmetrical ripples		87%	10%	3%
Current ripples Climbing ripples		8%	38%	54%
HCS/SCS		92%	-	8%
Low-angle lamination		52%	24%	24%
Lenticular/wavy/ flaser bedding		31%	42%	27%
Cross-strata (unidirectional)		19%	48%	33%
Cross-strata (bi-directional)		10%	75%	15%
Bundles		6%	83%	11%
Rhythmic lamination		13%	81%	6%
Sigmoidal cross-strata		7%	71%	22%
Mud drapes		6%	86%	8%
Graded beds (event beds)		18%	4%	78%
Plane-parallel lamination		28%	30%	42%
Compound cross-strata		5%	74%	21%
Soft sediment deformation		13%	26%	61%
Texture/Bioturbation				
Process	w	t	r	
Sorting	Well sorted	Moderately to well sorted	Moderately to poorly sorted	
Grain roundness	Rounded	Sub-rounded/ Sub-angular	Sub-rounded to angular	
Coaly/Plant fragments	Scarce	Scarce/ abundant if concentrated in drapes	Abundant	
Bioturbation	Moderate to high bioturbation intensity (during fairweather) Fully marine	Low to high bioturbation intensity (can be in discrete horizons); stressed Fully marine or brakish	Low bioturbation intensity; stressed. Can be locally concentrated in discrete horizons (interflood)	
Bed geometries/Architecture				

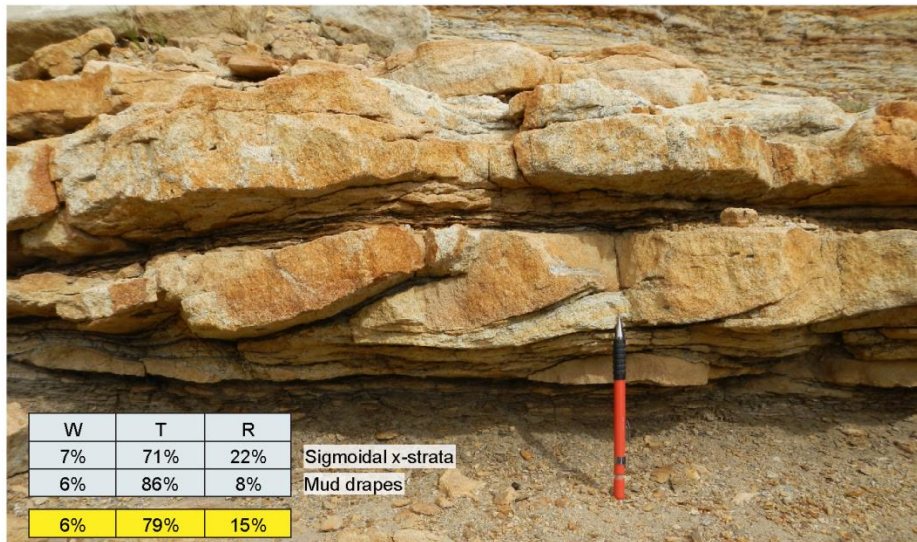


Figure 3.2: Example of how to calculate compound percentages. According to Table 3.1, sigmoidal cross strata have Pw=7%, Pt=71%, Pr=22%. However, the foresets of these cross-strata are draped by mud (Pw=6%, Pt=86%, Pr=8%). Therefore the total percentages that take into account both characteristics are: Pw=6%, Pt=79%, Pr=15%. This bed is located at 7 m from the bottom of the parasequence. Photo courtesy of Keith Adamson.

In order to evaluate possible trends and relations between sedimentary structures, hydrodynamic processes and different environments and sub-environments, several sedimentary logs from published literature (see Table 3.2 and Fig. 3.3) have been analyzed. Each log has been color-coded, using different colors for each sedimentary structure, process, and environment. Based on the thickness of each colored unit with respect to the total thickness, quantitative information on the relation between sedimentary structures, processes and environments can be calculated (see text below).

Table 3.2: List of references, location and age of the case studies used for the analysis of sedimentary logs.

Reference	Case Study
Bhattacharya and Walker (1991)	Dunvegan Formation, Alberta (Canada) – Upper Cretaceous
Choi (2011)	Gomso Bay, Korea – Modern
Fraser and Hester (1977)	Lake Michigan (USA) – Modern
Gani et al. (2009)	Wester Interior Seaway, Wyoming and Utah (USA) – Cretaceous
Kreisa and Moila (1986)	Curtis Formation, Utah (USA) – Upper Jurassic
Mellere and Steel (1996)	Bearreraig Sandstone Formation, Scotland – Middle Jurassic
Hampson (2000)	Blackhawk Formation, Utah (USA) – Upper Cretaceous
Mutti et al. (2000)	Trempe-Graus Basin, Spain – Eocene
Olariu and Bhattacharya (2006)	Lousiana, USA – Modern Ferron Sandstone, Utah (USA) – Cretaceous
Olariu et al. (2012)	Trempe-Graus Basin, Spain – Eocene
Plink-Björklund (2005)	Central Basin, Spitsbergen – Eocene
Pulham (1989)	Clare Basin, Ireland – Upper Carboniferous
Leva López et al. (2016)	Almond Formation, Wyoming (USA) – Upper Cretaceous
Ta et al. (2002)	Mekong River Delta, Vietnam – Late Holocene
Wightman and Pemberton (1997)	McMurray Formation, Alberta (Canada) – Lower Cretaceous
Rossi and Steel (2016)	Las Lajas Formation, Argentina – Middle-Late Jurassic



Figure 3.3: Location of the sedimentary logs published in the literature used to calculate the proportions of facies and processes in different environments and sub-environments.

Example 1: Las Lajas Fm. outcrop (Neuquén Basin)

A 15 meter thick parasequence of the Jurassic Lajas Formation of the Neuquén Basin, Argentina, is used to illustrate the proposed methodology. The Lajas Formation in the study area has been recently re-evaluated as a mixed-energy deltaic system characterized by river-, wave-, and tidal-influenced strata (Rossi and Steel, 2016). However, in order to unravel the range of process mixing a quantitative approach is needed. In the Lajas Formation, the same process variability present at the scale of the whole succession is also found at the parasequence scale. This is a good case study to quantify process variability and mixing.

In the studied deltaic parasequence (Fig. 3.4), the first 5 meters are dominated by hummocky strata (HCS), swaley strata (SCS) ($P_w = 92\%$, $P_r = 8\%$), and low-angle lamination ($P_w = 52\%$, $P_t = 24\%$, $P_r = 24\%$). These structures are associated with infrequent dune-generated cross-strata with bundled forests ($P_w = 6\%$, $P_t = 83\%$, $P_r = 11\%$) and ripple cross-lamination ($P_w = 8\%$, $P_t = 38\%$, $P_r = 54\%$). This interval presents

very fine to fine-grained, very well sorted sandstones, moderate to intense bioturbation (*Planolites*, *Paleophycus*, *Ophiomorpha*, *Thalassinoides*, *Macaronichnus* and *Cruziana*) and shell fragments, which confirm the interpretation that the lower part of the parasequence was deposited in a fully marine environment dominated by wave processes (Fig. 3.4).

The middle part of the parasequence is dominated by erosionally-based coarse-grained graded beds (Pw = 18%, Pt = 4%, Pr = 78%), that erode into fine-grained, heterolithic sediments. However, cross-strata (Pw = 19%, Pt = 48%, Pr = 33%), sigmoidal cross-strata with mud drapes (Pw = 6%, Pt = 79%, Pr = 15%; Fig. 2), bi-directional cross-strata (Pw = 10%, Pt = 75%, Pr = 15%), low-angle lamination (Pw = 52%, Pt = 24%, Pr = 24%), and sporadic HCS (Pw = 92%, Pr = 8%) are present. These structures indicate that tidal and wave currents were likely reworking fluvially-emplaced sandstone strata (Fig. 3.4). Sandstone strata are interbedded with heterolithic, wavy to lenticular bedded, deposits (Fig. 3.4) characterized by mm-thick organic-rich laminae and thin siltstone and sandstone beds; these beds are usually a few centimeters thick with wave- and current-ripple lamination (sometimes bi-directional). These heterolithic, fine-grained sediments represent deposition in a low-energy environment. Bioturbation is moderate and with marine trace fossils (*Paleophycus*, *Ophiomorpha*, *Planolites*). Grains are usually sub-rounded and the sorting is from moderate to good.

The upper part of the parasequence is dominated by cross-strata (Pw = 19%, Pt = 48%, Pr = 33%), some of which show mud or organic-rich drapes (Pw = 6%, Pt = 86%, Pr = 8%), bidirectional paleocurrents (Pw = 10%, Pt = 75%, Pr = 15%), and rarely foreset bundles (Pw = 6%, Pt = 83%, Pr = 11%). Compound cross-strata (Pw = 5%, Pt = 74%, Pr = 21%) are also present. However, erosional surfaces and wood fragments have become

increasingly abundant, pointing towards increased terrestrial input (Fig. 3.4), but the environment is still subaqueous, as indicated by trace fossils (*Dactyloidites* or *Cruziana*).

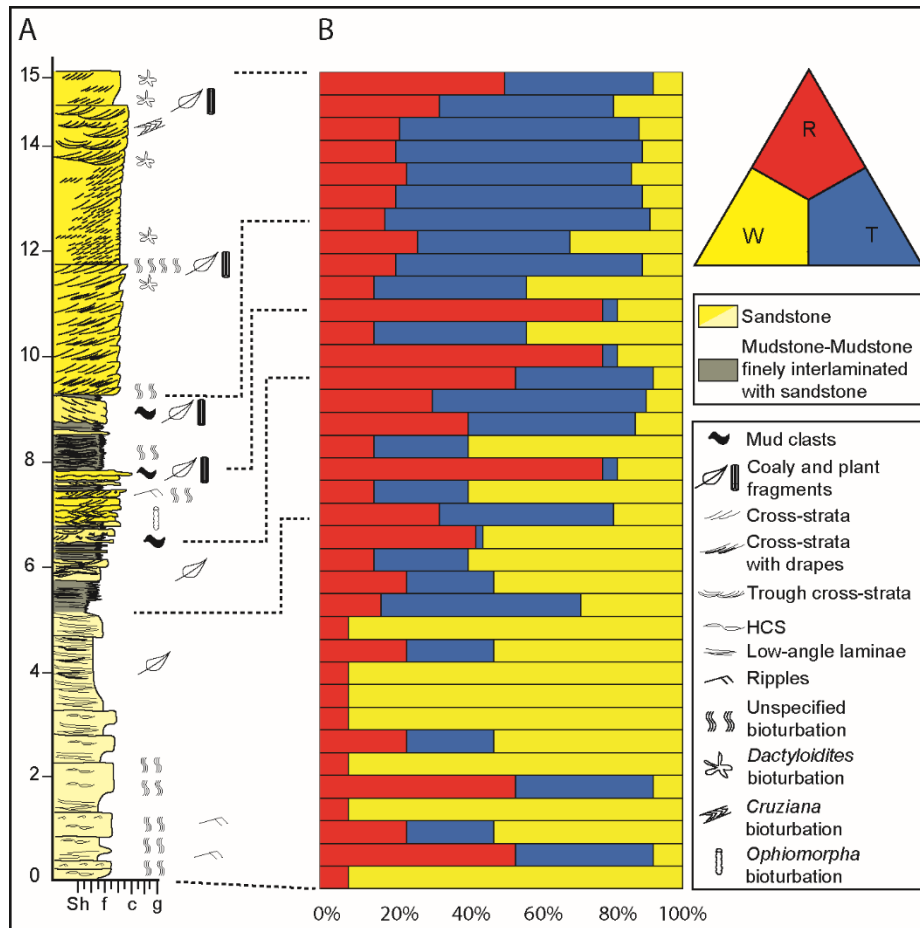


Figure 3.4: Sedimentological log of the described deltaic parasequence (A) and vertical (i.e. temporal) process changes (B). (A) shows the “classical” sedimentological log measured through the parasequence, whereas the probability graph shows the occurrence of river, wave and tidal processes through time. Yellow represents wave processes (W), red fluvial processes (R) and blue tidal processes (T). The lower part of the parasequence shows high probability of being the result of wave action. The middle part of the parasequence shows a complex mixture of wave, river and tidal processes. The upper part of the parasequence shows similar probabilities of being the result of fluvial and tidal currents.

Example 2: sedimentary logs database

The data collected from several sedimentary logs of different basins worldwide (Fig. 3.3) can be used to assess the likelihood of associations of sedimentary structures to a certain process and to certain depositional sub-environments. In the same way, the relation between different sub-environments and hydrodynamic processes can be quantified. Figure 3.5 shows the relation between sedimentary structures and hydrodynamic processes, whereas Figures 3.6, 3.7, 3.8 show the relation between sedimentary structures and sub-environments. For example, delta front environments are very variable in terms of sedimentary structures (Fig. 3.6); thick sets of stacked cross-strata and compound cross-strata are very typical of shelf bars and ridges (Figure 3.7). This relation of structures to different sub-environments can further help to reduce uncertainties in the interpretation of process variability of sedimentary successions, by helping to exclude certain processes. Some structures such as cross-strata and parallel laminations seems to be common to all three (river, wave and tidal) processes (Fig. 3.5) despite cross-strata are traditionally linked with fluvial, non-marine deposits. Other structures are more specific to a given process such as HCS or symmetrical ripples to waves, bidirectional, bundles, rhythmic laminations for tidal, normal grading or unidirectional ripples for river (Fig. 3.5) despite these are not necessarily the most frequent sedimentary structures built by that particular process.

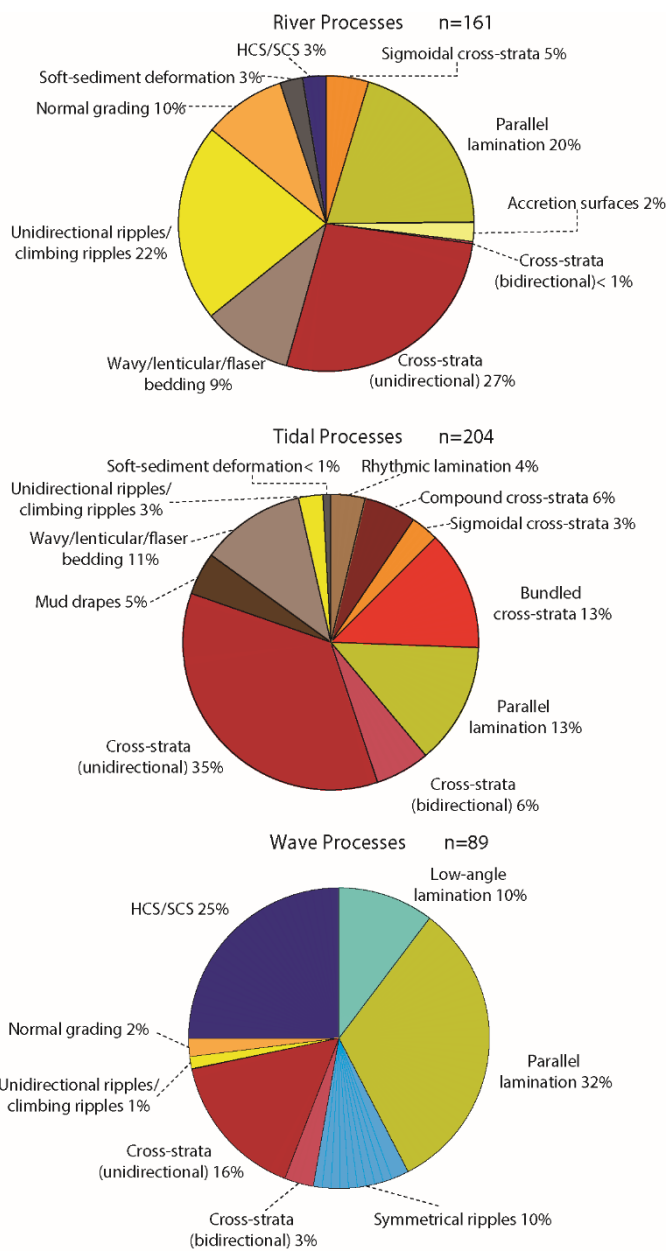


Figure 3.5: Relation between sedimentary structures and hydrodynamic processes (river, wave, tide); *n* represents the total number of facies units (stratal units characterized by the same structure) counted to calculate the percentages.

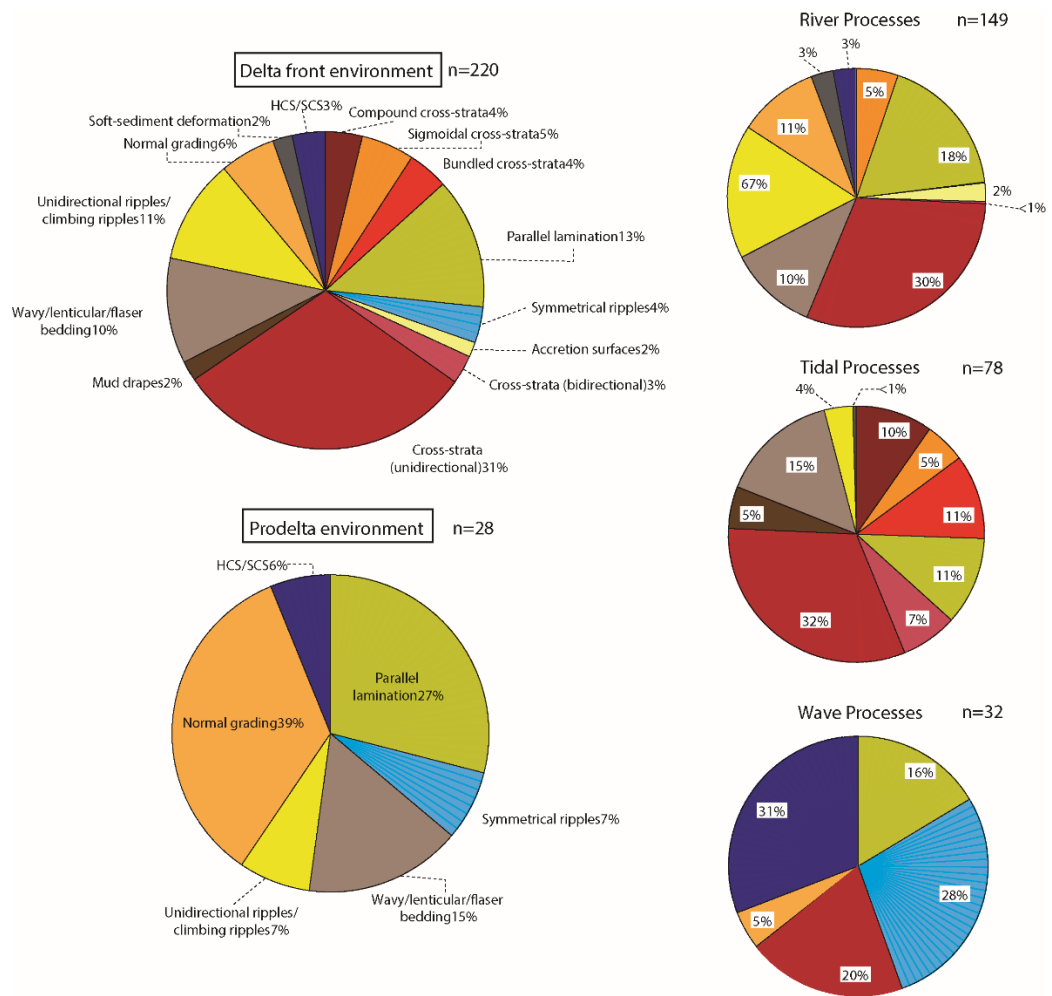


Figure 3.6: Sedimentary structures and processes in deltaic environment; *n* represents the total number of facies units counted to calculate the percentages.

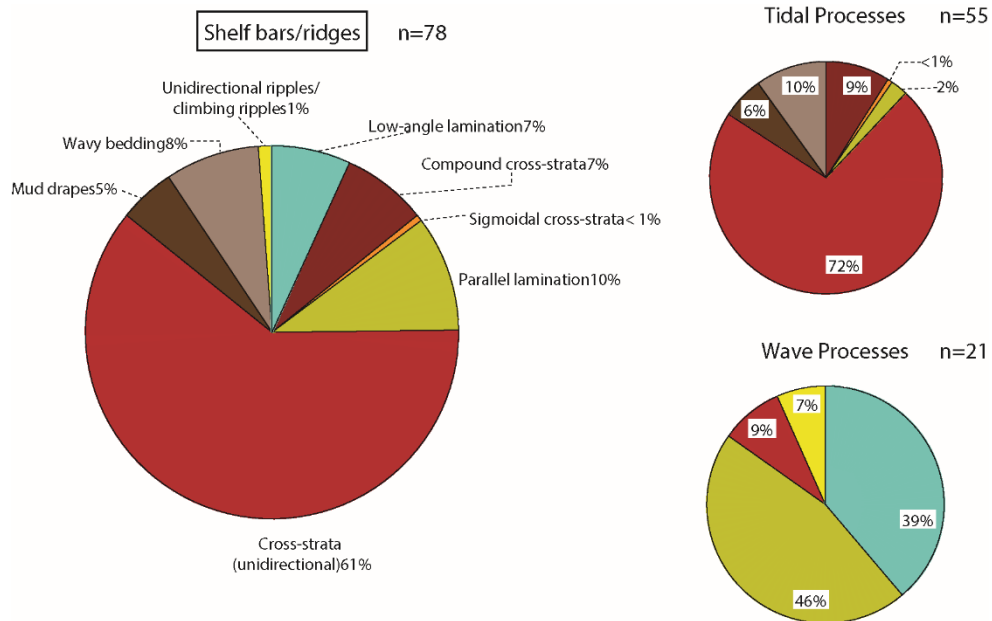


Figure 3.7: Sedimentary structures and processes in shelf bars and ridges; *n* represents the total number of facies units counted to calculate the percentages.

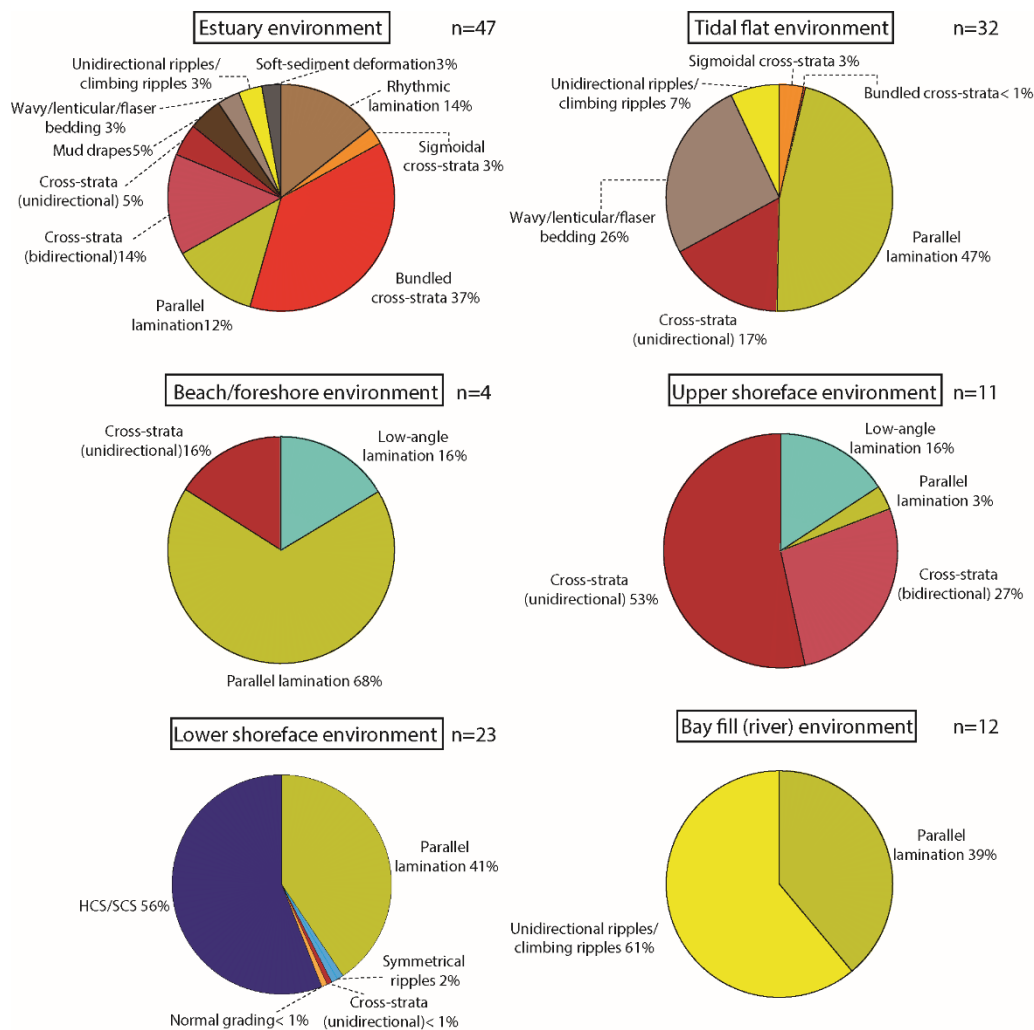


Figure 3.8: Relations between sedimentary structures and different environments; *n* represents the total number of facies units counted to calculate the percentages.

DISCUSSION

Process Probability Graph (PPG)

The application of Table 3.1 to the described deltaic parasequence in example 1 allows the creation of a probability graph (Fig. 3.4B), showing the relative importance of the three processes: waves, rivers and tides. The graph is built using the percentage values calculated for each bed.

The process probability graph constructed for the parasequence studied (Fig. 3.4B) clearly shows that from bottom to top (i.e. from more distal settings to more proximal settings) wave energy decreased while river influence increased. Tidal influence decreased in the most distal settings, but persisted in the proximal ones, where it co-existed with river processes. However, this general trend is not linear. In the middle part of the parasequence all three processes co-exist with similar probabilities, creating a complex pattern (Fig. 3.4). The graph allows a more precise interpretation of the history of process changes. Furthermore, it emphasizes likely autogenic process changes, sometimes underestimated in favor of high frequency base level changes (e.g. Van Wagoner, 1992). The presented methodology can be efficiently coupled to classical facies analysis to gain more precise and quantitative information on the process regimes of the study successions.

Limitations of the methodology

A possible major limitation of the methodology is its reliance on literature-derived interpretations of ancient successions, which can be subjective and may be biased by the popularity of a particular facies model at the time of the original study (see also Colombera et al., 2012b). In the same way, studies based on modern depositional systems are limited by the resolution of the instruments used and the ability to effectively record processes in areas with limited accessibility (e.g. deep waters on the shelf).

Nonetheless, even taking these limitations into account, the application of this methodology, following an initial conventional interpretation of the depositional environments or sub-environments of the succession of interest, can provide increased insight into process variability changes in time, space, as well as a better overview of the uncertainty.

Finally, we want to point out that this methodology should be considered as a first step towards the quantification of process variability and related uncertainty, but it cannot represent the ultimate, final or definitive solution. As knowledge advances and depositional processes and systems are better understood, there is an expectation that the percentage values here proposed will change. A possible solution is to make the data available in an open source format, so that it can be edited and refined. The methodology and results presented here should help future studies that aim for a quantification of process variability; it can also increase awareness of current biases in interpretations.

CONCLUSIONS

A new approach to facies interpretation in sedimentary strata, highlighting the intrinsic complexity of mixed-energy coastal systems (MECS) is advocated, giving new insight into how different processes, often at the same time, create sedimentary successions. The traditional facies description and sedimentological analysis of sedimentary successions is still fundamental for the interpretation of sedimentary rocks. In addition, the new methodology can be applied to further characterize the sedimentary successions, attempting to quantify the preservation of paleo-environmental signals that we observe and describe, and highlighting the intrinsic complexity of natural systems.

Process probability graphs (PPG) identify and highlight the complexity of mixed-energy systems, but at the same time they offer new insight into the evolution of these systems.

The methodology presented is a useful tool to quantify process variability in ancient systems (both in outcrop and core) and it helps to better express geological uncertainty. Furthermore, it represents a starting point for comparing process change histories and for a more precise comparison between different systems (for example reservoir cores and their outcrop analogues, or modern and ancient systems).

ACKNOWLEDGEMENTS

We sincerely thank the Lajas Project sponsors, Statoil, Woodside, BHP Billiton and VNG Norge for providing valuable advice in the field and financial support, and Lajas Project PIs for discussion in the field.

REFERENCES

- Ainsworth, R. B., Vakarelov, B. K., and Nanson, R. A., 2011, Dynamic spatial and temporal prediction of changes in depositional processes on clastic shorelines: toward improved subsurface uncertainty reduction and management: AAPG bulletin, v. 95, no. 2, p. 267-297.
- Allen, J. R. L., 1982, Sedimentary structures, their character and physical basis, Elsevier.
- Bhattacharya, J. P., and Walker, R. G., 1991, River- and Wave-Dominated Depositional Systems of the Upper Cretaceous Dunvegan Formation, Northwestern Alberta: Bulletin of Canadian Petroleum Geology, v. 39, no. 2, p. 165-191.
- Boersma, J. R., and Terwindt, J. H. J., 1981, Neap–spring tide sequences of intertidal shoal deposits in a mesotidal estuary: Sedimentology, v. 28, no. 2, p. 151-170.
- Choi, K., 2011, Tidal rhythmites in a mixed-energy, macrotidal estuarine channel, Gomso Bay, west coast of Korea: Marine Geology, v. 280, no. 1–4, p. 105-115.
- Colombera, L., Felletti, F., Mountney, N. P., and McCaffrey, W. D., 2012a, A database approach for constraining stochastic simulations of the sedimentary heterogeneity of fluvial reservoirs: AAPG bulletin, v. 96, no. 11, p. 2143-2166.
- Colombera, L., Mountney, N. P., Hodgson, D. M., and McCaffrey, W. D., 2016, The Shallow-Marine Architecture Knowledge Store: A database for the characterization of shallow-marine and paralic depositional systems: Marine and Petroleum Geology, v. 75, p. 83-99.
- Colombera, L., Mountney, N. P., and McCaffrey, W. D., 2012b, A relational database for the digitization of fluvial architecture: concepts and example applications: Petroleum Geoscience, v. 18, no. 1, p. 129-140.
- Dalrymple, B. W., 2010, Tidal depositional systems, *in* James, N. P., and Dalrymple, B. W., eds., Facies models, Volume 4, Geological Association of Canada, p. 201-231.
- Dalrymple, R. W., Knight, R. J., and Lambiase, J. J., 1978, Bedforms and their hydraulic stability relationships in a tidal environment, Bay of Fundy, Canada: Nature, v. 275, p. 100-104.
- Dalrymple, R. W., Knight, R. J., Zaitlin, B. A., and Middleton, G. V., 1990, Dynamics and facies model of a macrotidal sand-bar complex, Cobequid Bay—Salmon River Estuary (Bay of Fundy): Sedimentology, v. 37, no. 4, p. 577-612.

- De Raaf, J. F. M., Boersma, J. R., and Van Gelder, A., 1977, Wave-generated structures and sequences from a shallow marine succession, Lower Carboniferous, County Cork, Ireland: *Sedimentology*, v. 24, no. 4, p. 451-483.
- Dumas, S., Arnott, R., and Southard, J. B., 2005, Experiments on oscillatory-flow and combined-flow bed forms: implications for interpreting parts of the shallow-marine sedimentary record: *Journal of Sedimentary research*, v. 75, no. 3, p. 501-513.
- Fraser, G. S., and Hester, N. C., 1977, Sediments and sedimentary structures of a beach-ridge complex, southwestern shore of Lake Michigan: *Journal of Sedimentary Research*, v. 47, no. 3.
- Gani, M. R., Bhattacharya, J. P., and MacEachern, J. A., 2009, Using ichnology to determine relative influence of waves, storms, tides, and rivers in deltaic deposits: examples from Cretaceous Western Interior Seaway, USA, *in* MacEachern, J. A., Bann, K. L., Gingras, M. K., and Pemberton, S. G., eds., *Applied Ichnology*, Volume 52, SEPM SHort Course Notes, p. 209-225.
- Hampson, G. J., 2000, Discontinuity Surfaces, Clinoforms, and Facies Architecture in a Wave-Dominated, Shoreface-Shelf Parasequence: *Journal of Sedimentary Research*, v. 70, no. 2, p. 325-340.
- Jopling, A. V., and Walker, R. G., 1968, Morphology and origin of ripple-drift cross-lamination, with examples from the Pleistocene of Massachusetts: *Journal of Sedimentary Research*, v. 38, no. 4, p. 971-984.
- Kreisa, R. D., and Moila, R. J., 1986, Sigmoidal tidal bundles and other tide-generated sedimentary structures of the Curtis Formation, Utah: *Geological Society of America Bulletin*, v. 97, no. 4, p. 381-387.
- Kvale, E. P., Archer, A. W., and Johnson, H. R., 1989, Daily, monthly, and yearly tidal cycles within laminated siltstones of the Mansfield Formation (Pennsylvanian) of Indiana: *Geology*, v. 17, no. 4, p. 365-368.
- Leva López, J., Rossi, V. M., Olariu, C., and Steel, R. J., 2016, Architecture and recognition criteria of ancient shelf ridges; an example from Campanian Almond Formation in Hanna Basin, USA: *Sedimentology*.
- Mellere, D., and Steel, R. J., 1996, Tidal sedimentation in Inner Hebrides half grabens, Scotland: the Mid-Jurassic Berreraig Sandstone Formation: *Geological Society, London, Special Publications*, v. 117, no. 1, p. 49-79.
- Mutti, E., Tinterri, R., Di Biase, D., Fava, L., Mavilla, N., Angella, S., and Calabrese, L., 2000, Delta-front facies associations of ancient flood-dominated fluvio-deltaic systems: *Rev. Soc. Geol. Espana*, v. 13, no. 2, p. 165-190.
- Nio, S.-D., and Yang, C.-S., 1991, Diagnostic attributes of clastic tidal deposits: a review.
- Olariu, C., 2014, Autogenic process change in modern deltas: lessons for the ancient, *in* Martinius, A. W., Ravnås, R., Howell, J. A., Steel, R. J., and Wonham, J. P., eds., *From Depositional Systems to Sedimentary Successions on the Norwegian Continental Margin* Volume 46, *International Association of Sedimentologists*, p. 149-166.

- Olariu, C., and Bhattacharya, J. P., 2006, Terminal Distributary Channels and Delta Front Architecture of River-Dominated Delta Systems: *Journal of Sedimentary Research*, v. 76, no. 2, p. 212-233.
- Olariu, M. I., Olariu, C., Steel, R. J., Dalrymple, R. W., and Martinius, A. W., 2012, Anatomy of a laterally migrating tidal bar in front of a delta system: Esdolomada Member, Roda Formation, Tremp-Graus Basin, Spain: *Sedimentology*, v. 59, no. 2, p. 356-U332.
- Plink-Björklund, P., 2005, Stacked fluvial and tide-dominated estuarine deposits in high-frequency (fourth-order) sequences of the Eocene Central Basin, Spitsbergen: *Sedimentology*, v. 52, no. 2, p. 391-428.
- Plink-Björklund, P., 2008, Wave-to-tide facies change in a Campanian shoreline complex, Chimney Rock Tongue, Wyoming-Utah, USA, *in* Hampson, G. J., Steel, R. J., Burgess, P. M., and Dalrymple, B. W., eds., *Recent advances in models of shallow-marine stratigraphy: SEPM Special Publication, Volume 90*, p. 265-291.
- Pulham, A. J., 1989, Controls on internal structure and architecture of sandstone bodies within Upper Carboniferous fluvial-dominated deltas, County Clare, western Ireland, *in* Whateley, M. K. G., and Pickering, K. T., eds., *Deltas: Traps for Fossil Fuels, Volume 41*: London, Geol. Soc. Spec. Publ., p. 179-203.
- Rossi, V. M., and Steel, R. J., 2016, The role of tidal, wave and river currents in the evolution of mixed-energy deltas: Example from the Lajas Formation (Argentina): *Sedimentology*, v. 63, no. 4, p. 824-864.
- Ta, T. K. O., Nguyen, V. L., Tateishi, M., Kobayashi, I., Saito, Y., and Nakamura, T., 2002, Sediment facies and Late Holocene progradation of the Mekong River Delta in Bentre Province, southern Vietnam: an example of evolution from a tide-dominated to a tide- and wave-dominated delta: *Sedimentary Geology*, v. 152, no. 3-4, p. 313-325.
- Vakarelov, B. K., Ainsworth, R. B., and MacEachern, J. A., 2012, Recognition of wave-dominated, tide-influenced shoreline systems in the rock record: Variations from a microtidal shoreline model: *Sedimentary Geology*, v. 279, p. 23-41.
- Van Wagoner, J. C., 1992, High-frequency sequence stratigraphy and facies architecture of the Sego sandstone in the Book Cliffs of western Colorado and eastern Utah, AAPG, Sequence stratigraphy applications to shelf sandstone and sandstone reservoirs; outcrop to subsurface examples: AAPG Field Conference.
- Wightman, D. M., and Pemberton, S. G., 1997, The Lower Cretaceous (Aptian) McMurray Formation: an overview of the Fort McMurray area, northeastern, Alberta, *in* Pemberton, S. G., and James, D. P., eds., *Petroleum Geology of the Cretaceous Mannville Group, Western Canada Volume 18*, Canadian Society of Petroleum Geologists p. 312-344.
- Yoshida, S., Steel, R. J., and Dalrymple, R. W., 2007, Changes in Depositional Processes—An Ingredient in a New Generation of Sequence-Stratigraphic Models: *Journal of Sedimentary Research*, v. 77, no. 6, p. 447-460.

Chapter 4: Impact of tidal currents on delta-channel deepening, stratigraphic architecture, and sediment bypass beyond the shoreline³

ABSTRACT

Deltas are sensitive indicators of coastal processes (e.g., waves and tides) and show dynamic changes in shoreline morphology, distributary channel network, and stratigraphic architecture in response to coastal forcing. Numerical modeling has long been used to show delta evolution associated with a single dominant coastal process, but rarely to examine the sensitivity of deltas to mixed processes. Physics-based morphodynamic simulations (Delft3D) are used to investigate the influence of tidal currents on deltas. Tidal amplitude and the sand:mud ratio of subsurface sediment have been varied in the model. The results show that increasing tidal amplitude causes deeper and more stable distributary channels and more rugose planform shoreline patterns. A new metric for channel geometry quantifies tidal influence on the distributary channel network. Stable distributary channels act as an efficient mechanism for ebb-enhanced currents to (1) bypass sediment across the delta plain, and (2) extend channel tips seaward through mouth bar erosion. The basinward channel extension leads to sandier deposits in the tide-influenced deltas than in their river-dominated counterparts. The delta-front bathymetry also reflects sediment redistribution, changing the delta-front profile from concave to convex with compound geometries as tidal amplitude increases. These results suggest that channel overdeepening is a possible tidal signature that should

³ This chapter has been published as: Rossi, V. M., Kim, W., Leva López, J., Edmonds, D., Geleynse, N., Olariu, C., Steel, R. J., Hiatt, M., Passalacqua, P., 2016, Impact of tidal currents on delta-channel deepening, stratigraphic architecture, and sediment bypass beyond the shoreline: *Geology*, doi:10.1130/G38334.1. I was the primary author of this work.

be considered when interpreting ancient systems, and that sand may be bypassed much farther basinward in tide-influenced than in purely river-dominated deltas.

INTRODUCTION

Deltas are sensitive to environmental changes and thus undergo dynamic changes in planform shoreline geometry, distributary channel network, and stratigraphic architecture in response to coastal processes, sediment input, subsidence, eustatic change, and climate variations over a wide range of time scales.

Delta morphology is thought to reflect the dominant coastal processes. Galloway (1975) used such reasoning to propose the widely used ternary classification for deltas. However, even over short distances and small time spans, a delta can bear overlapping signals of multiple coastal processes that affect its morphology and stratigraphy (Olariu, 2014), making most deltas mixed energy systems. For example, the Mahakam Delta (Indonesia) has evolved from a river-dominated delta to a tide-influenced one during the Holocene, while the Mekong Delta (Vietnam) shows a temporal shift in the dominant coastal process from tides to waves (Olariu, 2014). The Wax Lake Delta (Louisiana, USA) has been classified as a river-dominated delta. However, recent studies reveal that even small-amplitude tides can strongly affect the evolution of distributary channels (Shaw and Mohrig, 2014). Ultimately, it is important to quantify and understand how mixed coastal processes are imprinted on the delta morphology and the related stratigraphic record.

In this paper we present results of numerical modeling using Delft3D software ([https://oss .deltares .nl /web /delft3d/](https://oss.deltares.nl/web/delft3d/)) with the tidal simulation that was presented in Geleynse et al. (2011). Tidal controls on shoreline planform pattern, distributary channel geometry, sediment partitioning in the downstream direction, delta-front geometry, and stratigraphic architecture have been examined. A new metric for channel geometry to

quantify tidal influence on the modeling results has been introduced and applied to modern deltas to better constrain mechanisms of natural fluvio-deltaic channel formation under tidal influence.

METHODOLOGY

Delft3D is a numerical modeling software package that models hydrodynamics, sediment transport, and topographic evolution in fluvial and coastal environments (e.g., Edmonds and Slingerland, 2010; Geleynse et al., 2011). Details of tidal simulation in Delft3D and initial test results were presented by Geleynse et al. (2011).

The model has a 20×10 km domain (Fig. 4.1) with square 50×50 m grid cells. Initially, a straight river (12 km long, 5 m deep, and 550 m wide) is set at the center of the basin that flows over a flat floodplain and then debouches into a linearly sloping basin ($\sim 0.14^\circ$). The initial shoreline is straight and located at 12 km from the upstream boundary.

We performed a total of 24 runs (see Table C.1 in Appendix C for the model parameters) with a constant river discharge ($Q_w = 2000 \text{ m}^3/\text{s}$) and no waves. Fine sediment (diameter $D = 50 \text{ }\mu\text{m}$) discharge (Q_{fines}) is $0.04 \text{ kg}/\text{m}^3$, while sand ($D = 200 \text{ }\mu\text{m}$) discharge (Q_{sand}) is given by a Neumann condition at the upstream end of the river. Tides in the model are simulated as a harmonic oscillation with amplitude $A = 1.5 \text{ m}$, 0.5 m , 0.25 m , and 0 m at a frequency of $30^\circ/\text{h}$ (i.e., semidiurnal tides) for distinct model runs. Sea level was kept constant and no subsidence was applied. We varied the ratio of sand to mud in the receiving basin substrate from 25:75, to 50:50, to 100:0. The substrate compositions have been chosen not to mimic a particular modern delta, but to understand the effect of tidal processes under a wide range of possible scenarios.

The first set of 12 runs (herein RL runs) produced results of long-term deltaic evolution (~ 7 yr of simulated time at bankfull condition, representing ~ 20 – 200 yr),

whereas the second set of 12 runs (herein RS) produced results with a higher temporal resolution over ~ 4 months total run time. The first set is used to analyze time-integrated tidal effects on delta morphology, channel network, and stratigraphy, whereas the second set is used to visualize the changes in suspended and bedload sediment transport and their spatial distribution over tidal cycles.

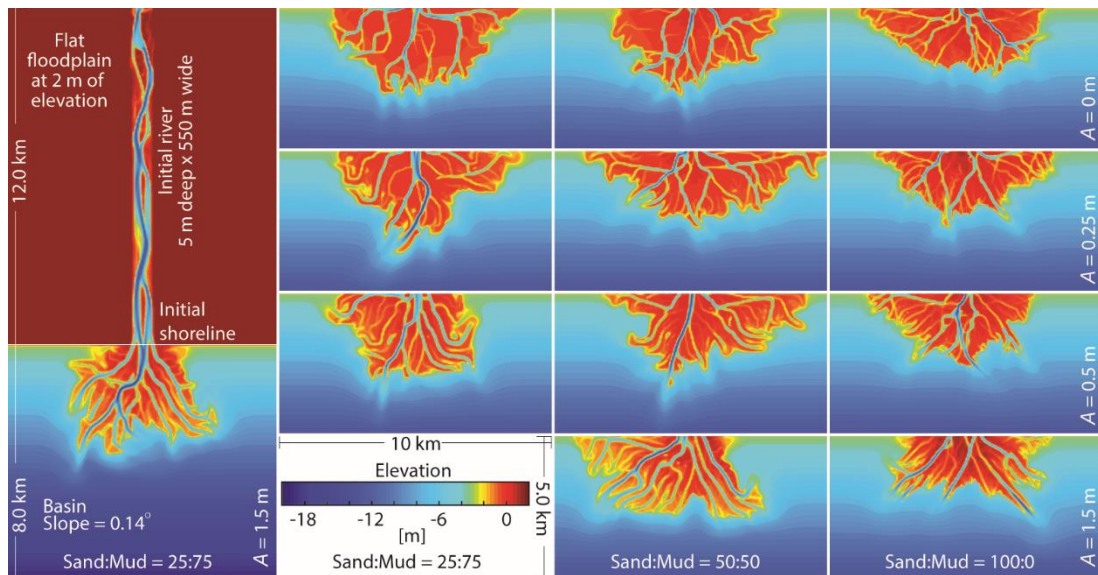


Figure 4.1: Topographic surfaces collected at 7.2 yr (final run time), showing shoreline morphologies and distributary channel networks for deltas simulated under different tidal amplitudes (A) and sand:mud ratios.

FLUVIO-DELTAIC CHANNEL AND SHORELINE EVOLUTION

Figure 4.1 shows the topographic surfaces of RL runs at the final stage. The control runs with tidal amplitude $A = 0$ show radially growing deltas with mouth bar formation inducing channel bifurcation, which increases progressively in the downstream direction. A distributary channel network with minor interdistributary bays develops.

Channels avulse into new locations while the previously abandoned channels are filled with sediment.

Under higher tidal amplitudes ($A = 0.5$ m and $A = 1.5$ m), mouth bars develop only at the major distributary channel tips, but rarely cause channel bifurcation due to erosion and downstream migration of the mouth bars. In these runs there is also a reduction in channel lateral mobility and bifurcation frequency. Increased stability in distributary channels of tide-influenced deltas has previously been suggested (Olariu and Bhattacharya, 2006). As a consequence, individual active channels are deeper and extend farther downstream, the overall delta morphology becomes more elongated, and the planform pattern of the shoreline becomes more rugose. Substrate sediment composition has a similar control on delta and channel morphology as the sediment mixture with more fines (i.e., more cohesive) produces deeper channels and an elongated delta shape.

Figure 4.2 shows channel depth at the distributary channel tips of the major distributaries as a function of tidal prism. We use two dimensionless numbers to scale channel depth (H^*) and tidal amplitude (A^*) as

$$H^* = \frac{H}{D}, \quad (1)$$

and

$$A^* = \frac{A^2 \cdot \Lambda}{s S_t T_t Q_w}, \quad (2)$$

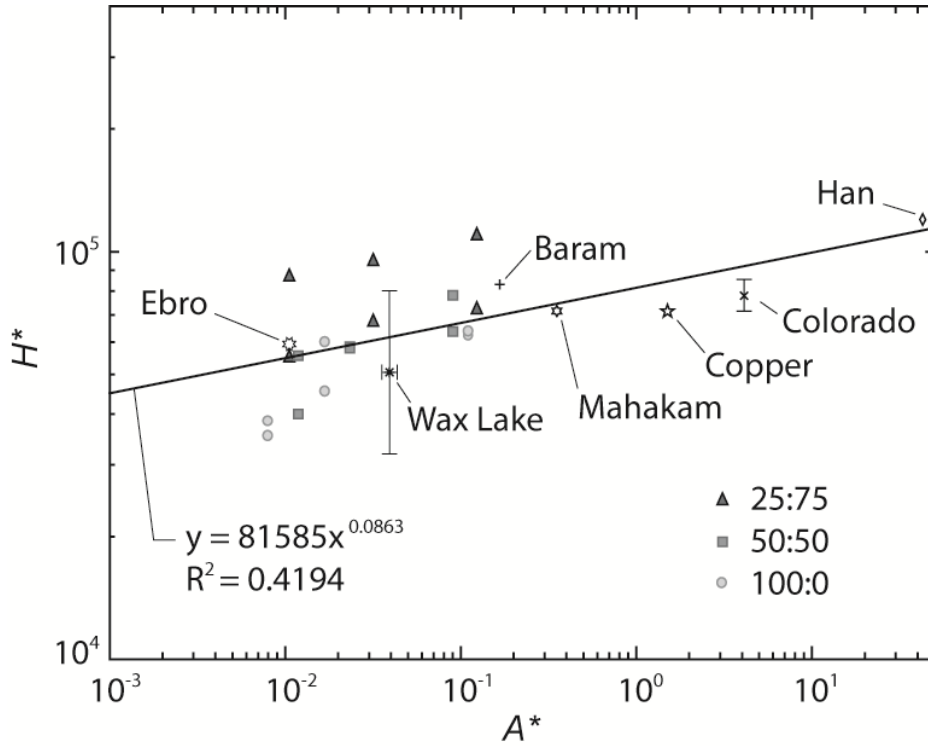


Figure 4.2: Relationship between dimensionless tidal amplitude and channel depth (A^* and H^*). Modern deltas are labeled with their names; bars show range of variability.

where H is the channel depth at the distributary channel tip, D is mean bed grain size, Λ denotes the delta's surface area, s is the maximum distance from the delta apex to the shoreline, S_t denotes the average delta topset slope, and T_t is half of the tidal period. Data are collected at the final time step of all runs (Table C.2). The channel depths and grain sizes were measured in the two deepest distributary channels at the shoreline (Fig. C.1). In Equation 2, A^* scales the relative influence of tide over river discharge (modified from Luketina, 1998). The dimensionless channel depth H^* increases with higher A^* following a power law relationship (Fig. 4.2). Channels are also deeper in the runs with more fine sediment due to cohesion of the banks, aiding flow confinement. We calculated shoreline

rugosity at the final stage of the runs following Wolinsky et al. (2010). The shoreline was picked at the seaward limit of the delta plain at mean sea level (-0.2 m contour line) for all the runs. The shoreline rugosity increases with tidal amplitude, similar to the trend in channel depth against tidal prism (Fig. C.2). Therefore, an increase in tidal amplitude and in tidal prism produces a more rugose shoreline planform and deeper channels.

SUBAQUEOUS DELTA PLATFORM AND STRATAL DEVELOPMENT

Figure 4.3 shows cross sections of the final deltaic stratigraphy through the location of maximum deltaic progradation for the runs with the 50:50 substrate sediment composition. The spatial distribution of channel and lobe facies between the runs indicates progressively less lateral channel mobility and reworking, and instead deeper channel incision as the tidal amplitude increases. In the control run with $A = 0$ m, the channel facies are distributed widely across the delta topset and individual channel depths are relatively shallow. Runs with 25:75 and 100:0 substrate sediment compositions (not shown here) have similar trends in the tidal runs compared to the control runs in their sets.

Delta-front geometry becomes more convex with higher tidal amplitudes (Figs. 4.3A–4.3D). The control run remains concave up throughout the run, whereas the tidal runs are characterized by a gradual change in the delta-front profile from concave up to convex up as the delta evolves. For the case of $A = 1.5$ m (Fig. 4.3D), tidal currents further shape the delta front into a compound clinoform.

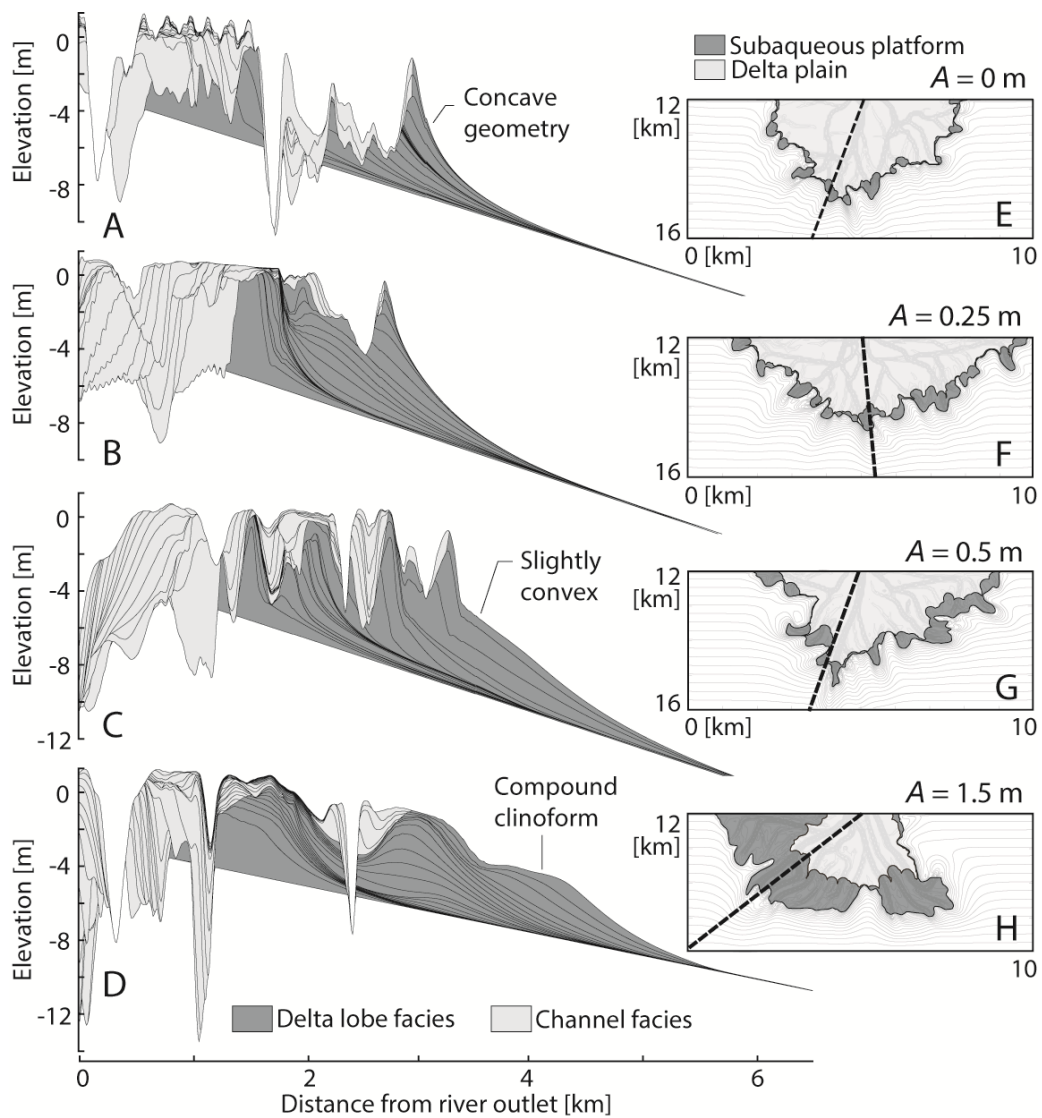


Figure 4.3: (A-D) Stratigraphic cross sections for model runs with a substrate sand:mud ratio of 50:50. (E-H) Plan-view images of the deltas. Dashed lines show the locations of the cross sections in A-D. A - tidal amplitude.

The subaqueous delta platform is a shallow area between the subaerial delta plain and the rollover point of the delta front, usually producing a compound clinoform geometry with both shoreline and upper delta-front rollovers (e.g., Swenson et al., 2005). The subaqueous delta platform has been recognized in both modern and ancient deltas

affected by strong marine reworking (e.g., Goodbred and Saito, 2012; Rossi and Steel, 2016). In the modeled runs the subaqueous delta platform (Figs. 4.3E–4.3H) area is overall larger in runs with higher tidal amplitudes. To compare delta-front profiles consistently, we normalized the delta-front slopes with the maximum slope of each transect (Fig. 4.4). The profiles (Fig. 4.4A) show that for low tidal amplitudes ($A = 0$ and 0.25 m) the delta-front slope decreases gradually in a basinward direction. However, for higher tidal amplitudes ($A = 0.5$ and 1.5 m) the slope becomes increasingly more irregular (pronounced double peaks), reflecting the presence of a compound clinoform. Different substrate sediment compositions do not significantly affect this result. Figure 4.4B shows the normalized slopes against the basinward extent of the deposits for only $A = 0$ and 1.5 m in all other runs with different sediment compositions. In all three cases, higher tidal amplitudes generate irregular slopes basinward, whereas smaller amplitudes produce asymptotic decreases in slope with distance from the shoreline. We applied the same analysis to the tide-influenced Mahakam Delta and the tide-dominated Han Delta (South Korea) (Fig. 4.4B), and found a similar double-peak pattern.

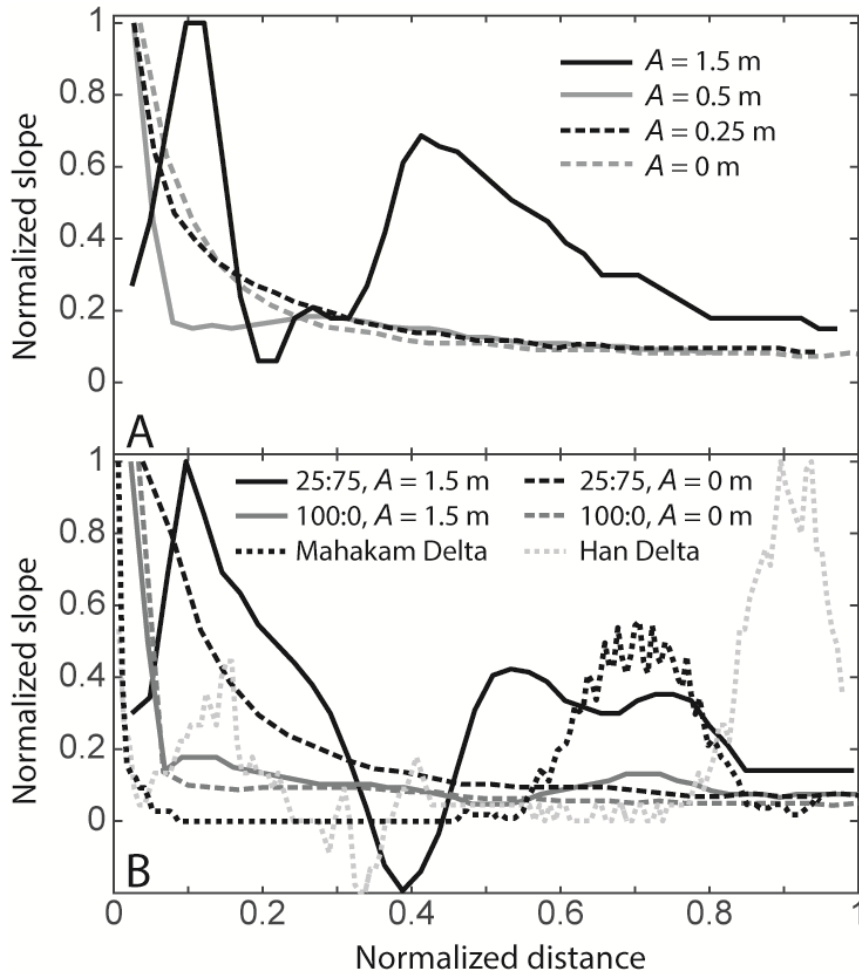


Figure 4.4: (A) Normalized delta-front slopes for the model runs with a substrate sand:mud ratio of 50:50. (B) Slopes for the model runs with a substrate sand:mud ratio of 25:75 and 100:0 for tidal amplitude $A = 0$ and $A = 1.5$ m, and two tide-influenced and tide-dominated modern deltas (Cummings et al., 2016).

DISCUSSION

Sediment partitioning

Tidal cycles involve changes in sea level and current velocity, and consequently influence suspended and bedload sediment fluxes in the distributary channels. Figure 4.5 shows the width-averaged parameters that were measured at four locations along the

deepest channel from the delta apex up to the channel tip (1–4 in Fig. 4.5, from proximal to distal; see Fig. C.3 for locations); data were collected from the 50:50 substrate sediment composition runs with $A = 0$ and 1.5 m. During ebb-tide drawdown for $A = 1.5$ m, suspended and bedload fluxes at the delta apex are increased ~ 3.5 and ~ 4 times, respectively (Fig. 4.5A), with respect to the control run (Fig. 4.5B). In addition, during ebb-tide drawdown, both bedload and suspended loads are fairly consistent in the three upstream locations (1–3) but reduced only beyond the shoreline (4). This indicates significant bypass of sediment through the entire delta plain with deposition beyond the shoreline. Therefore, tidal currents play an important role in creating more stable and deeper distributary channels that act as conduits for transporting sediment farther downstream.

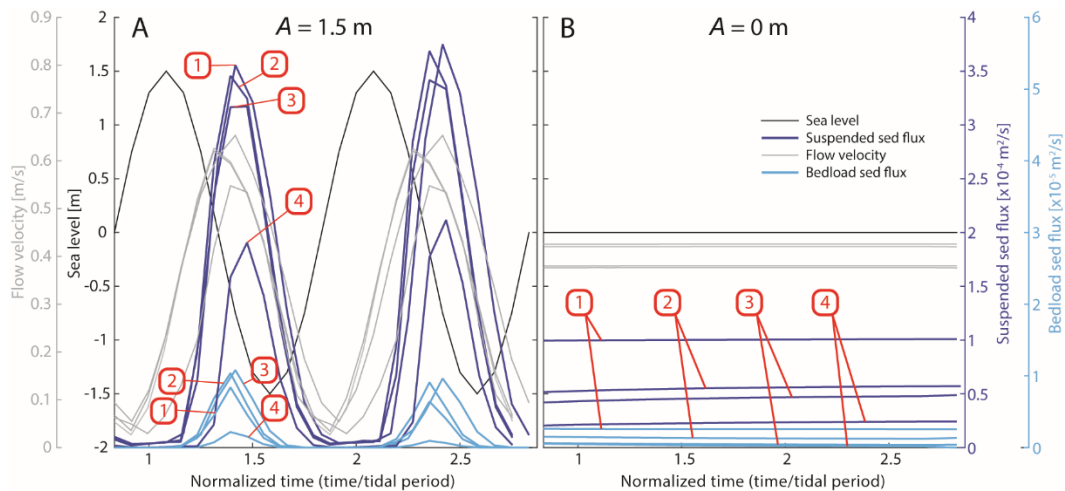


Figure 4.5: Suspended and bedload sediment (sed) fluxes, sea level, and flow velocity versus normalized time at four locations from upstream (1) to downstream (4) (Fig. C.3) along the main distributary channel in the model runs with a substrate sand:mud ratio of 50:50. (A) Tidal amplitude $A=1.5$ m. (B) $A=0$ m.

The distribution of sand and mud across these two deltas captures the control that tidal currents exert over sediment partitioning (Fig. 4.6). For $A = 1.5$ m the deposits remain sand rich (i.e., >50% sand) even beyond the shoreline (dashed line in Fig. 4.6), whereas for $A = 0$ the deposits are sand rich only in the proximal to medial reaches of the subaerial delta (see Fig. C.4 for the positions of the cross sections). In the modern Mississippi Delta (Louisiana, USA), which lacks significant tidal influence, sand deposits are located only in close proximity to the distributary channels (Fisk, 1961), whereas in the tide-dominated Han Delta, sand is transported tens of kilometers away from the shoreline (Cummings et al., 2016), suggesting that ebb-enhanced currents are an important agent for sand distribution. However, it has to be kept in mind that the deposits of tide-dominated deltas can be highly heterolithic in places, with thin but continuous mud beds (Willis, 2005; Dalrymple, 2010).

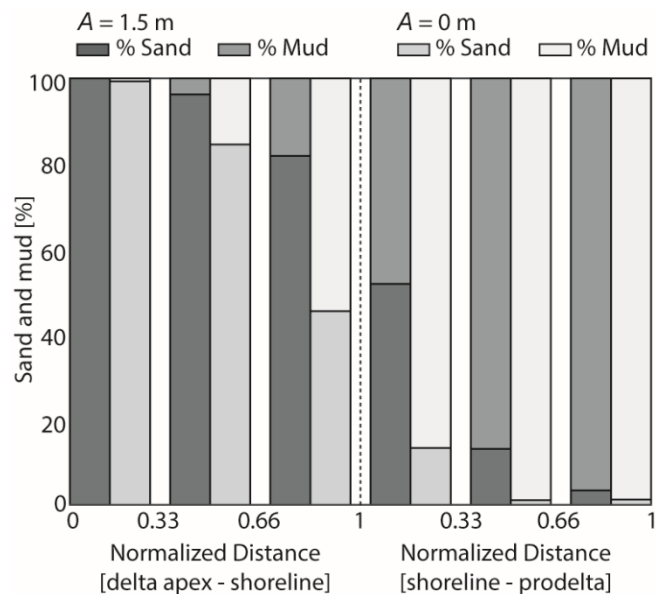


Figure 4.6: Percentages of sand and mud calculated radially from the delta apex to the shoreline and from the shoreline to the prodelta (Fig. C.4). The shoreline position is marked by a dashed line. A - tidal amplitude.

Tidal processes in modern river deltas

Shaw and Mohrig (2014) documented important tidal modulation of river flow (ebb drawdown) that extended the distributary channels as much as 6 km beyond the emerged delta in the Wax Lake Delta, even though the Atchafalaya Bay is microtidal. A similar morphodynamic change is captured in the modeling runs with moderate to high values of A^* , which increases H^* systematically. We used previously published data of modern deltas with different degrees of tidal influence to calculate A^* and H^* (Fig. 4.2). The modern deltas are well within the trend obtained from the modeling results. This relationship can prove useful to obtain a first-order prediction of either tidal prism using channel depth and grain-size data or paleochannel depth using grain-size and tidal prism data.

The Mahakam Delta shows a temporal transition from river-dominated to tide-influenced delta and it now has a compound clinoform geometry with a well-developed subaqueous platform (Roberts and Sydow, 2003). Compound clinoforms are also observed in other mud-rich deltas, such as the Amazon and Ganges-Brahmaputra Deltas (Goodbred and Saito, 2012). The model runs with high tidal amplitude show similar geometries. As a delta grows, the delta topset area becomes bigger and the shoreline progradation decelerates (Kim et al., 2006), causing reduced sediment delivery to the shoreline. This allows for a stronger reworking of sediments by tidal currents, producing funnel-shaped distributary channels [e.g., Mahakam Delta and Fly River Delta (Papua New Guinea); Dalrymple et al., 2003; Sassi et al., 2012]. The funnel-shaped channel geometry in modern tide-influenced and tide-dominated deltas reflects the evolution under tidal influence over several thousands of years (e.g., Dalrymple et al., 2003). The delta distributary channels in model runs with high tidal amplitudes were mostly elongated and deepened rather than funnel shaped. This is likely due to short modeling

duration (less than hundreds of years) and/or modeling limitations. With time, they likely evolve into a form similar to the Mahakam Delta, where the sediment discharge at the shoreline is significantly smaller and the tidal prism is sufficiently increased. We therefore suggest that when fluvial sediment supply and discharge to the shoreline are relatively high compared to tidal current reworking, tidal influence on the channel network is expressed by channel deepening and elongation.

CONCLUSIONS

Our results show that tidal currents have significant effects on fluvio-deltaic evolution. Stronger tidal currents cause (1) deeper and more stable distributary channels with less frequent channel bifurcation and avulsion events, (2) greater shoreline rugosity, and (3) wider subaqueous platforms.

The power law relationship between dimensionless channel depth and tidal amplitude normalized by river discharge shows that channel deepening can be considered an indication of tidal influence on the distributary channel network. This signature should also be considered when interpreting ancient tide-influenced systems.

Deltaic clinofolds are more concave in the case of river-dominated deltas and develop a more convex or compound clinofold geometry in the case of tide-influenced deltas.

Ebb-enhanced currents (river plus tide) are capable of transporting suspended and bedload sediment farther basinward, developing deeper and more stable channels that act as efficient conduits for sediment bypass, and thus creating deposits more sand rich than in the case of a fluvial outflow in the absence of tides. Counterintuitively, tide-influenced deltas have the potential to funnel sand-rich deposits farther from the shoreline than river-dominated deltas.

ACKNOWLEDGMENTS

We acknowledge support from National Science Foundation grant EAR-1135427 to Kim, Edmonds, and Passalacqua and grant EAR-1426997 to Edmonds. We thank G. Hampson, J. Bhattacharya, D. Cummings, and editor J. Parrish for constructive comments.

REFERENCES

- Cummings, D., Dalrymple, R., Choi, K., and Jin, J., 2016, The Tide-dominated Han River Delta, Korea: Geomorphology, Sedimentology, and Stratigraphic Architecture, Elsevier.
- Dalrymple, B. W., 2010, Tidal depositional systems, *in* James, N. P., and Dalrymple, B. W., eds., *Facies models*, Volume 4, Geological Association of Canada, p. 201-231.
- Dalrymple, R. W., Baker, E. K., Harris, P. T., and Hughes, M. G., 2003, Sedimentology and stratigraphy of a tide-dominated, foreland-basin delta (Fly River, Papua New Guinea), *in* Sidi, F. H., Nummedal, D., Imbert, P., Darman, H., and Posamentier, H. W., eds., *Tropical Deltas of Southeast Asia—Sedimentology, Stratigraphy, and Petroleum Geology*, Volume 76, SEPM Special Publication, p. 147-173.
- Edmonds, D. A., and Slingerland, R. L., 2010, Significant effect of sediment cohesion on delta morphology: *Nature Geosci.*, v. 3, no. 2, p. 105-109.
- Fisk, H. N., 1961, Bar-finger sands of Mississippi delta, *Geometry of sandstone bodies*: Tulsa, Oklahoma, AAPG, p. 29-52.
- Galloway, W. E., 1975, Process framework for describing the morphologic and stratigraphic evolution of deltaic depositional systems, *in* Broussard, M. L., ed., *Deltas, Models for Exploration*, p. 87-98.
- Geleynse, N., Storms, J. E. A., Walstra, D.-J. R., Jagers, H. R. A., Wang, Z. B., and Stive, M. J. F., 2011, Controls on river delta formation; insights from numerical modelling: *Earth and Planetary Science Letters*, v. 302, no. 1–2, p. 217-226.
- Goodbred Jr, S. L., and Saito, Y., 2012, Tide-dominated deltas, *in* Davis Jr, R. A., and Dalrymple, B. W., eds., *Principles of Tidal Sedimentology*, Springer Netherlands, p. 129-149.
- Kim, W., Paola, C., Voller, V. R., and Swenson, J. B., 2006, Experimental Measurement of the Relative Importance of Controls on Shoreline Migration: *Journal of Sedimentary Research*, v. 76, no. 2, p. 270-283.
- Luketina, D., 1998, Simple Tidal Prism Models Revisited: *Estuarine, Coastal and Shelf Science*, v. 46, no. 1, p. 77-84.
- Olariu, C., 2014, Autogenic process change in modern deltas: lessons for the ancient, *in* Martinius, A. W., Ravnås, R., Howell, J. A., Steel, R. J., and Wonham, J. P., eds.,

- From Depositional Systems to Sedimentary Successions on the Norwegian Continental Margin Volume 46, International Association of Sedimentologists, p. 149-166.
- Olariu, C., and Bhattacharya, J. P., 2006, Terminal Distributary Channels and Delta Front Architecture of River-Dominated Delta Systems: *Journal of Sedimentary Research*, v. 76, no. 2, p. 212-233.
- Roberts, H. H., and Sydow, J., 2003, Late Quaternary stratigraphy and sedimentology of the offshore Mahakam delta, east Kalimantan (Indonesia), *in* Sidi, F. H., Nummedal, D., Imbert, P., Darman, H., and Posamentier, H. W., eds., *Tropical Deltas of Southeast Asia—Sedimentology, Stratigraphy, and Petroleum Geology*, Volume 76, SEPM Special Publication, p. 125-145.
- Rossi, V. M., and Steel, R. J., 2016, The role of tidal, wave and river currents in the evolution of mixed-energy deltas: Example from the Lajas Formation (Argentina): *Sedimentology*, v. 63, no. 4, p. 824-864.
- Sassi, M. G., Hoitink, A. J. F., de Brye, B., and Deleersnijder, E., 2012, Downstream hydraulic geometry of a tidally influenced river delta: *Journal of Geophysical Research: Earth Surface*, v. 117, no. F04022.
- Shaw, J. B., and Mohrig, D., 2014, The importance of erosion in distributary channel network growth, Wax Lake Delta, Louisiana, USA: *Geology*, v. 42, no. 1, p. 31-34.
- Swenson, J. B., Paola, C., Pratson, L., Voller, V. R., and Murray, A. B., 2005, Fluvial and marine controls on combined subaerial and subaqueous delta progradation: Morphodynamic modeling of compound-clinoform development: *Journal of Geophysical Research: Earth Surface*, v. 110, no. F2, p. 1-16.
- Willis, B. J., 2005, Deposits of tide-influenced river deltas, *in* Giosan, L., and Bhattacharya, J. P., eds., *River Deltas - Concepts, Models, and Examples*, Volume 83, SEPM Special Publication, p. 87-129.
- Wolinsky, M. A., Edmonds, D. A., Martin, J., and Paola, C., 2010, Delta allometry: Growth laws for river deltas: *Geophysical Research Letters*, v. 37, no. 21.

Chapter 5: Tidal and fluvial process interplay in an early Pleistocene, delta-fed, strait margin (Calabria, southern Italy)⁴

ABSTRACT

The architecture and morphodynamics of modern and ancient tidal straits is one of the challenging research tasks of sedimentary geology. In particular, the deposits of strait-margin zones have been significantly understudied compared to the axial zone depositional environment. This paper presents a detailed sedimentological and stratigraphic analysis of an early Pleistocene marginal-marine succession deposited along the northern margin of the Siderno paleostrait (southern Italy). This area represents an excellent case study of sedimentation occurring along a margin where syn-depositional tectonics produced a complex coastal morphology, significantly influencing sedimentation and hydrodynamic processes. Along the strait margin, the emplacement of an isolated tectonic high (Piano Fossati) created a *ca* 3.5 km-wide local passageway. This uncommon morpho-structural element induced interplays between fluvio-deltaic processes (fed from the northern strait margin) and tidal current reworking (active within the marine strait). The field-based facies-analysis documents how highstand shallow-marine sedimentation across the strait margin was initially strongly conditioned from the inherited topography. A subsequent regression caused river-generated hyperpycnal flows and the transfer of large volumes of pebbly and shelly sandstones into slightly deeper water. In the delta front area, strong tidal currents were able to rework river-derived sediments generating large dune fields. The strong tidal influence imposed on the delta-

⁴ This chapter has been submitted as: Rossi, V. M., Longhitano, S. G., Mellere, D., Chiarella, D., Steel, R. J., Olariu, C., Dalrymple, R. W., Tidal and fluvial process interplay in an early Pleistocene, delta-fed, strait margin (Calabria, southern Italy), *Marine and Petroleum Geology*, Special Issue Sedimentology in Italy: recent advances and insights. I was the primary author of this work.

front induced a deflection and a consequent elongation of sand bodies in a direction parallel to the marine strait axis. This process became progressively enhanced during the following transgression, when tide-modulated currents reworked biocalcarenitic sands over the previous delta deposits, generating southeasterly migrating dunes. At the end of the transgression, strandplain progradation caused the closure of this marginal branch of the Siderno Strait. This last stage of sedimentation was followed by a dramatic regional-scale structural uplift, which interrupted the oceanographic circulation within the strait.

INTRODUCTION

Tidal straits are narrow marine passageways between emerged land areas and linking two adjacent basins (Pugh, 1987). Their oceanography is governed mainly by current convergence and amplification, due to the restriction of the cross-sectional area (Defant, 1961). In modern straits (e.g., the San Francisco Strait, the Messina Strait, the Dover Strait and the Torres Strait), tidal currents commonly flow in reversal phases between the two connected basins, and exert great influence on the sediments, producing a partitioning of by-pass areas and specific depositional zones (Longhitano, 2013). Bedload parting zones and associated scour zones can be developed in relation to flow constrictions (i.e. commonly in the narrowest point in the strait) and local bottom stress maxima, whereas sand transport paths are developed in the direction of the peak tidal current, and along two oppositely directed pathways away from the location of bedload parting (Harris et al., 1995). As a consequence, sediments in straits are commonly accumulated across two main depositional zones, symmetrically located away from the local bedload parting, and occurring at both ends of the strait. Tidal transport pathways control the spatial distribution of tidal sedimentary facies, so that sand-rich tidal bedform fields pass down-current and laterally to finer-grained sheets (e.g., Belderson et al., 1982; Harris et al., 1995; Reynaud and Dalrymple, 2012).

However, the margins of modern and ancient tidal straits can introduce important volumes of sedimentary deposits (Frey and Dashtgard, 2011; Longhitano et al., 2012b; Longhitano, 2013; Longhitano and Steel, 2016). Depending on the coastal gradient, strait margins can be steeply-inclined by-pass slopes, or gently-sloping depositional shelves, where shorefaces and river deltas develop, impinge upon and interact with the fields of tidal dunes (e.g., Longhitano and Steel, 2016).

River deltas entering into such tide-dominated passageways can be strongly impacted by the effect of tidal currents, but differently than in ‘classical’ tide-dominated deltas (e.g., Dalrymple et al., 2003; Goodbred Jr and Saito, 2012; Cummings et al., 2016; Eide et al., 2016). Rather than simply being influenced by flood and ebb currents through the delta distributary channels, such deltas are confronted by tidal currents that move mainly parallel to the strait coastline, causing asymmetrical deflection of the delta-front sands, and creating considerable elongation of tidally-reworked, dune-bedded sand bodies in the direction of the dominant tidal flow (e.g., the Klang Delta in the Malacca Strait; the Elwha Delta and the south-west coast of Vancouver Island in the Juan de Fuca Strait; Uroza, 2008; Frey and Dashtgard, 2011; Longhitano, 2015; Longhitano and Steel, 2015, 2016). In this type of system, the initial processes are dominantly fluvial-derived flows capable of transporting large quantities of clastic sediments, but these become significantly reworked at the delta front by tidal currents flowing at a high angle with respect to the delta progradation direction. This paper documents stratigraphic sections measured across the northern margin of the early-middle Pleistocene Siderno Strait, located in the Calabro-Peloritani Arc, southern Italy (Fig. 5.1A).

The Siderno Strait represents an exceptionally well-preserved example of an ancient tide-dominated passageway. In particular, in the eastern side of the basin (Fig. 5.1C), magnificent cross-stratified mixed siliciclastic-bioclastic complexes exhibiting

large-scale (meter-thick) tidal foresets occur (Longhitano et al., 2012a). The northern border of the Siderno Strait was a tectonically-controlled margin during the strait's formation and infilling, and it was characterized by the development of an infra-strait tectonic high (Fig. 5.1B). This constriction generated hydraulic amplification of tidal currents flowing roughly parallel to the margin (i.e., towards the SE), having great influence on the progradation of deltaic systems laterally impinging into this *ca* 3.5 km-wide passageway. The objectives are: 1) to document the sedimentary facies and architectures that develop along a strait margin; 2) to investigate how sedimentation respond to local morpho-structural constrictions; 3) to show how tidal circulation significantly impacted the incoming deltaic wedge.

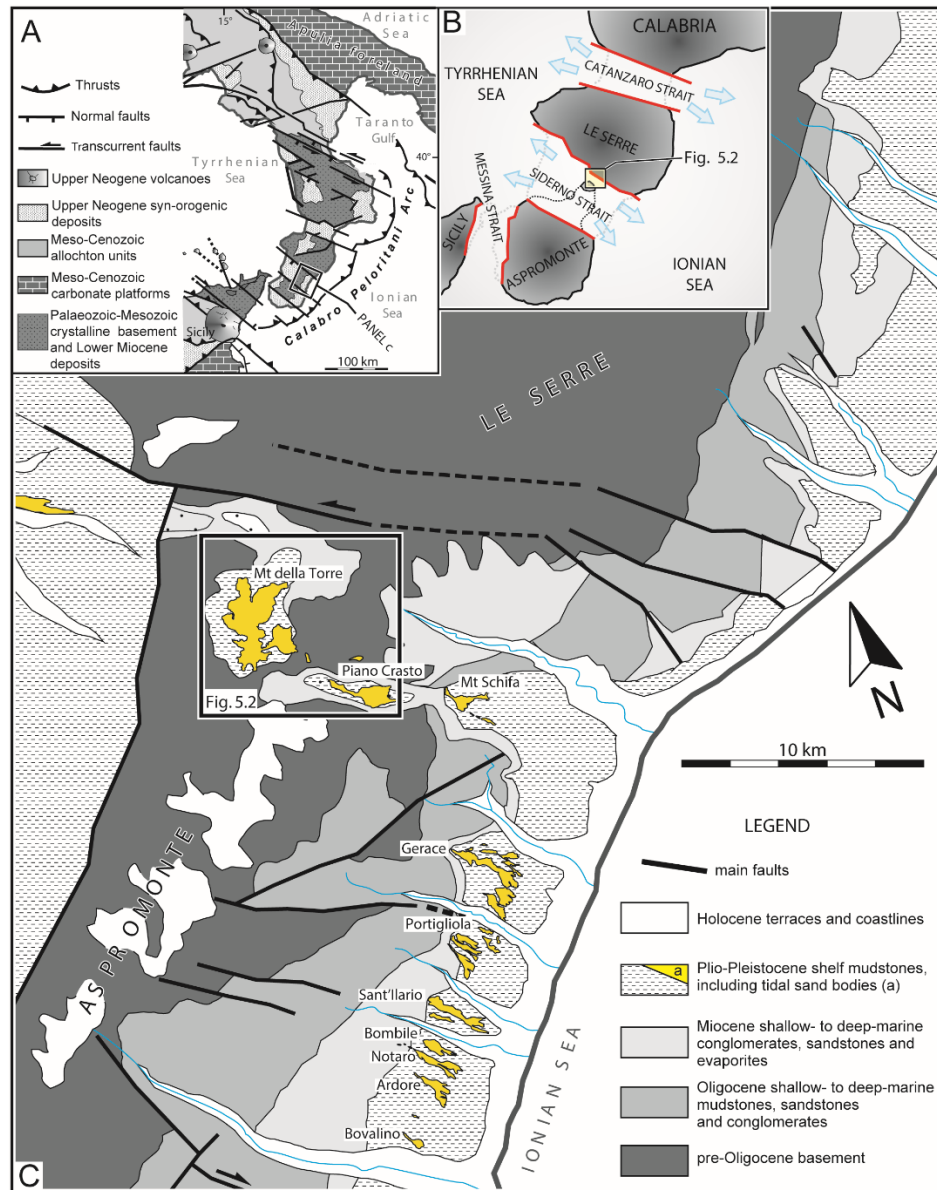


Figure 5.1: (A) Regional-scale structural sketch of the Calabro-Peloritani Arc, showing the main Plio-Pleistocene shear zones responsible for the south-eastward tectonic migration towards the Ionian Basin (modified from Tansi et al., 2007). (B) Paleogeographic reconstruction of the Siderno Strait during the Pleistocene, with the studied sector indicated in the rectangle. Note the occurrence of other adjacent tidal straits. (C) Simplified geological map of the central-eastern sector of the Siderno Basin, showing the main tidal sand bodies and the area documented in this work (modified from Cavazza et al., 1997).

GENERAL GEOLOGICAL SETTING OF THE SIDERNO BASIN

General tectonic setting

The Calabro-Peloritani Arc is a small orogen located in the central Mediterranean (Fig. 5.1A) consisting of Palaeozoic magmatic and crystalline basement rocks overlain by Meso-Cenozoic sedimentary cover (Amodio-Morelli et al., 1976; Tortorici, 1982; Critelli, 1999). Starting from the late Miocene onwards, the arc migrated towards the Ionian Basin, as the effect of crustal convergence between the northward moving African Plate that was subducting beneath the southward-overriding European Plate (Knott and Turco, 1991; Van Dijk et al., 2000; Tansi et al., 2007 and references therein). The south-eastward structural migration of the Calabro-Peloritani Arc towards the Ionian foreland basin occurred by means of a number of regional-scale strike-slip zones that separated the orogen into segments (Fig. 5.1A) with different rates of tectonic deformation (e.g., Goes et al., 2004). All these zones became narrow-elongate marine basins separated by tectonic highs (Sylvester, 1988), which connected the Tyrrhenian to the Ionian Sea, turning into tidal straits during the early-middle Pleistocene (i.e., the Catanzaro and the Messina straits) (Fig. 5.1B).

The Siderno Basin (Fig. 5.1C) is a WNW-ESE-elongate, *ca* 50 km long and 20 km wide, pull-apart basin between the Serre Massif to the north and the Aspromonte Massif to the south, developed during the Neogene-Quaternary within the proximal sector of the Calabrian forearc basin-fill (Van Dijk, 1992; Cavazza et al., 1997; Van Dijk et al., 2000; Cavazza and Ingersoll, 2005). The northern boundary of the basin represents one of the regional shear zones dissecting the Calabro-Peloritani Arc with left strike-slip kinematics (Knott and Turco, 1991), and that separated the Palaeozoic crystalline basement to the north and the sedimentary deposits filling the strait to the south. The

southern limit corresponds to another shear zone with right-slip kinematics, which was probably less active compared to the northern fault (Van Dijk, 1993; Tripodi et al., 2013).

The present-day exposure of the Pliocene-Pleistocene deposits that accumulated within the Siderno Strait is markedly unequal between the Tyrrhenian and the Ionian sides of the basin (Fig. 5.1C), with more abundant and better exposures on the Ionian side. This is due to the effect of a late Pleistocene NW-SE-trending extensional tectonics, related to the recent evolution of the Tyrrhenian Basin (Westaway, 1993; Tortorici et al., 1995; Galli and Peronace, 2015).

Neogene-to-Quaternary stratigraphy of the Siderno Basin

The Siderno basin-fill is represented by > 2,000 m-thick, Oligocene-to-Quaternary sedimentary succession, unconformably overlying the pre-Cenozoic basement (Patterson et al., 1995; Cavazza et al., 1997; Bonardi et al., 2001) (Fig. 5.1C).

The study interval lies at the top of a thick succession (> 800 m thick) of shallow-marine to deep-water Oligocene to Pleistocene sediments (Cavazza and DeCelles, 1993; Bonardi et al., 2001; Cavazza and Ingersoll, 2005). The study succession consists of mixed siliciclastic-bioclastic sediments up to 60 m thick which sharply overlie light-colored shelf marls and fine-grained sandstones (Cavazza et al., 1997). They are characterized by tidal cross-stratification and are considered to record of the onset of a tidal circulation in the Siderno Strait (Colella and D'alessandro, 1988; Cavazza et al., 1997; Longhitano et al., 2012a). The cross-stratified tidal deposits are unconformably overlain by gravels and sands belonging to different generations of marine terraces (Fig. 5.1C), lying up to 1,000 m above sea level. These terraces record a phase of tectonic uplift that caused the emergence of the Calabro-Peloritani block during the last 700 Kyr (Tortorici et al., 1995).

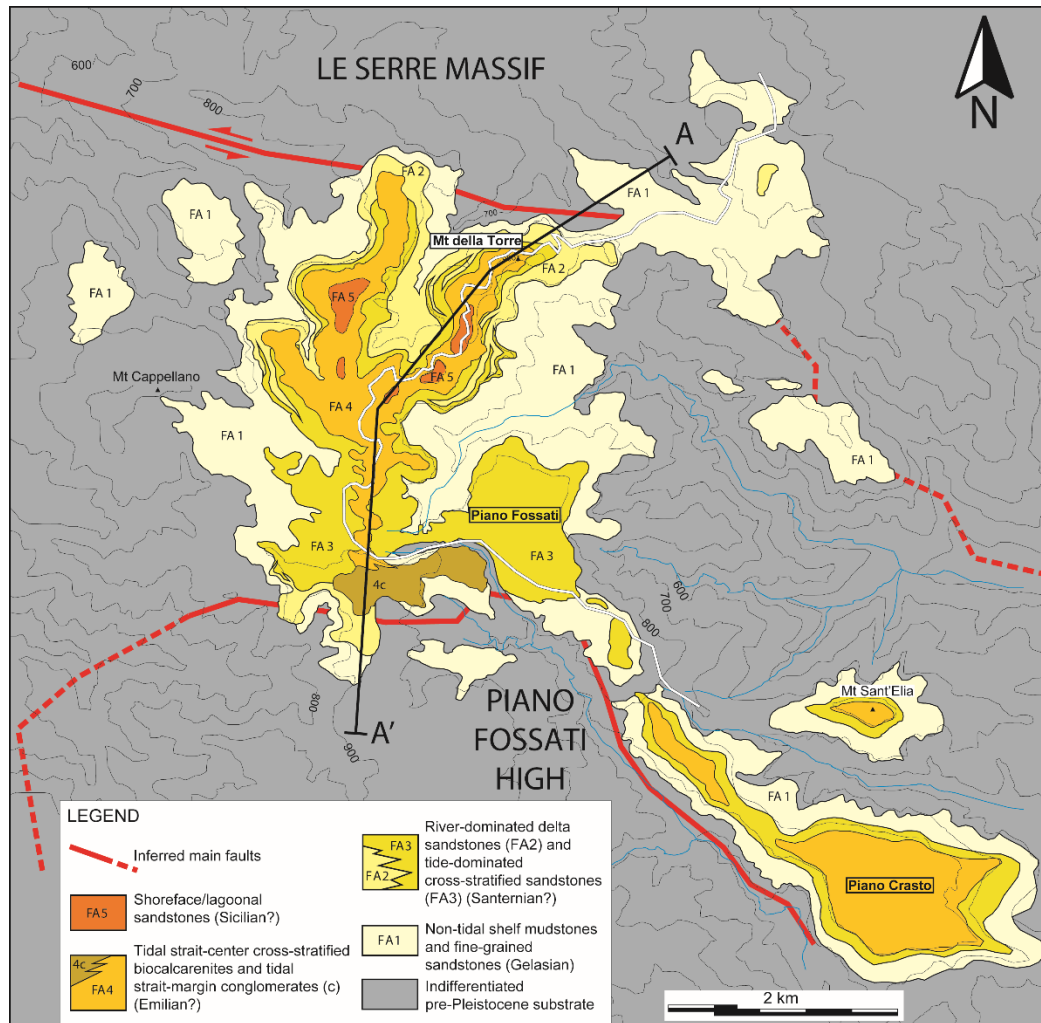


Figure 5.2: Detailed facies map of the studied area (see location in Fig. 5.1C). The present-day exposures of the lower-middle Pleistocene succession form elongate bodies. Cross-section A-A' is in Fig. 5.9.

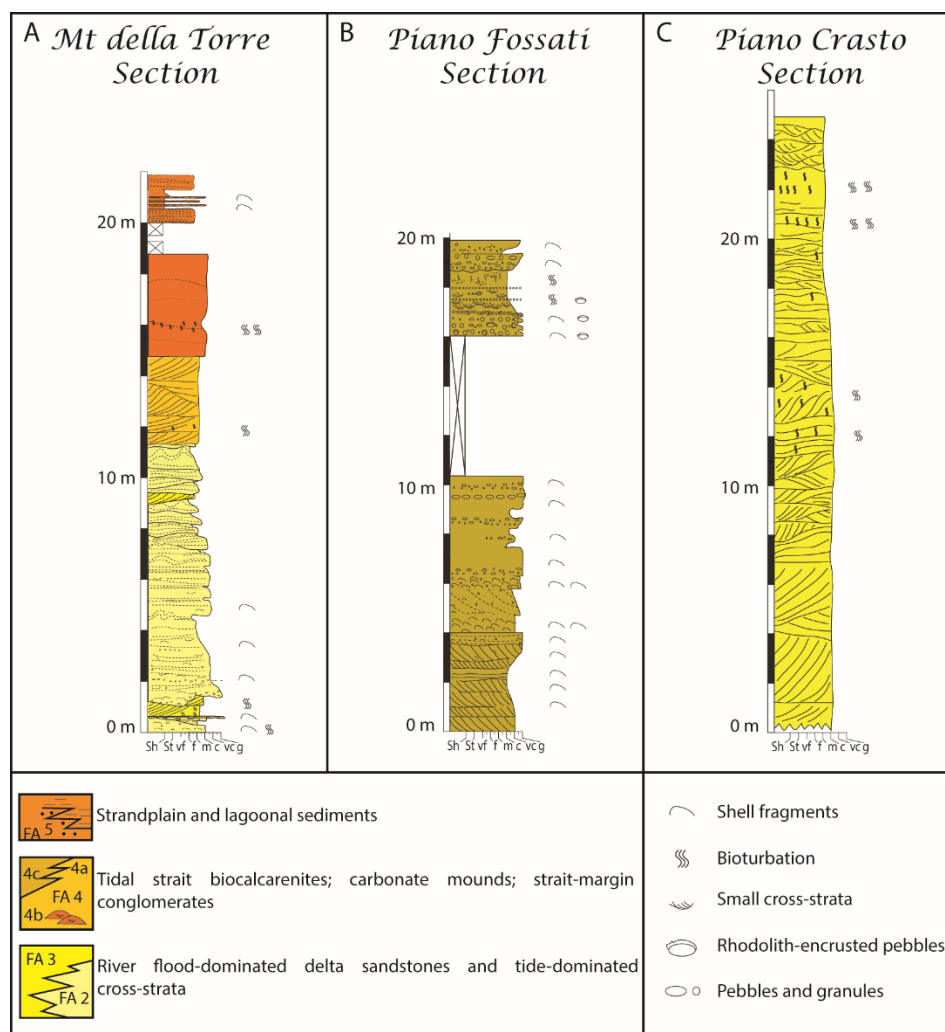


Figure 5.3: Main stratigraphic logs measured across the studied succession.

FACIES AND FACIES ASSOCIATIONS

This work is based on geological mapping (Fig. 5.2) coupled with the detailed logging of stratigraphic sections at key locations, paleocurrent measurements in cross-bedded sets and the collection of outcrop photomosaics for bedding architecture. The main outcrops are exposed on the Ionian side of the ancient Siderno Strait, between Mt della Torre (see also Colella and D'alessandro, 1988) and Piano Fossati (Fig. 5.2).

The sedimentological analysis has documented 12 sedimentary facies, which have been grouped into 5 main facies associations (Table 5.1).

Facies Association 1 (shelf mudstones and marlstones)

This facies association (*FAI*) includes the deposits in the lowermost stratigraphic interval of the study area, at the base of the hills and along modern incised valleys (Fig. 5.2). The deposits consist of a 60-70 m-thick monotonous coarsening-upward succession of light-colored mudstones that consist of tabular beds about 1 m thick (*facies 1a*) (Fig. 4), with common intercalations of thinner bedded mudstone and fine-grained, structureless and faintly laminated, sandstone towards the top (*facies 1b*) (Fig. 5.4). The base of the succession lies on the Zanclean Trubi Fm. and older substrates, forming a paraconformity surface (Cavazza et al., 1997), whereas the top of the succession is sharp and in places erosional. *FAI* deposits are commonly associated with *Zoophycos* ichnofacies, and have abundant planktonic Foraminifera dominated by *Sphaerodinellopsis* spp. and *Globorotalia margaritae* (Colella and D'alessandro, 1988).

Interpretation: Sediment textures and the micro-palaeontological content of *FAI* deposits indicate typical hemi-pelagic suspension fall-out in an open shelf environment. However, the coarsening-upward trend represented by progressively more abundant mudstone and sandstone intercalations towards the top, suggests a shallowing trend. The fine-grained deposits of *FAI* appear to infill pre-existent topography, consisting of narrow valleys and interfluves (Fig. 5.2) originated during a previous sea-level lowstand, which was responsible for the formation of the regional-scale unconformity documented at the base of this formation (Cavazza et al., 1997).

Table 5.1: List of facies

Facies associations	Facies	Description of the sedimentary facies	Interpretation of the depositional processes and environments	System tract
FA5	5c	Fine-grained and very well sorted sandstones, forming a sand body up to 5-6-m-thick and elongated perpendicularly with respect to the strait margins.	<p style="text-align: center;">Strandplain- lagoon regressive complex</p> Shoreface-strandplain system, including a lagoonal environment. It possibly marks the turn-around from transgression to regression at the beginning of the relative sea-level highstand.	HST
	5b	Alternation of mudstone and coarse sandstone, including also bioclastic-rich and silty interlayers, ranging in thickness from a few centimeters to ca. 10 cm, with bivalve and gastropod fragments.		
	5a	Light colored upper-fine to lower-medium sandstones, well sorted and normally-graded with sub-rounded grains, with few bioclasts, including low-angle laminae and normally-graded beds.		
FA4	4c	Cross-stratified, clast-supported, well-rounded conglomerates and sandstones, associated with algal rhodoliths, serpulids, bivalves, and rhodoliths.	<p style="text-align: center;">Tidal strait-margin late transgressive complex</p> Dune-bedded strait zone developed during a late stage of relative sea-level rise under the action of tidal currents flowing axially to the strait. This zone merged laterally to a strait-margin zone, flanked by a tectonic basement high and hosting pocket gravel beaches.	late TST
	4b	Isolated carbonate mounds, 10-m-wide and ca. 3-4-m-thick, including large-size balanides, barnacles, bryozoans, brachiopods, and abundant solitary cm-size corals.		
	4a	Cross-stratified, coarse-grained biocalcarenites made up of bivalves, bryozoans, echinoids and corals mixed with 10-30% of siliciclastic, sand-size fraction, forming two- and three-dimensional cross-strata up to 4 m thick, with paleo-currents pointing towards N125E.		
FA3	3b	Three-dimensional large-scale cross stratified sandstones and biocalcarenites up to 6 m thick.	<p style="text-align: center;">Deflected, tide-dominated delta-front regressive-transgressive complex</p> Series of superimposed dune fields developed on a delta-front environment, reworked by powerful tidal currents flowing at high angle with respect to the delta progradational axis.	LST - early TST
	3a	Two-dimensional cross-stratified sandstone up to 6 m thick, with paleo-currents ranging from N45 to N100. They include meniscate forms and biocalcarenitic intercalations made up of bivalves, bryozoans, barnacles, brachiopods and corals.		
FA2	2b	Cross-stratified lenticular sandstone intercalations bounded by erosional surfaces, showing sigmoidal, angular or tangential foresets up to 2 m thick. In places very bioturbated (meniscate <i>Scolicia</i> traces).	<p style="text-align: center;">River-dominated, tide-influenced deltaic regressive complex</p> River-dominated deltaic deposits, dominated by hyperpycnal and hyper-concentrated flows occurring during high-energy fluvial discharges and entering a tide influenced shallow-marine setting.	RST + LST(?)
	2a	Moderately- to poorly-sorted, normally-graded sandstones and subordinate conglomerates, forming lenticular strata, 0.4 to 5-6 m thick. Erosional basal surfaces marked by mud chips and lithic/shell fragments.		
FA1	1b	Thin mudstone and fine-grained sandstone intercalations.	<p style="text-align: center;">Shelf mudstones and marlstones</p> Regressive sedimentation in an open shelf setting, receiving even more siliciclastic input because of a generalized shallowing tendency due to a normal regression.	HST
	1a	Whitish mudstone tabular strata each ca. 1 m thick, associated with <i>Zoophycos</i> ichnofacies, and yield abundant planktonic Foraminifera dominated by <i>Sphaerodinellopsis</i> spp. and <i>Globorotalia margaritae</i> .		

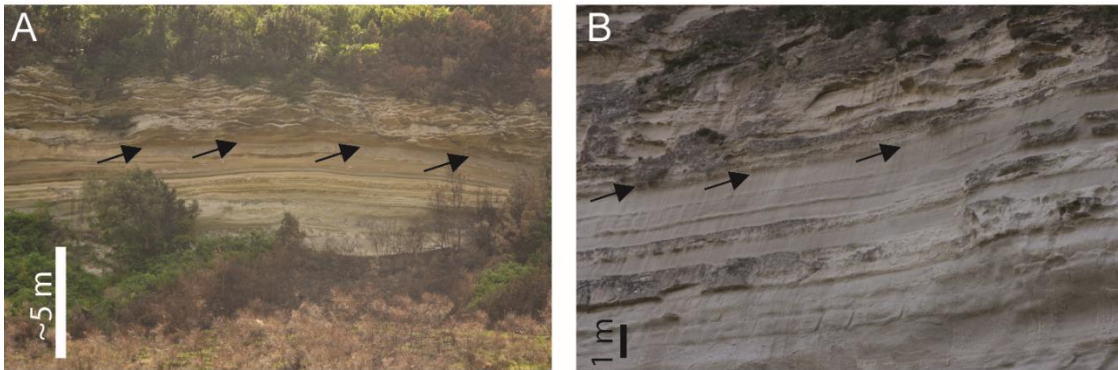


Figure 5.4: (A) Shelf mudstones and marlstones belonging to *FA1*. Arrows indicate the sharp contact with the overlying *FA3* tidal sandstones. (B) Detail of the surface separating *FA1* from the overlying *FA2-FA3* tidal cross-stratified sandstones.

Facies Association 2 (river-dominated, tide-influenced deltaic deposits)

The deposits of *FA2* have been subdivided into two facies: *2a* and *2b* (Table 5.1).

Facies 2a consists of sandstones with subordinate conglomerates, organized into irregular strata, ranging in thickness from 0.4 up to 5-6 m (Fig. 5.5A). The base of each bed commonly scours deeply into the underlying deposits. Towards the top of this succession, beds bounding surfaces display undulate and convex geometries with a wavelength of several meters (Fig. 5.5B). Granules and small pebbles, composed of sub-angular lithic fragments, mud chips and shell fragments, commonly mark the basal erosional surfaces. The individual beds show a subtle fining-upward trend, from conglomerate or very coarse/coarse-grained sandstones, to coarse- and medium-grained sandstones (Fig. 5.5A). Sandstones consist of moderately to poorly sorted siliciclastic grains (rich in mica and biotite), commonly containing abundant shell and bioclastic fragments (10-20%) concentrated in the lowermost strata intervals. The shell fragments are usually sub-horizontal, and not in a hydrodynamically stable position, although near

the base of the beds they can be convex upwards and slightly imbricated (in small pockets). Indistinct plane-parallel and faint low-angle inclined laminations associated with gently undulating laminations occur. Soft-sediment deformation structures (SSDS) are present and usually occur in the uppermost part of each bed (Fig. 5.5A and 5.5D).

Facies 2b occurs as localized intercalations within *facies 2a*. It is characterized by a lenticular geometry, as it often fills pre-existing scours, and it is erosionally bounded at the top (Fig. 5.5A and 5.5C). *Facies 2b* is cross-stratified, forming sigmoidal, angular and tangential foresets up to 2 m thick (Fig. 5.5C). These sediments are composed of upper medium-lower coarse and lower medium-upper fine sandstones and contain sparse sub-angular pebbles and granules, as well as shell fragments. The cross-strata typically display segregation of bioclastic-siliciclastic laminae and set-climber ripples, cyclic alternation of angular and tangential toesets, as well as reactivation surfaces. The overlying deposits belonging to *facies 2a* usually truncate the upper part of the foresets (Fig. 5.5C). SSDS are absent in *facies 2b*. In places, *facies 2b* is intensely bioturbated, displaying abundant poorly preserved meniscate *Scolicia* traces. Paleocurrent measurements of *facies 2b* cross-strata indicate a dominant direction towards the SW (Fig. 5.5A).

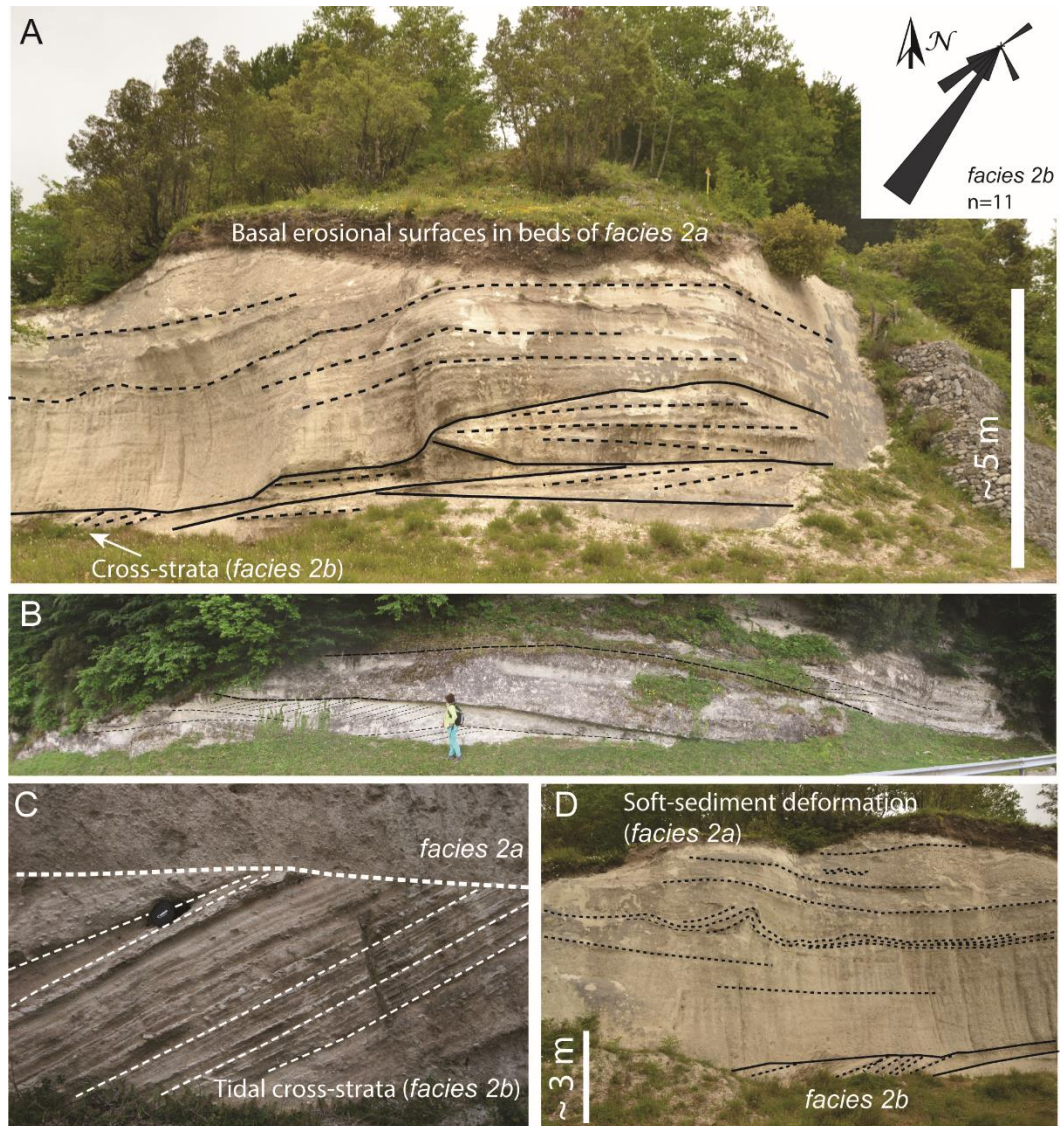


Figure 5.5: Overview of *FA2* deposits. (A) Typical erosional surfaces of *facies 2a*; note how *facies 2b* is eroded by *facies 2a*. (B) Undulate erosional surfaces. (C) Tidal foreset lamination within *facies 2b* erosionally overlain by the deposits of *facies 2a*. (D) Soft sediment deformation in *facies 2a*.

Interpretation: *FA2* deposits are interpreted as the result of fluviably-derived sediments entering a shallow-marine area in a deltaic proximal setting, based on the sediment texture, sorting, occurrence of shell fragments, bed geometries and sedimentary structures.

Facies 2a deposits are interpreted as the result of river flood-generated hyperpycnal flows (Mutti et al., 1996; Mutti et al., 2000; Mutti et al., 2003). Sedimentation may have occurred through an initial phase of scouring of the underlying deposits which is usually characteristic of high-energy river flash floods (Nemec and Muszynski, 1982; Sohn et al., 1999). The coarse-grained, poorly sorted lower portion of *facies 2a* strata would represent the basal hyperconcentrated flow produced when sediment-laden flows entered seawaters in association with a flood event (Mutti et al., 1996; Mutti et al., 2000). Bed scouring, with associated rip-ups and shell debris, is very common in this type of flows (Mutti et al., 2000; Rossi and Craig, 2016). The presence of shells not in hydrodynamic position further supports the lack of traction currents, but rather the presence of very high depositional rates or high sediment concentrations. The finer-grained and finely laminated upper part of each bed can represent the waning stage of the event or a decrease in sediment concentration (i.e., more diluted turbulent flows; Mutti et al., 2000). Alternatively, the laminations within each bed can be interpreted as internal scour surfaces or as antidunes (Southard and Boguchwal, 1990), related to the passage and deposition of sediment surges. The SSDSs can be caused by allogenic triggers (e.g. earthquakes) linked to the fault activity along the basin margin, or autogenic triggered responses in the bed related to rapid deposition and/or high sediment concentrations.

Facies 2b cross-strata have been deposited or reworked under the influence of tidal currents, based on the alternations of siliciclastic and bioclastic laminae, reactivation surfaces, cyclic alternation of angular and tangential toset geometry and set-climber ripples (e.g., Longhitano, 2011; Chiarella, 2016). We therefore argue that *facies 2b* cross-strata were formed in inter-flood periods, when tidal currents had enough time to rework the sediments emplaced during the previous river flood event. Moreover, the lack of

SSDSs in *facies 2b* suggests that deposition of *facies 2a* occurred when the sediments were already dewatered (Chiarella et al., 2016). *Facies 2b* cross-strata are only sporadically preserved and truncated by *facies 2a* deposits, suggesting that each high-energy flood event was able to remove tidally-reworked interflood deposits in the most proximal areas.

In summary, *FA2* sediments suggest accumulation in a flood-dominated, proximal deltaic setting, that most likely is inter-gradational between a river-delta system and a fan-delta system (cf. Mutti et al., 1996; Mutti et al., 2000), characterized by high-energy scouring (likely related to high-energy flood events) and deposition associated with hyperpycnal flows. Tidal currents were present in the marine basin, but they were able to rework the fluviially-derived sediments only during interflood periods. The preservation potential of tidally-reworked sediments in this proximal deltaic setting is fairly low, due to the high degree of erosion occurring during river flood events.

Facies Association 3 (deflected, tide-dominated delta-front)

FA3 is the volumetrically most important part of the study succession, reaching *ca* 70 m-thick of moderately- to well-sorted medium- to coarse-grained siliciclastic sandstones, biocalcarenic intervals and rare conglomeratic pavements (Figs. 5.6A and 5.6B). *FA3* forms vertically-stacked packages (up to 24 m thick) separated by wide and undulate erosional master surfaces (Figs. 5.6B and 5.6C). Each unit is characterized by stacked cross-strata. Cross-stratal sets have tabular to lenticular geometries and range in thickness from 1 to 6 m. Both trough (*facies 3a*) and planar (*facies 3b*) cross-strata are present, with paleocurrents ranging from 45°N to 100° N. However, moving from Mt della Torre to Piano Crasto areas (Fig. 5.2), cross-strata geometries change from being mainly 3D to 2D (Fig. 5.6A and 5.6D). Foresets exhibit reactivation surfaces, rhythmic foresets bundles, alternation of angular and tangential toesets, herringbone stratifications

and segregated (siliciclastic-bioclastic) laminae (Fig. 5.6D). Trace fossils are meniscate forms both parallel to and cross-cutting the foresets, whereas the biocalcarenitic intercalations are dominated by bivalves, bryozoans and less abundant barnacles, small-size brachiopods and corals.

In cliff exposures, *FA3* cross-strata appear to alternate and interfinger with *FA2* deposits, becoming thicker and more abundant towards the top (Fig. 5.6E and 5.6F).

Interpretation: The *FA3* cross-stratified sandstone succession is interpreted as a series of superimposed dune fields, derived from the reworking of distal delta-front deposits generated by tractional tidal currents flowing at a high angle with respect to the main deltaic progradational axis (see also Longhitano and Steel, 2016). We interpret *FA3* deposits to have been generated in a distal delta-front setting, more exposed to the action of the tidal currents that were flowing within the strait. The greater abundance of tidal cross-strata relative to river-dominated facies indicates the dominance of tidal currents in this part of the basin and the deflection of the delta front progressively towards the main tidal current direction, which was roughly parallel to the local margin of the strait.

Tidal current strength possibly decreased down-current (i.e. from Mt della Torre to Piano Crasto), due to the progressive enlargement of the passageway cross-section, generating a downcurrent transition from three- to two-dimensional tidal dunes, as observed in other modern and ancient tidal straits (e.g., Longhitano, 2013; Longhitano et al., 2014).

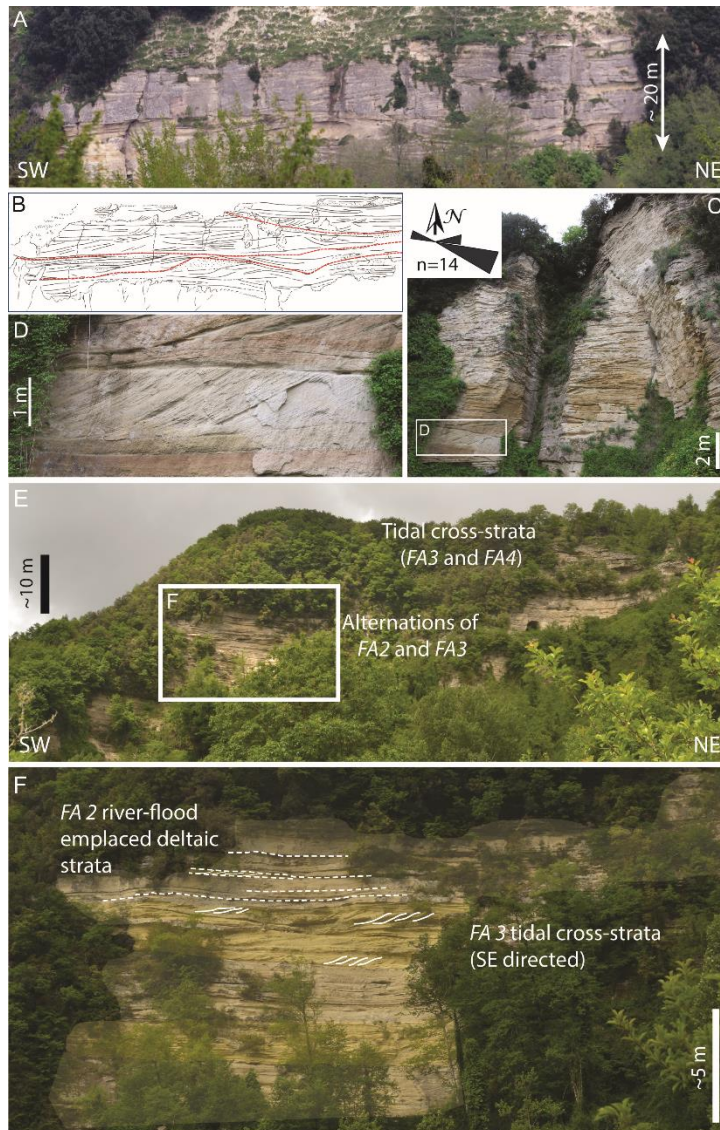


Figure 5.6: Outcrop photographs of *FA3*. (A) Piano Fossati section showing large-scale cross-stratification with abundant three-dimensional cross-strata. (B) Line-drawing of the photograph in A. Note cross-cutting sets and the dominant foreset dip towards the left (E-SE). (C) Piano Crasto section, which lies down-current from the section shown in A and B (see Fig. 5.2), shows, instead, dominant two-dimensional cross-strata with unimodal foreset direction. (D) Details of the photo in panel C, showing internal features of the tidal cross strata. (E) Cliff exposure in Mt della Torre, showing alternation of *FA2* and *FA3* deposits, with *FA3* deposits becoming more abundant towards the top. (F) Detail of the cliff in (E), showing the interfingering between *FA2* and *FA3*.

The basal interval of this association is slightly inclined towards the main sedimentary transport direction, indicating a low-angle downcurrent-dipping slope, a geometry that also contributes to the flow expansion that generated the down-current decrease in tidal-current speeds. The thickness of these strata is also probably the result of a certain confinement exerted by the previous topography and the presence of the Piano Fossati tectonic high (Fig. 5.2).

Facies Association 4 (tidal strait-margin complex)

FA4 includes three main *facies 4a, 4b* and *4c*.

At Mt della Torre, *facies 4a* forms a *ca* 30 m-thick succession of coarse-grained biocalcarenic sandstones, composed of fragments of bivalves, bryozoans, echinoids and corals mixed with a variable amount (10-30%) of quartz-rich siliciclastic material. The biocalcarenites sharply overly the deltaic siliciclastic deposits, recording an abrupt enrichment in the carbonate content of the deposits (Fig. 5.7A). *FA4* deposits are diffusely cross-stratified, forming individual sets of trough and planar cross-strata up to 2 m thick (Fig. 5.7B). Paleocurrents suggest a general direction towards 125°N, although the dataset is extremely limited due to poor outcrop accessibility.

Facies 4b represents isolated carbonate mounds, 10 m-wide and *ca* 3-4 m thick, organized in a compensational stacking pattern (Fig. 5.7C). Mounds includes clusters of large *Megabalanus tulipiformis* (Colella and D'alessandro, 1988), associated with abundant barnacles, bryozoans and brachiopods. However, solitary cm-size corals (Fig. 5.7D) represent the recurrent species. In places, the mounds show intense bioturbation, especially close to their base.

At Piano Fossati, the correlative deposits are represented by *facies 4c* (Fig. 5.7E and 5.7F), consisting of conglomerates and mixed siliciclastic-bioclastic sandstones, organized into three vertically-stacked, coarsening-upward lenticular units. The latter

exhibit several scour surfaces and extensive, low-angle accretionary surfaces that pass into distal fine-grained deposits southeastwards (parallel to the strait axis). Conglomerate clasts, pebble to boulder grades, derived from granitoid basement rocks. They are sub-angular to well-rounded and discoidal with maximum particle size of *ca* 10 cm in diameter, commonly encrusted by algal rhodoliths. Some layers are rich in serpulids, bivalves, and rhodoliths (Fig. 5.7F). Most of the strata are normally or inversely graded, containing abundant shells and barnacles, including also a medium grained arenite matrix enriched in echinoids, bivalves and bryozoans. Cross-stratification occurs in places, forming 9 to 20 cm thick sets. Bioturbation is sparse, but can be quite pervasive in certain intervals where only ghosts of cross-strata are preserved.

Interpretation: The biocalcarenes of *FA4* are characterized by two- and three-dimensional cross-strata very similar to those observed in the previous interval (*FA3*), and similar cross-stratified biocalcarenes pervasively occur at the top of a number of other stratigraphic sections in the Siderno Strait, as well as in other correlative basins of southern Italy (Longhitano et al., 2012a). For these reasons, we argue that tidal currents (flowing axially to the passageway between Mt della Torre and Piano Fossati) were controlling the deposition of *FA4* biocalcarenes as well.

If compared to *FA2* and *FA3*, the abrupt enrichment in bioclasts and the occurrence of localized carbonate mounds in *FA4* point towards a reduction of siliciclastic (deltaic) input in the basin and sediment starvation, which in turn allowed favorable conditions for the development of faunal communities. Siliciclastic starvation in the basin could have occurred for two main reasons: 1) climatic change and reduction in water and sediment supply to the basin (i.e. deactivation of fluvial systems); 2) relative sea level rise and consequent deepening of the Siderno Strait, and back-stepping of the fluvio-deltaic systems.

The presence in the carbonate mounds of solitary corals of small dimensions points towards a relatively deep environment, which can possibly be related to a rapid rise of relative sea-level (Colella and D'alessandro, 1988). These deposits merged laterally and across the outcrop localities into the coarse-grained deposits of *facies 4c*, that are interpreted as beach sediments reworked by currents and storms in an upper shoreface setting, along the Piano Fossati tectonic high.

Facies Association 5 (shoreface and lagoon complex)

The deposits of *FA5* represent the uppermost stratigraphic interval of the investigated succession. They have been subdivided into three facies: *5a*, *5b* and *5c*.

Facies 5a consists of light colored upper-fine to lower-medium-grained sandstones, well sorted and with sub-rounded grains, with few bioclasts (Fig. 5.8A). These deposits are characterized by low-angle laminae and normally-graded beds.

Facies 5b overlies *facies 5a* (Fig. 5.8A) and forms an alternation of mudstones and coarse sandstone beds, including also bioclastic-rich beds, 1-10 cm thick (Fig. 5.8B). The bioclastic intervals mostly contain bivalve and gastropod fragments, ranging from shell hash, to larger fragments (Fig. 5.8C).

Facies 5c has been recognized at the very top of the succession, and consists of 5-6 m-thick lower medium-grained very well sorted sandstones with ghosts of low-angle laminations (Fig. 5.8D), forming an elongate sand body stretching perpendicularly with respect to the strait (see Fig. 5.2).

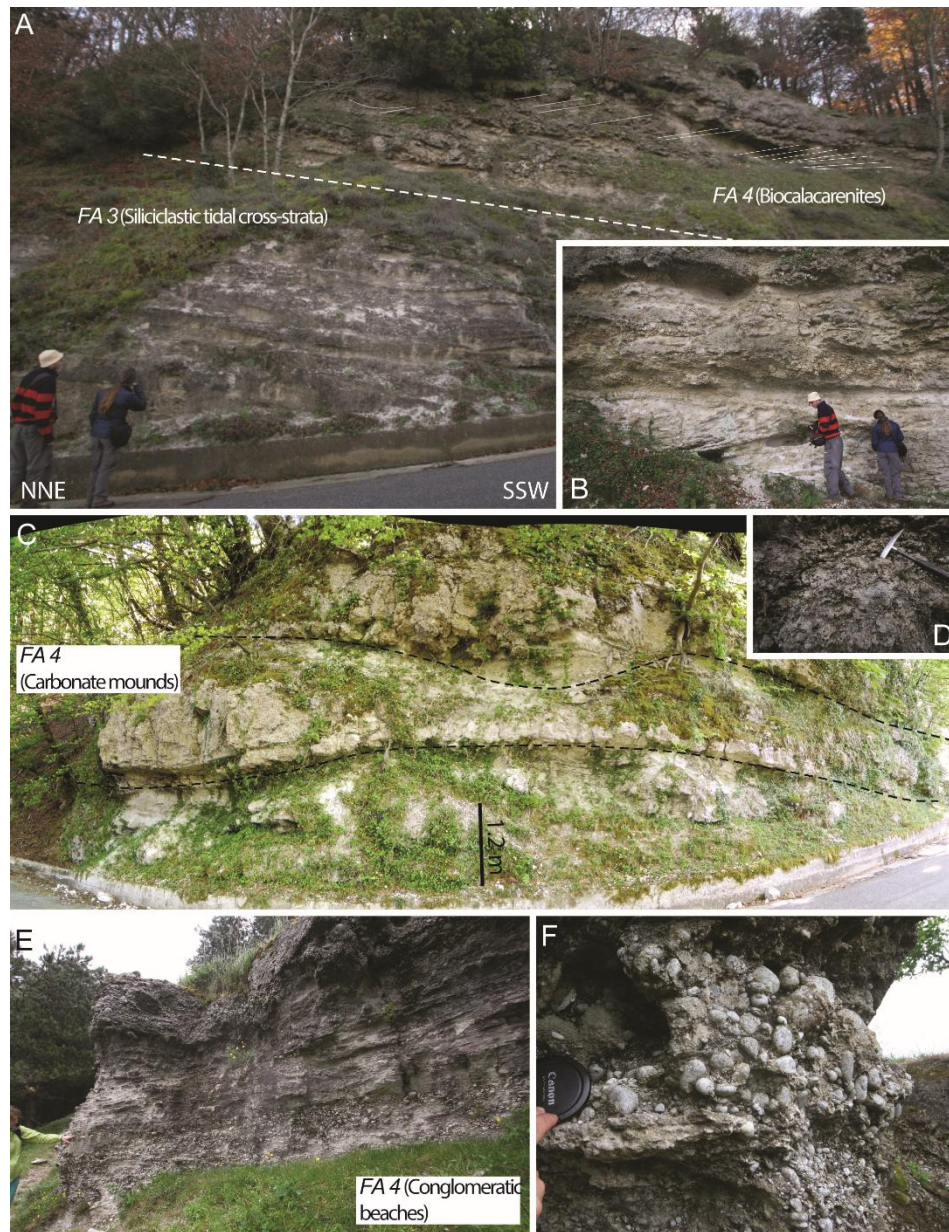


Figure 5.7: Outcrops of *FA4*. (A) Vertical transition at the Monte della Torre section between *FA3* and *FA4* (dotted line). (B) Detail of cross-stratified biocalcarenes of *facies 4a*. (C) Carbonate mounds of *facies 4b*, organized in a lateral compensation pattern. (D) Close-up view from the previous photograph. (E) Conglomerates and sandstones of *facies 4c* at Piano Fossati. (F) Detail from the previous photograph.

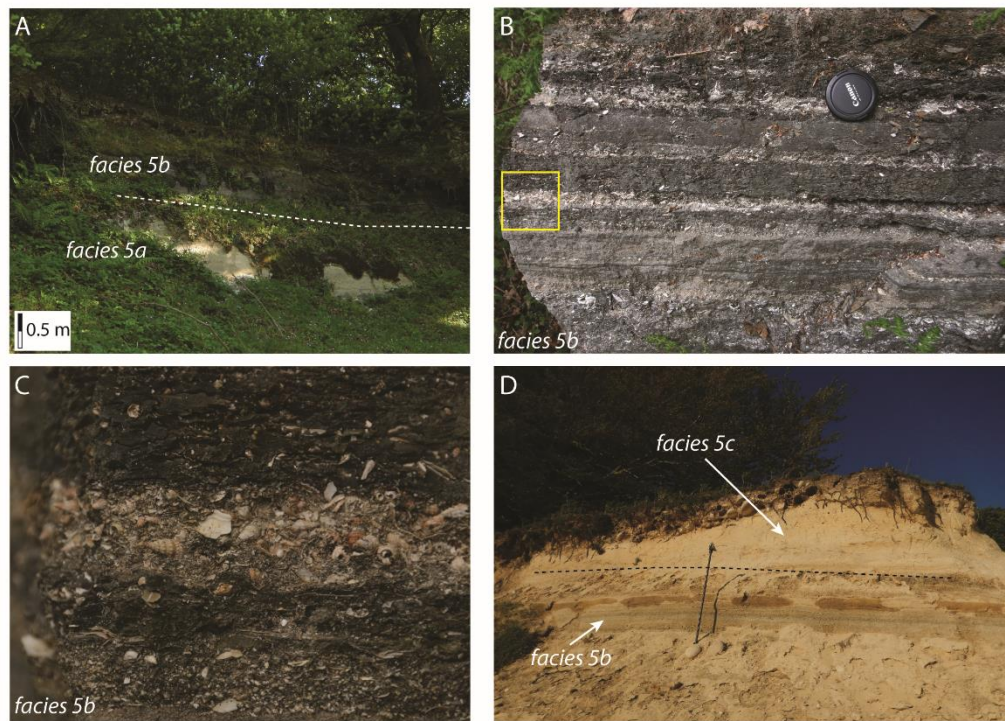


Figure 5.8: Deposits belonging to *FA5*. (A) Cross-laminated foreshore sandstones (*facies 5a*) overlain by lagoonal fine-grained, bioclastic sandstones (*facies 5b*). (B) Alternation of mudstones and bioclastic sandstones interpreted as lagoonal deposits (rectangle indicates the detail in panel C). (C) Bioclastic-rich interval encased in muddy sediments (*facies 5b*). For location, see rectangle in (B). (D) Laminated, fine-grained sandstones interpreted as aeolian deposits overlying *facies 5b* (Jacob staff for scale is 1.1 m tall).

Interpretation: *FA5* is interpreted as a shoreface–strandplain system, including a lagoonal environment (cf. Boothroyd et al., 1985; Ashley and Grizzle, 1988; Nichols, 1989). It may have been the barrier bar inherited from the prior transgression, but became now a regressive shoreface or strandplain (possibly marking the turn-around from transgression to regression at the beginning of the relative sea-level highstand). The coarse-grained sandstone layers and bioclastic-rich layers could represent sediments

reworked by waves/storms. *Facies 5c* could possibly represent small aeolian dunes (backshore environment), part of a spit or of a tombolo. The deposits of *FA5* are significantly shallower and more proximal than the underlying deposits belonging to *FA4*, indicating an overall shallowing trend.

DISCUSSION: MARGINAL-MARINE SEDIMENTATION ALONG THE SIDERNO STRAIT NORTHERN MARGIN

The sedimentary succession exposed along the northern margin of the Siderno Strait shows a regressive-transgressive-regressive, vertical facies trend, from shelf mudstones, to deltaic tidal-influenced cross-bedded sandstones, to tidal strait cross-bedded biocalcarenites, up to regressive shoreface non-tidal sandstones (Fig. 5.9A). The northern margin of the Siderno Strait represents a peculiar case, where the local morpho-structural conditions influenced sedimentation and hydrodynamic processes. The northern margin was characterized by a highly irregular morphology, due to the emplacement of an isolated tectonic high (i.e. Piano Fossati), which narrowed the strait to form a *ca* 3.5 km-wide local passageway. This uncommon morpho-structural element may have triggered a pronounced interplay between deltaic processes and tidal current reworking.

Deltaic vs. tidal strait processes

The sedimentary deposits documented in the present study are interpreted as depositional environments belonging to an ancient delta impinging onto a narrow tidal passageway, along the margin of a wider tidal strait.

River-flood deposits in straits

As observed in cliff exposures (Fig. 5.6E and 5.6F), river-flood dominated deltaic deposits (*FA2*) and tidal cross-strata (*FA3*) alternate in the stratigraphy, pointing to an interplay between fluvial and tidal processes (Fig. 5.9) in the deltaic environment (*facies 2a*). The fluvial system feeding the delta was draining the tectonically active Serre Massif (Fig. 5.2), providing the siliciclastic source for the gravel- and sand-size material shed into the strait. Within *FA2*, cross-strata produced by tidal current reworking (*facies 2b*) are preserved in places (Fig. 5.9). The occurrence but poor preservation potential of tidal cross-beds within fluvially-emplaced sediments in *FA2* indicates that fluvial processes were dominant over marine reworking. In contrast, *FA3* is characterized by a predominance of medium- to large-scale tidal cross-strata, which are well developed in Mt della Torre and Piano Fossati areas, as well as further downcurrent in Piano Crasto area (see Figs. 5.2 and 5.3). *FA3* is interpreted as the product of a strong reworking of sediments by tidal currents, oriented axially within the strait (i.e., south-eastward). Based on facies characteristics and on the lateral and vertical relationships between facies associations, we argue that fluvially-derived sediments were feeding a deltaic system that built transversely out from the northern margin of the Siderno Strait, entering a narrow setting, due to the presence of the Piano Fossati structural high (Fig. 5.9). Tidal currents were flowing axially within the strait and were mainly directed towards the south-east (i.e., towards the Ionian Sea). In the study area, tidal currents were further enhanced by the presence of a morphological constriction, which created a 3.5 km-wide passageway, between the Siderno Strait northern margin and the Piano Fossati high.

Intensity of tidal current reworking of the delta front

Tidal currents in straits tend to be stronger in the axial part of the passageway and weaker along the shallower margins, due to frictional dissipation (Frey and Dashtgard,

2011; Longhitano, 2013). This energy variation controlled the greater preservation of fluviially-derived sediments (i.e., *FA2*) in the proximal delta-front environment, and the occurrence of more tide-influenced facies (i.e., *FA3*) in the distal delta front and strait center. This specific hydrodynamic partition of the tidal flow in narrow straits or passageways can exert a considerably influence in shaping sand accumulations at the bottom, forming elongate bodies oriented roughly parallel to the dominant tidal flows, as well as to the strait margins. This phenomenon has been interpreted in a number of modern and ancient river deltas that impinge tidal straits, where delta-front sands deflected with respect to the deltaic main progradational axis, were asymmetrically distributed for considerable distances along the coast, even eventually producing detached sand banks or isolated tidal dune fields. (e.g., Longhitano and Steel, 2016). The delta-front deflection is also recorded in the studied deposits, in terms of the distribution of *FA3* deposits in a downcurrent direction (from Mt della Torre area to Piano Crasto area) (Fig. 5.2).

Tidal reworking of sediments is well-documented from transgressive shallow-marine shelf settings (e.g., Trentesaux et al., 1999; Olariu et al., 2012; Reynaud and Dalrymple, 2012; Leva López et al., 2016; Michaud and Dalrymple, 2016). Among these examples, the Roda Formation shows some remarkable similarities with the study succession, as it was also deposited in an elongated marine corridor in a tectonically active basin, where tidal currents were amplified and deltaic systems were present along the basin margins. According to Olariu et al. (2012) and Michaud and Dalrymple (2016), in the Roda Formation tidal currents were able to rework delta-fed sediments only during transgressive phases, and only in deltaic parasequences that significantly protruded into the basin (Michaud and Dalrymple, 2016).

In the deposits described here, on the contrary, tidal currents were amplified along the Siderno Strait northern margin, because of the presence of a structural high. For this reason, tidal currents were able to rework delta-fed sediments not only during transgressive phases, but also during deltaic progradation. Rather than tidal bars and ridges as in the Roda Formation example (Olariu et al., 2012; Michaud and Dalrymple, 2016), in the Siderno Strait delta-fed sediments were reworked into dune fields. Tinterri (2007) also described the interaction between river flood-dominated mouth bars present in some sandstone tongues of the Roda Formation and tidally-reworked deposits. According to Tinterri (2007), river and tidal interaction in the most distal delta deposits of the Roda Formation were common due to local structural confinement, in a scenario similar to what we have suggested in the present case study.

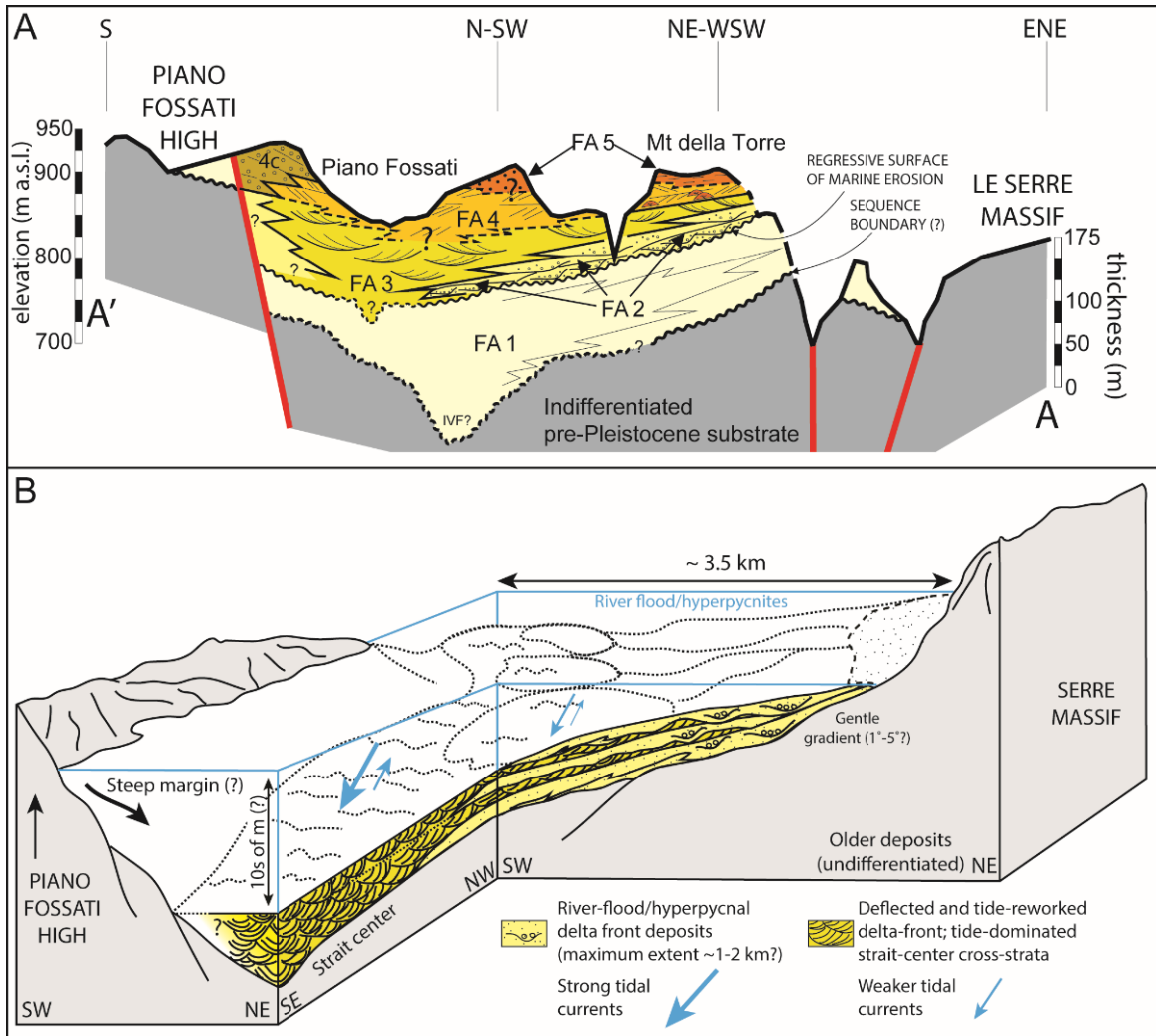


Figure 5.9: (A) Cross-section reconstructed along the trace A'-A indicated in Fig. 5.2. (B) Conceptual depositional model showing the relationships between river-dominated deltaic deposits and tidal cross-strata interpreted in the present work.

The early Pleistocene Siderno strait-margin evolution and the onset of a tidal circulation

The non-tidal shelf mudstones (*FA1*) occur at the base of the studied succession and are widespread in the Siderno Basin. The tabular strata are made up of mudstones, marlstones and fine sandstones containing open-marine micro-fauna. In the studied sector, as well as in other sections exposed in the eastern side of the basin, they crop out discontinuously, or infill lowstand valleys, incised into the older substrate (Fig. 5.10A).

The overlying deltaic tidally-influenced cross-bedded sandstones (*FA2-FA3*) lie erosionally on top of the shelfal mudstones (Fig. 5.4). The contact between them can be interpreted as a regressive surface of marine erosion (Plint, 1988; Helland-Hansen and Martinsen, 1996). This surface, which is conformable in the southern correlative successions, presumably originated during a virtually continuous phase of relative sea-level lowering induced by the activation of the structurally-controlled Siderno Strait northern margin, and further scoured by strong tidal currents. From this stage onwards, the Siderno Basin records the action of tidal currents, turning a non-tidal shelf passageway into a tidal strait (Fig. 5.10B) (Longhitano et al., 2012a). This change was probably a consequence of the inception of a morpho-structural cross-section of the basin that favored the switch-on of tidal-modulated current exchanges between the Tyrrhenian and the Ionian basins (e.g., Anastas et al., 2006; Longhitano et al., 2014).

During an episode of relative sea level rise, the marginal passageway of the northern Siderno Strait was still affected by strong tidal currents (Fig. 5.10C). As the siliciclastic input in the basin progressively decreased, local carbonate mounds developed, enriching the tidal-reworked sands with abundant bioclastic hash (Fig. 5.7).

As the rate of relative sea level rise slowed or stabilized, sediments along the strait margin in Mt della Torre area accumulated in a shallower environment, characterized by shoreface and lagoonal environments (*FA5*). The absence of any tidal

signature in the deposits of *FA5* suggests that at this time, tidal circulation diminished or stopped in this sector of the basin. At the last stage of deposition, before the rapid tectonic event that uplifted the area, these sediments probably merged southwards with the conglomeratic shoreface deposits shed from the steep-sloping cliffs of the Piano Fossati high (Fig. 5.10D). Based on the cartographic distribution of *FA5*, it is possible that the passageway between Mt della Torre and Piano Fossati became progressively closed due to the progradation of a sandy spit or tombolo linking the two adjacent sides (Fig. 5.10D). This last stage of sedimentation resulted from the likely severe decrease of the tidal circulation, prior to the definitive closure of the passageway. This in turn would suggest that the strait had shallowed to the point that friction was too great and tidal flow stopped before *FA5* deposits formed (Anastas et al., 2006). This last episode of sedimentation preceded an important phase of regional tectonic uplift, the demise of any marine circulation in the rest of the Siderno Strait and a break in the oceanographic linkage between the Tyrrhenian and Ionian basins.

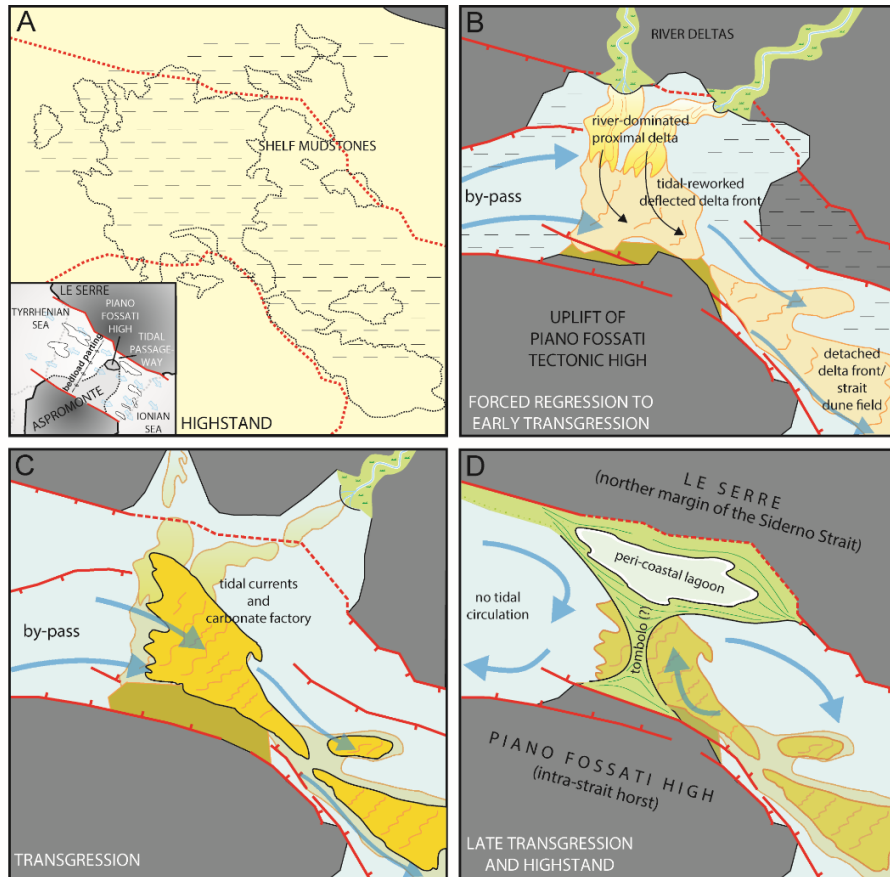


Figure 5.10: Palaeogeographic reconstructions showing the evolution of the northern margin of the Siderno Strait (inset), and the associated tide-dominated passageway during the early-middle Pleistocene. (A) At the end of the early Gelasian transgression, non-tidal open-shelf mudstones filled an inherited topography incised into older deposits during a previous stage of relative sea-level fall. (B) A subsequent phase of regional-scale tectonic activity in this part of the Calabro-Peloritani Arc was probably the cause of the onset of tide-modulated current exchange between the Tyrrhenian and the Ionian seas in the Siderno Strait (as well as in the adjacent Catanzaro and Messina straits; see reconstruction in Fig. 5.1C). Block-faulting of this part of the Siderno Strait margin caused the uplift of the Piano Fossati high, creating a 3.5-km-wide passageway that became dominated by strong tidal currents with a dominant SE-directed flow. Deltas prograded into this narrow corridor from the Serre Massif, but due to the presence of strong tidal currents, the delta front deposits became skewed. (C) The continued transgression caused the delta to back-step, and deposition became dominated by bioclastic tidal dunes and in-situ carbonate factories. (D) Highstand sedimentation caused coastal progradation and, possibly, the closure of this sector of the Siderno Strait margin.

CONCLUSIONS

This paper documents the sedimentology and stratigraphy of an early Pleistocene succession deposited along the northern margin of the Siderno tide-dominated paleo Strait. This area records sedimentary architectures along a morphologically complex margin, due to the presence of a structural high, which created a localized 3.5 km-wide passageway, responsible for the interaction between tidal and fluvial processes. Fluvially-fed sediments were shed from the northern margin during flood events into this area, accumulating river-dominated deltaic deposits. Tidal currents flowing roughly parallel to the strait margin reworked the delta-front sediments into southeastward migrating tidal dunes, oriented at a high angle with respect to the deltaic progradation direction. Tidal reworking was stronger in the most distal deltaic locations, and was weaker in the proximal sectors, so that the thickest cross-strata are located near the passageway axis, whereas deltaic deposits were dominated by river currents closer to the strait margin. Tidal reworking continued to affect sediment transport and deposition even when the siliciclastic input to the basin was shut off and sediments were mainly fed from carbonate factories. During the latest stage of strait-margin filling, tidal currents presumably decreased in strength, imparting even less influence on sediment accumulation and favoring the progradation of coastal strandplain deposits that progressively closed the narrow passageway. The dramatic regional-scale tectonic uplift that affected this segment of the Calabro-Peloritani Arc during the late Pleistocene marked the definitive deactivation of any tidal influence in the passageway, as well as in the whole Siderno Strait.

ACKNOWLEDGMENTS

This study represents the results of a field-based research module of the first author's PhD project, based at the University of Texas at Austin, financially supported by the University of Basilicata, UT Austin and GSA Research Grant (10724-14), and spent in southern Italy during Spring 2015.

REFERENCES

- Amodio-Morelli, L., Bonardi, G., Colonna, V., Dietrich, D., Giunta, G., Ippolito, F., Liguori, V., Lorenzoni, S., Paglionico, A., Perrone, V., Piccarreta, G., Russo, M., Scandone, P., Zanettin Lorenzoni, E., and Zuppetta, A., 1976, L'arco Calabro-Peloritano nell'orogene Appenninico-Maghrebide: *Mem. Soc. Geol. It.*, v. 17, p. 1-60.
- Anastas, A. S., Dalrymple, R. W., James, N. P., and Nelson, C. S., 2006, Lithofacies and dynamics of a cool-water carbonate seaway; mid-Tertiary, Te Kuiti Group, New Zealand: *Geological Society Special Publications*, v. 255, p. 245-268.
- Ashley, G. M., and Grizzle, R. E., 1988, The Hydrodynamics and Sedimentology of a Back-Barrier Lagoon-Salt Marsh System Interactions between hydrodynamics, benthos and sedimentation in a tide-dominated coastal lagoon: *Marine Geology*, v. 82, no. 1, p. 61-81.
- Belderson, R. H., Johnson, M. A., and Kenyon, N. H., 1982, Bedforms, *in* Stride, A. H., ed., *Offshore Tidal Sands*: London, Chapman and Hall, p. 27-57.
- Bonardi, G., Cavazza, W., Perrone, V., and Rossi, S., 2001, Calabria-Peloritani terrane and northern Ionian Sea, *in* Vai, G. B., and Martini, I. P., eds., *Anatomy of an Orogen: the Apennines and Adjacent Mediterranean Basins*: Dordrecht, Springer Netherlands, p. 287-306.
- Boothroyd, J. C., Friedrich, N. E., and McGinn, S. R., 1985, Barrier Islands Geology of microtidal coastal lagoons: Rhode Island: *Marine Geology*, v. 63, no. 1, p. 35-76.
- Cavazza, W., Blenkinsop, J., de Celles, P. G., Patterson, R. T., and Reinhardt, E. G., 1997, Stratigrafia e sedimentologia della sequenza sedimentaria oligocenica-quadernaria del bacino calabro-ionico: *Bollettino della Societa Geologica Italiana*, v. 116, no. 1, p. 51-77.
- Cavazza, W., and DeCelles, P. G., 1993, Geometry of a Miocene submarine canyon and associated sedimentary facies in southeastern Calabria, southern Italy: *Geological Society of America Bulletin*, v. 105, no. 10, p. 1297-1309.
- Cavazza, W., and Ingersoll, R. V., 2005, Detrital Modes of the Ionian Forearc Basin Fill (Oligocene-Quaternary) Reflect the Tectonic Evolution of the Calabria-Peloritani Terrane (Southern Italy): *Journal of Sedimentary Research*, v. 75, no. 2, p. 268-279.

- Chiarella, D., Angular and tangential toset geometry in tidal cross-strata: an additional feature of current-modulated deposits, *in* Proceedings Contributions to Modern and Ancient Tidal Sedimentology: Proceedings of the Tidalites 2012 Conference 2016, Volume 47, IAS Special Publication, p. 185-195.
- Chiarella, D., Moretti, M., Longhitano, S. G., and Muto, F., 2016, Deformed cross-stratified deposits in the Early Pleistocene tidally-dominated Catanzaro strait-fill succession, Calabrian Arc (Southern Italy): Triggering mechanisms and environmental significance: *Sedimentary Geology*.
- Colella, A., and D'alessandro, A., 1988, Sand waves, Echinocardium traces and their bathyal depositional setting (Monte Torre Palaeostrait, Plio-Pleistocene, southern Italy): *Sedimentology*, v. 35, no. 2, p. 219-237.
- Critelli, S., 1999, The interplay of lithospheric flexure and thrust accomodation in forming stratigraphic sequences in the southern Apennines foreland basin system, Italy: *Rendiconti Accademia dei Lincei*, v. 10, no. 9, p. 257-326.
- Cummings, D., Dalrymple, R., Choi, K., and Jin, J., 2016, The Tide-dominated Han River Delta, Korea: Geomorphology, Sedimentology, and Stratigraphic Architecture, Elsevier.
- Dalrymple, R. W., Baker, E. K., Harris, P. T., and Hughes, M. G., 2003, Sedimentology and stratigraphy of a tide-dominated, foreland-basin delta (Fly River, Papua New Guinea), *in* Sidi, F. H., Nummedal, D., Imbert, P., Darman, H., and Posamentier, H. W., eds., *Tropical Deltas of Southeast Asia—Sedimentology, Stratigraphy, and Petroleum Geology*, Volume 76, SEPM Special Publication, p. 147-173.
- Defant, A., 1961, Water bodies and stationary current conditions at boundary surfaces: *Physical Oceanography*, v. 1, p. 451-475.
- Eide, C. H., Howell, J. A., Buckley, S. J., Martinius, A. W., Oftedal, B. T., and Henstra, G. A., 2016, Facies model for a coarse-grained, tide-influenced delta: Gule Horn Formation (Early Jurassic), Jameson Land, Greenland: *Sedimentology*, p. n/a-n/a.
- Frey, S. E., and Dashtgard, S. E., 2011, Sedimentology, ichnology and hydrodynamics of strait-margin, sand and gravel beaches and shorefaces: Juan de Fuca Strait, British Columbia, Canada: *Sedimentology*, v. 58, no. 6, p. 1326-1346.
- Galli, P. A. C., and Peronace, E., 2015, Low slip rates and multimillennial return times for Mw 7 earthquake faults in southern Calabria (Italy): *Geophysical Research Letters*, v. 42, no. 13, p. 5258-5265.
- Goes, S., Giardini, D., Jenny, S., Hollenstein, C., Kahle, H. G., and Geiger, A., 2004, A recent tectonic reorganization in the south-central Mediterranean: *Earth and Planetary Science Letters*, v. 226, no. 3-4, p. 335-345.
- Goodbred Jr, S. L., and Saito, Y., 2012, Tide-dominated deltas, *in* Davis Jr, R. A., and Dalrymple, B. W., eds., *Principles of Tidal Sedimentology*, Springer Netherlands, p. 129-149.
- Harris, P. T., Pattiaratchi, C. B., Collins, M. B., and Dalrymple, R. W., 1995, What is a Bedload Parting?, *in* Flemming, B. W., and Bartholoma, A., eds., *Tidal Signatures in Modern and Ancient Sediments*, Volume 24, International Association of Sedimentologists Special Publication, p. 3-18.

- Helland-Hansen, W., and Martinsen, O. J., 1996, Shoreline trajectories and sequences: description of variable depositional-dip scenarios: *Journal of Sedimentary Research*, v. 66, no. 4.
- Knott, S. D., and Turco, E., 1991, Late Cenozoic kinematics of the Calabrian Arc, southern Italy: *Tectonics*, v. 10, no. 6, p. 1164-1172.
- Leva López, J., Rossi, V. M., Olariu, C., and Steel, R. J., 2016, Architecture and recognition criteria of ancient shelf ridges; an example from Campanian Almond Formation in Hanna Basin, USA: *Sedimentology*.
- Longhitano, S. G., 2011, The record of tidal cycles in mixed silici-bioclastic deposits: examples from small Plio-Pleistocene peripheral basins of the microtidal Central Mediterranean Sea: *Sedimentology*, v. 58, no. 3, p. 691-719.
- , 2013, A facies-based depositional model for ancient and modern, tectonically-confined tidal straits: *Terra Nova*, v. 25, no. 6, p. 446-452.
- Longhitano, S. G., 2015, Deflected steep-marginal deltas in confined tidal straits an outcrop analogue from the upper Miocene Amantea Basin, southern Italy, *Sedimentology of paralic reservoirs: recent advances and their applications: Piccadilly, London, Burlington House*, p. 94-95.
- Longhitano, S. G., Chiarella, D., Di Stefano, A., Messina, C., Sabato, L., and Tropeano, M., 2012a, Tidal signatures in Neogene to Quaternary mixed deposits of southern Italy straits and bays: *Sedimentary Geology*, v. 279, no. 0, p. 74-96.
- Longhitano, S. G., Chiarella, D., and Muto, F., 2014, Three-dimensional to two-dimensional cross-strata transition in the lower Pleistocene Catanzaro tidal strait transgressive succession (southern Italy): *Sedimentology*, v. 61, no. 7, p. 2136-2171.
- Longhitano, S. G., Mellere, D., Steel, R. J., and Ainsworth, R. B., 2012b, Tidal depositional systems in the rock record: A review and new insights: *Sedimentary Geology*, v. 279, no. 0, p. 2-22.
- Longhitano, S. G., and Steel, R. J., 2015, Deltas sourcing tidal straits: observations from some field case studies., 31st Meeting of the International Association of Sedimentologists: Krakow, p. 313.
- , 2016, Deflection of the progradational axis and asymmetry in tidal seaway and strait deltas: insights from two outcrop case studies, *Paralic Reservoir: London, Geological Society - Special Publication*.
- Michaud, K. J., and Dalrymple, R. W., Facies, architecture and stratigraphic occurrence of headland-attached tidal sand ridges in the Roda Formation, Northern Spain, *in Proceedings Contributions to Modern and Ancient Tidal Sedimentology: Proceedings of the Tidalites 2012 Conference 2016*, John Wiley & Sons, p. 313.
- Mutti, E., Davoli, G., Tinterri, R., and Zavala, C., 1996, The importance of ancient fluvio-deltaic systems dominated by catastrophic flooding in tectonically active basins: *Memorie di Scienze Geologiche*, v. 48, p. 233-291.
- Mutti, E., Tinterri, R., Benevelli, G., Biase, D. d., and Cavanna, G., 2003, Deltaic, mixed and turbidite sedimentation of ancient foreland basins: *Marine and Petroleum Geology*, v. 20, no. 6-8, p. 733-755.

- Mutti, E., Tinterri, R., Di Biase, D., Fava, L., Mavilla, N., Angella, S., and Calabrese, L., 2000, Delta-front facies associations of ancient flood-dominated fluvio-deltaic systems: *Rev. Soc. Geol. Espana*, v. 13, no. 2, p. 165-190.
- Nemec, W., and Muszyński, A., Volcaniclastic alluvial aprons in the Tertiary of Sofia district (Bulgaria), *in Proceedings Annales Societatis Geologorum Poloniae* 1982, Volume 52, p. 239-303.
- Nichols, M. M., 1989, Physical Processes and Sedimentology of Siliciclastic-Dominated Lagoonal Systems Sediment accumulation rates and relative sea-level rise in lagoons: *Marine Geology*, v. 88, no. 3, p. 201-219.
- Olariu, M. I., Olariu, C., Steel, R. J., Dalrymple, R. W., and Martinius, A. W., 2012, Anatomy of a laterally migrating tidal bar in front of a delta system: Esdolomada Member, Roda Formation, Tremp-Graus Basin, Spain: *Sedimentology*, v. 59, no. 2, p. 356-U332.
- Patterson, R. T., Blenkinsop, J., and Cavazza, W., 1995, Planktic foraminiferal biostratigraphy and $^{87}\text{Sr}/^{86}\text{Sr}$ isotopic stratigraphy of the Oligocene-to-Pleistocene sedimentary sequence in the southeastern Calabrian microplate, southern Italy: *Journal of Paleontology*, v. 69, p. 7-20.
- Plint, A., 1988, Sharp-based shoreface sequences and “offshore bars” in the Cardium Formation of Alberta: their relationship to relative changes in sea level: *Sea-Level Changes: An Integrated Approach: SEPM, Special Publication*, v. 42, p. 357-370.
- Pugh, D. T., 1987, *Tides, Surges and Mean Sea-Level*, New York, John Wiley.
- Reynaud, J.-Y., and Dalrymple, R. W., 2012, Shallow-marine tidal deposits, *in* Davis Jr, R. A., and Dalrymple, B. W., eds., *Principles of Tidal Sedimentology*: New York, Springer, p. 335-370.
- Rossi, M., and Craig, J., 2016, A new perspective on sequence stratigraphy of syn-orogenic basins: insights from the Tertiary Piedmont Basin (Italy) and implications for play concepts and reservoir heterogeneity: *Geological Society, London, Special Publications*, v. 436.
- Sohn, Y. K., Rhee, C. W., and Kim, B. C., 1999, Debris Flow and Hyperconcentrated Flood-Flow Deposits in an Alluvial Fan, Northwestern Part of the Cretaceous Yongdong Basin, Central Korea: *The Journal of Geology*, v. 107, no. 1, p. 111-132.
- Southard, J. B., and Boguchwal, L. A., 1990, Bed configurations in steady unidirectional water flows. Part 2. Synthesis of flume data: *Journal of Sedimentary Research*, v. 60, no. 5.
- Sylvester, A. G., 1988, Strike-slip faults: *Geological Society of America Bulletin*, v. 100, no. 11, p. 1666-1703.
- Tansi, C., Muto, F., Critelli, S., and Iovine, G., 2007, Neogene-Quaternary strike-slip tectonics in the central Calabrian Arc (southern Italy): *Journal of Geodynamics*, v. 43, no. 3, p. 393-414.
- Tinterri, R., 2007, The Lower Eocene Roda Sandstone (south Central Pyrenees): an example of a flood-dominated river-delta system in a tectonically controlled basin: *Rivista Italiana di Paleontologia e Stratigrafia (Research In Paleontology and Stratigraphy)*, v. 113, no. 2, p. 223-255.

- Tortorici, L., 1982, Lineamenti geologico-strutturali dell'arco Calabro-Peloritano: Società Italiana di Mineralogia e Petrografia, v. 38, p. 927-940.
- Tortorici, L., Monaco, C., Tansi, C., and Cocina, O., 1995, Kinematics of distributed deformation in plate boundary zones with emphasis on the Mediterranean, Anatolia and Eastern Asia Recent and active tectonics in the Calabrian arc (Southern Italy): Tectonophysics, v. 243, no. 1, p. 37-55.
- Trentesaux, A., Stolk, A., and Berne, S., 1999, Sedimentology and stratigraphy of a tidal sand bank in the southern North Sea: Marine Geology, v. 159, no. 1-4, p. 253-272.
- Tripodi, V., Muto, F., and Critelli, S., 2013, Structural style and tectono-stratigraphic evolution of the Neogene–Quaternary Siderno Basin, southern Calabrian Arc, Italy: International Geology Review, v. 55, no. 4, p. 468-481.
- Uroza, C. A., 2008, Processes and Architectures of Deltas in Shelf-break and Ramp Platforms: Examples from the Eocene of West Spitsbergen (Norway), the Pliocene Paleo-Orinoco Delta (SE Trinidad), and the Cretaceous Western Interior Seaway (S Wyoming and NE Utah) [PhD: the University of Texas at Austin, 261 p.
- Van Dijk, J. P., 1992, Late Neogene fore-arc basin evolution in the Calabrian Arc (central Mediterranean); tectonic sequence stratigraphy and dynamic geohistory, Utrecht University.
- Van Dijk, J. P., 1993, Three-Dimensional Quantitative Restoration of Central Mediterranean Neogene Basins: The Dynamic Geohistory Approach, *in* Spencer, A. M., ed., Generation, Accumulation and Production of Europe's Hydrocarbons III: Special Publication of the European Association of Petroleum Geoscientists No. 3: Berlin, Heidelberg, Springer Berlin Heidelberg, p. 267-280.
- Van Dijk, J. P., Bello, M., Brancaleoni, G. P., Cantarella, G., Costa, V., Frixia, A., Golfetto, F., Merlini, S., Riva, M., Torricelli, S., Toscano, C., and Zerilli, A., 2000, A regional structural model for the northern sector of the Calabrian Arc (southern Italy): Tectonophysics, v. 324, no. 4, p. 267-320.
- Westaway, R., 1993, Quaternary uplift of southern Italy: Journal of Geophysical Research: Solid Earth, v. 98, no. B12, p. 21741-21772.

Appendix A: Correlation panel of the Lajas outcrop at Lohan Mahuida

A correlation panel was created based on the measured stratigraphic sections. The outcrop belt is *ca* 7 km long and the total stratigraphic thickness is *ca* 300 m. The location of the measured sections is in figure 1.2B. The colors in the correlation panel represent interpreted facies associations (see text in Chapter 2 for detailed descriptions).

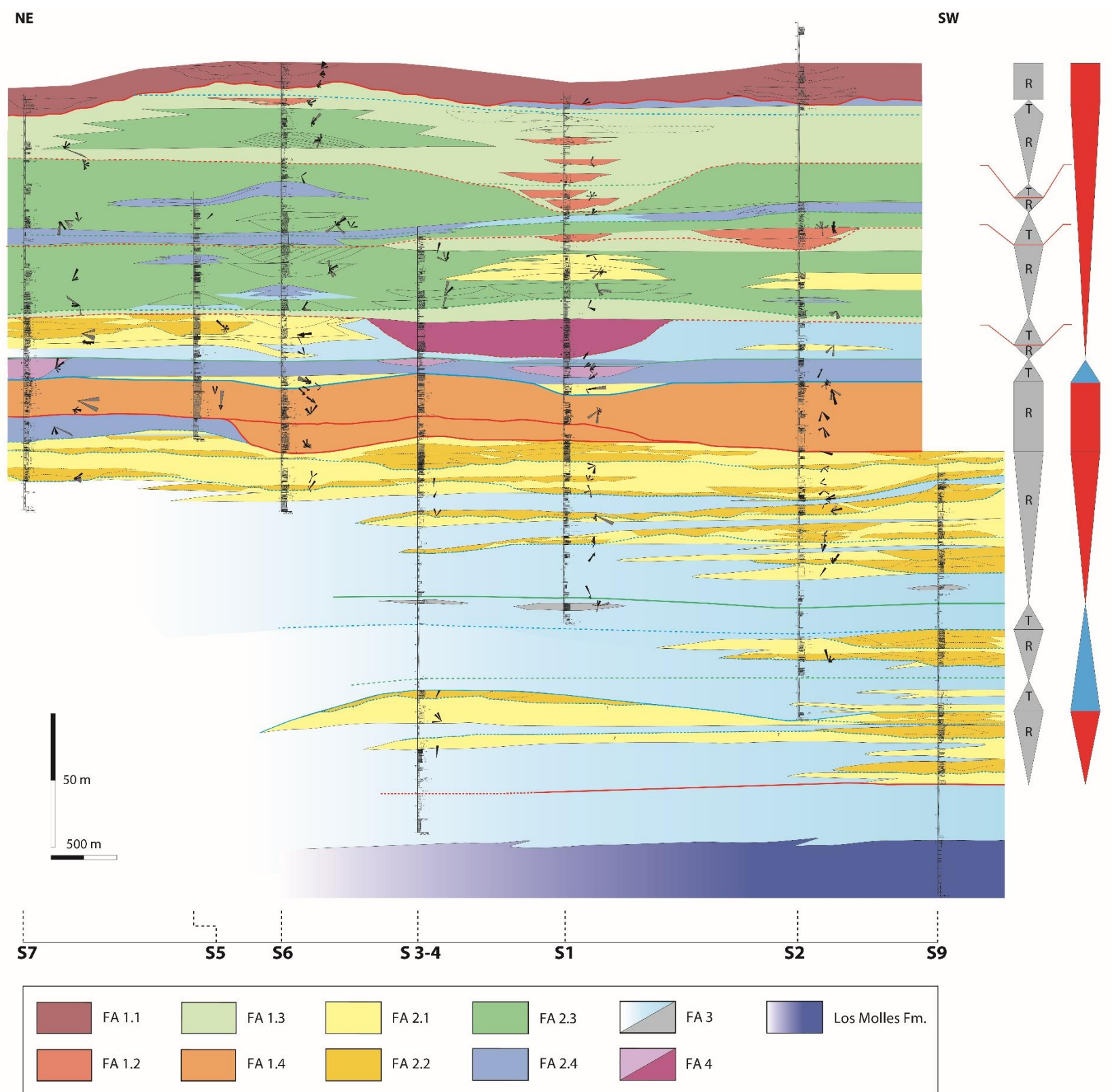


Figure A.1: Correlation panel of the Lajas Formation at Lohan Mahuida. The cross-section is slightly oblique to strike, but overall the progradation is from the south-west to north-east. Stratigraphic surfaces are color-coded as follows: red represents sequence boundaries, blue represents flooding surfaces, green represents maximum flooding surfaces. Solid lines represent 3rd order surfaces, dashed lines represents 4th order and 5th order surfaces.

Appendix B: Supplementary material for process probability calculations

This appendix provides the complete list of references used to calculate the percentages of each sedimentary structure (Table B.1). Tables B.2 and B.3 present additional analysis on unidirectional cross-strata and inverse grading.

Table B.1: Complete list of references used to calculate the percentages of each sedimentary structure.

Sedimentary Structures	Number of data	References
Symmetrical ripples	w = 27 t = 3 r = 1	Clifton (1976); De Raaf et al. (1977); Homewood and Allen (1981); Clifton (1982); Pulham (1989); Bhattacharya and Walker (1991); Willis et al. (1999); Coates and MacEachern (2000); Kirschbaum and Hettinger (2004); McIlroy (2004); Dumas et al. (2005); Anastas et al. (2006); Dumas and Arnott (2006); Olariu and Bhattacharya (2006); Gani and Bhattacharya (2007); Plink-Björklund (2008); Bhattacharya and MacEachern (2009); Gani et al. (2009); Ichaso and Dalrymple (2009); Pontén and Plink-Björklund (2009); MacEachern et al. (2010); Plint (2010); Olariu et al. (2012b); Scasso et al. (2012); Chen et al. (2014); Hurd et al. (2014); Ichaso and Dalrymple (2014)
Current ripples/ climbing ripples	w = 4 t = 19 r = 27	Jopling and Walker (1968); Collinson (1970); Clifton (1976); De Raaf et al. (1977); Dalrymple et al. (1978); Allen (1980); Homewood and Allen (1981); Howard and Reineck (1981); Clifton (1982); Mutti et al. (1985); Kreisa and Moila (1986); Rossi and Rogledi (1988); Tessier and Gigot (1989); Bhattacharya and Walker (1991); Allen and Posamentier (1994); Greb and Archer (1995); De Boer (1998); Gingras et al. (1998); Willis et al. (1999); Coates and MacEachern (2000); Bhattacharya and Giosan (2003); Kirschbaum and Hettinger (2004); McIlroy (2004); Dumas et al. (2005); Olariu et al. (2005); Dumas and Arnott (2006); Olariu and Bhattacharya (2006); Gani and Bhattacharya (2007); Pontén and Plink-Björklund (2007); Plink-Björklund (2008); Bhattacharya and MacEachern (2009); Gani et al. (2009); Pontén and Plink-Björklund (2009); Charvin et al. (2010); Choi (2010); Olariu et al. (2010); Olariu et al. (2012a); Olariu et al. (2012b); Plink-Björklund (2012); Scasso et al. (2012); Chen et al. (2014); Hurd et al. (2014); Ichaso and Dalrymple (2014)

Table B.1: Continued.

HCS/SCS	w = 22 t = - r = 2	Bhattacharya and Walker (1991); Greb and Archer (1995); Coates and MacEachern (2000); Mutti et al. (2000); Willis and Gabel (2003); Kirschbaum and Hettlinger (2004); Dumas et al. (2005); Anastas et al. (2006); Dumas and Arnott (2006); Olariu and Bhattacharya (2006); Gani and Bhattacharya (2007); Plink-Björklund (2008); Bhattacharya and MacEachern (2009); Ichaso and Dalrymple (2009); Pontén and Plink-Björklund (2009); Charvin et al. (2010); Plint (2010); Plink-Björklund (2012); Chen et al. (2014); Hurd et al. (2014); Ichaso and Dalrymple (2014)
Low-angle lamination	w = 11 t = 5 r = 5	Duncan Jr (1964); Coleman and Wright (1975); Boersma and Terwindt (1981); Kreisa and Moila (1986); Coates and MacEachern (2000); Mutti et al. (2003); Dumas et al. (2005); Dumas and Arnott (2006); Pontén and Plink-Björklund (2007); Plink-Björklund (2008); Gani et al. (2009); Charvin et al. (2010); MacEachern et al. (2010); Olariu et al. (2010); Plint (2010); Hurd et al. (2014)
Lenticular/ wavy/ flaser bedding	w = 14 t = 19 r = 12	Coleman and Gagliano (1965); Reineck and Wunderlich (1968); McCave (1970); De Raaf et al. (1977); Galloway (1981); Homewood and Allen (1981); Terwindt (1981); Clifton (1982); Pulham (1989); Tye and Coleman (1989); Bhattacharya and Walker (1991); Nichols et al. (1991); Nio and Yang (1991); Tessier (1993); Brooks et al. (1995); Greb and Archer (1995); De Boer (1998); Borgeld et al. (1999); Willis et al. (1999); Coates and MacEachern (2000); Martin (2000); Ta et al. (2002); Kirschbaum and Hettlinger (2004); Wheatcroft et al. (2006); Plink-Björklund (2008); Olariu et al. (2012a); Plink-Björklund (2012); Scasso et al. (2012); Chen et al. (2014); Hurd et al. (2014)
Unidirectional cross-strata	w = 17 t = 42 r = 29	Collinson (1970); Clifton (1976); Kumar and Sanders (1976); Dalrymple et al. (1978); Allen (1980); Boersma and Terwindt (1981); Homewood and Allen (1981); Clifton (1982); Dalrymple (1984); Kreisa and Moila (1986); Pulham (1989); Bhattacharya and Walker (1991); Greb and Archer (1995); Mellere and Steel (1995, 1996); Wightman and Pemberton (1997); De Boer (1998); Gingras et al. (1998); Bhattacharya and Giosan (2003); Choi et al. (2004); Kirschbaum and Hettlinger (2004); McIlroy (2004); Dumas et al. (2005); Longhitano and Nemeč (2005); Olariu et al. (2005); Anastas et al. (2006); Dumas and Arnott (2006); Olariu and Bhattacharya (2006); Reynaud et al. (2006); (Gani and Bhattacharya, 2007); Pontén and Plink-Björklund (2007); Longhitano (2008); Plink-Björklund (2008); Gani et al. (2009); Ichaso and Dalrymple (2009); Pontén and Plink-Björklund (2009); Charvin et al. (2010); Dalrymple (2010); Plint (2010); Longhitano (2011); Longhitano et al. (2012); Olariu et al. (2012a); Olariu et al. (2012b); Plink-Björklund (2012); Scasso et al. (2012); Longhitano (2013); Reynaud et al. (2013); Chen et al. (2014); Hurd et al. (2014); Ichaso and Dalrymple (2014); Longhitano et al. (2014)

Table B.1: Continued.

Bidirectional cross-strata	w = 4 t = 30 r = 6	De Raaf and Boersma (1971); Coleman and Wright (1975); De Raaf et al. (1977); Fraser and Hester (1977); Allen (1980); Boersma and Terwindt (1981); Homewood and Allen (1981); Howard and Reineck (1981); Clifton (1982); Dalrymple (1984); De Mowbray and Visser (1984); Alam et al. (1985); Tessier and Gigot (1989); Brown et al. (1990); Nio and Yang (1991); Greb and Archer (1995); De Boer (1998); Willis et al. (1999); McIlroy (2004); Willis (2005); Gani and Bhattacharya (2007); Van den Berg et al. (2007); Plink-Björklund (2008); Gani et al. (2009); Ichaso and Dalrymple (2009); Pontén and Plink-Björklund (2009); Dalrymple (2010); Choi (2011); Ainsworth et al. (2012); Olariu et al. (2012a); Olariu et al. (2012b); Plink-Björklund (2012); Scasso et al. (2012); Chen et al. (2014); Ichaso and Dalrymple (2014); Rossi and Craig (2016)
Foreset bundles	w = 1 t = 15 r = 2	De Raaf and Boersma (1971); Visser (1980); Allen (1981); Homewood and Allen (1981); De Mowbray and Visser (1984); Kreisa and Moila (1986); Tessier and Gigot (1989); Nio and Yang (1991); Wightman and Pemberton (1997); De Boer (1998); McIlroy (2004); Kvale (2006); Van den Berg et al. (2007); Yang et al. (2008); Dalrymple (2010); Ainsworth et al. (2012)
Rhythmic lamination	w = 2 t = 13 r = 1	Clifton (1982); Kvale et al. (1989); Brown et al. (1990); Dalrymple et al. (1991); Nio and Yang (1991); Greb and Archer (1995); Willis (2005); Kvale (2006); Bhattacharya and MacEachern (2009); Choi (2011); Plink-Björklund (2012); Scasso et al. (2012); Chen et al. (2014)
Sigmoidal cross-strata	w = 1 t = 10 r = 3	De Raaf et al. (1977); Mutti et al. (1985); Kreisa and Moila (1986); Nio and Yang (1991); Wightman and Pemberton (1997); Mutti et al. (2000); Mutti et al. (2003); Kirschbaum and Hettlinger (2004); Willis (2005); Pontén and Plink-Björklund (2007, 2009); Tinterri (2011); Plink-Björklund (2012); Rossi and Craig (2016)
Mud drapes	w = 2 t = 31 r = 3	De Raaf and Boersma (1971); Allen (1980); Visser (1980); Allen (1981); Boersma and Terwindt (1981); Clifton (1982); De Mowbray and Visser (1984); Kreisa and Moila (1986); Kvale et al. (1989); Bhattacharya and Walker (1991); Nio and Yang (1991); Greb and Archer (1995); Wightman and Pemberton (1997); De Boer (1998); Willis et al. (1999); Willis and Gabel (2003); Kirschbaum and Hettlinger (2004); McIlroy (2004); Willis (2005); Gani and Bhattacharya (2007); Pontén and Plink-Björklund (2007); Van den Berg et al. (2007); Plink-Björklund (2008); Gani et al. (2009); Ichaso and Dalrymple (2009); Pontén and Plink-Björklund (2009); Dalrymple (2010); Ainsworth et al. (2012); Olariu et al. (2012a); Olariu et al. (2012b); Plink-Björklund (2012); Scasso et al. (2012); Chen et al. (2014); Ichaso and Dalrymple (2014)

Table B.1: Continued.

Graded beds/ structureless	w = 4 t = 1 r = 18	Rossi and Rogledi (1988); De Boer (1998); Mutti et al. (2000); Martinius et al. (2001); Mutti et al. (2003); Budillon et al. (2005); Olariu et al. (2005); Olariu and Bhattacharya (2006); Gani and Bhattacharya (2007); Pontén and Plink-Björklund (2007); Ainsworth et al. (2008); Plink-Björklund (2008); Bhattacharya and MacEachern (2009); Pontén and Plink-Björklund (2009); Charvin et al. (2010); Plink-Björklund (2012); Rossi and Craig (2016)
Plane-parallel lamination	w = 14 t = 15 r = 21	Clifton (1976); Kumar and Sanders (1976); Allen (1980); Howard and Reineck (1981); Clifton (1982); Dalrymple (1984); Kreisa and Moila (1986); Rossi and Rogledi (1988); Pulham (1989); Bhattacharya and Walker (1991); De Boer (1998); Willis et al. (1999); Coates and MacEachern (2000); Mutti et al. (2000); Mutti et al. (2003); Kirschbaum and Hettlinger (2004); McIlroy (2004); Dumas et al. (2005); Olariu et al. (2005); Anastas et al. (2006); Dumas and Arnott (2006); Olariu and Bhattacharya (2006); Gani and Bhattacharya (2007); Pontén and Plink-Björklund (2007); Plink-Björklund (2008); Gani et al. (2009); Pontén and Plink-Björklund (2009); Charvin et al. (2010); Dalrymple (2010); MacEachern et al. (2010); Olariu et al. (2010); Olariu et al. (2012a); Plink-Björklund (2012); Scasso et al. (2012); Rossi and Craig (2016)
Compound cross-strata	w = 1 t = 14 r = 4	Allen (1980); Dalrymple (1984); Wightman and Pemberton (1997); Kirschbaum and Hettlinger (2004); Anastas et al. (2006); Gani and Bhattacharya (2007); Pontén and Plink-Björklund (2007); Plink-Björklund (2008); Ainsworth et al. (2012); Longhitano et al. (2012); Olariu et al. (2012a); Olariu et al. (2012b); Plink-Björklund (2012); Chen et al. (2014)
Soft-sediment deformation	w = 3 t = 6 r = 14	Bhattacharya and Walker (1991); De Boer (1998); Willis et al. (1999); Coates and MacEachern (2000); Mutti et al. (2000); Mutti et al. (2003); (Choi et al., 2004); Kirschbaum and Hettlinger (2004); Olariu and Bhattacharya (2006); Gani and Bhattacharya (2007); Greb and Archer (2007); Plink-Björklund (2008); Bhattacharya and MacEachern (2009); Gani et al. (2009); Pontén and Plink-Björklund (2009); Charvin et al. (2010); Scasso et al. (2012); Chen et al. (2014)
Inverse grading		Mutti et al. (2000); Mutti et al. (2003); Bhattacharya and MacEachern (2009); Ichaso and Dalrymple (2014)

Table B.2: Within unidirectional cross-strata it is possible in some cases to distinguish between tabular and trough cross-strata. Percentages have been calculated for tabular (2D) cross-strata and trough (3D) cross-strata.

Sedimentary structures	P(w)	P(t)	P(r)
2D cross-strata	17%	57%	26%
3D cross-strata	22%	49%	29%

Table B.3: Percentages related to inverse grading and inverse-to-normal grading. This structure is very diagnostic of river processes. However, the number of papers referencing it is very limited. For this reason this structure is shown only in the Appendix.

Sedimentary structures	P(w)	P(t)	P(r)
Inverse grading and inverse-to-normal grading	-	-	100%

REFERENCES

- Ainsworth, R. B., Flint, S. S., and Howell, J. A., 2008, Predicting coastal depositional style: influence of basin morphology and accommodation to sediment supply ratio within a sequence stratigraphic framework: Recent advances in models of shallow-marine stratigraphy: SEPM Special Publication, v. 90, p. 237-263.
- Ainsworth, R. B., Hasiotis, S. T., Amos, K. J., Krapf, C. B. E., Payenberg, T. H. D., Sandstrom, M. L., Vakarelov, B. K., and Lang, S. C., 2012, Tidal signatures in an intracratonic playa lake: *Geology*, v. 40, no. 7, p. 607-610.
- Alam, M. M., Crook, K. A. W., and Taylor, G., 1985, Fluvial herring-bone cross-stratification in a modern tributary mouth bar, Coonamble, New South Wales, Australia: *Sedimentology*, v. 32, no. 2, p. 235-244.
- Allen, G. P., and Posamentier, H. W., 1994, Transgressive facies and sequence architecture in mixed tide-and wave-dominated incised valleys: example from the Gironde Estuary, France, *Incised-valley Systems: Origin and Sedimentary Sequences*, Volume 51, SEPM Special Publication.
- Allen, J. R. L., 1980, Sand waves: a model of origin and internal structure: *Sedimentary Geology*, v. 26, no. 4, p. 281-328.
- , 1981, Lower Cretaceous tides revealed by cross-bedding with mud drapes: *Nature*, v. 289, no. 5798, p. 579-581.
- Anastas, A. S., Dalrymple, R. W., James, N. P., and Nelson, C. S., 2006, Lithofacies and dynamics of a cool-water carbonate seaway; mid-Tertiary, Te Kuiti Group, New Zealand: *Geological Society Special Publications*, v. 255, p. 245-268.
- Bhattacharya, J. P., and Giosan, L., 2003, Wave-influenced deltas: geomorphological implications for facies reconstruction: *Sedimentology*, v. 50, no. 1, p. 187-210.
- Bhattacharya, J. P., and MacEachern, J. A., 2009, Hyperpycnal Rivers and Prodeltaic Shelves in the Cretaceous Seaway of North America: *Journal of Sedimentary Research*, v. 79, no. 4, p. 184-209.
- Bhattacharya, J. P., and Walker, R. G., 1991, River- and Wave-Dominated Depositional Systems of the Upper Cretaceous Dunvegan Formation, Northwestern Alberta: *Bulletin of Canadian Petroleum Geology*, v. 39, no. 2, p. 165-191.
- Boersma, J. R., and Terwindt, J. H. J., 1981, Neap-spring tide sequences of intertidal shoal deposits in a mesotidal estuary: *Sedimentology*, v. 28, no. 2, p. 151-170.
- Borgeld, J. C., Hughes Clarke, J. E., Goff, J. A., Mayer, L. A., and Curtis, J. A., 1999, Acoustic backscatter of the 1995 flood deposit on the Eel shelf: *Marine Geology*, v. 154, no. 1-4, p. 197-210.
- Brooks, G. R., Jack, L. K., Shea, P., Williams, S. J., and McBride, R. A., 1995, East Louisiana Continental Shelf Sediments: A Product of Delta Reworking: *Journal of Coastal Research*, v. 11, no. 4, p. 1026-1036.
- Brown, M. A., Archer, A. W., and Kvale, E. P., 1990, Neap-spring tidal cyclicity in laminated carbonate channel-fill deposits and its implications: Salem Limestone (Mississippian), south-central Indiana, USA: *Journal of Sedimentary Research*, v. 60, no. 1.

- Budillon, F., Violante, C., Conforti, A., Esposito, E., Insinga, D., Iorio, M., and Porfido, S., 2005, Event beds in the recent prodelta stratigraphic record of the small flood-prone Bonea Stream (Amalfi Coast, Southern Italy): *Marine Geology*, v. 222–223, no. 0, p. 419-441.
- Charvin, K., Hampson, G. J., Gallagher, K. L., and Labourdette, R., 2010, Intra-parasequence architecture of an interpreted asymmetrical wave-dominated delta: *Sedimentology*, v. 57, no. 3, p. 760-785.
- Chen, S., Steel, R. J., Dixon, J. F., and Osman, A., 2014, Facies and architecture of a tide-dominated segment of the Late Pliocene Orinoco Delta (Morne L'Enfer Formation) SW Trinidad: *Marine and Petroleum Geology*, v. 57, no. 0, p. 208-232.
- Choi, K., 2010, Rhythmic Climbing-Ripple Cross-Lamination in Inclined Heterolithic Stratification (IHS) of a Macrotidal Estuarine Channel, Gomso Bay, West Coast of Korea: *Journal of Sedimentary Research*, v. 80, no. 6, p. 550-561.
- , 2011, Tidal rhythmites in a mixed-energy, macrotidal estuarine channel, Gomso Bay, west coast of Korea: *Marine Geology*, v. 280, no. 1–4, p. 105-115.
- Choi, K., Dalrymple, R. W., Chun, S. S., and Kim, S.-P., 2004, Sedimentology of Modern, Inclined Heterolithic Stratification (IHS) in the Macrotidal Han River Delta, Korea: *Journal of Sedimentary Research*, v. 74, no. 5, p. 677-689.
- Clifton, H. E., 1976, Wave-formed sedimentary structures—a conceptual model, *in* Davis Jr, R. A., and Ethington, R. L., eds., *Beach and Nearshore Sedimentation*, Volume 24, SEPM Spec. Publ., p. 126-148.
- Clifton, H. E., 1982, Estuarine deposits, *in* Scholle, P. A., and Spearing, D., eds., *Sandstone Depositional Environments*: Tulsa, OK, American Association of Petroleum Geologists, p. 179-189.
- Coates, L., and MacEachern, J., Differentiating river-and wave-dominated deltas from shorefaces: Examples from the Cretaceous Western Interior Seaway, Alberta, Canada, *in* *Proceedings GeoCanada 2000, Millennium Geoscience Summit*, Calgary, Alberta, 2000, p. unpaginated.
- Coleman, J. M., and Gagliano, S. M., 1965, Sedimentary structures: Mississippi river deltaic plain, *in* Middleton, G. V., ed., *Sedimentary Structures and Their Hydrodynamic Interpretation*, Volume 12, Soc. Econ. Paleontologists Mineralogists Spec. Publ., p. 133-148.
- Coleman, J. M., and Wright, L. D., 1975, Modern River Deltas: Variability of Processes and Sand Bodies, *in* Broussard, M. L., ed., *Deltas - Models for Exploration*, Houston Geological Society, p. 99-149.
- Collinson, J. D., 1970, Bedforms of the Tana River, Norway: *Geografiska Annaler. Series A, Physical Geography*, v. 52, no. 1, p. 31-56.
- Dalrymple, B. W., 2010, Tidal depositional systems, *in* James, N. P., and Dalrymple, B. W., eds., *Facies models*, Volume 4, Geological Association of Canada, p. 201-231.
- Dalrymple, R. W., 1984, Morphology and internal structure of sandwaves in the Bay of Fundy: *Sedimentology*, v. 31, no. 3, p. 365-382.

- Dalrymple, R. W., Knight, R. J., and Lambiase, J. J., 1978, Bedforms and their hydraulic stability relationships in a tidal environment, Bay of Fundy, Canada: *Nature*, v. 275, p. 100-104.
- Dalrymple, R. W., Makino, Y., and Zaitlin, B. A., 1991, Temporal and spatial patterns of rhythmite deposition on mud flats in the macrotidal Cobequid Bay-Salmon River estuary, Bay of Fundy, Canada.
- De Boer, P. L., 1998, Intertidal sediments: composition and structure, *in* Eisma, D., ed., *Intertidal Deposits. River Mouths, Tidal Flats, and Coastal Lagoons*: Boca Raton, CRC Press, p. 345-361.
- De Mowbray, T., and Visser, M. J., 1984, Reactivation surfaces in subtidal channel deposits, Oosterschelde, Southwest Netherlands: *Journal of Sedimentary Research*, v. 54, no. 3, p. 811-824.
- De Raaf, J. F. M., and Boersma, J. R., 1971, Tidal deposits and their sedimentary structures: *Netherlands Journal of Geosciences/Geologie en Mijnbouw*, v. 50, no. 3, p. 479-504.
- De Raaf, J. F. M., Boersma, J. R., and Van Gelder, A., 1977, Wave-generated structures and sequences from a shallow marine succession, Lower Carboniferous, County Cork, Ireland: *Sedimentology*, v. 24, no. 4, p. 451-483.
- Dumas, S., Arnott, R., and Southard, J. B., 2005, Experiments on oscillatory-flow and combined-flow bed forms: implications for interpreting parts of the shallow-marine sedimentary record: *Journal of Sedimentary research*, v. 75, no. 3, p. 501-513.
- Dumas, S., and Arnott, R. W. C., 2006, Origin of hummocky and swaley cross-stratification— The controlling influence of unidirectional current strength and aggradation rate: *Geology*, v. 34, no. 12, p. 1073-1076.
- Duncan Jr, J. R., 1964, The effects of water table and tide cycle on swash-backwash sediment distribution and beach profile development: *Marine Geology*, v. 2, no. 3, p. 186-197.
- Fraser, G. S., and Hester, N. C., 1977, Sediments and sedimentary structures of a beach-ridge complex, southwestern shore of Lake Michigan: *Journal of Sedimentary Research*, v. 47, no. 3.
- Galloway, W. E., 1981, Depositional architecture of Cenozoic Gulf Coastal Plain fluvial systems, *in* Ethridge, F. G., and Flores, R. M., eds., *Recent and Ancient Nonmarine Depositional Environments*, Volume 31, Soc. Econ. Palaeontol. Mineral. Spec. Publ., p. 127-156.
- Gani, M. R., and Bhattacharya, J. P., 2007, Basic Building Blocks and Process Variability of a Cretaceous Delta: Internal Facies Architecture Reveals a More Dynamic Interaction of River, Wave, and Tidal Processes Than Is Indicated by External Shape: *Journal of Sedimentary Research*, v. 77, no. 4, p. 284-302.
- Gani, M. R., Bhattacharya, J. P., and MacEachern, J. A., 2009, Using ichnology to determine relative influence of waves, storms, tides, and rivers in deltaic deposits: examples from Cretaceous Western Interior Seaway, USA, *in* MacEachern, J. A.,

- Bann, K. L., Gingras, M. K., and Pemberton, S. G., eds., Applied Ichnology, Volume 52, SEPM SHort Course Notes, p. 209-225.
- Gingras, M. K., MacEachern, J. A., and Pemberton, S. G., 1998, A comparative analysis of the ichnology of wave-and river-dominated allomembers of the Upper Cretaceous Dunvegan Formation: *Bulletin of Canadian Petroleum Geology*, v. 46, no. 1, p. 51-73.
- Greb, S. F., and Archer, A. W., 1995, Rhythmic sedimentation in a mixed tide and wave deposit, Hazel Patch Sandstone (Pennsylvanian), eastern Kentucky coal field: *Journal of Sedimentary Research*, v. 65, no. 1.
- Greb, S. F., and Archer, A. W., 2007, Soft-sediment deformation produced by tides in a meizoseismic area, Turnagain Arm, Alaska: *Geology*, v. 35, no. 5, p. 435-438.
- Homewood, P., and Allen, P., 1981, Wave-controlled, tide-controlled, and current-controlled sandbodies of Miocene molasse, western Switzerland: *Aapg Bulletin-American Association of Petroleum Geologists*, v. 65, no. 12, p. 2534-2545.
- Howard, J. D., and Reineck, H.-E., 1981, Depositional facies of high-energy beach-to-offshore sequence: comparison with low-energy sequence: *AAPG Bulletin*, v. 65, no. 5, p. 807-830.
- Hurd, T. J., Fielding, C. R., and Hutsky, A. J., 2014, Variability In Sedimentological and Ichnological Signatures Across A River-Dominated Delta Deposit: Peay Sandstone Member (Cenomanian) of the Northern Bighorn Basin, Wyoming, U.S.A: *Journal of Sedimentary Research*, v. 84, no. 1, p. 1-18.
- Ichaso, A. A., and Dalrymple, R. W., 2009, Tide- and wave-generated fluid mud deposits in the Tilje Formation (Jurassic), offshore Norway: *Geology*, v. 37, no. 6, p. 539-542.
- , 2014, Eustatic, tectonic and climatic controls on an early synrift mixed-energy delta, Tilje Formation (early Jurassic, Smørbukk Field, offshore mid-Norway), in Martinius, A. W., Ravnås, R., Howell, J. A., Steel, R. J., and Wonham, J. P., eds., *Depositional Systems to Sedimentary Successions on the Norwegian Continental Shelf*, Volume 46, International Association of Sedimentologists Special Publication, p. 339-388.
- Jopling, A. V., and Walker, R. G., 1968, Morphology and origin of ripple-drift cross-lamination, with examples from the Pleistocene of Massachusetts: *Journal of Sedimentary Research*, v. 38, no. 4, p. 971-984.
- Kirschbaum, M. A., and Hettinger, R. D., 2004, Facies analysis and sequence stratigraphic framework of Upper Campanian strata (Neslen and mount Garfield Formations, Bluecastle Tongue of the Castlegate Sandstone, and Mancos Shale), eastern Book cliffs, Colorado and Utah, U.S. Geological Survey Digital Data Report.
- Kreisa, R. D., and Moila, R. J., 1986, Sigmoidal tidal bundles and other tide-generated sedimentary structures of the Curtis Formation, Utah: *Geological Society of America Bulletin*, v. 97, no. 4, p. 381-387.
- Kumar, N., and Sanders, J. E., 1976, Characteristics of shoreface storm deposits: modern and ancient examples: *Journal of Sedimentary Research*, v. 46, no. 1, p. 145-162.

- Kvale, E. P., 2006, The origin of neap–spring tidal cycles: *Marine Geology*, v. 235, no. 1–4, p. 5-18.
- Kvale, E. P., Archer, A. W., and Johnson, H. R., 1989, Daily, monthly, and yearly tidal cycles within laminated siltstones of the Mansfield Formation (Pennsylvanian) of Indiana: *Geology*, v. 17, no. 4, p. 365-368.
- Longhitano, S. G., 2008, Sedimentary facies and sequence stratigraphy of coarse-grained Gilbert-type deltas within the Pliocene thrust-top Potenza Basin (Southern Apennines, Italy): *Sedimentary Geology*, v. 210, no. 3–4, p. 87-110.
- , 2011, The record of tidal cycles in mixed silici–bioclastic deposits: examples from small Plio–Pleistocene peripheral basins of the microtidal Central Mediterranean Sea: *Sedimentology*, v. 58, no. 3, p. 691-719.
- , 2013, A facies-based depositional model for ancient and modern, tectonically–confined tidal straits: *Terra Nova*, v. 25, no. 6, p. 446-452.
- Longhitano, S. G., Chiarella, D., and Muto, F., 2014, Three-dimensional to two-dimensional cross-strata transition in the lower Pleistocene Catanzaro tidal strait transgressive succession (southern Italy): *Sedimentology*, v. 61, no. 7, p. 2136-2171.
- Longhitano, S. G., Mellere, D., Steel, R. J., and Ainsworth, R. B., 2012, Tidal depositional systems in the rock record: A review and new insights: *Sedimentary Geology*, v. 279, no. 0, p. 2-22.
- Longhitano, S. G., and Nemeč, W., 2005, Statistical analysis of bed-thickness variation in a Tortonian succession of biocalcarenic tidal dunes, Amantea Basin, Calabria, southern Italy: *Sedimentary Geology*, v. 179, no. 3–4, p. 195-224.
- MacEachern, J. A., Pemberton, S. G., Gingras, M. K., and Bann, K. L., 2010, Ichnology and facies models, *in* James, N. P., and Dalrymple, R. W., eds., *Facies models*, Volume 4, Geological Association of Canada.
- Martin, A. J., 2000, Flaser and wavy bedding in ephemeral streams: a modern and an ancient example: *Sedimentary Geology*, v. 136, no. 1–2, p. 1-5.
- Martinius, A. W., Kaas, I., Næss, A., Helgesen, G., Kjærefjord, J. M., and Leith, D. A., 2001, Sedimentology of the heterolithic and tide-dominated tilje formation (Early Jurassic, Halten Terrace, Offshore Mid-Norway), *in* Martinsen, O. J., and Dreyer, T., eds., *Sedimentary Environments Offshore Norway — Palaeozoic to Recent*, Volume Volume 10, Norwegian Petroleum Foundation Special Publications, p. 103-144.
- McCave, I. N., 1970, Deposition of fine-grained suspended sediment from tidal currents: *Journal of Geophysical Research*, v. 75, no. 21, p. 4151-4159.
- McIlroy, D., 2004, Ichnofabrics and sedimentary facies of a tide-dominated delta: Jurassic Ile Formation of Kristin field, Haltenbanken, offshore mid-Norway, *in* McIlroy, D., ed., *The Application of Ichnology to Palaeoenvironmental and Stratigraphic Analysis: Lyell Meeting 2003*, Volume 228, The Geological Society of London, Special Publication, p. 237-272.

- Mellere, D., and Steel, R. J., 1995, Facies architecture and sequentiality of nearshore and shelf sandbodies - Haystack Mountains Formation, Wyoming, USA: *Sedimentology*, v. 42, no. 4, p. 551-574.
- , 1996, Tidal sedimentation in Inner Hebrides half grabens, Scotland: the Mid-Jurassic Bearreraig Sandstone Formation: Geological Society, London, Special Publications, v. 117, no. 1, p. 49-79.
- Mutti, E., Rosell, J., Allen, G. P., Fonnesu, F., and Sgavetti, M., 1985, The Eocene Baronia tide-dominated delta-shelf system in the Ager Basin, *in* Mila, M. D., and Rosell, J., eds., *Excursion Guidebook: VI Eur. Ref. Mtg. I.A.S.*: Lerida, Spain, p. 579-600.
- Mutti, E., Tinterri, R., Benevelli, G., Biase, D. d., and Cavanna, G., 2003, Deltaic, mixed and turbidite sedimentation of ancient foreland basins: *Marine and Petroleum Geology*, v. 20, no. 6-8, p. 733-755.
- Mutti, E., Tinterri, R., Di Biase, D., Fava, L., Mavilla, N., Angella, S., and Calabrese, L., 2000, Delta-front facies associations of ancient flood-dominated fluvio-deltaic systems: *Rev. Soc. Geol. Espana*, v. 13, no. 2, p. 165-190.
- Nichols, M. M., Johnson, G. H., and Peebles, P., 1991, Modern Sediments and Facies Model for a Microtidal Coastal Plain Estuary, The James Estuary, Virginia: *Journal of Sedimentary Petrology*, v. 61, no. 6, p. 883-899.
- Nio, S.-D., and Yang, C.-S., 1991, Diagnostic attributes of clastic tidal deposits: a review.
- Olariu, C., and Bhattacharya, J. P., 2006, Terminal Distributary Channels and Delta Front Architecture of River-Dominated Delta Systems: *Journal of Sedimentary Research*, v. 76, no. 2, p. 212-233.
- Olariu, C., Bhattacharya, J. P., Xu, X., Aiken, C. L. V., Zeng, X., and McMechan, G. A., 2005, Integrated study of ancient delta-front deposits, using outcrop, ground-penetrating radar, and three-dimensional photorealistic data: Cretaceous Panther Tongue Sandstone, Utah, USA, *in* Giosan, L., and Bhattacharya, J. P., eds., *River Deltas: Concepts, Models, and Examples*, Volume 83, SEPM Special Publication.
- Olariu, C., Steel, R. J., Dalrymple, R. W., and Gingras, M. K., 2012a, Tidal dunes versus tidal bars: The sedimentological and architectural characteristics of compound dunes in a tidal seaway, the lower Baronia Sandstone (Lower Eocene), Ager Basin, Spain: *Sedimentary Geology*, v. 279, p. 134-155.
- Olariu, C., Steel, R. J., and Petter, A. L., 2010, Delta-front hyperpycnal bed geometry and implications for reservoir modeling: Cretaceous Panther Tongue delta, Book Cliffs, Utah: *AAPG bulletin*, v. 94, no. 6, p. 819-845.
- Olariu, M. I., Olariu, C., Steel, R. J., Dalrymple, R. W., and Martinus, A. W., 2012b, Anatomy of a laterally migrating tidal bar in front of a delta system: Esdolomada Member, Roda Formation, Tremp-Graus Basin, Spain: *Sedimentology*, v. 59, no. 2, p. 356-U332.
- Plink-Björklund, P., 2008, Wave-to-tide facies change in a Campanian shoreline complex, Chimney Rock Tongue, Wyoming-Utah, USA, *in* Hampson, G. J., Steel, R. J., Burgess, P. M., and Dalrymple, B. W., eds., *Recent advances in*

- models of shallow-marine stratigraphy: SEPM Special Publication, Volume 90, p. 265-291.
- Plink-Björklund, P., 2012, Effects of tides on deltaic deposition: Causes and responses: *Sedimentary Geology*, v. 279, no. 0, p. 107-133.
- Plint, A. G., 2010, Wave-and storm-dominated shoreline and shallow-marine systems, *in* Dalrymple, B. W., and James, N. P., eds., *Facies models*, Volume 4, Geological Association of Canada, p. 167-199.
- Pontén, A., and Plink-Björklund, P., 2007, Depositional environments in an extensive tide-influenced delta plain, Middle Devonian Gauja Formation, Devonian Baltic Basin: *Sedimentology*, v. 54, no. 5, p. 969-1006.
- , 2009, Process Regime Changes Across a Regressive to Transgressive Turnaround in a Shelf-Slope Basin, Eocene Central Basin of Spitsbergen: *Journal of Sedimentary Research*, v. 79, no. 1, p. 2-23.
- Pulham, A. J., 1989, Controls on internal structure and architecture of sandstone bodies within Upper Carboniferous fluvial-dominated deltas, County Clare, western Ireland, *in* Whateley, M. K. G., and Pickering, K. T., eds., *Deltas: Traps for Fossil Fuels*, Volume 41: London, Geol. Soc. Spec. Publ., p. 179-203.
- Reineck, H.-E., and Wunderlich, F., 1968, Classification and Origin of Flaser and Lenticular Bedding: *Sedimentology*, v. 11, no. 1-2, p. 99-104.
- Reynaud, J.-Y., Dalrymple, R. W., Vennin, E., Parize, O., Besson, D., and Rubino, J.-L., 2006, Topographic Controls on Production and Deposition of Tidal Cool-Water Carbonates, Uzès Basin, SE France: *Journal of Sedimentary Research*, v. 76, no. 1, p. 117-130.
- Reynaud, J.-Y., Ferrandini, M., Ferrandini, J., Santiago, M., Thinon, I., André, J.-P., Barthet, Y., Guennoc, P. O. L., and Tessier, B., 2013, From non-tidal shelf to tide-dominated strait: The Miocene Bonifacio Basin, Southern Corsica: *Sedimentology*, v. 60, no. 2, p. 599-623.
- Rossi, M., and Craig, J., 2016, A new perspective on sequence stratigraphy of syn-orogenic basins: insights from the Tertiary Piedmont Basin (Italy) and implications for play concepts and reservoir heterogeneity: Geological Society, London, Special Publications, v. 436.
- Rossi, M. E., and Rogledi, S., 1988, Relative sea-level changes, local tectonic settings and basin margin sedimentation in the interference zone between two orogenic belts: seismic stratigraphic examples from Padan foreland basin, northern Italy, *in* Nemeč, W., and Steel, R. J., eds., *Fan Deltas: Sedimentology and Tectonic Settings*: Glasgow, Blakie and Son, p. 368-384.
- Scasso, R., Dozo, M. T., Cuitiño, J. I., and Bouza, P., 2012, Meandering tidal-fluvial channels and lag concentration of terrestrial vertebrates in the fluvial-tidal transition of an ancient estuary in Patagonia: *Lat. Am. J. Sedimentol. Basin Anal.*, v. 19, p. 27-45.
- Ta, T. K. O., Nguyen, V. L., Tateishi, M., Kobayashi, I., Saito, Y., and Nakamura, T., 2002, Sediment facies and Late Holocene progradation of the Mekong River Delta in Bentre Province, southern Vietnam: an example of evolution from a tide-

- dominated to a tide- and wave-dominated delta: *Sedimentary Geology*, v. 152, no. 3–4, p. 313-325.
- Terwindt, J. H. J., 1981, Origin and sequences of sedimentary structures in inshore mesotidal deposits of the North Sea, *in* Nio, S. D., Shuttenhelm, R. T. E., and van Weering, T. C., eds., *Holocene marine sedimentation in the North Sea Basin*, Volume 5, *Internat. Assoc. Sedimentologists Spec. Publ.*, p. 4-26.
- Tessier, B., 1993, Upper intertidal rhythmites in the Mont-Saint-Michel Bay (NW France): Perspectives for paleoreconstruction: *Marine Geology*, v. 110, no. 3–4, p. 355-367.
- Tessier, B., and Gigot, P., 1989, A vertical record of different tidal cyclicities: an example from the Miocene Marine Molasse of Digne (Haute Provence, France): *Sedimentology*, v. 36, no. 5, p. 767-776.
- Tinterri, R., 2011, Combined flow sedimentary structures and the genetic link between sigmoidal-and hummocky-cross stratification: *GeoActa*, v. 10, p. 1-43.
- Tye, R. S., and Coleman, J. M., 1989, Depositional Processes and Stratigraphy of Fluvially Dominated Lacustrine Deltas: Mississippi Delta Plain: *Journal of Sedimentary Petrology*, v. 59, no. 6, p. 973-996.
- Van den Berg, J. H., Boersma, J. R., and Van Gelder, A., 2007, Diagnostic sedimentary structures of the fluvial-tidal transition zone—Evidence from deposits of the Rhine and Meuse: *Netherlands Journal of Geosciences/Geologie en Mijnbouw*, v. 86, no. 3, p. 287-306.
- Visser, M., 1980, Neap-spring cycles reflected in Holocene subtidal large-scale bedform deposits: a preliminary note: *Geology*, v. 8, no. 11, p. 543-546.
- Wheatcroft, R. A., Stevens, A. W., Hunt, L. M., and Milligan, T. G., 2006, The large-scale distribution and internal geometry of the fall 2000 Po River flood deposit: Evidence from digital X-radiography: *Continental Shelf Research*, v. 26, no. 4, p. 499-516.
- Wightman, D. M., and Pemberton, S. G., 1997, The Lower Cretaceous (Aptian) McMurray Formation: an overview of the Fort McMurray area, northeastern, Alberta, *in* Pemberton, S. G., and James, D. P., eds., *Petroleum Geology of the Cretaceous Mannville Group, Western Canada Volume 18*, *Canadian Society of Petroleum Geologists* p. 312-344.
- Willis, B. J., 2005, Deposits of tide-influenced river deltas, *in* Giosan, L., and Bhattacharya, J. P., eds., *River Deltas - Concepts, Models, and Examples*, Volume 83, *SEPM Special Publication*, p. 87-129.
- Willis, B. J., Bhattacharya, J. P., Gabel, S. L., and White, C. D., 1999, Architecture of a tide-influenced river delta in the Frontier Formation of central Wyoming, USA: *Sedimentology*, v. 46, no. 4, p. 667-688.
- Willis, B. J., and Gabel, S. L., 2003, Formation of Deep Incisions into Tide-Dominated River Deltas: Implications for the Stratigraphy of the Sego Sandstone, Book Cliffs, Utah, U.S.A: *Journal of Sedimentary Research*, v. 73, no. 2, p. 246-263.

Yang, B., Gingras, M. K., Pemberton, S. G., and Dalrymple, R. W., 2008, Wave-generated tidal bundles as an indicator of wave-dominated tidal flats: *Geology*, v. 36, no. 1, p. 39-42.

Appendix C: Supplementary material for the modeling simulations (Delft3D)

This appendix provides the supplementary material for the study presented in Chapter 4. In particular, all the runs used in this study are listed in Table C.1. Table C.2 provides all the data used to calculate A^* and H^* (Fig. 4.2) for both the model runs and modern deltas. The locations where the parameters presented in Chapter 4 have been calculated are presented in Figures C.1, C.2, C.3 and C.4.

Table C.1: Complete list of the 24 runs used in this study.

Run Name	Tidal Amplitude [m]	Initial sediment composition [%sand-%mud]	Total simulation time [days]	
RL-A ₃ -S ₁	1.5	25-75	2640	
RL-A ₂ -S ₁	0.5			
RL-A ₁ -S ₁	0.25			
RL-A ₀ -S ₁	0			
RL-A ₃ -S ₂	1.5	50-50		
RL-A ₂ -S ₂	0.5			
RL-A ₁ -S ₂	0.25			
RL-A ₀ -S ₂	0			
RL-A ₃ -S ₃	1.5	100-0		
RL-A ₂ -S ₃	0.5			
RL-A ₁ -S ₃	0.25			
RL-A ₀ -S ₃	0			
RS-A ₃ -S ₁	1.5	25-75		110
RS-A ₂ -S ₁	0.5			
RS-A ₁ -S ₁	0.25			
RS-A ₀ -S ₁	0			
RS-A ₃ -S ₂	1.5	50-50		
RS-A ₂ -S ₂	0.5			
RS-A ₁ -S ₂	0.25			
RS-A ₀ -S ₂	0			
RS-A ₃ -S ₃	1.5	100-0		
RS-A ₂ -S ₃	0.5			
RS-A ₁ -S ₃	0.25			
RS-A ₀ -S ₃	0			

Table C.2: Data used to calculate A^* and H^* in all the runs and in modern deltas. Data for modern deltas is from Thompson (1968), Allen et al. (1979), Caline and Huong (1992), Guillen and Palanques (1992), Carriquiry and Sánchez (1999), Lambiase et al. (2002), Syvitski and Saito (2007), Baitis (2008), Kim et al. (2009), Sassi et al. (2011), Shaw et al. (2013), Shaw and Mohrig (2014), Cummings et al. (2016).

Initial Sediment Composition	Tidal Amplitude [m]	Shoreline [m]	Area [m ²]	Slope [-]	Qw [m ³ /s]	½ Tidal Period [s]	H ₁ Depth [m]	H ₁ Grainsize [mm]	H ₂ Depth [m]	H ₂ Grainsize [mm]	A^*	H_1^*	H_2^*
100-0	0				2000	-	6.94	0.21	6.31	0.194	0	33068.1	32553.09
100-0	0.25	2265.3	7250893	0.00057	2000	22050	7.27	0.189	6.78	0.192	0.00795852	38462.96	35320.83
100-0	0.5	2374.39	7018459	0.001	2000	22050	12.00	0.2	9.13	0.2	0.01675680	60027.5	45635.5
100-0	1.5	2386.14	5140991	0.001	2000	22050	12.76	0.2	12.51	0.2	0.10992458	63801.5	62574
50-50	0				2000	-	8.85	0.15	6.59	0.156	0	59039.33	42282.69
50-50	0.25	2610.7	9762638	0.00045	2000	22050	9.96	0.179	5.85	0.146	0.01177712	55670.95	40055.48
50-50	0.5	2753.39	7972377	0.0007	2000	22050	9.66	0.165	5.32	0.092	0.02344895	58570.91	57879.35
50-50	1.5	2395.55	4206146	0.001	2000	22050	13.31	0.17	10.21	0.16	0.08958247	78286.47	63834.37
25-75	0				2000	-	6.23	0.116	6.22	0.128	0	53702.58	48574.22
25-75	0.25	2764.7	8480778	0.00041	2000	22050	12.94	0.15	7.78	0.142	0.01060340	86312.66	54826.76
25-75	0.5	2776.45	6678393	0.00043	2000	22050	11.67	0.124	8.32	0.124	0.03171137	94112.09	67104.84
25-75	1.5	2510.21	4497021	0.00074	2000	22050	15.96	0.146	10	0.139	0.12351709	109316.44	71942.44
WLD	0.2	10000	104719755	0.0001	4800	22050	5	0.094			0.03957662	53290.41	
WLD	0.2	8000	67020643	0.0001	4800	22050	4	0.094			0.03166130	42632.33	
Han	4.5	45000	2.1e+09	0.0002	5000	22050	30	0.25			42.8571428	120000	
Mahakam	0.6	41000	1.3e+09	0.0005	3000	22050	5	0.07			0.35287695	71428.57	
Copper	1.7	40000	1.92e+09	0.0006	7000	22050	5	0.07			1.49789439	71428.57	
Colorado (CA)	2.5	50000	6.34e+08	0.0004	2182	22050	5	0.07	6	0.07	4.11790136	71428.57	85714.2857
Baram	0.85	26000	3e+08	0.0005	2270	44100	5	0.06			0.16655256	83333.33	
Ebro	0.1	28000	3.38e+08	0.00021	2475	22050	6	0.101			0.01053308	59405.94	

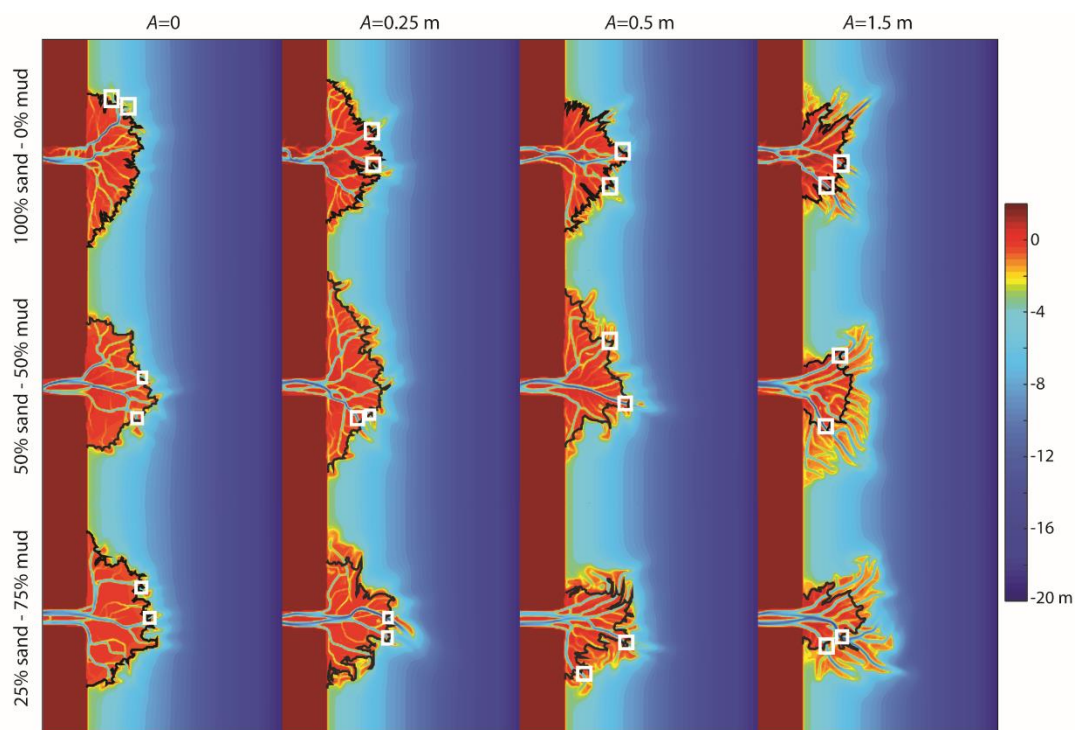


Figure C.1: Location of the two deepest channels (white rectangles) used to calculate H^* (see Table C.2). The shoreline position is marked by the black line.

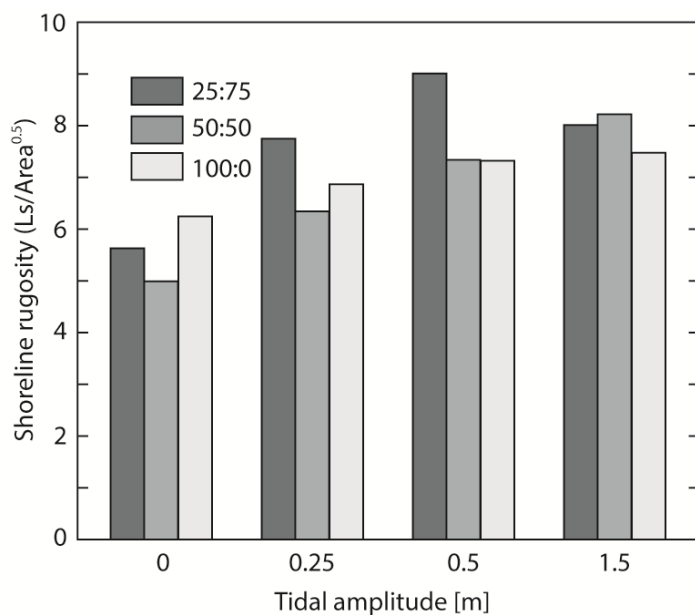


Figure C.2: Final shoreline rugosity for all model runs.

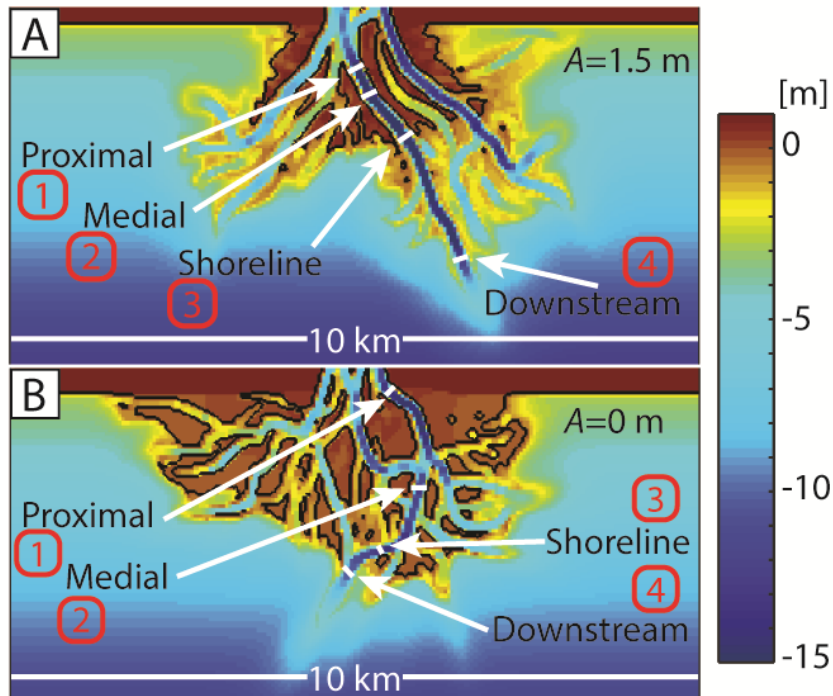


Figure C.3: Position of the four locations along the main distributary channel in which the width-averaged parameters shown in Fig. 4.5 (base level, flow velocity, suspended sediment flux, bedload sediment flux) have been calculated. (A) Locations in the 50:50 run with $A=1.5$ m. (B) Locations in the 50:50 run with $A=0$ m.

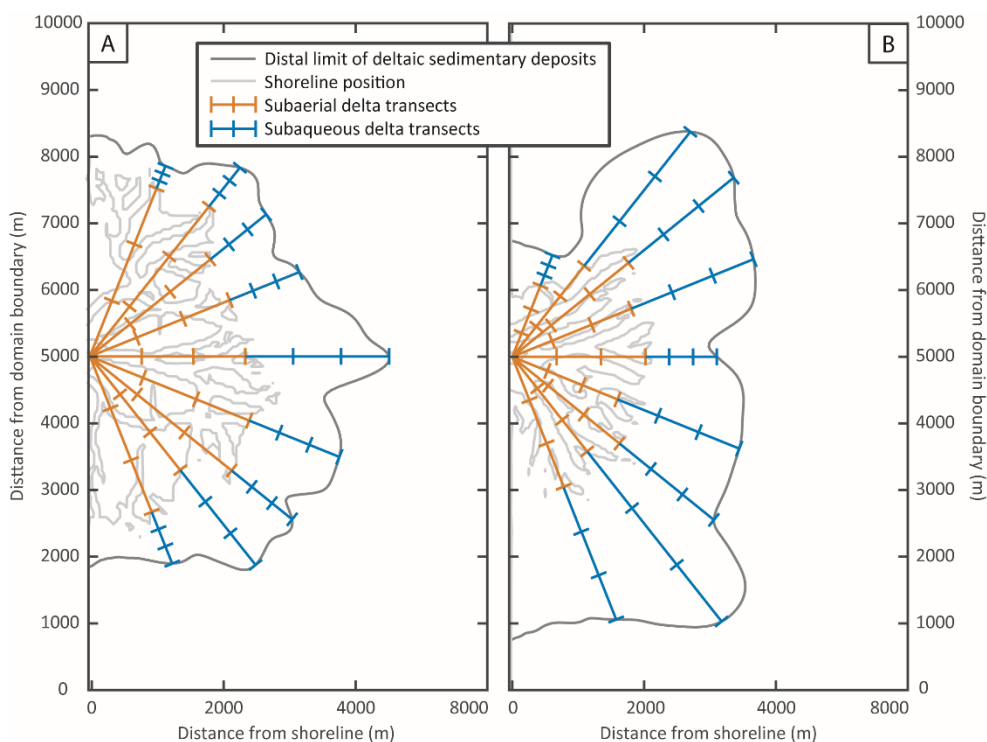


Figure C.4: Position of the transects along which the percentages of sand and mud in the deltaic deposits (Fig. 4.6) have been calculated. (A) Position of the transects in the 50:50 run with $A=0$. (B) Position of the transects in the 50:50 run with $A=1.5$ m. The subaerial delta transects include deposits from the delta apex to the shoreline. The subaqueous delta transects include deposits from the shoreline to the prodelta.

REFERENCES

- Allen, G. P., Laurier, D., and Thouvein, J., 1979, Étude sédimentologique du delta de la Mahakam, Compagnie française des pétroles - Total, Notes et Mémoires.
- Baitis, E., 2008, Grain Sizes of Recent Siliciclastic Deposits in Wax Lake Delta, Louisiana [BSc: The University of Texas at Austin.
- Caline, B., and Huong, J., 1992, New insight into the recent evolution of the Baram Delta from satellite imagery: Geological Society of Malaysia Bulletin, v. 32, p. 1-13.
- Carriquiry, J. D., and Sánchez, A., 1999, Sedimentation in the Colorado River delta and Upper Gulf of California after nearly a century of discharge loss: Marine Geology, v. 158, no. 1-4, p. 125-145.

- Cummings, D., Dalrymple, R., Choi, K., and Jin, J., 2016, *The Tide-dominated Han River Delta, Korea: Geomorphology, Sedimentology, and Stratigraphic Architecture*, Elsevier.
- Guillen, J., and Palanques, A., 1992, Sediment dynamics and hydrodynamics in the lower course of a river highly regulated by dams: the Ebro River: *Sedimentology*, v. 39, no. 4, p. 567-579.
- Kim, W., Mohrig, D., Twilley, R., Paola, C., and Parker, G., 2009, Is it feasible to build new land in the Mississippi River Delta: *Eos*, v. 90, no. 42, p. 373-374.
- Lambiase, J. J., Rahim, A. A. b. A., and Peng, C. Y., 2002, Facies distribution and sedimentary processes on the modern Baram Delta: implications for the reservoir sandstones of NW Borneo: *Marine and Petroleum Geology*, v. 19, no. 1, p. 69-78.
- Sassi, M. G., Hoitink, A. J. F., de Brye, B., Vermeulen, B., and Deleersnijder, E., 2011, Tidal impact on the division of river discharge over distributary channels in the Mahakam Delta: *Ocean Dynamics*, v. 61, no. 12, p. 2211-2228.
- Shaw, J. B., and Mohrig, D., 2014, The importance of erosion in distributary channel network growth, Wax Lake Delta, Louisiana, USA: *Geology*, v. 42, no. 1, p. 31-34.
- Shaw, J. B., Mohrig, D., and Whitman, S. K., 2013, The morphology and evolution of channels on the Wax Lake Delta, Louisiana, USA: *Journal of Geophysical Research: Earth Surface*, v. 118, no. 3, p. 1562-1584.
- Syvitski, J. P. M., and Saito, Y., 2007, Morphodynamics of deltas under the influence of humans: *Global and Planetary Change*, v. 57, no. 3-4, p. 261-282.
- Thompson, R. W., 1968, Tidal Flat Sedimentation on the Colorado River Delta, Northwestern Gulf of California: *Geological Society of America Memoirs*, v. 107, p. 1-132.

Bibliography

- Agirrezabala, L. M., and de Gibert, J. M., 2004, Paleodepth and Paleoenvironment of *Dactyloidites ottoi* (Geinitz, 1849) from Lower Cretaceous Deltaic Deposits (Basque-Cantabrian Basin, West Pyrenees): *PALAIOS*, v. 19, no. 3, p. 276-291.
- Ainsworth, R. B., Flint, S. S., and Howell, J. A., 2008, Predicting coastal depositional style: influence of basin morphology and accommodation to sediment supply ratio within a sequence stratigraphic framework: Recent advances in models of shallow-marine stratigraphy: *SEPM Special Publication*, v. 90, p. 237-263.
- Ainsworth, R. B., Hasiotis, S. T., Amos, K. J., Krapf, C. B. E., Payenberg, T. H. D., Sandstrom, M. L., Vakarelov, B. K., and Lang, S. C., 2012, Tidal signatures in an intracratonic playa lake: *Geology*, v. 40, no. 7, p. 607-610.
- Ainsworth, R. B., Vakarelov, B. K., Lee, C., MacEachern, J. A., Montgomery, A. E., Ricci, L. P., and Dashtgard, S. E., 2015, Architecture and Evolution of A Regressive, Tide-Influenced Marginal Marine Succession, Drumheller, Alberta, Canada: *Journal of Sedimentary Research*, v. 85, no. 6, p. 596-625.
- Ainsworth, R. B., Vakarelov, B. K., and Nanson, R. A., 2011, Dynamic spatial and temporal prediction of changes in depositional processes on clastic shorelines: toward improved subsurface uncertainty reduction and management: *AAPG bulletin*, v. 95, no. 2, p. 267-297.
- Alam, M. M., Crook, K. A. W., and Taylor, G., 1985, Fluvial herring-bone cross-stratification in a modern tributary mouth bar, Coonamble, New South Wales, Australia: *Sedimentology*, v. 32, no. 2, p. 235-244.
- Allen, G. P., and Posamentier, H. W., 1994, Transgressive facies and sequence architecture in mixed tide-and wave-dominated incised valleys: example from the Gironde Estuary, France, *Incised-valley Systems: Origin and Sedimentary Sequences*, Volume 51, *SEPM Special Publication*.
- Allen, J. R. L., 1980, Sand waves: a model of origin and internal structure: *Sedimentary Geology*, v. 26, no. 4, p. 281-328.
- , 1981, Lower Cretaceous tides revealed by cross-bedding with mud drapes: *Nature*, v. 289, no. 5798, p. 579-581.
- , 1982, *Sedimentary structures, their character and physical basis*, Elsevier.
- Allen, P. A., and Homewood, P., 1984, Evolution and mechanics of a Miocene tidal sandwave: *Sedimentology*, v. 31, no. 1, p. 63-81.
- Amir Hassan, M. H., Johnson, H. D., Allison, P. A., and Abdullah, W. H., 2013, Sedimentology and stratigraphic development of the upper Nyalau Formation (Early Miocene), Sarawak, Malaysia: A mixed wave- and tide-influenced coastal system: *Journal of Asian Earth Sciences*, v. 76, no. 0, p. 301-311.
- Amodio-Morelli, L., Bonardi, G., Colonna, V., Dietrich, D., Giunta, G., Ippolito, F., Liguori, V., Lorenzoni, S., Paglionico, A., Perrone, V., Piccarreta, G., Russo, M., Scandone, P., Zanettin Lorenzoni, E., and Zuppetta, A., 1976, L'arco Calabro-Peloritano nell'orogene Appenninico-Maghrebide: *Mem. Soc. Geol. It.*, v. 17, p. 1-60.

- Anastas, A. S., Dalrymple, R. W., James, N. P., and Nelson, C. S., 1997, Cross-stratified calcarenites from New Zealand: subaqueous dunes in a cool-water, Oligo-Miocene seaway: *Sedimentology*, v. 44, no. 5, p. 869-891.
- Anastas, A. S., Dalrymple, R. W., James, N. P., and Nelson, C. S., 2006, Lithofacies and dynamics of a cool-water carbonate seaway; mid-Tertiary, Te Kuiti Group, New Zealand: *Geological Society Special Publications*, v. 255, p. 245-268.
- Ashley, G. M., and Grizzle, R. E., 1988, The Hydrodynamics and Sedimentology of a Back-Barrier Lagoon-Salt Marsh System Interactions between hydrodynamics, benthos and sedimentation in a tide-dominated coastal lagoon: *Marine Geology*, v. 82, no. 1, p. 61-81.
- Ayranci, K., Lintern, D. G., Hill, P. R., and Dashtgard, S. E., 2012, Tide-supported gravity flows on the upper delta front, Fraser River delta, Canada: *Marine Geology*, v. 326–328, no. 0, p. 166-170.
- Belderson, R. H., Johnson, M. A., and Kenyon, N. H., 1982, Bedforms, *in* Stride, A. H., ed., *Offshore Tidal Sands*: London, Chapman and Hall, p. 27-57.
- Bhattacharya, J. P., 2010, Deltas, *in* Dalrymple, B. W., and James, N. P., eds., *Facies models*, Volume 4, Geological Association of Canada, p. 233-264.
- Bhattacharya, J. P., and Giosan, L., 2003, Wave-influenced deltas: geomorphological implications for facies reconstruction: *Sedimentology*, v. 50, no. 1, p. 187-210.
- Bhattacharya, J. P., and MacEachern, J. A., 2009, Hyperpycnal Rivers and Prodeltaic Shelves in the Cretaceous Seaway of North America: *Journal of Sedimentary Research*, v. 79, no. 4, p. 184-209.
- Bhattacharya, J. P., and Walker, R. G., 1991, River- and Wave-Dominated Depositional Systems of the Upper Cretaceous Dunvegan Formation, Northwestern Alberta: *Bulletin of Canadian Petroleum Geology*, v. 39, no. 2, p. 165-191.
- Bhattacharya, J. P., and Willis, B. J., 2001, Lowstand Deltas in the Frontier Formation, Powder River Basin, Wyoming: Implications for Sequence Stratigraphic Models: *AAPG Bulletin*, v. 85, no. 2, p. 261-294.
- Boersma, J. R., and Terwindt, J. H. J., 1981, Neap–spring tide sequences of intertidal shoal deposits in a mesotidal estuary: *Sedimentology*, v. 28, no. 2, p. 151-170.
- Bonardi, G., Cavazza, W., Perrone, V., and Rossi, S., 2001, Calabria-Peloritani terrane and northern Ionian Sea, *in* Vai, G. B., and Martini, I. P., eds., *Anatomy of an Orogen: the Apennines and Adjacent Mediterranean Basins*: Dordrecht, Springer Netherlands, p. 287-306.
- Boothroyd, J. C., Friedrich, N. E., and McGinn, S. R., 1985, Barrier Islands Geology of microtidal coastal lagoons: Rhode Island: *Marine Geology*, v. 63, no. 1, p. 35-76.
- Borgeld, J. C., Hughes Clarke, J. E., Goff, J. A., Mayer, L. A., and Curtis, J. A., 1999, Acoustic backscatter of the 1995 flood deposit on the Eel shelf: *Marine Geology*, v. 154, no. 1–4, p. 197-210.
- Brandsæter, I., McIlroy, D., Lia, O., Ringrose, P., and Næss, A., 2005, Reservoir modelling and simulation of Lajas Formation outcrops (Argentina) to constrain tidal reservoirs of the Halten Terrace (Norway): *Petroleum Geoscience*, v. 11, no. 1, p. 37-46.

- Brooks, G. R., Jack, L. K., Shea, P., Williams, S. J., and McBride, R. A., 1995, East Louisiana Continental Shelf Sediments: A Product of Delta Reworking: *Journal of Coastal Research*, v. 11, no. 4, p. 1026-1036.
- Brown, M. A., Archer, A. W., and Kvale, E. P., 1990, Neap-spring tidal cyclicity in laminated carbonate channel-fill deposits and its implications: Salem Limestone (Mississippian), south-central Indiana, USA: *Journal of Sedimentary Research*, v. 60, no. 1.
- Budillon, F., Violante, C., Conforti, A., Esposito, E., Insinga, D., Iorio, M., and Porfido, S., 2005, Event beds in the recent prodelta stratigraphic record of the small flood-prone Bonea Stream (Amalfi Coast, Southern Italy): *Marine Geology*, v. 222–223, no. 0, p. 419-441.
- Burgess, P. M., Flint, S., and Johnson, S., 2000, Sequence stratigraphic interpretation of turbiditic strata: An example from Jurassic strata of the Neuquén basin, Argentina: *Geological Society of America Bulletin*, v. 112, no. 11, p. 1650-1666.
- Carle, L., and Hill, P. R., 2009, Subaqueous Dunes of the Upper Slope of the Fraser River Delta (British Columbia, Canada): *Journal of Coastal Research*, v. 25, no. 2, p. 448-458.
- Cattaneo, A., and Steel, R. J., 2003, Transgressive deposits: a review of their variability: *Earth-Science Reviews*, v. 62, no. 3–4, p. 187-228.
- Cavazza, W., Blenkinsop, J., de Celles, P. G., Patterson, R. T., and Reinhardt, E. G., 1997, Stratigrafia e sedimentologia della sequenza sedimentaria oligocenica-quadernaria del bacino calabro-ionico: *Bollettino della Societa Geologica Italiana*, v. 116, no. 1, p. 51-77.
- Cavazza, W., and DeCelles, P. G., 1993, Geometry of a Miocene submarine canyon and associated sedimentary facies in southeastern Calabria, southern Italy: *Geological Society of America Bulletin*, v. 105, no. 10, p. 1297-1309.
- Cavazza, W., and Ingersoll, R. V., 2005, Detrital Modes of the Ionian Forearc Basin Fill (Oligocene-Quaternary) Reflect the Tectonic Evolution of the Calabria-Peloritani Terrane (Southern Italy): *Journal of Sedimentary Research*, v. 75, no. 2, p. 268-279.
- Charvin, K., Hampson, G. J., Gallagher, K. L., and Labourdette, R., 2010, Intra-parasequence architecture of an interpreted asymmetrical wave-dominated delta: *Sedimentology*, v. 57, no. 3, p. 760-785.
- Chen, S., Steel, R. J., Dixon, J. F., and Osman, A., 2014, Facies and architecture of a tide-dominated segment of the Late Pliocene Orinoco Delta (Morne L'Enfer Formation) SW Trinidad: *Marine and Petroleum Geology*, v. 57, no. 0, p. 208-232.
- Chiarella, D., Angular and tangential toset geometry in tidal cross- strata: an additional feature of current- modulated deposits, *in Proceedings Contributions to Modern and Ancient Tidal Sedimentology: Proceedings of the Tidalites 2012 Conference 2016*, Volume 47, IAS Special Publication, p. 185-195.
- Chiarella, D., Moretti, M., Longhitano, S. G., and Muto, F., 2016, Deformed cross-stratified deposits in the Early Pleistocene tidally-dominated Catanzaro strait-fill

- succession, Calabrian Arc (Southern Italy): Triggering mechanisms and environmental significance: *Sedimentary Geology*.
- Choi, K., 2010, Rhythmic Climbing-Ripple Cross-Lamination in Inclined Heterolithic Stratification (IHS) of a Macrotidal Estuarine Channel, Gomso Bay, West Coast of Korea: *Journal of Sedimentary Research*, v. 80, no. 6, p. 550-561.
- , 2011, Tidal rhythmites in a mixed-energy, macrotidal estuarine channel, Gomso Bay, west coast of Korea: *Marine Geology*, v. 280, no. 1-4, p. 105-115.
- Choi, K., Dalrymple, R. W., Chun, S. S., and Kim, S.-P., 2004, Sedimentology of Modern, Inclined Heterolithic Stratification (IHS) in the Macrotidal Han River Delta, Korea: *Journal of Sedimentary Research*, v. 74, no. 5, p. 677-689.
- Clifton, H. E., 1976, Wave-formed sedimentary structures—a conceptual model, *in* Davis Jr, R. A., and Ethington, R. L., eds., *Beach and Nearshore Sedimentation*, Volume 24, SEPM Spec. Publ., p. 126-148.
- Clifton, H. E., 1982, Estuarine deposits, *in* Scholle, P. A., and Spearing, D., eds., *Sandstone Depositional Environments*: Tulsa, OK, American Association of Petroleum Geologists, p. 179-189.
- Clifton, H. E., and Phillips, R. L., 1980, Lateral trends and vertical sequences in estuarine sediments, Willapa Bay, Washington, *in* Field, M. E., Bouma, A. H., Colburn, I. P., Douglas, R. G., and Ingle, J. C., eds., *Quaternary Depositional Environments of the Pacific Coast*, Volume Pacific Coast Paleogeography Symposium 4, Society of Economic Paleontologists and Mineralogists Pacific Section, p. 55-71.
- Coates, L., and MacEachern, J., Differentiating river- and wave-dominated deltas from shorefaces: Examples from the Cretaceous Western Interior Seaway, Alberta, Canada, *in* *Proceedings GeoCanada 2000*, Millennium Geoscience Summit, Calgary, Alberta, 2000, p. unpaginated.
- Colella, A., and D'alessandro, A., 1988, Sand waves, Echinocardium traces and their bathyal depositional setting (Monte Torre Palaeostrait, Plio- Pleistocene, southern Italy): *Sedimentology*, v. 35, no. 2, p. 219-237.
- Coleman, J. M., and Gagliano, S. M., 1965, Sedimentary structures: Mississippi river deltaic plain, *in* Middleton, G. V., ed., *Sedimentary Structures and Their Hydrodynamic Interpretation*, Volume 12, Soc. Econ. Paleontologists Mineralogists Spec. Publ., p. 133-148.
- Coleman, J. M., and Wright, L. D., 1975, Modern River Deltas: Variability of Processes and Sand Bodies, *in* Broussard, M. L., ed., *Deltas - Models for Exploration*, Houston Geological Society, p. 99-149.
- Collinson, J. D., 1970, Bedforms of the Tana River, Norway: *Geografiska Annaler. Series A, Physical Geography*, v. 52, no. 1, p. 31-56.
- Colombera, L., Felletti, F., Mountney, N. P., and McCaffrey, W. D., 2012a, A database approach for constraining stochastic simulations of the sedimentary heterogeneity of fluvial reservoirs: *AAPG bulletin*, v. 96, no. 11, p. 2143-2166.
- Colombera, L., Mountney, N. P., Hodgson, D. M., and McCaffrey, W. D., 2016, The Shallow-Marine Architecture Knowledge Store: A database for the

- characterization of shallow-marine and paralic depositional systems: *Marine and Petroleum Geology*, v. 75, p. 83-99.
- Colombera, L., Mountney, N. P., and McCaffrey, W. D., 2012b, A relational database for the digitization of fluvial architecture: concepts and example applications: *Petroleum Geoscience*, v. 18, no. 1, p. 129-140.
- Crevello, P., Morley, C., Lambiase, J., and Simmons, M., The Interaction of Tectonics and Depositional Systems on the Stratigraphy of the Active Tertiary Deltaic Shelf Margin of Brunei Darussalam, *in Proceedings Proceedings of the Petroleum Systems of SE Asia and Australasia Conference 1997*, p. 767-772.
- Critelli, S., 1999, The interplay of lithospheric flexure and thrust accommodation in forming stratigraphic sequences in the southern Apennines foreland basin system, Italy: *Rendiconti Accademia dei Lincei*, v. 10, no. 9, p. 257-326.
- Cummings, D., Dalrymple, R., Choi, K., and Jin, J., 2016, The Tide-dominated Han River Delta, Korea: Geomorphology, Sedimentology, and Stratigraphic Architecture, Elsevier.
- Cummings, D. I., Arnott, R. W. C., and Hart, B. S., 2006, Tidal signatures in a shelf-margin delta: *Geology*, v. 34, no. 4, p. 249-252.
- Dalrymple, B. W., 2010, Tidal depositional systems, *in* James, N. P., and Dalrymple, B. W., eds., *Facies models*, Volume 4, Geological Association of Canada, p. 201-231.
- Dalrymple, R. W., 1984, Morphology and internal structure of sandwaves in the Bay of Fundy: *Sedimentology*, v. 31, no. 3, p. 365-382.
- Dalrymple, R. W., Baker, E. K., Harris, P. T., and Hughes, M. G., 2003, Sedimentology and stratigraphy of a tide-dominated, foreland-basin delta (Fly River, Papua New Guinea), *in* Sidi, F. H., Nummedal, D., Imbert, P., Darman, H., and Posamentier, H. W., eds., *Tropical Deltas of Southeast Asia—Sedimentology, Stratigraphy, and Petroleum Geology*, Volume 76, SEPM Special Publication, p. 147-173.
- Dalrymple, R. W., and Choi, K., 2007, Morphologic and facies trends through the fluvial-marine transition in tide-dominated depositional systems: A schematic framework for environmental and sequence-stratigraphic interpretation: *Earth-Science Reviews*, v. 81, no. 3-4, p. 135-174.
- Dalrymple, R. W., Knight, R. J., and Lambiase, J. J., 1978, Bedforms and their hydraulic stability relationships in a tidal environment, Bay of Fundy, Canada: *Nature*, v. 275, p. 100-104.
- Dalrymple, R. W., Knight, R. J., Zaitlin, B. A., and Middleton, G. V., 1990, Dynamics and facies model of a macrotidal sand-bar complex, Cobequid Bay—Salmon River Estuary (Bay of Fundy): *Sedimentology*, v. 37, no. 4, p. 577-612.
- Dalrymple, R. W., Makino, Y., and Zaitlin, B. A., 1991, Temporal and spatial patterns of rhythmite deposition on mud flats in the macrotidal Cobequid Bay-Salmon River estuary, Bay of Fundy, Canada.
- Dalrymple, R. W., Zaitlin, B. A., and Boyd, R., 1992a, Estuarine facies models: conceptual basis and stratigraphic implications: perspective: *Journal of Sedimentary Research*, v. 62, no. 6.

- Dalrymple, R. W., Zaitlin, B. A., and Boyd, R., 1992b, Estuarine facies models; conceptual basis and stratigraphic implications: *Journal of Sedimentary Research*, v. 62, no. 6, p. 1130-1146.
- Dalrymple, R. W., and Choi, K., 2007, Morphologic and facies trends through the fluvial-marine transition in tide-dominated depositional systems: A schematic framework for environmental and sequence-stratigraphic interpretation: *Earth-Science Reviews*, v. 81, no. 3-4, p. 135-174.
- Dashtgard, S., Venditti, J., Hill, P., Sisulak, C., Johnson, S., and La Croix, A., 2012a, Sedimentation across the tidal-fluvial transition in the lower Fraser River, Canada: *Sediment. Rec*, v. 10, p. 4-9.
- Dashtgard, S. E., Gingras, M. K., and MacEachern, J. A., 2009, Tidally Modulated Shorefaces: *Journal of Sedimentary Research*, v. 79, no. 11, p. 793-807.
- Dashtgard, S. E., MacEachern, J. A., Frey, S. E., and Gingras, M. K., 2012b, Tidal effects on the shoreface: Towards a conceptual framework: *Sedimentary Geology*, v. 279, no. 0, p. 42-61.
- Dastgheib, A., Roelvink, J. A., and Wang, Z. B., 2008, Long-term process-based morphological modeling of the Marsdiep Tidal Basin: *Marine Geology*, v. 256, no. 1-4, p. 90-100.
- Davis Jr, R. A., and Dalrymple, R. W., 2011, *Principles of tidal sedimentology*, Springer Science & Business Media.
- De Boer, P. L., 1998, Intertidal sediments: composition and structure, *in* Eisma, D., ed., *Intertidal Deposits. River Mouths, Tidal Flats, and Coastal Lagoons*: Boca Raton, CRC Press, p. 345-361.
- de Gibert, J. M., Martinell, J., and Domènech, R., 1995, The rosetted feeding trace fossil *Dactyloidites otto* (Geinitz) from the Miocene of Catalonia: *Geobios*, v. 28, no. 6, p. 769-776.
- de Jong, J. D., 1977, Dutch tidal flats: *Sedimentary Geology*, v. 18, no. 1, p. 13-23.
- De Mowbray, T., and Visser, M. J., 1984, Reactivation surfaces in subtidal channel deposits, Oosterschelde, Southwest Netherlands: *Journal of Sedimentary Research*, v. 54, no. 3, p. 811-824.
- De Raaf, J. F. M., and Boersma, J. R., 1971, Tidal deposits and their sedimentary structures: *Netherlands Journal of Geosciences/Geologie en Mijnbouw*, v. 50, no. 3, p. 479-504.
- De Raaf, J. F. M., Boersma, J. R., and Van Gelder, A., 1977, Wave-generated structures and sequences from a shallow marine succession, Lower Carboniferous, County Cork, Ireland: *Sedimentology*, v. 24, no. 4, p. 451-483.
- Defant, A., 1961, Water bodies and stationary current conditions at boundary surfaces: *Physical Oceanography*, v. 1, p. 451-475.
- Dumas, S., Arnott, R., and Southard, J. B., 2005, Experiments on oscillatory-flow and combined-flow bed forms: implications for interpreting parts of the shallow-marine sedimentary record: *Journal of Sedimentary research*, v. 75, no. 3, p. 501-513.

- Dumas, S., and Arnott, R. W. C., 2006, Origin of hummocky and swaley cross-stratification— The controlling influence of unidirectional current strength and aggradation rate: *Geology*, v. 34, no. 12, p. 1073-1076.
- Duncan Jr, J. R., 1964, The effects of water table and tide cycle on swash-backwash sediment distribution and beach profile development: *Marine Geology*, v. 2, no. 3, p. 186-197.
- Edmonds, D., Slingerland, R., Best, J., Parsons, D., and Smith, N., 2010, Response of river-dominated delta channel networks to permanent changes in river discharge: *Geophysical Research Letters*, v. 37, no. 12, p. L12404.
- Edmonds, D. A., and Slingerland, R. L., 2010, Significant effect of sediment cohesion on delta morphology: *Nature Geosci*, v. 3, no. 2, p. 105-109.
- Eide, C. H., Howell, J. A., Buckley, S. J., Martinius, A. W., Oftedal, B. T., and Henstra, G. A., 2016, Facies model for a coarse-grained, tide-influenced delta: Gule Horn Formation (Early Jurassic), Jameson Land, Greenland: *Sedimentology*, p. n/a-n/a.
- Fisk, H. N., 1961, Bar-finger sands of Mississippi delta, *Geometry of sandstone bodies*: Tulsa, Oklahoma, AAPG, p. 29-52.
- FitzGerald, D., Buynevich, I., and Hein, C., 2012, Morphodynamics and Facies Architecture of Tidal Inlets and Tidal Deltas, *in* Davis Jr, R. A., and Dalrymple, R. W., eds., *Principles of Tidal Sedimentology*, Springer Netherlands, p. 301-333.
- Franzese, J., Spalletti, L., Pérez, I. G., and Macdonald, D., 2003, Tectonic and paleoenvironmental evolution of Mesozoic sedimentary basins along the Andean foothills of Argentina (32°–54°S): *Journal of South American Earth Sciences*, v. 16, no. 1, p. 81-90.
- Franzese, J. R., Veiga, G. D., Schwarz, E., and Gómez-Pérez, I., 2006, Tectonostratigraphic evolution of a Mesozoic graben border system: the Chachil depocentre, southern Neuquén Basin, Argentina: *Journal of the Geological Society*, v. 163, no. 4, p. 707-721.
- Fraser, G. S., and Hester, N. C., 1977, Sediments and sedimentary structures of a beach-ridge complex, southwestern shore of Lake Michigan: *Journal of Sedimentary Research*, v. 47, no. 3.
- Frey, S. E., and Dashtgard, S. E., 2011, Sedimentology, ichnology and hydrodynamics of strait-margin, sand and gravel beaches and shorefaces: Juan de Fuca Strait, British Columbia, Canada: *Sedimentology*, v. 58, no. 6, p. 1326-1346.
- Fürsich, F. T., and Bromley, R. G., 1985, Behavioural interpretation of a rosetted spreite trace fossil: *Dactyloidites ottoii* (Geinitz): *Lethaia*, v. 18, no. 3, p. 199-207.
- Fürsich, F. T., and Oschmann, W., 1993, Shell beds as tools in basin analysis: the Jurassic of Kachchh, western India: *Journal of the Geological Society*, v. 150, no. 1, p. 169-185.
- Galli, P. A. C., and Peronace, E., 2015, Low slip rates and multimillennial return times for Mw 7 earthquake faults in southern Calabria (Italy): *Geophysical Research Letters*, v. 42, no. 13, p. 5258-5265.

- Galloway, W. E., 1975, Process framework for describing the morphologic and stratigraphic evolution of deltaic depositional systems, *in* Broussard, M. L., ed., *Deltas, Models for Exploration*, p. 87-98.
- Galloway, W. E., 1976, Sediments and stratigraphic framework of the Copper River fan-delta, Alaska: *Journal of Sedimentary Research*, v. 46, no. 3, p. 726-737.
- Galloway, W. E., 1981, Depositional architecture of Cenozoic Gulf Coastal Plain fluvial systems, *in* Ethridge, F. G., and Flores, R. M., eds., *Recent and Ancient Nonmarine Depositional Environments*, Volume 31, Soc. Econ. Palaeontol. Mineral. Spec. Publ., p. 127-156.
- Gani, M. R., and Bhattacharya, J. P., 2007, Basic Building Blocks and Process Variability of a Cretaceous Delta: Internal Facies Architecture Reveals a More Dynamic Interaction of River, Wave, and Tidal Processes Than Is Indicated by External Shape: *Journal of Sedimentary Research*, v. 77, no. 4, p. 284-302.
- Gani, M. R., Bhattacharya, J. P., and MacEachern, J. A., 2009, Using ichnology to determine relative influence of waves, storms, tides, and rivers in deltaic deposits: examples from Cretaceous Western Interior Seaway, USA, *in* MacEachern, J. A., Bann, K. L., Gingras, M. K., and Pemberton, S. G., eds., *Applied Ichnology*, Volume 52, SEPM SHort Course Notes, p. 209-225.
- Geleynse, N., Storms, J. E. A., Walstra, D.-J. R., Jagers, H. R. A., Wang, Z. B., and Stive, M. J. F., 2011, Controls on river delta formation; insights from numerical modelling: *Earth and Planetary Science Letters*, v. 302, no. 1-2, p. 217-226.
- Gingras, M. K., MacEachern, J. A., and Pemberton, S. G., 1998, A comparative analysis of the ichnology of wave-and river-dominated allomembers of the Upper Cretaceous Dunvegan Formation: *Bulletin of Canadian Petroleum Geology*, v. 46, no. 1, p. 51-73.
- Goes, S., Giardini, D., Jenny, S., Hollenstein, C., Kahle, H. G., and Geiger, A., 2004, A recent tectonic reorganization in the south-central Mediterranean: *Earth and Planetary Science Letters*, v. 226, no. 3-4, p. 335-345.
- Goodbred Jr, S. L., and Saito, Y., 2012, Tide-dominated deltas, *in* Davis Jr, R. A., and Dalrymple, B. W., eds., *Principles of Tidal Sedimentology*, Springer Netherlands, p. 129-149.
- Goodbred, S. L., and Kuehl, S. A., 1999, Holocene and modern sediment budgets for the Ganges-Brahmaputra river system: Evidence for highstand dispersal to flood-plain, shelf, and deep-sea depocenters: *Geology*, v. 27, no. 6, p. 559-562.
- Greb, S. F., and Archer, A. W., 1995, Rhythmic sedimentation in a mixed tide and wave deposit, Hazel Patch Sandstone (Pennsylvanian), eastern Kentucky coal field: *Journal of Sedimentary Research*, v. 65, no. 1.
- Greb, S. F., and Archer, A. W., 2007, Soft-sediment deformation produced by tides in a meizoseismic area, Turnagain Arm, Alaska: *Geology*, v. 35, no. 5, p. 435-438.
- Guzman, J. I., and Fisher, W. L., 2006, Early and middle Miocene depositional history of the Maracaibo Basin, western Venezuela: *AAPG bulletin*, v. 90, no. 4, p. 625-655.

- Hampson, G. J., 2000, Discontinuity Surfaces, Clinoforms, and Facies Architecture in a Wave-Dominated, Shoreface-Shelf Parasequence: *Journal of Sedimentary Research*, v. 70, no. 2, p. 325-340.
- Harris, P. T., Pattiaratchi, C. B., Collins, M. B., and Dalrymple, R. W., 1995, What is a Bedload Parting?, *in* Flemming, B. W., and Bartholoma, A., eds., *Tidal Signatures in Modern and Ancient Sediments*, Volume 24, International Association of Sedimentologists Special Publication, p. 3-18.
- Hayes, M. O., 1980, General morphology and sediment patterns in tidal inlets: *Sedimentary Geology*, v. 26, no. 1-3, p. 139-156.
- Helland-Hansen, W., and Hampson, G. J., 2009, Trajectory analysis: concepts and applications: *Basin Research*, v. 21, no. 5, p. 454-483.
- Helland-Hansen, W., and Martinsen, O. J., 1996, Shoreline trajectories and sequences: description of variable depositional-dip scenarios: *Journal of Sedimentary Research*, v. 66, no. 4.
- Hillen, M. M., 2009, Wave reworking of a delta: process-based modelling of sediment reworking under wave conditions in the deltaic environment [Master thesis: TU Delft].
- Hillen, M. M., Geleynse, N., Storms, J. E. A., Walstra, D. J. R., and Groenenberg, R. M., 2014, Morphodynamic modelling of wave reworking of an alluvial delta and application of results in the standard reservoir modelling workflow, *in* Martinius, A. W., Ravnås, R., Howell, J. A., Steel, R. J., and Wonham, J. P., eds., *From Depositional Systems to Sedimentary Successions on the Norwegian Continental Margin (Special Publication 46 of the IAS)*, Volume 46, International Association of Sedimentologists, p. 167-186.
- Homewood, P., and Allen, P., 1981, Wave-controlled, tide-controlled, and current-controlled sandbodies of Miocene molasse, western Switzerland: *Aapg Bulletin-American Association of Petroleum Geologists*, v. 65, no. 12, p. 2534-2545.
- Howard, J. D., and Reineck, H.-E., 1981, Depositional facies of high-energy beach-to-offshore sequence: comparison with low-energy sequence: *AAPG Bulletin*, v. 65, no. 5, p. 807-830.
- Hurd, T. J., Fielding, C. R., and Hutsky, A. J., 2014, Variability In Sedimentological and Ichnological Signatures Across A River-Dominated Delta Deposit: Peay Sandstone Member (Cenomanian) of the Northern Bighorn Basin, Wyoming, U.S.A: *Journal of Sedimentary Research*, v. 84, no. 1, p. 1-18.
- Ichaso, A. A., and Dalrymple, R. W., 2009, Tide- and wave-generated fluid mud deposits in the Tilje Formation (Jurassic), offshore Norway: *Geology*, v. 37, no. 6, p. 539-542.
- , 2014, Eustatic, tectonic and climatic controls on an early synrift mixed-energy delta, Tilje Formation (early Jurassic, Smørbukk Field, offshore mid-Norway), *in* Martinius, A. W., Ravnås, R., Howell, J. A., Steel, R. J., and Wonham, J. P., eds., *Depositional Systems to Sedimentary Successions on the Norwegian Continental Shelf*, Volume 46, International Association of Sedimentologists Special Publication, p. 339-388.

- Jablonski, B. V. J., 2012, Process Sedimentology and Three-Dimensional Facies Architecture of a Fluvially Dominated, Tidally Influenced Point Bar: Middle McMurray Formation, Lower Steepbank River Area, Northeastern Alberta, Canada [MSc MSc Thesis]: Queen's University.
- Jablonski, B. V. J., and Dalrymple, B. W., 2014, Fluvial Seasonality: A Predictive Tool for Deciphering the Sedimentological Complexity of Inclined Heterolithic Stratification Deposited on Large-Scale Tidal-Fluvial Point Bars?, CSPG/CSEG/CWLS GeoConvention 2013, (Integration: Geoscience engineering Partnership), AAPG/CSPG©2014: Calgary TELUS Convention Centre & ERCB Core Research Centre, Calgary, AB, Canada, 6-12 May 2013.
- Jopling, A. V., and Walker, R. G., 1968, Morphology and origin of ripple-drift cross-lamination, with examples from the Pleistocene of Massachusetts: *Journal of Sedimentary Research*, v. 38, no. 4, p. 971-984.
- Kidwell, S. M., Time scales of fossil accumulation: patterns from Miocene benthic assemblages, *in* Proceedings Third North American Paleontological Convention, Proceedings 1982, Volume 1, p. 295-300.
- Kidwell, S. M., and Bosence, D. W. J., 1991, Taphonomy and time-averaging of marine shelly faunas, *in* Allison, P. A., and Briggs, D. E. G., eds., *Taphonomy: Releasing the Data Locked in the Fossil Record.* : New York, Plenum Press, p. 115-209.
- Kidwell, S. M., Fürsich, F. T., and Aigner, T., 1986, Conceptual Framework for the Analysis and Classification of Fossil Concentrations: *Palaios*, v. 1, no. 3, p. 228-238.
- Kim, W., Paola, C., Voller, V. R., and Swenson, J. B., 2006, Experimental Measurement of the Relative Importance of Controls on Shoreline Migration: *Journal of Sedimentary Research*, v. 76, no. 2, p. 270-283.
- Kirschbaum, M. A., and Hettinger, R. D., 2004, Facies analysis and sequence stratigraphic framework of Upper Campanian strata (Neslen and mount Garfield Formations, Bluecastle Tongue of the Castlegate Sandstone, and Mancos Shale), eastern Book cliffs, Colorado and Utah, U.S. Geological Survey Digital Data Report.
- Klein, G. D., 1963, Bay of Fundy intertidal zone sediments: *Journal of Sedimentary Research*, v. 33, no. 4.
- Klein, G. D., 1971, A Sedimentary Model for Determining Paleotidal Range: *Geological Society of America Bulletin*, v. 82, no. 9, p. 2585-2592.
- Klein, G. D., and Sanders, J. E., 1964, Comparison of sediments from Bay of Fundy and Dutch Wadden Sea tidal flats: *Journal of Sedimentary Research*, v. 34, no. 1.
- Knott, S. D., and Turco, E., 1991, Late Cenozoic kinematics of the Calabrian Arc, southern Italy: *Tectonics*, v. 10, no. 6, p. 1164-1172.
- Kollmann, H. A., 2014, The extinct Nerineoidea and Acteonelloidea (Heterobranchia, Gastropoda): a palaeobiological approach: *Geodiversitas*, v. 36, no. 3, p. 349-383.
- Kreisa, R. D., and Moila, R. J., 1986, Sigmoidal tidal bundles and other tide-generated sedimentary structures of the Curtis Formation, Utah: *Geological Society of America Bulletin*, v. 97, no. 4, p. 381-387.

- Kuehl, S. A., Levy, B. M., Moore, W. S., and Allison, M. A., 1997, Subaqueous delta of the Ganges-Brahmaputra river system: *Marine Geology*, v. 144, no. 1–3, p. 81-96.
- Kumar, N., and Sanders, J. E., 1976, Characteristics of shoreface storm deposits: modern and ancient examples: *Journal of Sedimentary Research*, v. 46, no. 1, p. 145-162.
- Kurcinka, C., 2014, Sedimentology and facies architecture of the tide-influenced, river-dominated delta-mouth bars in the lower Lajas Formation (Jurassic), Argentina [MSc MSc Thesis]: Queen's University.
- Kvale, E. P., 2006, The origin of neap–spring tidal cycles: *Marine Geology*, v. 235, no. 1–4, p. 5-18.
- Kvale, E. P., Archer, A. W., and Johnson, H. R., 1989, Daily, monthly, and yearly tidal cycles within laminated siltstones of the Mansfield Formation (Pennsylvanian) of Indiana: *Geology*, v. 17, no. 4, p. 365-368.
- Lambiase, J. J., Damit, A. R., Simmons, M. D., Abdoerrias, R., and Hussin, A., 2003, A Depositional model and the stratigraphic development of modern and ancient tide-dominated deltas in NW Borneo, *in* Sidi, F. H., Nummedal, D., Imbert, P., Darman, H., and Posamentier, H. W., eds., *Tropical Deltas of Southeast Asia—Sedimentology, Stratigraphy, and Petroleum Geology* Volume SEPM Special Publication 76, p. 109-123.
- Lambiase, J. J., Rahim, A. A. b. A., and Peng, C. Y., 2002, Facies distribution and sedimentary processes on the modern Baram Delta: implications for the reservoir sandstones of NW Borneo: *Marine and Petroleum Geology*, v. 19, no. 1, p. 69-78.
- Leva López, J., Rossi, V. M., Olariu, C., and Steel, R. J., 2016, Architecture and recognition criteria of ancient shelf ridges; an example from Campanian Almond Formation in Hanna Basin, USA: *Sedimentology*.
- Longhitano, S. G., 2008, Sedimentary facies and sequence stratigraphy of coarse-grained Gilbert-type deltas within the Pliocene thrust-top Potenza Basin (Southern Apennines, Italy): *Sedimentary Geology*, v. 210, no. 3–4, p. 87-110.
- , 2011, The record of tidal cycles in mixed silici–bioclastic deposits: examples from small Plio–Pleistocene peripheral basins of the microtidal Central Mediterranean Sea: *Sedimentology*, v. 58, no. 3, p. 691-719.
- , 2013, A facies-based depositional model for ancient and modern, tectonically–confined tidal straits: *Terra Nova*, v. 25, no. 6, p. 446-452.
- Longhitano, S. G., 2015, Deflected steep-marginal deltas in confined tidal straits an outcrop analogue from the upper Miocene Amantea Basin, southern Italy, *Sedimentology of paralic reservoirs: recent advances and their applications: Piccadilly, London, Burlington House*, p. 94-95.
- Longhitano, S. G., Chiarella, D., Di Stefano, A., Messina, C., Sabato, L., and Tropeano, M., 2012a, Tidal signatures in Neogene to Quaternary mixed deposits of southern Italy straits and bays: *Sedimentary Geology*, v. 279, no. 0, p. 74-96.
- Longhitano, S. G., Chiarella, D., and Muto, F., 2014, Three-dimensional to two-dimensional cross-strata transition in the lower Pleistocene Catanzaro tidal strait transgressive succession (southern Italy): *Sedimentology*, v. 61, no. 7, p. 2136-2171.

- Longhitano, S. G., Mellere, D., Steel, R. J., and Ainsworth, R. B., 2012b, Tidal depositional systems in the rock record: A review and new insights: *Sedimentary Geology*, v. 279, no. 0, p. 2-22.
- Longhitano, S. G., and Nemeč, W., 2005, Statistical analysis of bed-thickness variation in a Tortonian succession of biocalcarenic tidal dunes, Amantea Basin, Calabria, southern Italy: *Sedimentary Geology*, v. 179, no. 3-4, p. 195-224.
- Longhitano, S. G., and Steel, R. J., 2015, Deltas sourcing tidal straits: observations from some field case studies., 31st Meeting of the International Association of Sedimentologists: Krakow, p. 313.
- , 2016, Deflection of the progradational axis and asymmetry in tidal seaway and strait deltas: insights from two outcrop case studies, Paralic Reservoir: London, Geological Society - Special Publication.
- Luketina, D., 1998, Simple Tidal Prism Models Revisited: *Estuarine, Coastal and Shelf Science*, v. 46, no. 1, p. 77-84.
- MacEachern, J. A., Pemberton, S. G., Gingras, M. K., and Bann, K. L., 2010, Ichnology and facies models, *in* James, N. P., and Dalrymple, R. W., eds., *Facies models*, Volume 4, Geological Association of Canada.
- Martin, A. J., 2000, Flaser and wavy bedding in ephemeral streams: a modern and an ancient example: *Sedimentary Geology*, v. 136, no. 1-2, p. 1-5.
- Martínez, M. A., Prámparo, M. B., Quattrocchio, M. E., and Zavala, C. A., 2008, Depositional environments and hydrocarbon potential of the Middle Jurassic Los Molles Formation, Neuquén Basin, Argentina: palynofacies and organic geochemical data: *Revista Geológica de Chile*, v. 35, no. 2, p. 279-305.
- Martínez, M. A., Quattrocchio, M. E., and Zavala, C. A., 2002, Análisis palinofacial de la Formación Lajas (Jurásico Medio), Cuenca Neuquina, Argentina. Significado paleoambiental y paleoclimático: *Revista Española de Micropaleontología*, v. 34, no. 1, p. 81-104.
- Martinius, A. W., and Gowland, S., 2011, Tide- influenced fluvial bedforms and tidal bore deposits (Late Jurassic Lourinhã Formation, Lusitanian Basin, Western Portugal): *Sedimentology*, v. 58, no. 1, p. 285-324.
- Martinius, A. W., Kaas, I., Næss, A., Helgesen, G., Kjærefjord, J. M., and Leith, D. A., 2001, Sedimentology of the heterolithic and tide-dominated tilje formation (Early Jurassic, Halten Terrace, Offshore Mid-Norway), *in* Martinsen, O. J., and Dreyer, T., eds., *Sedimentary Environments Offshore Norway — Palaeozoic to Recent*, Volume Volume 10, Norwegian Petroleum Foundation Special Publications, p. 103-144.
- Martinius, A. W., Ringrose, P. S., Brostrøm, C., Elfenbein, C., Næss, A., and Ringås, J. E., 2005, Reservoir challenges of heterolithic tidal sandstone reservoirs in the Halten Terrace, mid-Norway: *Petroleum Geoscience*, v. 11, no. 1, p. 3-16.
- McCave, I. N., 1970, Deposition of fine-grained suspended sediment from tidal currents: *Journal of Geophysical Research*, v. 75, no. 21, p. 4151-4159.
- McIlroy, D., 2004, Ichnofabrics and sedimentary facies of a tide-dominated delta: Jurassic Ile Formation of Kristin field, Haltenbanken, offshore mid-Norway, *in*

- McIlroy, D., ed., *The Application of Ichnology to Palaeoenvironmental and Stratigraphic Analysis: Lyell Meeting 2003*, Volume 228, The Geological Society of London, Special Publication, p. 237-272.
- McIlroy, D., Flint, S., Howell, J. A., and Timms, N., 2005, *Sedimentology of the tide-dominated Jurassic Lajas Formation, Neuquén Basin, Argentina*: Geological Society, London, Special Publications, v. 252, no. 1, p. 83-107.
- McIlroy, D., Flint, S. S., and Howell, J. A., 1999, Applications of high-resolution sequence stratigraphy to reservoir prediction and flow unit definition in aggradational tidal successions, *in* Hentz, T., ed., *Advanced Reservoir Characterization for the 21st Century.*, Volume 19, GCSSEPM Special Publications, p. 121-132.
- Mellere, D., and Steel, R. J., 1995, Facies architecture and sequentiality of nearshore and shelf sandbodies - Haystack Mountains Formation, Wyoming, USA: *Sedimentology*, v. 42, no. 4, p. 551-574.
- , 1996, Tidal sedimentation in Inner Hebrides half grabens, Scotland: the Mid-Jurassic Berreraig Sandstone Formation: Geological Society, London, Special Publications, v. 117, no. 1, p. 49-79.
- Michaud, K. J., and Dalrymple, R. W., Facies, architecture and stratigraphic occurrence of headland- attached tidal sand ridges in the Roda Formation, Northern Spain, *in* *Proceedings Contributions to Modern and Ancient Tidal Sedimentology: Proceedings of the Tidalites 2012 Conference* 2016, John Wiley & Sons, p. 313.
- Morgans-Bell, H. S., and McIlroy, D., 2005, Palaeoclimatic implications of Middle Jurassic (Bajocian) coniferous wood from the Neuquén Basin, west-central Argentina: Geological Society, London, Special Publications, v. 252, no. 1, p. 267-278.
- Mutti, E., Davoli, G., Tinterri, R., and Zavala, C., 1996, The importance of ancient fluvio-deltaic systems dominated by catastrophic flooding in tectonically active basins: *Memorie di Scienze Geologiche*, v. 48, p. 233-291.
- Mutti, E., Rosell, J., Allen, G. P., Fonnesu, F., and Sgavetti, M., 1985, The Eocene Baronia tide-dominated delta-shelf system in the Ager Basin, *in* Mila, M. D., and Rosell, J., eds., *Excursion Guidebook: VI Eur. Ref. Mtg. I.A.S.: Lerida, Spain*, p. 579-600.
- Mutti, E., Tinterri, R., Benevelli, G., Biase, D. d., and Cavanna, G., 2003, Deltaic, mixed and turbidite sedimentation of ancient foreland basins: *Marine and Petroleum Geology*, v. 20, no. 6-8, p. 733-755.
- Mutti, E., Tinterri, R., Di Biase, D., Fava, L., Mavilla, N., Angella, S., and Calabrese, L., 2000, Delta-front facies associations of ancient flood-dominated fluvio-deltaic systems: *Rev. Soc. Geol. Espana*, v. 13, no. 2, p. 165-190.
- Myrow, P. M., Lukens, C., Lamb, M. P., Houck, K., and Strauss, J., 2008, Dynamics of a Transgressive Prodeltaic System: Implications for Geography and Climate Within a Pennsylvanian Intracratonic Basin, Colorado, U.S.A: *Journal of Sedimentary Research*, v. 78, no. 8, p. 512-528.

- Nemec, W., and Muszyński, A., Volcaniclastic alluvial aprons in the Tertiary of Sofia district (Bulgaria), *in* Proceedings Annales Societatis Geologorum Poloniae 1982, Volume 52, p. 239-303.
- Nichols, M. M., 1989, Physical Processes and Sedimentology of Siliciclastic-Dominated Lagoonal Systems Sediment accumulation rates and relative sea-level rise in lagoons: *Marine Geology*, v. 88, no. 3, p. 201-219.
- Nichols, M. M., and Biggs, R. B., 1985, Estuaries, *in* Davis Jr, R. A., ed., *Coastal Sedimentary Environments*: New York, Springer-Verlag, p. 77-186.
- Nichols, M. M., Johnson, G. H., and Peebles, P., 1991, Modern Sediments and Facies Model for a Microtidal Coastal Plain Estuary, The James Estuary, Virginia: *Journal of Sedimentary Petrology*, v. 61, no. 6, p. 883-899.
- Nio, S.-D., and Yang, C.-S., 1991, Diagnostic attributes of clastic tidal deposits: a review.
- Nittroer, C. A., Kuehl, S. A., Figueiredo, A. G., Allison, M. A., Sommerfield, C. K., Rine, J. M., Faria, L. E. C., and Silveira, O. M., 1996, The geological record preserved by Amazon shelf sedimentation: *Continental Shelf Research*, v. 16, no. 5-6, p. 817-841.
- Olariu, C., 2014, Autogenic process change in modern deltas: lessons for the ancient, *in* Martinius, A. W., Ravnås, R., Howell, J. A., Steel, R. J., and Wonham, J. P., eds., *From Depositional Systems to Sedimentary Successions on the Norwegian Continental Margin Volume 46*, International Association of Sedimentologists, p. 149-166.
- Olariu, C., and Bhattacharya, J. P., 2006, Terminal Distributary Channels and Delta Front Architecture of River-Dominated Delta Systems: *Journal of Sedimentary Research*, v. 76, no. 2, p. 212-233.
- Olariu, C., Bhattacharya, J. P., Xu, X., Aiken, C. L. V., Zeng, X., and McMechan, G. A., 2005, Integrated study of ancient delta-front deposits, using outcrop, ground-penetrating radar, and three-dimensional photorealistic data: Cretaceous Panther Tongue Sandstone, Utah, USA, *in* Giosan, L., and Bhattacharya, J. P., eds., *River Deltas: Concepts, Models, and Examples*, Volume 83, SEPM Special Publication.
- Olariu, C., Steel, R. J., Dalrymple, R. W., and Gingras, M. K., 2012a, Tidal dunes versus tidal bars: The sedimentological and architectural characteristics of compound dunes in a tidal seaway, the lower Baronia Sandstone (Lower Eocene), Ager Basin, Spain: *Sedimentary Geology*, v. 279, p. 134-155.
- Olariu, C., Steel, R. J., and Petter, A. L., 2010, Delta-front hyperpycnal bed geometry and implications for reservoir modeling: Cretaceous Panther Tongue delta, Book Cliffs, Utah: *AAPG bulletin*, v. 94, no. 6, p. 819-845.
- Olariu, M. I., Olariu, C., Steel, R. J., Dalrymple, R. W., and Martinius, A. W., 2012b, Anatomy of a laterally migrating tidal bar in front of a delta system: Esdolomada Member, Roda Formation, Tremp-Graus Basin, Spain: *Sedimentology*, v. 59, no. 2, p. 356-U332.
- Patterson, R. T., Blenkinsop, J., and Cavazza, W., 1995, Planktic foraminiferal biostratigraphy and $^{87}\text{Sr}/^{86}\text{Sr}$ isotopic stratigraphy of the Oligocene-to-

- Pleistocene sedimentary sequence in the southeastern Calabrian microplate, southern Italy: *Journal of Paleontology*, v. 69, p. 7-20.
- Pirmez, C., Pratson, L. F., and Steckler, M. S., 1998, Clinof orm development by advection-diffusion of suspended sediment: Modeling and comparison to natural systems: *Journal of Geophysical Research: Solid Earth*, v. 103, no. B10, p. 24141-24157.
- Plink-Björklund, P., 2005, Stacked fluvial and tide-dominated estuarine deposits in high-frequency (fourth-order) sequences of the Eocene Central Basin, Spitsbergen: *Sedimentology*, v. 52, no. 2, p. 391-428.
- Plink-Björklund, P., 2008, Wave-to-tide facies change in a Campanian shoreline complex, Chimney Rock Tongue, Wyoming-Utah, USA, *in* Hampson, G. J., Steel, R. J., Burgess, P. M., and Dalrymple, B. W., eds., Recent advances in models of shallow-marine stratigraphy: SEPM Special Publication, Volume 90, p. 265-291.
- Plink-Björklund, P., 2012, Effects of tides on deltaic deposition: Causes and responses: *Sedimentary Geology*, v. 279, no. 0, p. 107-133.
- Plint, A., 1988, Sharp-based shoreface sequences and “offshore bars” in the Cardium Formation of Alberta: their relationship to relative changes in sea level: *Sea-Level Changes: An Integrated Approach*: SEPM, Special Publication, v. 42, p. 357-370.
- Plint, A. G., 2010, Wave-and storm-dominated shoreline and shallow-marine systems, *in* Dalrymple, B. W., and James, N. P., eds., *Facies models*, Volume 4, Geological Association of Canada, p. 167-199.
- Pontén, A., and Plink-Björklund, P., 2007, Depositional environments in an extensive tide-influenced delta plain, Middle Devonian Gauja Formation, Devonian Baltic Basin: *Sedimentology*, v. 54, no. 5, p. 969-1006.
- , 2009, Process Regime Changes Across a Regressive to Transgressive Turnaround in a Shelf-Slope Basin, Eocene Central Basin of Spitsbergen: *Journal of Sedimentary Research*, v. 79, no. 1, p. 2-23.
- Pugh, D. T., 1987, *Tides, Surges and Mean Sea-Level*, New York, John Wiley.
- Pulham, A. J., 1989, Controls on internal structure and architecture of sandstone bodies within Upper Carboniferous fluvial-dominated deltas, County Clare, western Ireland, *in* Whateley, M. K. G., and Pickering, K. T., eds., *Deltas: Traps for Fossil Fuels*, Volume 41: London, Geol. Soc. Spec. Publ., p. 179-203.
- Quattrocchio, M. E., Zavala, C. A., García, V., and Volkheimer, W., Paleogeographic changes during the Middle Jurassic in the southern part of the Neuquén Basin, Argentina, *in* *Proceedings Advances in Jurassic Research*. Transtec Publications, Geo Research Forum, Switzerland, 1996, Volume 1-2, p. 467-484.
- Reineck, H.-E., and Wunderlich, F., 1968, Classification and Origin of Flaser and Lenticular Bedding: *Sedimentology*, v. 11, no. 1-2, p. 99-104.
- Reynaud, J.-Y., and Dalrymple, R. W., 2012, Shallow-marine tidal deposits, *in* Davis Jr, R. A., and Dalrymple, B. W., eds., *Principles of Tidal Sedimentology*: New York, Springer, p. 335-370.

- Reynaud, J.-Y., Dalrymple, R. W., Vennin, E., Parize, O., Besson, D., and Rubino, J.-L., 2006, Topographic Controls on Production and Deposition of Tidal Cool-Water Carbonates, Uzès Basin, SE France: *Journal of Sedimentary Research*, v. 76, no. 1, p. 117-130.
- Reynaud, J.-Y., Ferrandini, M., Ferrandini, J., Santiago, M., Thinon, I., André, J.-P., Barthet, Y., Guennoc, P. O. L., and Tessier, B., 2013, From non-tidal shelf to tide-dominated strait: The Miocene Bonifacio Basin, Southern Corsica: *Sedimentology*, v. 60, no. 2, p. 599-623.
- Reynolds, A. D., 1999, Dimensions of paralic sandstone bodies: *AAPG bulletin*, v. 83, no. 2, p. 211-229.
- Rieu, R., van Heteren, S., van der Spek, A. J. F., and De Boer, P. L., 2005, Development and Preservation of a Mid-Holocene Tidal-Channel Network Offshore the Western Netherlands: *Journal of Sedimentary Research*, v. 75, no. 3, p. 409-419.
- Roberts, H. H., and Sydow, J., 2003, Late Quaternary stratigraphy and sedimentology of the offshore Mahakam delta, east Kalimantan (Indonesia), *in* Sidi, F. H., Nummedal, D., Imbert, P., Darman, H., and Posamentier, H. W., eds., *Tropical Deltas of Southeast Asia—Sedimentology, Stratigraphy, and Petroleum Geology*, Volume 76, SEPM Special Publication, p. 125-145.
- Rosenfeld, U., 1978, Litología y sedimentología de la formación Lajas (Jurásico Medio) en la parte austral de la Cuenca Neuquina, Argentina: *Acta Geológica Lilloana*.
- Rossi, M., and Craig, J., 2016, A new perspective on sequence stratigraphy of syn-orogenic basins: insights from the Tertiary Piedmont Basin (Italy) and implications for play concepts and reservoir heterogeneity: *Geological Society, London, Special Publications*, v. 436.
- Rossi, M. E., and Rogledi, S., 1988, Relative sea-level changes, local tectonic settings and basin margin sedimentation in the interference zone between two orogenic belts: seismic stratigraphic examples from Padan foreland basin, northern Italy, *in* Nemeč, W., and Steel, R. J., eds., *Fan Deltas: Sedimentology and Tectonic Settings*: Glasgow, Blakie and Son, p. 368-384.
- Rossi, V. M., Kim, W., Leva López, J., Edmonds, D., Geleynse, N., Olariu, C., Steel, R. J., Hiatt, M., and Passalacqua, P., 2016, Impact of tidal currents on delta-channel deepening, stratigraphic architecture, and sediment bypass beyond the shoreline: *Geology*, v. 44, no. 11, p. 927-930.
- Rossi, V. M., and Steel, R. J., 2016, The role of tidal, wave and river currents in the evolution of mixed-energy deltas: Example from the Lajas Formation (Argentina): *Sedimentology*, v. 63, no. 4, p. 824-864.
- Saller, A., and Blake, G., 2003, Sequence stratigraphy and syndepositional tectonics of upper Miocene and Pliocene deltaic sediments, offshore Brunei Darussalam, *in* Sidi, F. H., Nummedal, D., Imbert, P., Darman, H., and Posamentier, H. W., eds., *Tropical Deltas of Southeast Asia — Sedimentology, Stratigraphy, and Petroleum Geology* SEPM Special Publication 76, p. 219-234.

- Sassi, M. G., Hoitink, A. J. F., de Brye, B., and Deleersnijder, E., 2012, Downstream hydraulic geometry of a tidally influenced river delta: *Journal of Geophysical Research: Earth Surface*, v. 117, no. F04022.
- Scasso, R., Dozo, M. T., Cuitiño, J. I., and Bouza, P., 2012, Meandering tidal-fluvial channels and lag concentration of terrestrial vertebrates in the fluvial-tidal transition of an ancient estuary in Patagonia: *Lat. Am. J. Sedimentol. Basin Anal.*, v. 19, p. 27-45.
- Schwarz, E., 2012, Sharp-based marine sandstone bodies in the Mulichinco Formation (Lower Cretaceous), Neuquén Basin, Argentina: remnants of transgressive offshore sand ridges: *Sedimentology*, p. no-no.
- Shaw, J. B., and Mohrig, D., 2014, The importance of erosion in distributary channel network growth, Wax Lake Delta, Louisiana, USA: *Geology*, v. 42, no. 1, p. 31-34.
- Sohn, Y. K., Rhee, C. W., and Kim, B. C., 1999, Debris Flow and Hyperconcentrated Flood-Flow Deposits in an Alluvial Fan, Northwestern Part of the Cretaceous Yongdong Basin, Central Korea: *The Journal of Geology*, v. 107, no. 1, p. 111-132.
- Southard, J. B., and Boguchwal, L. A., 1990, Bed configurations in steady unidirectional water flows. Part 2. Synthesis of flume data: *Journal of Sedimentary Research*, v. 60, no. 5.
- Spalletti, L., Veiga, G., and Schwarz, E., 2010, Facies and stratigraphic sequences of the Mesozoic Neuquén Basin (Western Argentina): continental to deep marine settings. , *in* del Papa, C. A., R., ed., *Field Excursion Guidebook*, 18th International Sedimentological Congress, Mendoza, Argentina, FE-C3 Mendoza, Argentina, p. 1-79.
- Steel, R. J., Plink-Bjorklund, P., and Aschoff, J., 2012, Tidal Deposits of the Campanian Western Interior Seaway, Wyoming, Utah and Colorado, USA, *in* Davis Jr, R. A., and Dalrymple, R. W., eds., *Principles of Tidal Sedimentology*, Springer Netherlands, p. 437-471.
- Swenson, J. B., Paola, C., Pratson, L., Voller, V. R., and Murray, A. B., 2005, Fluvial and marine controls on combined subaerial and subaqueous delta progradation: Morphodynamic modeling of compound- clinoform development: *Journal of Geophysical Research: Earth Surface*, v. 110, no. F2, p. 1-16.
- Sylvester, A. G., 1988, Strike-slip faults: *Geological Society of America Bulletin*, v. 100, no. 11, p. 1666-1703.
- Ta, T. K. O., Nguyen, V. L., Tateishi, M., Kobayashi, I., Saito, Y., and Nakamura, T., 2002a, Sediment facies and Late Holocene progradation of the Mekong River Delta in Bentre Province, southern Vietnam: an example of evolution from a tide-dominated to a tide- and wave-dominated delta: *Sedimentary Geology*, v. 152, no. 3-4, p. 313-325.
- Ta, T. K. O., Nguyen, V. L., Tateishi, M., Kobayashi, I., Tanabe, S., and Saito, Y., 2002b, Holocene delta evolution and sediment discharge of the Mekong River, southern Vietnam: *Quaternary Science Reviews*, v. 21, no. 16-17, p. 1807-1819.

- Tänavsuu-Milkeviciene, K., and Plink-Björklund, P., 2009, Recognizing Tide-Dominated Versus Tide-Influenced Deltas: Middle Devonian Strata of the Baltic Basin: *Journal of Sedimentary Research*, v. 79, no. 12, p. 887-905.
- Tansi, C., Muto, F., Critelli, S., and Iovine, G., 2007, Neogene-Quaternary strike-slip tectonics in the central Calabrian Arc (southern Italy): *Journal of Geodynamics*, v. 43, no. 3, p. 393-414.
- Terwindt, J. H. J., 1981, Origin and sequences of sedimentary structures in inshore mesotidal deposits of the North Sea, *in* Nio, S. D., Shuttenhelm, R. T. E., and van Weering, T. C., eds., *Holocene marine sedimentation in the North Sea Basin*, Volume 5, Internat. Assoc. Sedimentologists Spec. Publ. , p. 4-26.
- Tessier, B., 1993, Upper intertidal rhythmites in the Mont-Saint-Michel Bay (NW France): Perspectives for paleoreconstruction: *Marine Geology*, v. 110, no. 3-4, p. 355-367.
- Tessier, B., and Gigot, P., 1989, A vertical record of different tidal cyclicities: an example from the Miocene Marine Molasse of Digne (Haute Provence, France): *Sedimentology*, v. 36, no. 5, p. 767-776.
- Thrana, C., Næss, A., Leary, S., Gowland, S., Brekken, M., and Taylor, A., 2014, Updated depositional and stratigraphic model of the Lower Jurassic Åre Formation, Heidrun Field, Norway, *From Depositional Systems to Sedimentary Successions on the Norwegian Continental Margin*, John Wiley & Sons, Ltd, p. 253-289.
- Tinterri, R., 2007, The Lower Eocene Roda Sandstone (south Central Pyrenees): an example of a flood-dominated river-delta system in a tectonically controlled basin: *Rivista Italiana di Paleontologia e Stratigrafia (Research In Paleontology and Stratigraphy)*, v. 113, no. 2, p. 223-255.
- , 2011, Combined flow sedimentary structures and the genetic link between sigmoidal- and hummocky-cross stratification: *GeoActa*, v. 10, p. 1-43.
- Tortorici, L., 1982, Lineamenti geologico-strutturali dell'arco Calabro-Peloritano: *Società Italiana di Mineralogia e Petrografia*, v. 38, p. 927-940.
- Tortorici, L., Monaco, C., Tansi, C., and Cocina, O., 1995, Kinematics of distributed deformation in plate boundary zones with emphasis on the Mediterranean, Anatolia and Eastern Asia Recent and active tectonics in the Calabrian arc (Southern Italy): *Tectonophysics*, v. 243, no. 1, p. 37-55.
- Trentesaux, A., Stolk, A., and Berne, S., 1999, Sedimentology and stratigraphy of a tidal sand bank in the southern North Sea: *Marine Geology*, v. 159, no. 1-4, p. 253-272.
- Tripodi, V., Muto, F., and Critelli, S., 2013, Structural style and tectono-stratigraphic evolution of the Neogene-Quaternary Siderno Basin, southern Calabrian Arc, Italy: *International Geology Review*, v. 55, no. 4, p. 468-481.
- Tye, R. S., and Coleman, J. M., 1989a, Depositional Processes and Stratigraphy of Fluvially Dominated Lacustrine Deltas: Mississippi Delta Plain: *Journal of Sedimentary Petrology*, v. 59, no. 6, p. 973-996.

- , 1989b, Evolution of Atchafalaya lacustrine deltas, south-central Louisiana: *Sedimentary Geology*, v. 65, no. 1–2, p. 95-112.
- Uroza, C. A., 2008, Processes and Architectures of Deltas in Shelf-break and Ramp Platforms: Examples from the Eocene of West Spitsbergen (Norway), the Pliocene Paleo-Orinoco Delta (SE Trinidad), and the Cretaceous Western Interior Seaway (S Wyoming and NE Utah) [PhD: the University of Texas at Austin, 261 p.
- Vakarelov, B. K., and Ainsworth, R. B., 2013, A hierarchical approach to architectural classification in marginal-marine systems: Bridging the gap between sedimentology and sequence stratigraphy: *AAPG bulletin*, v. 97, no. 7, p. 1121-1161.
- Vakarelov, B. K., Ainsworth, R. B., and MacEachern, J. A., 2012, Recognition of wave-dominated, tide-influenced shoreline systems in the rock record: Variations from a microtidal shoreline model: *Sedimentary Geology*, v. 279, p. 23-41.
- Van Andel, T. H., 1967, The Orinoco Delta: *Journal of Sedimentary Petrology*, v. 37, no. 2, p. 297-310.
- Van den Berg, J. H., Boersma, J. R., and Van Gelder, A., 2007, Diagnostic sedimentary structures of the fluvial-tidal transition zone—Evidence from deposits of the Rhine and Meuse: *Netherlands Journal of Geosciences/Geologie en Mijnbouw*, v. 86, no. 3, p. 287-306.
- Van Dijk, J. P., 1992, Late Neogene fore-arc basin evolution in the Calabrian Arc (central Mediterranean); tectonic sequence stratigraphy and dynamic geohistory, Utrecht University.
- Van Dijk, J. P., 1993, Three-Dimensional Quantitative Restoration of Central Mediterranean Neogene Basins: The Dynamic Geohistory Approach, *in* Spencer, A. M., ed., *Generation, Accumulation and Production of Europe's Hydrocarbons III: Special Publication of the European Association of Petroleum Geoscientists No. 3*: Berlin, Heidelberg, Springer Berlin Heidelberg, p. 267-280.
- Van Dijk, J. P., Bello, M., Brancaleoni, G. P., Cantarella, G., Costa, V., Frixia, A., Golfetto, F., Merlini, S., Riva, M., Torricelli, S., Toscano, C., and Zerilli, A., 2000, A regional structural model for the northern sector of the Calabrian Arc (southern Italy): *Tectonophysics*, v. 324, no. 4, p. 267-320.
- van Maren, D. S., Hoekstra, P., and Hoitink, A. J. F., 2004, Tidal flow asymmetry in the diurnal regime: bed-load transport and morphologic changes around the Red River Delta: *Ocean Dynamics*, v. 54, no. 3-4, p. 424-434.
- Van Wagoner, J. C., 1992, High-frequency sequence stratigraphy and facies architecture of the Sego sandstone in the Book Cliffs of western Colorado and eastern Utah, AAPG, Sequence stratigraphy applications to shelf sandstone and sandstone reservoirs; outcrop to subsurface examples: AAPG Field Conference.
- Vergani, G. D., Tankard, A. J., Belotti, H. J., and Welsink, H. J., 1995, Tectonic Evolution and Paleogeography of the Neuquén Basin, Argentina, *in* Tankard, A. J., Suarez Soruco, R., and Welsink, H. J., eds., *Petroleum Basins of South America*: Tulsa, OK, AAPG Memoir 62, p. 383-402.

- Visser, M., 1980, Neap-spring cycles reflected in Holocene subtidal large-scale bedform deposits: a preliminary note: *Geology*, v. 8, no. 11, p. 543-546.
- Walsh, J. P., Nittrouer, C. A., Palinkas, C. M., Ogston, A. S., Sternberg, R. W., and Brunskill, G. J., 2004, Clinoform mechanics in the Gulf of Papua, New Guinea: *Continental Shelf Research*, v. 24, no. 19, p. 2487-2510.
- Warne, A. G., Guevara, E. H., and Aslan, A., 2002, Late Quaternary Evolution of the Orinoco Delta, Venezuela: *Journal of Coastal Research*, v. 18, no. 2, p. 225-253.
- Westaway, R., 1993, Quaternary uplift of southern Italy: *Journal of Geophysical Research: Solid Earth*, v. 98, no. B12, p. 21741-21772.
- Wheatcroft, R. A., Stevens, A. W., Hunt, L. M., and Milligan, T. G., 2006, The large-scale distribution and internal geometry of the fall 2000 Po River flood deposit: Evidence from digital X-radiography: *Continental Shelf Research*, v. 26, no. 4, p. 499-516.
- Wightman, D. M., and Pemberton, S. G., 1997, The Lower Cretaceous (Aptian) McMurray Formation: an overview of the Fort McMurray area, northeastern, Alberta, *in* Pemberton, S. G., and James, D. P., eds., *Petroleum Geology of the Cretaceous Mannville Group, Western Canada Volume 18*, Canadian Society of Petroleum Geologists p. 312-344.
- Willis, B. J., 2005, Deposits of tide-influenced river deltas, *in* Giosan, L., and Bhattacharya, J. P., eds., *River Deltas - Concepts, Models, and Examples*, Volume 83, SEPM Special Publication, p. 87-129.
- Willis, B. J., Bhattacharya, J. P., Gabel, S. L., and White, C. D., 1999, Architecture of a tide-influenced river delta in the Frontier Formation of central Wyoming, USA: *Sedimentology*, v. 46, no. 4, p. 667-688.
- Willis, B. J., and Gabel, S. L., 2003, Formation of Deep Incisions into Tide-Dominated River Deltas: Implications for the Stratigraphy of the Sejo Sandstone, Book Cliffs, Utah, U.S.A: *Journal of Sedimentary Research*, v. 73, no. 2, p. 246-263.
- Wolinsky, M. A., Edmonds, D. A., Martin, J., and Paola, C., 2010, Delta allometry: Growth laws for river deltas: *Geophysical Research Letters*, v. 37, no. 21.
- Wright, L. D., 1977, Sediment transport and deposition at river mouths: A synthesis: *Geological Society of America Bulletin*, v. 88, no. 6, p. 857-868.
- Xue, Z., Liu, J. P., DeMaster, D., Van Nguyen, L., and Ta, T. K. O., 2010, Late Holocene Evolution of the Mekong Subaqueous Delta, Southern Vietnam: *Marine Geology*, v. 269, no. 1-2, p. 46-60.
- Yang, B., Gingras, M. K., Pemberton, S. G., and Dalrymple, R. W., 2008, Wave-generated tidal bundles as an indicator of wave-dominated tidal flats: *Geology*, v. 36, no. 1, p. 39-42.
- Yang, B. C., Dalrymple, R. W., and Chun, S. S., 2005, Sedimentation on a wave-dominated, open-coast tidal flat, south-western Korea: summer tidal flat – winter shoreface: *Sedimentology*, v. 52, no. 2, p. 235-252.
- Yoshida, S., Steel, R. J., and Dalrymple, R. W., 2007, Changes in Depositional Processes—An Ingredient in a New Generation of Sequence-Stratigraphic Models: *Journal of Sedimentary Research*, v. 77, no. 6, p. 447-460.

Zavala, C. A., Sequence stratigraphy in continental to marine transitions. An example from the middle Jurassic Cuyo Group, South Neuquen Basin, Argentina, *in* Proceedings Advances in Jurassic Research Dürnten, Switzerland, 1996, Trans Tech Publications, GeoResearch Forum, p. 285-294.